Investigating the molecular regulation of adult neural stem cell quiescence

Isabelle Maria Blomfield

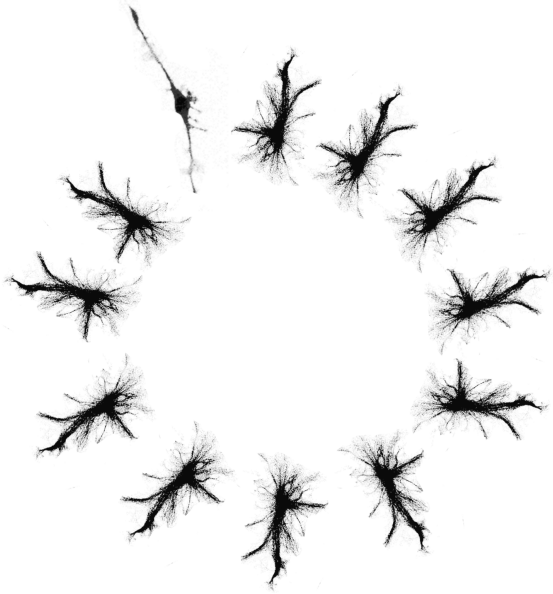

'"Quexit": How a stem cell decides to remain in, or exit, quiescence'

University College London

and

The Francis Crick Institute

PhD Supervisor: François Guillemot

A thesis submitted for the degree of

Doctor of Philosophy

University College London

September 2018

Declaration

I Isabelle Maria Blomfield confirm that the work presented in this thesis is my own. Where information has been derived from other sources, I confirm that this has been indicated in the thesis.

Abstract

Quiescence is essential for long-term maintenance of adult stem cells and tissue homeostasis. The adult mammalian brain was recently discovered to harbour populations of neural stem cells in at least two neurogenic regions: the subventricular zone (SVZ) of the lateral ventricles, and the subgranular zone (SGZ) of the hippocampus. Adult hippocampal neural stem cells (AHNSCs) are a mostly quiescent population, whose activation is tightly controlled by a complex range of signals derived from their niche. How exactly these signals are interpreted by AHNSCs to regulate quiescence is not fully understood. The proneural bHLH transcription factor Ascl1 is crucial for AHNSC activation, and degradation of Ascl1 protein by the E3 ubiquitin ligase Huwe1 is an important mechanism to allow active neural stem cells to return to quiescence.

Here I present the discovery that Ascl1 is unexpectedly expressed and transcribed in quiescent NSCs *in vivo*, and is suppressed at the protein level to maintain quiescence of NSCs. In order to investigate the molecular mechanisms regulating AHNSC quiescence, and to circumvent the complexities of the neurogenic niche, we have developed an *in vitro* model of AHNSC quiescence. We have found that the *in vitro* model robustly reproduces the quiescent stem cell state of NSCs *in vivo*. We undertook a candidate approach to identify regulators of Ascl1 protein and NSC quiescence and identified the inhibitor of differentiation (Id) protein, Id4, as a novel quiescence factor. Functional studies *in vitro* in combination with genetic approaches *in vivo* confirmed that Id4 is expressed in quiescent hippocampal NSCs, maintains NSC quiescence, and mediates the inhibition of Ascl1 protein in quiescent NSCs, by sequestration of its E-protein binding partners. Finally, we investigated the niche signals regulating Id4 expression, and discovered that it is regulated in a complex manner likely by more than one signalling pathway.

Acknowledgements

My first thanks and enormous gratitude go to my supervisor Dr. François Guillemot, and co-supervisor Dr. Noelia Urbán. The combined unwavering guidance I have received from two incredibly knowledgeable, patient and supportive supervisors has undoubtedly been the driving force behind the success and enjoyment I have experienced during my PhD. Thank you, François, for being a rare supervisor who not only provides excellent scientific guidance, but also encourages exploits beyond the lab. Also thank you for the many opportunities I have had to go to incredible international conferences over the last 5 years.

A double thank you Noelia as colleague and friend throughout the past 5 years, for your incredible supervision and collaboration, your advice and support in science and life, as well as many laughs and Friday beers!

Thank you, Mar, for the incredible help and support, both scientific and non, you have made these last couple of years immeasurably more manageable and enjoyable. The lab has evolved immensely since I joined in 2013, however I must thank my past labmates Koji, Debbie, Pat and Jimena, and current labmates Mar, Sophie, Marco, Lachlan, Michael, Clem, Cristina, Oana, Berta, Ale, Lan, Siew Lan, for all the scientific support, advice and discussions, as well as all the laughs and good times outside of the lab. I have thoroughly enjoyed feeling equally foreign in our international bubble!

Thank you to my thesis committee, Alex Gould, Mike Gilchrist, Sila Ultanir and Rita Sousa-Nuñes for the support, discussions and suggestions throughout my PhD.

My PhD colleagues and friends, in particular Pedro, Kathleen, Hannah, Luuk, and Johanna.

Finally, I will always be grateful to my mum Maria, dad Rob, and big brother Dan, for their endless support and encouragement. You have all kept me smiling!

Impact Statement

Our human bodies are constantly being regenerated thanks to populations of stem cells we keep with us throughout adult life. However, these stem cells can become dysfunctional and deregulated with age or disease. Too little activation will result in not enough tissue regeneration, too much could exhaust the stem cells too early, and complete deregulation of stem cells could lead to aggressive cancers.

Evidence is emerging that adult humans may have neural stem cells that actively contribute new neurons to the brain, but reduction or deregulation of this production is associated with depression, age-related cognitive decline, and neurodegeneration, all of which are major current health concerns in the United Kingdom and globally. These diseases lack effective treatments, and result in terrible suffering for patients and families, as well as disabling a large percentage of the workforce resulting in economic consequences.

However, research into the mechanisms regulating neural stem cells could hold a key to alleviating these diseases. We have discovered a novel mechanism which tightly controls the quiescent state of adult neural stem cells. The protein Id4 is expressed in neural stem cells and acts as a block on activation, holding stem cells back until they're needed.

The fields of adult neurogenesis and adult stem cell research will benefit from the discovery of this novel molecular mechanisms for future research, as well as by utilising the model of quiescent neural stem cells presented in this thesis.

This research also has implications for human health and ageing. By understanding what causes stem cells to maintain a healthy level of activity, we can begin to identify environmental factors that help this process, such as particular diets or social and learning activities, providing people with practical advice to maintain a healthy brain and body well into old age.

By specifically targeting Id4, with designer drugs for example, we could potentially activate stem cells that have become dormant with age or disease, thereby tapping into an endogenous regenerative capacity within the brain. This would be particularly useful for sufferers of depression and neurodegeneration, who require more therapeutic intervention.

Understanding how stem cells function in the brain is also important for guiding the development of stem cell therapies for brain injuries or stroke; if we know what causes stem cells to remain active or become dormant, we can ensure that stem cells transplanted into the brain remain active and generate the neurons when and where we want them to.

Finally, understanding how neural stem cell activity is regulated is valuable knowledge for research into brain cancers. Glioblastomas have stem-like cells which can be quiescent and evade chemotherapy, therefore if we discover Id4 is responsible for this quiescence, we can target it, potentially improving the primary treatment of the cancer and helping to prevent recurrence.

There is realistic scope to translate the research presented here into new drugs and therapies, and the work will be published in a well-respected peer-reviewed scientific journal.

Table of Contents

Abstract **3**
Acknowledgements **4**
Impact Statement **5**
Table of Contents **7**
Table of Figures **11**
List of Tables **14**
Abbreviations **15**
Chapter 1.Introduction **17**
1.1 Adult neurogenesis **18**
1.1.1 The history of adult neurogenesis 18
1.1.2 The 'what' and 'where' of adult neurogenesis 19
1.1.3 Adult neurogenesis in humans 20
1.1.4 Function of adult neurogenesis 21
1.2 The stem cell niche **23**
1.2.1 Common features of adult stem cell niches 23
1.2.2 The adult subventricular zone as a neurogenic niche 24
1.2.3 The neurogenic niche in the adult mouse hippocampus 26
1.2.4 RGLs: from astrocytes to neural stem cells 29
1.2.5 RGL heterogeneity 30
1.2.6 Embryonic origin of RGLs 32
1.3 Stem cell quiescence **33**
1.3.1 What is quiescence? 33
1.3.2 Transcriptional signature of quiescence 34
1.3.3 Function of quiescence 35
1.3.4 Identifying quiescent stem cells 37
1.4 Regulation of adult neural stem cells and neurogenesis **38**
1.4.1 Systemic regulation 38
1.4.2 Direct regulation of NSCs by the neurogenic niche 39
1.5 *In vitro* culture systems for studying adult NSCs **51**
1.6 Intrinsic mechanisms regulating NSC quiescence **53**
1.6.1 TLX 53
1.6.2 MicroRNAs 53
1.6.3 Ascl1 54
1.6.4 FoxO3 56
1.6.5 Pten 56
1.6.6 Cell cycle proteins; p21, p27, p57 57
1.6.7 REST 57
1.6.8 NFIX 58
1.6.9 Id proteins 58
1.7 The Inhibitor of Differentiation proteins **58**
1.7.1 Structure and conservation of Id proteins 58
1.7.2 Expression of Id proteins in embryonic and adult CNS 60
1.7.3 Regulation of Id expression 61
1.7.4 Function of Id proteins 61
1.8 Aims of the present work **65**

Chapter 2.Materials & Methods 67
2.1 Experimental model and subject details 67
2.1.1 Mouse models 67
2.1.2 Primary Cell Cultures 68
2.2 Method Details 68
2.2.1 Tamoxifen administration 68
2.2.2 Tissue preparation and immunofluorescence 68
2.2.3 RNA *in situ* hybridization 70
2.2.4 Microscopic analysis 71
2.2.5 Cell treatments 71
2.2.6 Constructs, plasmid transfection and viral transduction 74
2.2.7 FAC sorting 76
2.2.8 RNA extraction, cDNA synthesis and QPCR 76
2.2.9 RNA sequencing and analysis 77
2.2.10 Protein purification, Western Blot and Co-immunoprecipitation 78
2.3 Quantification and Statistical Analysis 80
2.3.1 Quantification of immunofluorescence 80
2.3.2 Statistics 80
Chapter 3.Results 1 83
3.1 Development of an *in vitro* model of adult hippocampal stem cell quiescence 83
3.1.1 Deriving adult hippocampal neural stem cells 83
3.1.2 BMP4-treated AHNSCs can be induced into a reversible quiescent-like state 84
3.1.3 BMP4-induced quiescent AHNSCs maintain their multipotency 88
3.1.4 BMP4-induced quiescent AHNSCs spontaneously enter the cell cycle and can re-enter quiescence 89
3.2 BMP4 induces more quiescence-like features in AHNSCs than just cell cycle arrest. 93
3.2.1 BMP4-induced quiescent AHNSCs have different metabolic, transcription and translation rates than active AHNSCs 94
3.2.2 Transcriptome-wide analysis reveals a quiescence “signature” of BMP4-treated AHNSCs 96
3.3 Refining the *in vitro* model of AHNSC quiescence 99
3.3.1 Withdrawal of EGF and titration of FGF2 generates a more physiological model of AHNSC quiescence without affecting stemness. 99
3.3.2 AHNSCs cultured in FGF2 alone can reversibly be induced into quiescence 103
3.3.3 Titrating BMP4 induces different “depths” of quiescence 104
3.4 Transcriptome-wide analysis of the refined *in vitro* model shows BMP4-treated AHNSCs are quiescent 107
3.4.1 BMP4 treatment (and not EGF withdrawal) induces a quiescence transcriptional “signature” similar to *in vivo* quiescent NSCs 107
3.4.2 “Shallow” and “deep” quiescent NSCs have specific transcriptional differences 110
Chapter 4.Results 2 113

4.1 Ascl1 is expressed at the transcriptional level, but inhibited at the protein level, in quiescent NSCs *in vivo* and *in vitro* 113
4.1.1 Many more RGLs *in vivo* express *Ascl1* mRNA than Ascl1 protein. 113
4.1.2 Ascl1 protein, but not mRNA, is inhibited by BMP4-induced quiescence in AHNSCs *in vitro* 119
4.1.3 Ascl1 protein is actively translated in NSCs *in vitro* 121
4.1.4 Proteasomal degradation of Ascl1 in quiescent NSCs is independent of Huwe1 122
4.2 Inhibitor of Differentiation 4 (Id4) is highly expressed in quiescent RGLs and NSCs, and anti-correlates with Ascl1 protein 123
4.2.1 Expression of the Id proteins *in vivo* 123
4.2.2 Id4 is the most enriched Id protein in quiescent AHNSCs *in vitro*, and anti-correlates with Ascl1 126
4.2.3 E-proteins are expressed in hippocampal NSCs and interact with Ascl1 and Id4 *in vitro* 129
4.3 Functional analysis of Id4 *in vitro* reveals its role in maintaining quiescence of NSCs 131
4.3.1 Over-expression of Id4 in active NSCs *in vitro* suppresses Ascl1 protein, and induces cell cycle arrest 131
4.3.2 Over-expression of Id4 in active NSCs *in vitro* induces transcriptional changes associated with quiescence 134
4.3.3 Over-expression of Id1 can induce cell-cycle arrest but does not suppress Ascl1 protein 139
4.3.4 Id1 only induces a small subset of the quiescence transcriptional signature, and does not regulate Ascl1 target genes 141
4.3.5 Inactivating Id4 in quiescent NSCs stabilises Ascl1 143
4.3.6 Inactivating Id4 in quiescent NSCs restores the function of Ascl1 145
4.3.7 Loss of Id4 in NSCs results in increased Ascl1 protein levels but does not prevent cell cycle arrest in BMP4-induced quiescence 147
4.4 Id4 maintains quiescence of RGLs *in vivo* 149
4.4.1 Acute conditional deletion of Id4 *in vivo* activates RGLs from quiescence 149
4.4.2 The effects of conditional Id4 deletion from RGLs are lost after 30 days 152
4.4.3 Perfusion technique and Ascl1 antibody species affects Ascl1 protein detection 155
4.4.4 Id1 and Id3 are upregulated in response to Id4 deletion 158
***4.5* Id4 expression is independent of Smad4 *in vivo* 160**
4.5.1 Smad signalling is active in a small number RGLs *in vivo*, in the presence or absence of Smad4 161
4.5.2 Conditional deletion of Smad4 *in vivo* does not affect Id4 expression or RGL activation 162
4.5.3 Conditional deletion of Smad4 in AHNSCs *in vitro* does not affect Id4 protein level, but does lead to a loss of Id1 and Id3 165
Chapter 5.Results 3 169
5.1 Modulating Notch signalling has different effects in different concentrations of BMP4 169
5.1.1 Notch signalling is active in NSCs *in vitro* 169

5.1.2 Active Notch signalling is required for low-level proliferation of quiescent NSCs, independent of Id4 and Ascl1 172
5.1.3 Notch regulates different genes depending on the level of BMP4 signalling 177
5.2 Investigating the effect of Notch signalling on Id4 *in vivo* 181
5.3 Notch-RBPJk signalling is not required to maintain Id4 expression in RGLs 182
5.4 Id4 expression in RGLs is independent of both Notch and BMP signalling *in vivo* 184
5.4.1 Double RBPJk-Smad4 conditional deletion does not strongly affect Id4 expression in RGLs 184
Chapter 6.Discussion 187
6.1 An *in vitro* model of adult hippocampal neural stem cell quiescence 187
6.1.1 BMP4-treated adult hippocampal neural stem cells robustly model RGL quiescence 188
6.1.2 Modulating extrinsic factors *in vitro* generates different NSC states 190
6.1.3 BMP4-treated AHNSCs model multiple features of neural stem cell quiescence 191
6.1.4 Future uses of the *in vitro* model of AHNSC quiescence 192
6.2 The unexpected expression of *Ascl1* in quiescent RGLs 194
6.2.1 Ascl1 mRNA is expressed in quiescent NSCs, but suppressed at the protein level 194
6.3 Identification of Id4 as a candidate for regulating Ascl1 protein in quiescence 197
6.3.1 Id4 is a marker of quiescent RGLs 197
6.3.2 Id4:E47 interaction is observed in quiescent AHNSCs 198
6.3.3 The function of Id4 in adult hippocampal NSCs 200
6.4 Hippocampal niche signals other than canonical BMP and Notch regulate Id4 expression 206
6.5 Crosstalk between BMP and Notch signalling 208
6.6 Conclusions and perspectives 210
Reference List 213

Table of Figures

Figure 1.1. Documented regions of neurogenesis in the adult rodent brain..... 19
Figure 1.2. Scheme of the neurogenic niche in the adult mouse subventricular zone 25
Figure 1.3. The neurogenic niche of the adult mouse hippocampus..... 27
Figure 1.4. Expression of genes defining the neurogenic lineage in the dentate gyrus..... 28
Figure 1.5. Molecular and metabolic features of hippocampal NSCs from quiescence to activation. 35
Figure 1.6. Sources of neural stem cell regulation in the hippocampal neurogenic niche. 51
Figure 1.7. Conservation of Id1-4 protein sequence. 59
Figure 1.8. Protein-protein interactions between IDs, Class II bHLHs and E-proteins 62
Figure 3.1. Scheme of *in vitro* model of adult-derived hippocampal neural stem cell quiescence 84
Figure 3.2. BMP4 induces reversible cell cycle exit in AHNSCs (legend next page) 87
Figure 3.3. BMP4-induced quiescent AHNSCs retain their multipotency..... 89
Figure 3.4. Analysis of cycling cells in BMP4-induced quiescence by EdU-BrdU pulse-chase 92
Figure 3.5. Analysis of mitochondria, RNA transcription and protein translation levels in AHNSCs. 95
Figure 3.6. RNAseq analysis of active (EGF+FGF2) vs quiescent (BMP4+FGF2) AHNSCs and comparison with quiescent NS5-NSCs 97
Figure 3.7. Withdrawal of EGF from active AHNSCs, and titration of FGF2 102
Figure 3.8. BMP4 induces reversible quiescence in AHNSCs propagated in FGF2 only 103
Figure 3.9. Titrating BMP4 induces quiescence in a dose-dependent manner (legend next page) 106
Figure 3.10. RNAseq analysis of active (FGF2 only) and quiescent (FGF2+BMP4) AHNSCs (legend next page) 109

Figure 3.11. Comparison of 1ng/mL vs 20ng/mL BMP4 in quiescent AHNSCs by RNAseq 112
Figure 4.1. Ascl1 mRNA and protein expression in hippocampal RGLs (legend next page) 117
Figure 4.2. Ascl1 mRNA and protein expression in AHNSCs *in vitro* 120
Figure 4.3. Ascl1 protein levels increase in AHNSCs following proteasomal inhibition 122
Figure 4.4. Inhibition of Ascl1 protein in quiescent AHNSCs is Huwe1-independent 123
Figure 4.5. Protein expression of Id1, 2, 3 and 4 in the dentate gyrus 125
Figure 4.6. Expression of Id1-4 in AHNSCs *in vitro* 128
Figure 4.7. E-protein expression and co-immunoprecipitation of E47, Id4 and Ascl1 in AHNSCs *in vitro* 131
Figure 4.8. Over-expression of Id4 in active AHNSCs *in vitro* 133
Figure 4.9. RNAseq analysis of Id4 over-expression in active AHNSCs *in vitro* (legend next page) 137
Figure 4.10. Over-expression of Id1 in active AHNSCs *in vitro* 140
Figure 4.11. RNAseq analysis of Id1 over-expression in active AHNSCs *in vitro* (legend next page) 142
Figure 4.12. Over-expression of E47 in quiescent AHNSCs *in vitro* 144
Figure 4.13. RNAseq analysis of E47 over-expression in quiescent AHNSCs *in vitro* 146
Figure 4.14. Expression of Id-4 and Ascl1 in AHNSCs derived from Id4flx mice 148
Figure 4.15. Effects of acute conditional deletion of Id4 from RGLs in the adult hippocampus (legend next page) 151
Figure 4.16. Long-term effects of Id4 deletion on RGL activity and Ascl1 protein level 154
Figure 4.17. Analysis of perfusion method and antibody on Ascl1 immunodetection 157
Figure 4.18. Effects on Id1 and Id3 expression following acute and long-term conditional deletion of Id4 from RGLs (legend next page) 159
Figure 4.19. Expression of phospho-Smad1/5/8 in the dentate gyri of control and *Smad4*^{cKO} mice (legend next page) 161

Figure 4.20. Effects of acute and long-term conditional deletion of Smad4 from RGLs (legend next page) 163
Figure 4.21. Analysis of Id levels in AHNSCs derived from Smad4flx mice 167
Figure 5.1. Scheme for inhibiting Notch signalling and expression of Notch components in AHNSCs *in vitro* 171
Figure 5.2. Effects of inhibiting Notch signalling in active and quiescent AHNSCs *in vitro* (legend next page)..... 175
Figure 5.3. RNAseq analysis of active, shallow quiescent and deep quiescent AHNSCs following Notch inhibition (legend next page) 180
Figure 5.4. Effects of acute deletion of Notch effector RBPJk in RGLs 183
Figure 5.5. Effects of acute deletion of both Smad4 and RBPJk in RGLs 185
Figure 6.1. Proposed mechanisms regulating the active and quiescent RGL state and *Id4*^{cKO} RGLs..... 211

List of Tables

Table 1. List of probes used for QPCR gene expression analysis 76
Table 2. Antibodies and *in situ* probes. 82
Table 3. Combinations of S-phase markers EdU and BrdU, and pan cell cycle marker Ki67 distinguish different cycling behaviours of the cells. 91
Table 4. Cell adhesion genes exclusively co-expressed in AHNSCs and SGZ RGLs, or NS5 NSCs and SGZ RGLs 99

Abbreviations

Adeno	Adenovirus
AHNSC	Adult hippocampal neural stem cell
Ascl1	Achaete-scute complex homolog-like 1
A.U.	Arbitrary units
bHLH	Basic helix-loop-helix
BMP	Bone morphogenetic protein
BrdU	5-bromo-2'-deoxyuridine
BSA	Bovine serum albumin
cDNA	Complementary DNA
cKO	Conditional knock out
Co-IP	Co-immunoprecipitation
CldU	Chloro-deoxyuridine
DAPI	6-diamidino-2-phenylindole
DAVID	Database for annotation, visualisation, and integrated discovery
ddCt	Delta delta cycle threshold
DG	Dentate gyrus
DMSO	Dimethyl sulfoxide
DNA	Deoxyribonucleic acid
dsDNA	Double stranded DNA
ECL	Enhanced chemiluminescence
EdU	5-ethynyl-2'-deoxyuridine
EGF	Epithelial growth factor
FACS	Fluorescence activated cell sorting
FGF2	Fibroblast growth factor 2
GABA	Gamma-Aminobutyric acid
GFAP	Glial fibrillary acidic protein
GFP	Green fluorescent protein
GLAST	Glutamate aspartate transporter
GO	Gene ontology
GSI	Gamma-secretase inhibitor
HA	Human influenza heamagglutinin

ID	Inhibitor of differentiation/DNA binding
IdU	Iodo-deoxyuridine
IF	Immunofluorescence
IHC	Immunohistochemistry
IRES	Internal ribosome entry site
IP	Immunoprecipitation
IPC	Intermediate progenitor cell
i.p.	Intraperitoneal
LY	LY411575 (GSI)
moi	Multiplicity of infection
mRNA	Messenger RNA
NBF	Neutral buffered formaldehyde
NDS	Normal donkey serum
NSC	Neural stem cell
OPP	O-propargyl-puromycin
P	Postnatal day
PBS	Phosphate buffered saline
PFA	Paraformaldehyde
PY	Pyronin Y
QPCR	Quantitative polymerase chain reaction
RGL	Radial glial neural stem cell
RNA	Ribonucleic acid
RNA-seq	RNA sequencing
RYFP	Rosa-26 YFP
SEM	Standard error of the mean
SVZ	Subventricular zone
SGZ	Subgranular zone
TAM	Tamoxifen
TBS	Tris-buffered saline
tdTomato	Tandem dimer Tomato (red) fluorescent protein
WB	Western blot
WT	*Wildtype*
YFP	Yellow fluorescent protein

Chapter 1. Introduction

Adult mammalian tissues need to be repaired and regenerated throughout life in order to maintain function in the face of environmental and cellular damage that occurs from injury, disease and ageing. Many cell types are constantly turned-over in adult humans to replace old or damaged cells, such as the skin, hair, blood, muscle and intestinal epithelium. The source of this regenerative capacity lies with populations of specialised stem cells that exist within the different tissues, where they can divide asymmetrically to self-renew and generate progenitor cells that will differentiate into the mature cell type of their tissue, replacing their old or damaged counterparts.

Up until the middle of the last century, it was strongly believed that the adult mammalian brain was excluded from the list of tissues with a regenerative capacity. The long-held dogma “no new neurons” referred to the idea that humans were born with all the neurons they would ever have, and once lost would not be replaced. However, after a series of experiments demonstrated the existence of proliferating cells within the adult rodent brain, the existence of functional neural stem cells in mammals has been found in (although not limited to) the subventricular zone (SVZ) of the lateral ventricles, and the subgranular zone (SGZ) of the dentate gyrus (DG) in the hippocampus.

In this thesis, I will explore the regulation of adult mammalian neural stem cells within the SGZ, specifically the mechanisms controlling the maintenance of and activation from quiescence. In the following chapter, I will summarise the current knowledge in the field of adult neurogenesis with a specific focus on the biology of neural stem cells and the regulation of their quiescence. I will explore the current understanding of the quiescent stem cell state, and the known signals and mechanisms regulating the activation of neural stem cells from quiescence, highlighting the importance of the neurogenic niche, as well as the methods used to study these cells. I will then introduce the Inhibitor of Differentiation (Id) family of proteins as a potential new regulator of NSC quiescence.

1.1 Adult neurogenesis

1.1.1 The history of adult neurogenesis

Adult neurogenesis is the process of generating new neurons in the adult brain. This was an unthinkable phenomenon up until the 1980's, where before the consensus amongst researchers was with the conclusions of celebrated neurobiologist Santiago Ramón y Cajal, who postulated (translated from Spanish), "In the adult centre, the nerve paths are something fixed, finished, immutable: everything may die, nothing may be regenerated." (Ramón y Cajal, 1928). Such a brutal conclusion was understandable in the light of the fact the brain is comprised primarily of post-mitotic neurons, however left small hope for therapies targeting regeneration in the brain. In the face of scepticism and criticism from his contemporaries, Joseph Altman challenged the long-held belief of "no new neurons" in 1963 with the publication of his research showing evidence of proliferating cells in the brains of adult rodents (Altman, 1963). Altman described cells labelled with a thymidine analogue [H^3]-thymidine, which gets incorporated into the DNA of dividing cells and can be detected by autoradiography, in several regions of the adult rodent brain, including a particularly proliferative zone in the dentate gyrus of the hippocampus (Altman, 1963; Altman and Das, 1965), as well as the neocortex and olfactory bulb (Altman, 1966, 1969). It wasn't until about two decades later that Altman's observations were corroborated, with the description of adult neurogenesis in canaries using the same technique (Goldman and Nottebohm, 1983). These studies in songbirds also started to provide a functional relevance of adult neurogenesis, namely in seasonal song learning, which helped to drive interest in the field. This was followed a decade later by the successful isolation of cells from the adult mouse brain (striatum and dissections including the hippocampus) which demonstrated stem cell properties *in vitro* (Reynolds and Weiss, 1992; Richards et al., 1992). Teleost fish including zebrafish were also shown to have widespread progenitor proliferation in the adult brain (Zupanc et al., 2005; Zupanc and Horschke, 1995). However, a major step forward in the field came from the introduction of a new thymidine analogue, the now widely-used bromodeoxyuridine (BrdU) (Kuhn et al., 1996) which is able to be detected by immunocytochemistry, and therefore much more practical. Gould and colleagues used BrdU to demonstrate the existence of adult neurogenesis in the neocortex of adult macaques (Gould et al., 1999), revealing adult neurogenesis was present in primates, and subsequent studies demonstrated adult neurogenesis in several other Old World and New World primates (reviewed by (Yuan

et al., 2014)). Finally, a handful of studies have found evidence for (and against) adult hippocampal neurogenesis in humans, which I will discuss in more depth in Section 1.1.3.

1.1.2 The 'what' and 'where' of adult neurogenesis

Neurogenesis is defined as the production of new functional neurons from precursor cells that are found within specialised locations in the brain, termed neurogenic niches, which provide vital physical and molecular cues to support the maintenance and activity of the stem cells. In the adult rodent brain, the areas of significant neurogenesis are the subventricular zone (SVZ) of the lateral ventricles, which generate newborn neurons that integrate into the olfactory bulb; and in the subgranular zone (SGZ) of the dentate gyrus (DG) in the hippocampus (Figure 1.1).

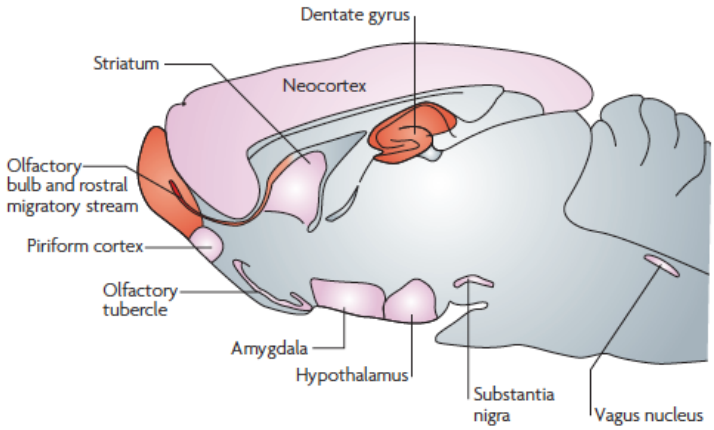

Figure 1.1. Documented regions of neurogenesis in the adult rodent brain
Shown in red are the two most well-studied neurogenic regions, the dentate gyrus in the hippocampus, and the olfactory bulb, for which new neurons arise from the subventricular zone and migrate via the rostral migratory stream. Areas of pink indicate regions for which low levels of neurogenesis have been reported, including the hypothalamus, amygdala, striatum and neocortex. Image reproduced from (Gould, 2007) with permission of the rights holder, Springer Nature.

Newborn neurons in the DG migrate very short distances to integrate into the granule cell layer. Other areas with low level neurogenesis have also been discovered, including in the amygdala, striatum and neocortex in rodents and macaques, as well as the hypothalamus in rodents (Gould, 2007) (Figure 1.1). I will describe neurogenesis in

the mouse SVZ and SGZ in more detail below in Section 1.1.5-6, as these are the neurogenic regions most relevant for the work presented in this thesis.

1.1.3 Adult neurogenesis in humans

The evidence for adult neurogenesis in humans was first shown in 1998 by Eriksson and colleagues, who controversially demonstrated the incorporation of BrdU in the hippocampus of cancer patients, whose brain tissue was analysed post-mortem (Eriksson et al., 1998). Further evidence for adult human neurogenesis *in vivo* has been more difficult to obtain for obvious reasons, however neural stem/progenitor cells have been isolated from adult human hippocampus and subventricular zone (SVZ) following surgical excision, and demonstrated to undergo *in vitro* neurogenesis (Kukekov et al., 1999; Roy et al., 2000). Post-mortem immunocytochemical staining for the neuronal precursor marker Doublecortin (Dcx) has also suggested the existence of neurogenesis in the adult human hippocampus (Knoth et al., 2010). More recently, two inspired studies measured the level of Carbon14 (^{14}C) in genomic DNA isolated from the striatum (Ernst et al., 2014) and hippocampus (Spalding et al., 2013) of human post-mortem brain tissue, from people who lived in an area that had been the site of nuclear bomb testing in 1955. By plotting the concentration of ^{14}C in neuronal cells at the time of post-mortem against the environmental ^{14}C concentration at the time of birth, the authors were able to estimate whether new carbon had been incorporated into these neuronal cells by cell division, and determined a small percentage of neuronal cells were newly generated in adulthood in the striatum (Ernst et al., 2014) whilst 700 new neurons were incorporated into the adult human hippocampus each day, with little decline into old age (Spalding et al., 2013). However, there has been debate about whether the levels of neurogenesis in humans was more than just negligible after adolescence (Kempermann, 2011b), and 2018 has seen the controversy intensify, with two of the most comprehensive analyses of adult human neurogenesis to date, presenting opposite findings. Sorrells and colleagues suggest there is no evidence for neurogenesis after childhood, based on the immunohistochemical analysis of markers of proliferating progenitors and immature neurons in 59 patient samples from foetal stage to 77 years old (Sorrells et al., 2018). In contrast, Boldrini et al., find evidence for neurogenesis in 28 men and women aged 14 to 79, with little decline over age (Boldrini et al., 2018). The authors of both studies used similar immunohistochemical analysis to determine the presence of neurogenesis, although the estimates of new neuronal production presented by

Boldrini et al., were from stereological analysis which may give an over-estimation. Clearly the presence of active and functional adult neurogenesis in humans is still yet to be fully clarified, which will require many more studies and new techniques before a consensus is reached (recently reviewed by (Kempermann et al., 2018)). In contrast to hippocampal neurogenesis, olfactory bulb neurogenesis is reportedly very low or absent in humans (Bergmann et al., 2012; Sanai et al., 2004; Wang et al., 2011).

1.1.4 Function of adult neurogenesis

In lieu of strong and conclusive direct evidence for neurogenesis in adult humans, understanding its function can help to inform whether it may exist and be relevant for human health. The dentate gyrus directly inputs into the hippocampus, the function of which is reported to include spatial navigation, learning and memory, and pattern separation, including integrating new information into a previously learned environment (Goncalves et al., 2016; Kempermann, 2012). Neurogenesis in the SGZ may actively contribute to the function of hippocampus, as retrovirally labelled newborn neurons have been observed to integrate into the hippocampal circuitry in mice and show electrophysiological properties of mature GC neurons after a period of 4-8 weeks (Gu et al., 2012; van Praag et al., 2002). Specifically reducing the number of newborn neurons in mice affects spatial memory, including the long-term memory required to tackle the Morris water maze, as well as context-dependent memory in fear conditioning tasks (Goncalves et al., 2016). These two memory functions are also thought to function in cognitive flexibility, or the ability to discern change in a previously learned environment, including pattern separation (Kempermann, 2012). An age-related decline in pattern separation performance has been reported for humans (Stark et al., 2010), which could imply a similar function of the hippocampus between rodents and humans.

Neurogenesis in the SVZ generates new neurons for the olfactory bulb, a structure in the forebrain that processes sensory inputs from olfactory neurons in the nasal cavity. A direct role for adult SVZ neurogenesis in odour discrimination has not been fully demonstrated, although levels of neurogenesis and olfactory reaction time have been shown to be positively correlated (Lazarini and Lledo, 2011). It is interesting that SVZ neurogenesis is active in mammals such as rodents and canines, but reportedly low in humans, which could be reflect our comparatively poor olfaction abilities, at least in

comparison with canines and rodents. Despite this, there is evidence to suggest impaired olfaction is a symptom of neurodegenerative and neurologic diseases (Godoy et al., 2015), which as I will discuss shortly, may result in some cases from impaired neurogenesis. This observation could suggest adult SVZ neurogenesis may be present and functional in humans, however it could also reflect a direct loss of the olfactory neurons, rather than impaired neurogenesis.

There are now many studies describing adult hippocampal neurogenesis in many different species, and by observing the phylogenetic map of adult neurogenesis we can make assumptions about the evolution and therefore potential function of adult neurogenesis (Kempermann, 2012). In his review, Kempermann suggests that hippocampal neurogenesis would provide an increased level of flexibility within the adult brain. Whilst a certain level of neuronal rigidity is required to remember important learned behaviours, a level of cognitive flexibility would allow for adaptation in changeable environments Therefore, one could imagine that neurogenesis in the hippocampus would facilitate adaptation to humans who were very mobile, both in terms of hunting, and also moving to new home environments.

An evolutionary perspective of adult neurogenesis can inform us to a point, but a more acute measure of the function of adult neurogenesis can be obtained from symptoms of disorders that reportedly show impaired neurogenesis in the DG. Humans frequently display an age-related cognitive decline (Lazarov and Marr, 2013), and there is evidence for decreased DG volume with age (O'Shea et al., 2016) and a modest age-related decline in hippocampal neurogenesis (Spalding et al., 2013), however it is not clear whether there is a direct link between decreased neurogenesis and cognitive performance in aged humans. Psychiatric disorders such as anxiety, depression and schizophrenia have been associated with altered neurogenesis and reduced hippocampal volume (Goncalves et al., 2016). Impaired neurogenesis is particularly implicated in depression, due to the observation that ablating neurogenesis in adult rodents leads to an increase in depression- and anxiety-like behaviours (Revest et al., 2009). Antidepressant drugs can also directly increase levels of neurogenesis in the SGZ (e.g. (Huang and Herbert, 2006); reviewed by (Miller and Hen, 2015)), and neurogenesis has been shown to be required for the behavioural effects of antidepressant treatment in mice (Miller and Hen, 2015; Santarelli et al., 2003). Impaired adult hippocampal neurogenesis has also been associated with

schizophrenia, particularly as mutations in DISC1, a well characterised susceptibility gene for schizophrenia, has been shown to play important roles in newborn GC neuron survival and maturation (Duan et al., 2007; Kvajo et al., 2008). Epilepsy is another human disorder associated with increased excitability in the DG, and seizures are able to activate neural stem cells, potentially leading to further aberrant neurogenesis and increased over-excitability (Jessberger and Parent, 2015). Neurodegenerative diseases in adult humans, such as Alzheimer's Disease (AD), Parkinson's Disease (PD) and Huntington's Disease (HD), also commonly display impaired neurogenesis as part of their pathology (reviewed by (Winner and Winkler, 2015)). Neurodegenerative disorders appear to combine the gradual loss of mature neurons through dysfunction and death, in combination with a reduction in neurogenesis. Moreover, many of the symptoms that appear years before a diagnosis of AD, PD or HD include those described as diseases of impaired hippocampal neurogenesis such as depression, anxiety, and learning and memory problems (Winner and Winkler, 2015). Therefore, gaining a thorough understanding of the factors that regulate adult neurogenesis, that are observed to be changed in early neurodegenerative conditions, may lead to improved early diagnosis and therapeutic interventions targeting neurogenesis in these patients.

1.2 The stem cell niche

1.2.1 Common features of adult stem cell niches

The concept of a stem cell "niche" was first put forward by R. Schofield in his study of haematopoietic stem cells, where he suggests that the behaviour or fate of the stem cell depends upon the surrounding cells it is associated with (Schofield, 1978). The "niche" concept was further brought into the spotlight by studies of the stem cell microenvironment in the Drosophila gonad (Lin, 2002). Niches have since been described for several adult mammalian stem cell populations, including the bone marrow haematopoietic stem cell niche (reviewed by (Boulais and Frenette, 2015)), the hair follicle for follicular bulge stem cells and the intestinal crypts for crypt base columnar stem cells (reviewed by (Moore and Lemischka, 2006)), and the muscle for satellite cells (reviewed by (Yin et al., 2013)). The definition of the niche has evolved to describe a microenvironment of cells organised in a specialised 3-dimensional architecture, such that it can provide the maintenance and survival of undifferentiated

stem cells, as well as acting as a hub of signalling such that it can exert spatiotemporal control of stem cell activity. These features are common amongst all the stem cell niches, and the importance of the niche in providing a protective environment promoting stemness is highlighted by the challenges faced attempting to culture various adult stem cells *in vitro* (McKee and Chaudhry, 2017). The challenge to recapitulate the *in vivo* niche has led to some ingenious developments, including micro-patterned culture substrates, 3-D culture protocols, and the use of various biomaterials to mimic the stiffness and 3D architecture of the niche (Griessinger et al., 2014; Joo et al., 2015; McKee and Chaudhry, 2017).

The important regulatory function of the hippocampal stem cell niche was demonstrated by early heterotopic transplantation experiments, in which cultured adult hippocampal progenitor cells were grafted into other neurogenic regions (the rostral migratory stream, containing neuroblasts generated from SVZ NSCs) or the non-neurogenic cerebellum (Suhonen et al., 1996). The engraftments of the progenitor cells into the RMS resulted in migration and differentiation into olfactory bulb neurons, whereas those in the cerebellum failed to differentiate, suggesting the neurogenic niche provides specific signalling cues to drive proper differentiation. I will next describe the architecture of the neurogenic niches in the SVZ and SGZ.

1.2.2 The adult subventricular zone as a neurogenic niche

The neurogenic niche in the subventricular zone (SVZ) of the lateral ventricles is located adjacent to an ependymal cell layer separating the ventricular space from the SVZ (Figure 1.2). The stem cells of the SVZ are astrocytic-like cells expressing GFAP, and were described to have stem cell properties and generate neurons by retroviral lineage tracing (Doetsch et al., 1999b). The SVZ neural stem cells, known as type B1 cells, extend an apical process with a primary cilium through the ependymal cell layer to contact the cerebrospinal fluid inside the lateral ventricle. The B1 cells are in very close association with the other niche cells, and are found surrounded by ciliated ependymal cells forming a stereotyped pinwheel structure with a single B1 cell in the centre (Bond et al., 2015; Fuentealba et al., 2012) (Figure 1.2). A dividing B1 cell will generate a proliferating intermediate progenitor cell (IPC or C cell) which will divide a number of times before becoming a neuroblast (A cell).

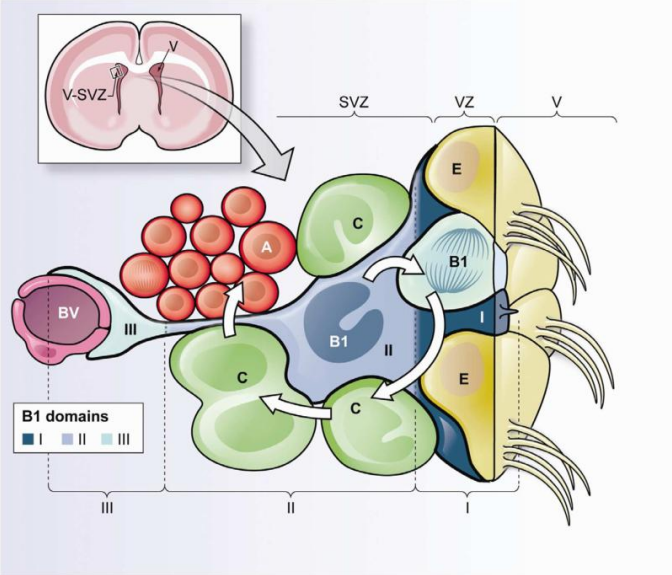

Figure 1.2. Scheme of the neurogenic niche in the adult mouse subventricular zone

The subventricular zone (SVZ) is located along the walls of the lateral ventricles (V), shown in the schematic coronal cross-section of an adult mouse brain (top left panel). The stem cells of the SVZ (light blue; type B1 cells) extend an apical process with primary cilium to contact the lateral ventricle, as well as a basal process which contacts the blood vessels (BV) of the vasculature. The NSCs are surrounded by their niche cells, including the ciliated ependymal cells (yellow; E cells) forming the characteristic pinwheel structure, as well as their intermediate progenitor cells (green; type C cells), which generate neuroblasts (red; type A cells) destined to migrate via the rostral-migratory stream to the olfactory bulb, where they integrate as mature olfactory neurons. Image reproduced from (Fuentealba et al., 2012) with permission of the rights holder, Elsevier.

The neuroblasts migrate away from the SVZ to join the rostral migratory stream (RMS), a chain of maturing neuroblasts that use one another as a migratory substrate, within a glial sheath (Bronner, 2014). During this migration, the neuroblasts will differentiate into different subtypes of interneuron, and eventually integrate into the olfactory bulb (Bond et al., 2015; Fuentealba et al., 2012). SVZ type B1 cells receive signals from the different components of the niche, including from the cell-cell contacts of ependymal cells, diffusible signals within the CSF via the primary cilium, as well as signalling from the IPCs, neuroblasts and innervation from surrounding neuronal cells. B1 cells also have a basal process that ends in a specialised end-foot that contacts blood vessels, providing yet another source of niche signalling (Fuentealba et al., 2012) (Figure 1.2).

1.2.3 The neurogenic niche in the adult mouse hippocampus

The hippocampal neurogenic niche is located in the subgranular zone (SGZ) of the dentate gyrus (DG) (Figure 1.3). The stem cells of the SGZ are radial astrocytic- or glial-like cells (RGLs). RGLs are identified by their characteristic morphology, with the nucleus in the SGZ (a thin layer of nuclei sandwiched between the granule cell layer and hilus), radial process extending through granule cell layer beyond which it branches into the molecular layer (Figure 1.3). Like SVZ type B1 cells, RGLs have primary cilium located at the base of the radial process (Breunig et al., 2008), enabling cilium-mediated signalling. RGLs generate granule neurons via a well characterised neurogenic lineage. RGLs in the adult mouse exist in a mostly quiescent state, with a small percentage that activate at any given time, to divide asymmetrically to generate another RGL and a daughter cell bearing only a short, thin process, which is a proliferating intermediate progenitor cell (IPC; type II a, and type II b cells). IPCs divide around 3 times, before maturing into neuroblasts or type III cells. These cells can then mature into granule cells (Figure 1.3), and if the right survival signals are received, will mature and integrate into the hippocampal circuitry (Gu et al., 2012; van Praag et al., 2002).

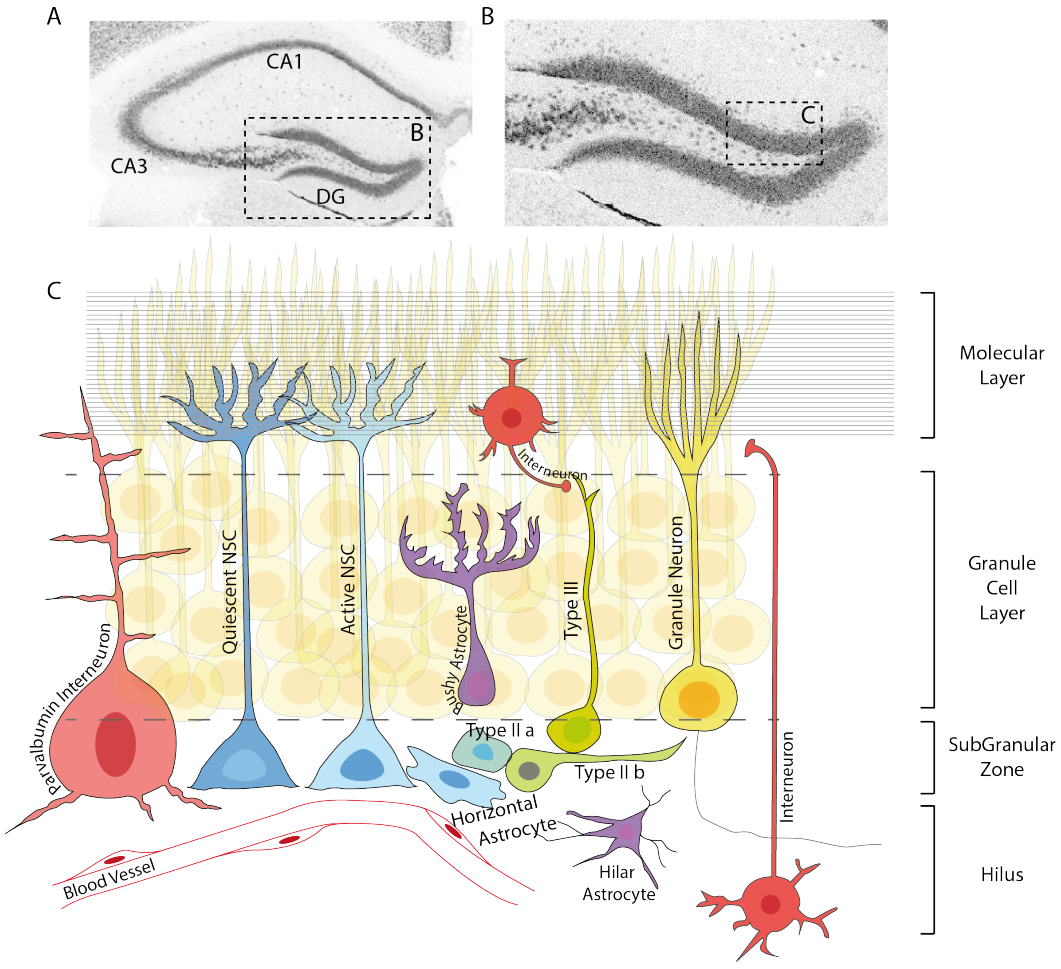

Figure 1.3. The neurogenic niche of the adult mouse hippocampus

A) The organisation of the mouse hippocampus, shown by immunohistochemistry for the neuronal maker NeuN. The CA1 and CA3 subfields of the hippocampus can be seen converging between the characteristic blades of the dentate gyrus (DG), highlighted within the dashed box. **B)** Close up of the dentate gyrus. The neurogenic niche is located in the subgranular zone of the inner blades of the DG. **C)** Schematic of the hippocampal neurogenic niche in the dentate gyrus. Radial glial-like stem cells (RGLs/NSCs) are seen with their nucleus in the subgranular zone (SGZ) with radial process extending through the granule cell layer, and processes branching into the molecular layer. Active RGLs or horizontal astrocytes will divide to produce intermediate progenitors (type II a and type II b cells), which will proliferate before differentiating over several days into neuroblasts (type III cells) and eventually fully differentiating into granule neurons, which migrate a short distance into the granule cell layer. The neurogenic lineage exists in close associated with other niche cells, including astrocytes (purple), interneurons (red) and blood vessels of the vasculature. Reproduced from (Urban and Guillemot, 2014) with permission of the rights holder, Frontiers.

The DG neurogenic lineage can also be characterised by the expression of particular neurogenic transcription factors and cellular markers, such as Tbr2 (IPCs), Dcx (neuroblasts) and NeuN (neurons) (Figure 1.4; (Hsieh, 2012; Urban and Guillemot, 2014)). RGLs are characterised by the expression of GFAP, GLAST, Nestin and Hes5 mRNA (Figure 1.4), which I will discuss in more detail in the next section.

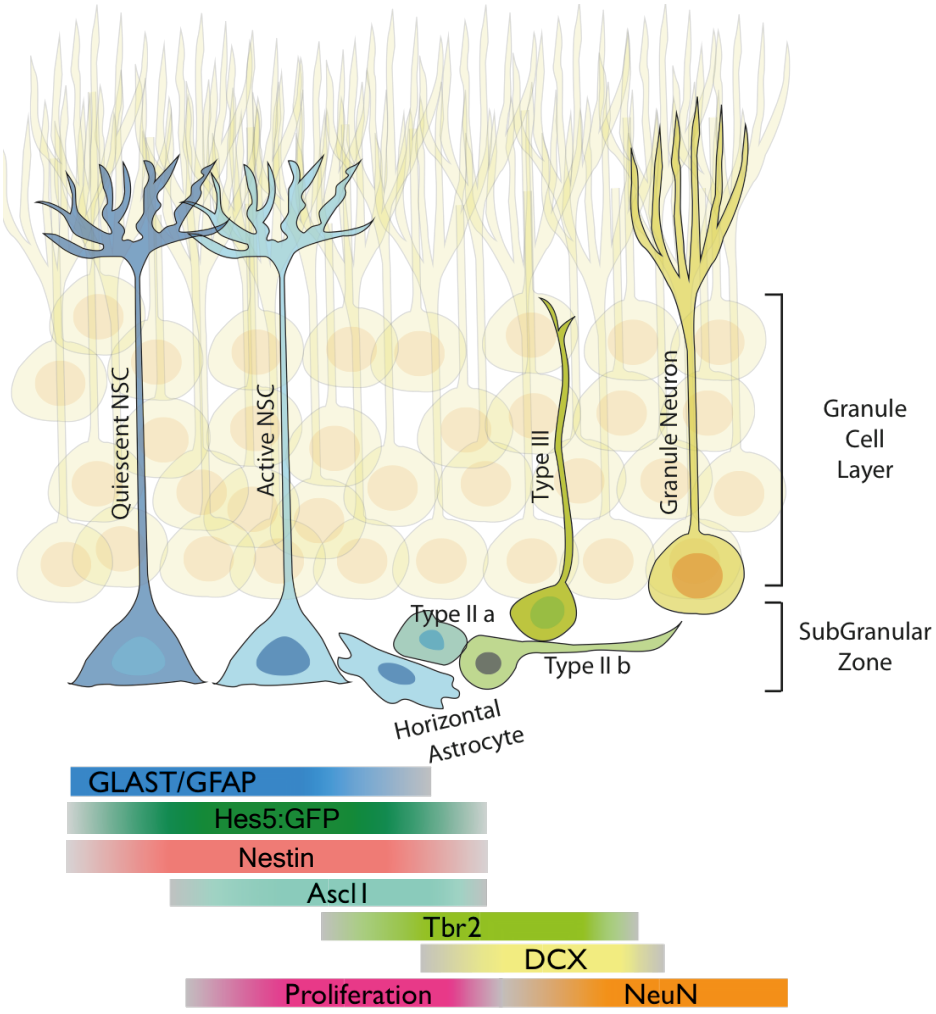

Figure 1.4. Expression of genes defining the neurogenic lineage in the dentate gyrus.

The neurogenic lineage in the subgranular zone of the dentate gyrus can be identified by stage-specific markers. Quiescent RGLs (NSCs) are identified by their expression of GLAST, GFAP, Nestin, a GFP-reporter of Hes5 transcription (Lugert et al., 2010), as well as the lack of expression of Ascl1 and proliferation markers. Ascl1 expression is found in active RGLs and intermediate progenitor cells (IPCs; type II a). IPCs also express the

transcription factor Tbr2, while Doublecortin (DCX) is switched on in neuroblasts (type II b), followed by NeuN, which labels more mature neuroblasts and newborn neurons. Modified from (Urban and Guillemot, 2014) with permission of the rights holder, Frontiers.

1.2.4 RGLs: from astrocytes to neural stem cells

RGLs share many properties with the other glial cells of the adult brain, as well as the radial glia of the developing CNS (Kriegstein and Alvarez-Buylla, 2009), and indeed they were first thought to be DG astrocytes. The characterisation of RGLs as bona fide SGZ NSCs began with utilising one of their defining markers, glial fibrillary acidic protein (GFAP), a marker of astrocytes but also identified as a marker of SVZ NSCs (Doetsch et al., 1999a; Laywell et al., 2000). Seri and colleagues demonstrated that retrovirally labelled GFAP+ radial cells, following ablation of dividing cells in the SGZ, divide and give rise to progeny that differentiate into granule neurons (Seri et al., 2001). These results were corroborated by genetic ablation of GFAP-expressing cells in the SGZ, which resulted in a loss of neurogenesis (Garcia et al., 2004). Since then, more markers of RGLs have been identified including glutamate aspartate transporter (GLAST; SLC1A3) (Namba et al., 2005), although GLAST and GFAP are also both expressed by astrocytes in the DG and hilus. RGLs also express Nestin (Fukuda et al., 2003; Seri et al., 2004), Sox2 (Episkopou, 2005; Pevny and Nicolis, 2010; Suh et al., 2007) and Hes5 (Lugert et al., 2010), however these markers are also expressed by IPCs (Figure 1.4). So far, no specific marker for RGLs has been identified, however the current markers have enabled a strong progression in the field, with the development of transgenic reporters for fate-mapping as well as transgenic manipulations to elucidate the behaviour and regulation of the stem cells (Bonaguidi et al., 2012). For example, clonal analysis of cells labelled in the tamoxifen inducible NestinCre^{ERT2};RosaYFP mouse line revealed that RGLs undergo different modes of division, including self-renewing symmetric divisions and asymmetric divisions generating neuronal progenitors or astroglia, as well as a few cases of direct differentiation without a self-renewing division (Bonaguidi et al., 2011). Interestingly, a study published at the same time using Nestin-GFP reporter mice reports that RGLs do not undergo expansive symmetric division, instead rapidly divide asymmetrically to generate IPCs, with the mother RGLs subsequently differentiating into astrocytes (Encinas et al., 2011). In this model, RGLs are lost at the population level, being consumed with increasing age (Encinas et al., 2011). The opposing conclusions from

Bonaguidi et al., and Encinas et al., reflects the important differences when analysing as a clonal versus population level. It also may highlight heterogeneity of the RGL pool, a concept which is gaining increased attention, due to the implications for studies of the regulation and long-term fate of the RGLs. More recently, an incredible feat was achieved to live-image RGLs in the adult dentate gyrus over several weeks, in order to closely record the self-renewal capacity and lineage relationships of RGLs and their progeny, in a longitudinal way (Pilz et al., 2018). RGLs were labelled with tdTomato in Ascl1 expressing neural stem and progenitor cells (Ascl1CreERT2 mice), and imaged via a cortical window, which revealed most RGLs divide asymmetrically, with a smaller proportion of symmetric divisions, as was found by clonal lineage tracing (Bonaguidi et al., 2011), and direct neurogenic divisions were also observed (Pilz et al., 2018). Interestingly, the authors did not observe any Ascl1-tdtomato RGL returning to quiescence for a substantial amount of time, which conversely had been observed by other groups (Bonaguidi et al., 2011; Urban et al., 2016), and could identify Ascl1-expressing RGLs as a more proliferative, dispensable population. This again suggests there may be subgroups of RGLs with different contributions to neurogenesis and distinct responses to regulating stimuli.

1.2.5 RGL heterogeneity

Heterogeneity among adult NSCs has been described in the SVZ, where different subsets of NSCs along the rostro-caudal axis of the SVZ generate distinct subtypes of interneuron (Merkle et al., 2007) (Merkle et al., 2014). A similar regionalisation of RGL identify in the DG has not yet been observed. However, RGL heterogeneity is highlighted by DeCarolis and colleagues who compared the dynamics and neurogenic contribution of RGLs labelled by either the transgenic reporter NestinCreERT2;Rosa26YFP or GLASTCreERT2;Rosa26-YFP (DeCarolis et al., 2013). The authors demonstrate that the differentially labelled RGLs contribute differently to the stem cell pool, with GLAST-expressing RGLs showing higher levels of proliferation and neurogenic contribution than Nestin-expressing RGLs, even after ablation of proliferating progenitors and activating the stem cells by exercise (mouse wheel running) (DeCarolis et al., 2013). Two morphologically distinct subtypes of RGL have also been proposed to exist, the classical radial glial-like stem cell and a non-dividing astrocytic-like cell lacking a radial process but co-expressing RGL markers (Steiner et al., 2006). These astrocytic-like RGLs could represent an early stage of astrocytic

differentiation of an RGL, however later studies using Sox2-GFP and Hes5-GFP fate mapping (Lugert et al., 2010; Suh et al., 2007) similarly observed two morphologically distinct populations of RGLs, the radial and non-radial or “horizontal” astrocyte. Interestingly, Suh et al., observed that non-radial Sox2+ cells are the major proliferating population in the SGZ, whilst the Sox2+ radial NSCs were rarely dividing (Suh et al., 2007). Similarly, Hes5:GFP labelled radial and non-radial/horizontal NSCs respond differently to neurogenic stimuli, with the non-radial portion proliferating more in response to stimulation but are lost with increasing age, whilst the radial NSCs proliferate less and persist with age (Lugert et al., 2010). More recently, single-cell transcriptomes have been generated from FAC sorted cells dissociated from the adult mouse dentate gyrus. This will be discussed in more detail below in Section 1.3.2. Single cell transcriptomic data could shed light on transcriptional heterogeneity of adult NSCs, however there are limitations. Firstly, such data only provides a single snapshot in time, therefore if subtypes of stem cell were identified, it would not be possible to follow the behaviour or fate of the cell, so the functional implication of the subtype would be difficult to infer. Secondly, single cell transcriptomes can suffer from low sequencing depth due to small amounts of mRNA, which creates difficulty distinguishing heterogeneity from noise, or distinguishing stable expression of a gene from an oscillating expression (although the oscillation of a gene may itself confer heterogeneity to a population of stem cells). Finally, this kind of analysis still relies on isolating NSCs based on the expression of known markers such as GLAST or Nestin, introducing bias which may result in unknown subtypes of NSC being excluded. On the other hand, a major benefit of single cell transcriptomic analysis of NSCs has been to shed light on the transcriptional signature of quiescent RGLs; their quiescent state can be inferred from the low or absent expression of cell cycle and activation genes, therefore associated transcriptional features can be observed (discussed in Section 1.3.2).

RGLs may also be heterogeneous with regards to their likelihood to activate or return to quiescence. Urbán and colleagues have identified two subtypes of quiescent RGL; the resting population, representing a small number RGLs that have activated and divided, and temporarily returned to quiescence; and the dormant population, representing the majority of stem cells, that have (very likely) never divided (Urban et al., 2016). Regulation of the resting pool is crucial for maintaining neurogenesis in the adult DG (Urban et al., 2016).

Overall, these studies highlight the possibility that all RGLs are not equal, and may be differentially regulated and contribute to neurogenesis in different ways. It is also not clear whether the current known markers of RGLs are able to label the entire population, or if in fact more subpopulations of RGLs exist. Considering the implications of a heterogeneous pool of RGLs for understanding the regulation of neurogenesis in homeostasis and disease, it will be highly important to elucidate the identity of all adult RGLs in the SGZ.

1.2.6 Embryonic origin of RGLs

One potential source of RGL heterogeneity could be differential origins of adult RGLs. The embryonic origin of adult DG NSCs is not fully known (Berg et al., 2018; Urban and Guillemot, 2014). Historically the assumption for the origin of adult DG NSCs has been that they originate from the whole length of the embryonic dentate neuroepithelium (DNE), from where GFAP-expressing cells migrate towards the SGZ, and give rise to granule neurons from early stages of DG development and continuing throughout adulthood (Seri et al., 2004). However, recent lineage tracing experiments of sonic hedgehog (SHH)-responsive cells suggests that a subset of adult neural stem cells are induced at peri-natal stages in the most ventral portion of the hippocampus, from where they are induced by SHH, and migrate dorsally to populate the whole length of the adult DG, where they contribute to adult DG neurogenesis (Li et al., 2013). This has opened up the possibility of separate populations of adult NSCs, originating from different embryonic or peri-natal stages of development. RGLs in the adult DG could potentially be either a continuation of RGLs from development, or a separate population of NSCs set-aside in development, becoming activated in adulthood (Berg et al., 2018; Encinas et al., 2013). Further lineage tracing experiments would help to fully elucidate the origins of adult SGZ NSCs, such as has been done for the embryonic origin of SVZ NSCs (Fuentealba et al., 2015). However, the recent explosion of single-cell RNA-sequencing has enabled a far deeper exploration into the transcriptional of identity of NSCs from development to adulthood. The Linnarsson lab has produced a database of single cell RNAseq data for all cells in the DG across postnatal development, an extraordinary feat that provides an unprecedented insight into the gene expression of RGLs throughout development and adulthood (Hochgerner et al., 2018). The authors show a shift in RGL identity from embryonic to adult during

the second postnatal week, and further critical examination of gene expression changes will surely reveal insights into the embryonic origin of adult DG RGLs, and potential novel mechanisms of their regulation.

1.3 Stem cell quiescence

Before I describe the known extrinsic and intrinsic mechanisms regulating neurogenesis, and specifically their effects on RGL activation, I will explore the concept of stem cell quiescence, discussing how it is defined and what is known of quiescence in RGLs. In this way, I will focus my discussion of the signals and molecules regulating RGLs on their influence on quiescence and activation, a central concept to my thesis.

1.3.1 What is quiescence?

Quiescence is defined as a reversible state of cell cycle exit, or when cells reside in the 'G0' cell cycle state often for prolonged periods of time, but with the ability to re-enter the cell cycle. It is distinct from terminal differentiation or senescence due to its reversibility under normal conditions (post-mitotic cells are in some cases able to re-enter the cycle e.g. reactive astrocytosis, however this is usually as a result of injury or other extreme stimulus). The G0 cell cycle state is not fully understood, currently defined by a 2n DNA content and the absence of cell cycle gene expression (Cheung and Rando, 2013). Historically, quiescence was thought to perhaps represent a very long or paused G1 phase, and particularly thought to be a state of inactivity with low levels of cellular activity. Early studies of cellular quiescence supported this view, such as the observation that serum deprivation results in inhibition of protein synthesis and induces quiescence of 3T3 cells (Larsson et al., 1985; Zetterberg and Larsson, 1985). Interestingly, these cells would only enter quiescence if they were in early G1 at the time of serum deprivation, indicating the quiescent state exists in close relationship with the cell cycle, and that it may be an actively regulated state, rather than a result of loss of cellular function. Techniques to evaluate the transcriptional and biological characteristics of quiescent cells have improved vastly over the past few years, resulting in a much more finessed understanding of quiescence as a distinct and complex cellular state. RNA sequencing, for example, has enabled the generation of a 'transcriptional signature' of quiescence.

1.3.2 Transcriptional signature of quiescence

Quiescence is akin to an actively maintained state of dormancy. Despite the observation that quiescent stem cells have a low RNA content (Fukada et al., 2007; Huttmann et al., 2001), recent transcriptomic studies on prospectively isolated quiescent stem cells has demonstrated quiescence to involve the active transcription of hundreds of genes (reviewed by (Cheung and Rando, 2013)), and has been performed for hair follicle stem cells (Blanpain et al., 2004), satellite cells (Fukada et al., 2007) haematopoietic stem cells (Forsberg et al., 2010), and adult neural stem cells. Common groups of genes were found to be regulated in all populations of quiescent stem cell, such as a downregulation of genes involved in cell cycle progression, DNA replication and RNA processing, and upregulation of genes involved in transcriptional regulation and stem cell maintenance (Cheung and Rando, 2013). Several studies have performed bulk or single-cell RNA sequencing on prospectively isolated quiescent NSCs from the adult SVZ, a feat made possible by the identification of a handful of markers specifically distinguishing quiescent from active NSCs, such as EGF receptor, and more recently LeX (Beckervordersandforth et al., 2010; Codega et al., 2014; Morizur et al., 2018). This is in contrast to the DG, where there are no good markers to distinguish quiescent and active NSCs by FACS. Nevertheless, single cell RNAseq analysis of quiescent DG RGLs was achieved by FAC sorting all RGLs from the adult dentate gyrus, followed by retrospective bioinformatic grouping of cells along a ‘pseudotime’ axis based on a continuum of transcriptional changes from most quiescent to most active (Shin et al., 2015). In this way, the genes most enriched in quiescent RGLs were identified. Much like for quiescent stem cells in other adult niches, quiescent SVZ and SGZ NSCs downregulate genes involved in cell cycle and RNA processing, but interestingly display a signature of upregulated genes involved in cell adhesion, cell-cell signalling, mitochondrial function and metabolic changes (Beckervordersandforth et al., 2010; Codega et al., 2014; Morizur et al., 2018; Shin et al., 2015) (Figure 1.5). Lipid metabolism is particular enriched in quiescent NSCs, and had been previously shown to be enriched in FAC sorted Sox2:GFP+ NSCs from the DG, highlighting metabolism as an important process in NSCs (Bracko et al., 2012). The metabolic state of quiescent radial glial-like cells is predominantly glycolytic with low levels of oxidative phosphorylation (OxPhos) and likely with de novo lipogenesis (Knobloch et al., 2013), but upon activation switches towards the mitochondrial

electron transport chain (ETC) and OxPhos for energy (Beckervordersandforth, 2017) (Figure 1.5). Moreover, the mitochondria themselves are shown to be distributed differently in quiescent vs active hippocampal NSCs *in vivo*, with a higher mitochondrial volume in the primary process of NSCs than of active NSCs/progenitor cells (Beckervordersandforth, 2017). Strikingly, NSC metabolism can directly regulate quiescence/activation, as shown by direct manipulation of NSC fatty acid metabolism, either via deletion of carnitine palmitoyltransferase 1a, or the metabolite malonyl-CoA, induced NSC exit from quiescence and increased proliferation (Knobloch et al., 2017).

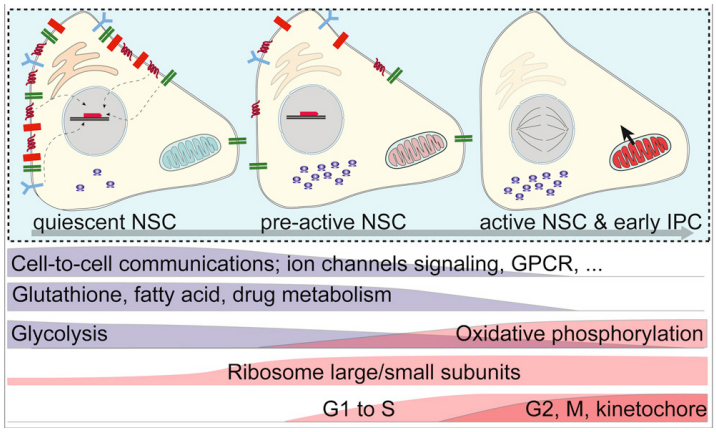

Figure 1.5. Molecular and metabolic features of hippocampal NSCs from quiescence to activation.

Single cell RNA sequencing of adult hippocampal NSCs identifies cellular features of NSC quiescence, including high expression of cell-cell signalling components such as receptors, a predominantly glycolytic metabolism with some fatty acid metabolism, low levels of ribogenesis which correlates with lower levels of transcription compared with active NSCs, and a G0 cell cycle state. Modified from (Shin et al., 2015) with permission of the rights holder, Elsevier.

1.3.3 Function of quiescence

Quiescence is a functionally important cell state for any long-lived organism, enabling preservation of self-renewing stem cells over many years. Quiescence allows stem cells to be maintained in a dormant state until required to generate a progenitor cell for tissue homeostasis. The benefit of this form of reversible dormancy, over having a continually proliferating pool for example, is likely to be the prevention of accumulation of DNA and cellular damage; if a stem cell only needs to divide once to generate a progenitor which itself can divide several more times, it will enable functional levels of

regeneration with a reduced number of proliferative stem cell divisions, reducing the risk of introducing deleterious DNA mutations, and preventing a stem cell from becoming senescent (irreversibly exited from the cell cycle). Nevertheless, any cell that persists in an organism for many years will eventually accumulate DNA damage, as well as be exposed to environmental stress, and risk accumulating damage such as from oxidative stress and hypoxia. The transcriptional and metabolic profile of quiescent stem cells suggests this cellular state actively protects the stem cell from these stresses (Cheung and Rando, 2013; Tsai, 2016). For example, the FOXO transcription factors are often highly expressed in quiescent stem cells, including FoxO3 in adult NSCs (Renault et al., 2009), and these TFs protect cells from oxidative stress and hypoxia by inducing the expression of protective genes (Yeo et al., 2013). Quiescence may also encourage genomic integrity by non-random segregation of sister chromosomes during mitosis, known as the 'immortal strand hypothesis', specifically segregating the newly synthesised strands of DNA to the new-born daughter cell, whilst sequestering the old template DNA in the self-renewing stem cell (Charville and Rando, 2011). Although not universally evident, some evidence for this hypothesis has been observed in satellite cells and intestinal stem cells (reviewed by (Cheung and Rando, 2013)) as well as adult neural stem cell cultures (Karpowicz et al., 2005). Ultimately, quiescence can function to prevent stem cell damage and depletion (from apoptosis or senescence), enabling proper tissue regeneration during age and injury.

Quiescence may also enable stem cells to be more permissive to many different regulating signals, and respond quickly. Quiescence is associated with low levels of mRNA, but is has been suggested that quiescent stem cells are poised to respond, quickly expressing mRNA in response to the dominating signal (Cheung and Rando, 2013). If too many genes were actively transcribed in quiescence, the response to a particular signal may be slowed down by cross-talk or interference. Therefore, the transcriptional activity of quiescence may enable rapid response of a stem cell to a changing environment.

Quiescence has also been observed in tumour stem-like cells, such as in glioblastoma (Lathia et al., 2015). Glioblastoma (GBM) is a highly aggressive brain tumour, with a high mortality rate due to its wide invasion of the surrounding brain. Isolation of primary brain tumours has led to the identification of self-renewing cancer stem cells contained

within the tumours, including those with quiescent-like properties (Chen et al., 2012). Glioma stem-like cells (GSCs) present a significant problem for treatment, as the quiescent state enables evasion from the classic anti-proliferative chemotherapies. The surviving quiescent cells are able to reinvade and generate new malignancies. GSCs are thought to bear similarities to NSCs, therefore gaining a thorough understanding of the molecular regulation of quiescence in adult NSCs should generate potential new strategies for targeting quiescent brain tumour cells, either by targeting them for destruction, or by preventing their eventual activation from quiescence, such as via manipulation of their interaction with their niche (Brooks and Parrinello, 2017; Chen et al., 2016).

1.3.4 Identifying quiescent stem cells

In the absence of a distinctive marker of quiescence (the lack of cell proliferation markers has generally been used to identify quiescent stem cells), S-phase label retention paradigms have been used to mark very slowly or infrequently dividing stem cells (Sottocornola and Lo Celso, 2012; Urban et al., 2016). In essence, mice are infused with a thymidine nucleotide analogue (BrdU, EdU, IdU or CldU) over a period of time, which will be taken up by all dividing cells, including any stem cell that happens to activate and divide in that period. A chase period follows, in which the nucleotide analogue is withdrawn, and enough time allowed for actively proliferating cells to dilute out the analogue and/or differentiate. Any cell retaining the analogue label at the end of the chase period is considered to be slowly dividing stem cell, or a stem cell having returned to quiescence, hence the term ‘label retaining cell’. However, this technique cannot identify stem cells that have not exited quiescence in the first place. This is important for analysis of stem cell activity in the adult neurogenic niches, considering the hypothesis that a distinct proportion of RGLs are dormant, having never activated and divided (Urban et al., 2016). The hypothesis suggests these cells have functional differences to the resting stem cells (Urban et al., 2016), so being able to differentiate a dormant RGL from a resting RGL that has temporarily returned to quiescence is important for delineating their differential responses to manipulation. It is not clear why the majority of RGLs are dormant, but they present an exciting prospect for potential therapeutic activation in the aged mouse, harnessing a dormant endogenous regenerative capacity within the hippocampus.

1.4 Regulation of adult neural stem cells and neurogenesis

Neurogenesis can be regulated at several stages of the neurogenic lineage. Global levels of neurogenesis can be determined by the proliferation rates of IPCs, or the survival of newborn neurons (Baptista and Andrade, 2018; Rolando and Taylor, 2014). Moreover, the selective elimination of IPCs by microglia is a major regulatory mechanism controlling levels of neurogenesis (Sierra et al., 2014; Sierra et al., 2010). Historically, most studies have reported regulation of neurogenesis at the population level, for example by quantifying total proliferating cells in the DG, or total number of NeuN+ newborn neurons. However, these studies often fail to interrogate the cell-specific effects of manipulations, particularly the effect on RGL activity and fate. Control of RGL activation and self-renewal is vital for ensuring a source of new progenitors, and maintenance of neurogenesis with age.

RGLs are in close proximity to many different sources of regulatory signals. Regulation can come from direct contact with IPCs; diffusible signals from granule neurons, interneurons and bushy astrocytes; innervation in molecular layer; and from blood vessels. Here I will describe the extrinsic systemic and niche signals that influence neurogenesis, specifically focussing on those signals that regulate RGL quiescence and activation.

1.4.1 Systemic regulation

Adult neurogenesis is highly sensitive to and dynamically regulated by physiological stimuli, which could reflect the possible function of adult hippocampal neurogenesis for adapting to a changing physical and social environment (Goncalves et al., 2016; Kempermann, 2012). Physical exercise has been well documented to increase levels of neurogenesis in rodents (Kronenberg et al., 2003; Lugert et al., 2010; Steiner et al., 2008; Suh et al., 2007; van Praag et al., 1999). Exercise specifically increases the number of GLAST-expressing RGLs in the DG (DeCarolis et al., 2013), potentially via increasing the vascular niche; exercise is thought to promote angiogenesis in the niche, which provides a rich source of regulatory signals, which I will describe in more detail in Section 1.5.2. Learning and environmental enrichment (EE) both promote neurogenesis (Gould et al., 1999; Rolando and Taylor, 2014), suggesting neuronal stimulation can affect hippocampal neurogenesis. The social environment also has

strong regulatory effects on neurogenesis, both positive and negative depending on the form of interaction. For example, social isolation and psychosocial stress, such as interaction with an aggressive individual, reduces neurogenesis (Czeh et al., 2007; Gould et al., 1997; Lieberwirth et al., 2012). Non-social chronic stress also reduces neurogenesis (Mirescu and Gould, 2006). Sex hormones and adrenal hormones modulate neurogenesis (Galea et al., 2013; Gould et al., 1992), and mating and maternal social interaction increases neurogenesis (Furuta and Bridges, 2005; Mak et al., 2007). Many of these reports measure global levels of neurogenesis, or regulate neurogenesis downstream of NSCs. Environmental enrichment for example was reporter to act on committed progenitors rather than RGLs (Steiner et al., 2008). Physical exercise also stimulated proliferation of IPCs, but not RGLs (Lugert et al., 2010; Steiner et al., 2008). Detailed analysis of RGL activity in response to physiological stimuli is required to identify physiological regulators of quiescence. This is worth investigating in light of the observation that neurogenesis and the stem cell pool decreases with age (sharply immediately after adolescence, then more slowly with age), whilst NSC quiescence increases (Encinas et al., 2011; Jaskelioff et al., 2011; Kempermann, 2011a; Lugert et al., 2010; Seib et al., 2013). Therefore, identifying environmental stimuli that could mitigate this decline could enable rejuvenation of neurogenesis, which would be highly useful for human health. Environmental and physiological stimuli may not directly act on NSCs; rather, they may modulate elements of the neurogenic niche, which in turn directly regulate NSC function. Indeed, ageing of the neurogenic niche can directly affect NSC function (Mosher and Schaffer, 2018). I will next explore the various mechanisms by which the neurogenic niche can directly regulate neural stem cell activity.

1.4.2 Direct regulation of NSCs by the neurogenic niche

1.4.2.1 Cell adhesion

The neurogenic niche is a highly complex environment, with various different cell types and sources of signalling, as described in Section 1.2. But it is also complicated in light of the fact it regulates both the maintenance of NSCs, whilst also regulating the proliferation and differentiation of progenitors, and survival of neurons. This multilevel regulation demonstrates how localised and specific the regulating signals must be, suggesting there is a highly dynamic system of extrinsic signals integrating with

intrinsic changes in the responding cell. Part of this specificity is likely achieved through adhesion to the niche and local, cell-cell signalling. Expression of vascular cell adhesion molecule-1 (VCAM1) is required in SVZ NSCs to maintain their correct niche positioning, and disruption of VCAM1-mediated adhesion leads to loss of NSC quiescence (Kokovay et al., 2012). Similarly, the integrins, a class of cell adhesion molecule, enable contact between NSCs and the endothelial cells of the vascular niche, and their expression regulates NSC activity. SVZ NSCs express the laminin receptor α6β1-integrin, which is required for NSCs to adhere to the vascular niche and maintain a level of quiescence (Shen et al., 2008). Similarly, β1-Integrin is selectively expressed on dividing NSCs in the SVZ, and was shown to be required to maintain appropriate levels of proliferation of NSCs and IPCs (Kazanis et al., 2010). These studies contradict to some extent the observations that proliferative NSCs lie close to the vasculature, and endothelial cells can induce proliferation of NSCs in co-culture conditions (Shen et al., 2004), highlighting the complexity of the interaction between NSCs and their niche. Ottone and colleagues (2014) demonstrated in the SVZ that direct endothelial-to-stem cell signalling via ephrinB2 and Jagged maintained the stem cells in a quiescent state. Interestingly, the regulation of NSC quiescence by eprhinB2 and Jagged functioned via independent pathways, highlighting the complexity and number of signals that act in combination to tightly control NSC quiescence. This is certainly true in the embryo, where β1-integrins in NSCs directly influence levels of Notch signalling (Campos et al., 2006), which is itself a highly potent regulator of NSC activity in adult neurogenic niches.

1.4.2.2 Notch

Notch is a well-known signal implicated in the regulation of stem cells in many niches (Mourikis and Tajbakhsh, 2014), including the regulation of neural stem cells during embryonic development, and has recently received a great deal of attention for its role in maintaining the pool of adult neural stem cells (Imayoshi and Kageyama, 2011; Kageyama et al., 2008). There are 4 Notch receptors in mammals, Notch1-4, which are composed of an extracellular domain, a single transmembrane pass, and an intracellular domain. There are also 5 Notch ligands: Dll1, Dll3, Dll4, Jag1, Jag2. Notch signalling can be initiated when a cell expresses a ligand and activates the receptor on a neighbouring cell, signalling in a *trans* interaction. Notch can also be activated in *cis,* when a cell expresses both the receptor and the ligand. When a ligand binds to a

Notch receptor, y-secretase proteases such as presenilins cleave the receptors to release the Notch intracellular domain (NICD). The NICD enters the nucleus and binds target DNA along with RBPJk, recruiting coactivators including MAML1 to induce target gene expression such as *Hes1* and *Hes5*. Notch pathway components are expressed in the neurogenic niche of the SVZ and SGZ. Specifically, RGLs in the adult SGZ are capable of receiving Notch signalling due to the expression of the Notch receptors Notch1, Notch2 and Notch3 on GFAP-expressing RGLS. Concurrent with the receptor expression, Notch signalling is active in more than 90% of GFAP+ RGLs and Sox2+ RGLs in the SGZ, as determined by the expression of NICD and genetic reporters of Hes1 and Hes5 expression (Breunig et al., 2007; Ehm et al., 2010; Imayoshi et al., 2010; Lugert et al., 2010; Ohtsuka et al., 2006). The Notch ligand Jagged1 is expressed by niche astrocytes and IPCs, and is crucial for maintenance of RGLs via feedback from the progenitors to induce a return to quiescence of the stem cells (Lavado and Oliver, 2014) (Figure 1.6). Another Notch ligand, Dll1, is similarly expressed in IPCs, following asymmetric distribution of the protein to the daughter cell during NSC division, and provides a feedback signal from progenitor to stem cell, instructing the stem cell to return to quiescence (Kawaguchi et al., 2013). The consensus in the field is that Notch is required to maintain the adult stem cell pool, a role conserved between rodents and fish (Chapouton et al., 2010), both by inhibiting proliferation and maintaining stemness of RGLs by inhibiting cell-cycle exit and differentiation, in both the SGZ and SVZ (Alexson et al., 2006; Andreu-Agullo et al., 2009; Androutsellis-Theotokis et al., 2006; Hitoshi et al., 2002). NSCs in the SVZ also express Notch1-3, with Notch3 preferentially expressed by quiescent NSCs (Kawai et al., 2017) Notch signalling via Jagged1 has been suggested to promote quiescence by inhibiting differentiation, rather than by regulating the cell cycle (Ottone et al., 2014), a role similarly suggested for satellite (muscle) stem cells (Bjornson et al., 2012; Mourikis et al., 2012; Mourikis and Tajbakhsh, 2014). Manipulation of Notch receptor expression has added to the understanding of the role of Notch in NSC regulation, particularly highlighting the differential roles of the three receptors in spite of their signalling via the same intracellular cascade. Conditional knockout of the Notch1 receptor in Nestin+ cells in the DG results in a loss of the NSC and IPC populations (Ables et al., 2010), which the authors report to be due to a failure of self-renewal of the stem cells, and precocious cell cycle exit. A similar result was obtained using genetic ablation of Notch1 in GFAP+ cells, which promoted cell-cycle exit of RGLs and neuronal fate determination of progenitors, whereas constitutively active Notch1 signalling increased

RGL proliferation (Breunig et al., 2007). In the SVZ, Notch1 is required for activated NSCs to self-renew and maintain their stemness (Basak et al., 2012). In contrast, Notch2 and Notch3 have been separately shown to be required to maintain quiescence of SVZ NSCs (Engler et al., 2018; Kawai et al., 2017). An alternative approach has been to conditionally delete RBPJk, the downstream transcriptional effector of canonical Notch signalling. Conversely, RBPJk cKO mice showed an initial increase in proliferation of the quiescent RGLs and progenitors, followed by a loss of long-term maintenance of the stem cell pool, in both the SGZ and SVZ (Ehm et al., 2010; Imayoshi et al., 2010). The discrepancy between Notch1 cKO and RBPJk cKO mice may be due to different levels of Notch inhibition; signalling via alternative Notch receptors in Notch1cKO mice may mediate the phenotype and prevent the activation of RGLs observed in RBPJk cKO mice (for which all canonical Notch signalling is blocked). Notch signalling is notoriously context dependent, which is evident from the differential effects of Notch1 deletion in SVZ NSCs, which results in increased NSC proliferation without a subsequent loss of the stem cell pool, unlike in the SGZ where the stem cell pool is depleted (Ables et al., 2010; Basak et al., 2012).

1.4.2.3 Neurotransmitters: GABA, Glutamate

As a result of being located in the brain, neural stem cells are uniquely exposed to regulation by neurotransmitters. NSCs in both the SVZ and hippocampus express receptors for neurotransmitters, several of which have been identified to regulate NSC quiescence. Evidence exists for serotonin, dopamine, glutamate, GABA, acetylcholine, nitric oxide, neuropeptide Y and noradrenaline promoting proliferation in the neurogenic niches (reviewed by (Berg et al., 2013)), reflecting a complex network of feedback from other parts of the brain in regulating NSC quiescence, although it is yet to be determined if these factors activate NSCs from quiescence directly.

SVZ NSCs are directly innervated by serotonergic axons originating in the raphe nuclei, and their release of 5HT promotes SVZ cell proliferation (Banasr et al., 2004; Encinas et al., 2006; Tong et al., 2014). The SVZ also receives innervation from GABAergic and glutamatergic neurons of the striatum and cortex, and neuromodulatory regulation from dopaminergic innervation from the substantia nigra, the latter of which is suggested to promote proliferation in the SVZ (reviewed by (Young et al., 2011)). POMC+ neurons of the hypothalamus also directly innervate SVZ

niche cells including NSCs, and their activity has been shown to promote NSC proliferation (Paul et al., 2017). GABA is expressed and tonically secreted by SVZ neuroblasts, activating signalling in proximal progenitor cells, limiting their proliferation via phosphorylation of histone variant H2AX (Alfonso et al., 2012; Fernando et al., 2011; Liu et al., 2005; Nguyen et al., 2003). Whether GABA can specifically promote quiescence of SVZ NSCs is unclear, however treatment with GABA antagonist bicuculline results in specific activation of quiescent NSCs (Pineda et al., 2013) suggesting it may also normally promote NSC quiescence.

The dentate gyrus is populated by parvalbumin-expressing (PV+) interneurons, and similarly to neuroblasts of the SVZ, the tonic release of GABA from these cells has been identified to act directly on hippocampal NSCs, maintaining their quiescence by promoting cell cycle exit, inhibiting symmetrical self-renewal and astrocytic differentiation (Song et al., 2012a). Interestingly, NSCs can fine-tune their own GABA signalling via the cell autonomous expression of diazepam binding inhibitor (DBI), which promotes their proliferation (Dumitru et al., 2017). The dentate gyrus also receives projections from glutamatergic Mossy Cells in the hilus of both ipsi- and contralateral dentate gyri, which directly innervate the NSCs. Interestingly, depending on their moderate or high level of activation, Mossy Cells can either indirectly promote NSC quiescence via stimulating the release of GABA from DG interneurons, or promote activation of the NSCs via direct release of glutamate onto NSCs, respectively (Yeh et al., 2018). Glutamate also indirectly induces the activation of hippocampal NSCs by inhibiting the release of the Wnt inhibitor Sfrp3 from neurons (Jang et al., 2013b), and it has been shown to mediate NSC activation following ischaemic injury (Nochi et al., 2012). Regulation of NSC quiescence by glutamate may be specific to hippocampal NSCs, as receptors for glutamate do not appear to be expressed by SVZ NSCs (Lee et al., 2005; Nochi et al., 2012).

1.4.2.4 Vasculature

As described above, the adult neurogenic niches are highly vascularised, and the endothelial cells can directly regulate NSC quiescence (Fuentealba et al., 2012; Shen et al., 2004). In the DG, new neurons are generated in close proximity to blood vessels (Palmer et al., 2000) and BrdU+Nestin+ or BrdU+GFAP+ NSCs/IPCs were found next to capillaries, suggesting the vasculature can provide activating or pro-proliferative

signals in the DG as well as the more intensely studied SVZ. I have already explored how cell-cell signalling can mediate this effect. However, the vasculature is also the gateway to many systemic stimuli carried by the blood. Components in the blood can pass the blood-brain-barrier into the SVZ, as shown by injection of a fluorescent dye found in the SVZ and not in the cortex (Tavazoie et al., 2008). Heterochronic parabiosis, or the exposure of aged animals to the blood of a young animal (and vice versa) has emerged as a fascinating insight into the changes that occur systemically with age and how they directly affect the functioning of stem cells. For example, 'old' blood inhibits muscle regeneration, whilst 'young' blood restored it (Conboy et al., 2005; Rebo et al., 2016) via increased Notch activation (Conboy et al., 2005), which I have already discussed as a crucial regulator of stem cell quiescence. Young blood has also been shown to rejuvenate the regenerative capacity of the liver (Conboy et al., 2005; Rebo et al., 2016), the CNS (Ruckh et al., 2012; Villeda et al., 2011). Infusion of 'young' blood also improved hippocampal function and increased numbers of Sox2+ cells and proliferating cells in the DG (Villeda et al., 2011), whilst 'old' blood severely deceased number of Sox2+Ki67+ cells in the DG (Rebo et al., 2016). Neither study specifically addressed the effect of old vs young blood on NSC quiescence/activation, therefore it would be interesting to investigate whether there is a specific effect, especially as quiescence of NSCs is reported to increase with age (Lugert et al., 2010; Yousef et al., 2015a). However, these studies highlight the vasculature to be a rich source of regulation for adult neurogenesis.

1.4.2.5 Vasculature-derived factors: IGF, VEGF, NT-3

A specific factor known to be carried in the blood and to have a direct effect on NSC activity is insulin-like growth factor1 and 2 (Figure 1.6). IGF2 is expressed in SGZ GFAP+ Nestin+ Sox2+ NSCs (Bracko et al., 2012), and direct infusion of IGF into the brains of adult rats increases progenitor proliferation and overall levels of neurogenesis (Aberg et al., 2000). It was not shown in this study whether the effects of IGF were direct on stem cell activity, however IGF2 has been shown to directly regulate NSC proliferation in an autocrine manner via Akt signalling (Bracko et al., 2012). A fascinating link is being uncovered between vascular-derived factors and environmental regulators of neurogenesis. For example, circulating liver-derived IGF1 is required to mediate the exercise-induced increase in neurogenesis in mice, although the effects were at the level of neuronal survival, rather than NSC/IPC proliferation

(Trejo et al., 2008). The discrepancy over whether IGF signalling directly regulates NSC activity of neuronal survival may be a reflection of the source of IGF, systemic vs local. Studies in *Drosophila* have shown that NSCs respond only to local insulin from glia in the stem cell niche, which secrete *Drosophila* insulin-like peptide (DILP), as opposed to systemic insulin/IGF signalling (Chell and Brand, 2010). The stem cell niche therefore has the capacity to buffer systemic signals, in order to fine-tune regulation of neurogenesis. Levels of IGF1 in the hippocampus have also been observed to decrease sharply by middle age in rodents, and remain steady thereafter (Shetty et al., 2005), mirroring the decline in neurogenesis seen with age, which may hint to a direct functional relationship between IGF levels and neurogenesis.

The same study also observed a decline in the neurotrophic factor vascular endothelial growth factor (VEGF) (Shetty et al., 2005). VEGF is secreted by endothelial cells and directly regulates NSC activity by promoting SGZ NSC self-renewal (Jin et al., 2002; Sun et al., 2003). Hippocampal NSCs express VEGF receptor 3, and signalling via this receptor both activates NSCs from quiescence, and is required for NSC activation (Han et al., 2015). Much like IGF, VEGF mediates environmental factors that regulate quiescence, including exercise (Fabel et al., 2003) and environmental enrichment (Cao et al., 2004).

Another endothelial-derived factor, neurotrophin 3 (NT-3) is expressed by endothelial cells of the vasculature, and is also found in the cerebrospinal fluid, to which the SVZ is exposed (Silva-Vargas and Doetsch, 2014). NT-3 promotes quiescence and the long-term maintenance of SVZ NSCs, by regulating the levels of endothelial nitric oxide synthase (eNOS) (Delgado et al., 2014). eNOS catalyses the production of nitric oxide (NO), a gaseous signalling molecule which has been shown to inhibit proliferation of NSCs in both the SVZ and SGZ (Estrada and Murillo-Carretero, 2005).

Overall, the vascular neurogenic niche is a rich source of local and systemic signals regulating neural stem cell activity, both via direct cell-cell contacts and from diffusible factors.

1.4.2.6 Wnt

Wnt signalling is prominent in the SGZ, regulating several stages of the neurogenic lineage, although its direct role in regulation RGL quiescence is less clear. Canonical Wnt signalling proceeds with the binding of diffusible Wnt ligands to the Frizzled Wnt receptors and co-receptors such as LRP5/6. Binding induces disassembly of the destruction complex, which normally functions to phosphorylate β-catenin, targeting it for degradation. Therefore, Wnt ligand binding results in stabilisation of β-catenin, which then enters the nucleus, binding TEF/LEF transcription factors, and activating target gene expression. Wnt3a is produced by hippocampal astrocytes (Figure 1.6), and cultured SGZ NSCs express Wnt receptor Frizzled1 and Dishevelled1 (Lie et al., 2005), suggesting RGLs have the capacity to respond to Wnt, and lineage tracing experiments demonstrated cells in the SVZ and SGZ are responsive to Wnt/ β-catenin signalling (Bowman et al., 2013). In co-culture conditions, SGZ NSCs respond to hippocampal-astrocyte derived Wnts, and the presence of the Wnt inhibitor sFRP2/3 inhibited their ability to differentiate into neurons (Lie et al., 2005). Secretion of Wnts has been observed for cultured SGZ NSCs, suggesting both autocrine and paracrine Wnt signalling for NSCs *in vitro* (Qu et al., 2010), but has not been shown *in vivo*. Wnt antagonists are also present in the niche; sFRP3 for example is highly expressed by DG granule neurons, and is secreted into the niche, and may mediate an indirect regulation of RGL quiescence by granule neurons (Jang et al., 2013a) (Figure 1.6). Similarly, Dkk1 is expressed by SGZ progenitor cells and neurons, and conditional deletion in Nestin+ cells results in increased activation and self-renewal of NSCs, in young and aged mice, although the effect on quiescent RGLs was not directly examined (Seib et al., 2013). Lentiviral mediated-expression of a Wnt inhibitor in the DG resulted in vastly reduced numbers of proliferating neuroblasts, although whether Wnt directly affected NSC proliferation was not examined (Lie et al., 2005). Dominant-negative β-catenin interferes with proliferation of IPCs but not RGLs (Kuwabara et al., 2009), suggesting Wnt signalling promotes progenitor proliferation, however it is still unclear if it can directly activate quiescent RGLs. Overall, Wnt signalling strongly promotes neurogenesis, but its role specifically in RGL quiescence/activation requires further investigation.

1.4.2.7 Shh

RGLs in the dentate gyrus originate from Shh-responsive progenitors during development (Li et al., 2013). Correspondingly, GFAP+ RGLS in the SGZ are Shh-responsive (Ahn and Joyner, 2005). Shh signalling proceeds via binding of the ligand to the receptor Patched (Ptch1) located on the primary cilium. Upon ligand binding, Ptch1 releases its repression of the G-protein-coupled receptor Smoothened (Smo). Smo subsequently activates the expression of the Gli family of transcription factors, of which there are activating (Gli1) and repressive forms (Gli2, Gli3). Shh has been repeatedly shown to be necessary for the maintenance and proliferation of SVZ NSCs (e.g. (Palma et al., 2005; Petrova et al., 2013) and it appears to be required in the same way for SGZ NSCs; loss of the primary cilium on SGZ NSCs, which is required for Shh signalling, results in cell cycle exit and reduced progenitor production (Breunig et al., 2008). Similarly, conditional deletion of an essential component for cilium assembly in GFAP+ RGLs led to a significant decrease in progenitor proliferation and subsequently impaired spatial learning, although RGL quiescence was not affected (Amador-Arjona et al., 2011). Treatment of cultured SGZ NSCs with Shh and overexpression of Shh in the DG also induced progenitor proliferation (Lai et al., 2003) although again the direct effect on stem cell activation was not examined. Direct induction of stem cell activity by Shh has been shown for SVZ NSCs; activating Shh in SVZ NSCs led to an increase in the stem cell pool by inducing self-renewing symmetric division of the stem cells (Ferent et al., 2014).

1.4.2.8 FGF2

Fibroblast growth factor 2 (FGF2) is a well-established neurogenic factor for both developmental and adult neurogenesis (Mudo et al., 2009; Woodbury and Ikezu, 2014). FGF receptor 1 (FGFR1) is essential for neural progenitor proliferation and hippocampal formation during development (Ohkubo et al., 2004), and its mRNA is expressed in GFAP+BLBP+ stem cells of the postnatal DG (Choubey et al., 2017). GFAP+Sox2+ NSCs in the postnatal SVZ also express *Fgfr1* (Choubey et al., 2017), indicating FGF signalling can modulate neurogenesis at the level of the stem cells in adult neurogenic niches. Indeed, there are several reports demonstrating the pro-proliferative and pro-neurogenic effects of FGF2 infusion in the SVZ (Mudo et al., 2009). There are conflicting reports regarding the effects of FGF2 on RGL activity in

the SGZ. Two studies show that infusion of FGF2 into the lateral ventricles and virus-mediated overexpression of FGF2 in the DG increases progenitor cell proliferation and enhances neurogenesis in the DG, respectively (Rai et al., 2007; Yoshimura et al., 2001). However, other studies show no effect on cell proliferation or neurogenesis in the SGZ following FGF2 treatment (Jin et al., 2003; Kuhn et al., 1997; Mudo et al., 2007). Interestingly, proliferation of SGZ RGLs and IPCs is not affected in FGF2 knockout mice (Werner et al., 2011). Although the use of FGF2-null mice in this study may introduce the confounding effects of altered hippocampal development, the results suggest endogenous hippocampal FGF2 is not required for basal or homeostatic levels of NSC proliferation, instead it may potentially mediate systemic or environmental neurogenic stimuli, in situations when FGF2 is increased above basal levels (Werner et al., 2011). Indeed, FGF2 levels are increased in the hippocampus after kainic acid-induced seizure or ischemic brain injuries (Bugra et al., 1994; Lin et al., 1997; Yoshimura et al., 2001), and the concurrent increase in progenitor proliferation was dependent on FGF2 (Yoshimura et al., 2001; Yoshimura et al., 2003). Similarly, infusion of FGF2 can restore levels of neurogenesis in the DG and SVZ of aged mice (Jin et al., 2003; Kang and Hebert, 2015). Most of these studies report the effects of FGF2 signalling at the level of total proliferation or neurogenesis, and do not report the specific effects on NSC quiescence and activation. However, FGF2 is a potent mitogen and self-renewal factor for *in vitro* cultures of SVZ and SGZ NSCs (Gage et al., 1995; Gritti et al., 1996; Palmer et al., 1995), which I will explore in more detail in Section 1.6 below.

1.4.2.9 BMP

Bone morphogenetic protein (BMP) signalling plays a prominent role in regulating neurogenesis, both during embryonic development, where it is required for the early specification of the medio-dorsal structures of the developing brain, including the hippocampus (Urban and Guillemot, 2014), and throughout adult neurogenesis in the dentate gyrus (Choe et al., 2015). BMPs are a subgroup of the transforming growth factor β (TGFβ) family of extracellular morphogens, which regulate the development of a vast number of tissues including the nervous system, and regulate a plethora of processes, including patterning, proliferation and differentiation (Liu and Niswander, 2005). BMP signalling is initiated by the binding of a BMP ligand, of which more than 20 members have been identified in vertebrates (Bragdon et al., 2011), to the BMP

serine-threonine kinase receptor complex. There are two subtypes of BMP receptor; the type I receptors comprising BMPRIA, BMPRIB and Activin receptor type 1 (ACVR1); and BMP type II receptor, or BMPRII. In canonical BMP signalling, upon ligand binding the type I receptors become activated and phosphorylate the C-termini of their downstream mediators, the Smad1/5/8 DNA-binding proteins, enabling them to form a stable heterodimer with Smad4, a common mediator-Smad protein on which the other Smads converge. This Smad complex then binds DNA and recruits transcriptional co-activators or co-repressors to modulate target gene expression (Liu and Niswander, 2005). There is also evidence for non-canonical, Smad-independent TGFβ/BMP signalling, via activation of p38, Jun N-terminal kinase (JNK) mitogen-activated protein kinase (MAPK), phosphoinositide 3-kinase(Pi3K)/Akt and extracellular signal-regulated kinase 1/2 (ERK1/2) pathways (Derynck and Zhang, 2003; Moustakas and Heldin, 2005; Mu et al., 2012). For example, Smad-independent BMP-induced p38/MAPK activity has been reported during differentiation of embryonic stem cells into myeloid progenitors (Cook and Evans, 2014); Smad4-deficient breast cancer cells have demonstrated TGFβ-induced JNK/MAPK activation (Engel et al., 1999), and in Smad4-null colon cancer cells BMP is able to signal via ERK1/2 (Beck and Carethers, 2007). Smad4 also acts redundantly with TGFβ-induced p38/MAPK signalling to pattern the oral epithelium during development (Xu et al., 2008).

Components of the BMP pathway are expressed in adult neurogenic niches, and have been shown to have a profound regulatory role in neurogenesis. In the DG, Nestin+GFAP+ RGLs express BMPRIA, whilst NeuN+ granule neurons express BMPRII (Mira et al., 2010). The source of BMP ligands in the SGZ is not completely know, although BMPs including BMP4 are chronically secreted by granule neurons and the stem cells themselves (Bonaguidi et al., 2005; Mikawa et al., 2006) (Figure 1.6), and BMP4 and BMP6 have been shown to co-localise with endothelial cells and microglia, respectively, suggesting several different niche cells can produce BMPs (Yousef et al., 2015b). Unlike during development where BMP ligands diffuse across tissue to create a morphogen gradient, such as in the neural plate and patterning of the spinal cord, BMP ligands in the neurogenic niche of the DG are thought to act more locally to the source of secretion, due to the fact the ligands strongly bind the extracellular matrix, impeding their diffusion (Hall and Miller, 2004). BMPs have a profound effect on adult neurogenesis, acting differentially at two stages of the lineage depending on the differential expression of BMP receptor subtype. In BMP receptor II-

expressing granule neurons, BMP suppresses their differentiation (Bond et al., 2014; Mira et al., 2010), whereas it maintains quiescence of BMPR1a-expressing RGLs (Mira et al., 2010) (Figure 1.6). Granule neurons, progenitors and Sox2+ RGLs are immunoreactive for phospho-Smad1 (Mira et al., 2010), indicating BMP signalling is active in these cells. P-Smad1 is specifically excluded from proliferating RGLs, which is a direct reflection of the role of BMP in maintaining quiescence of RGLs; when BMP signalling in the DG was inhibiting by acute intracerebroventricular infusion of the inhibitor Noggin, the number of proliferating RGLs was significantly increased (Bonaguidi et al., 2008; Mira et al., 2010). BMP is also required to maintain the pool of stem cells in the DG, as demonstrated by the increase in number of newborn NeuN+ granule neurons and DCX+ progenitors 21 days after Noggin infusion, at the expense of non-radial Sox2+ stem cells (Mira et al., 2010). Conditional deletion of the canonical BMP mediator, Smad4, in GLAST-expressing cells similarly led to a transient increase in proliferating cells in the DG (although it was not reported whether this included a specific increase of RGL proliferation), followed by a loss of the non-radial pool of Sox2+ cells, although the radial stem cell pool was spared (Mira et al., 2010). BMP signalling is dynamically regulated in the DG by the inhibitors Noggin and Chordin which are also expressed in the niche (Fan et al., 2003; Scott et al., 2000). BMP signalling also mediates systemic regulation of neurogenesis, such as the exercise-induced effects on neurogenesis, via an increase in *Noggin* expression and decrease in *Bmp4* (Gobeske et al., 2009). Similarly, an increase in BMP signalling in the aged hippocampus may mediate the age-related decline in neurogenesis by inhibiting progenitor proliferation (Yousef et al., 2015b). BMP signalling also induces quiescence of cultured SGZ NSCs, creating the opportunity to investigate this elusive stem cell state in a highly tractable *in vitro* system, described in more detail in Section 1.5 (Martynoga et al., 2013; Mira et al., 2010; Sun et al., 2011).

BMP signalling also actively regulates neurogenesis in the SVZ, although its direct effects on the stem cells is less clear. NSCs and IPCs in the SVZ express BMPRIA and BMPRII, as well as BMP2/4, and these cells have the strongest immunoreactivity for p-Smad1/5/8 (Colak et al., 2008; Lim et al., 2000). Basal levels of BMP in the SVZ promotes a neurogenic fate of progenitor cells (Colak et al., 2008), while elevated BMP inhibits neurogenesis (Gajera et al., 2010; Lim et al., 2000). The level of BMP in the niche can be modulated by Noggin released from ependymal cells (Lim et al., 2000). Injection of BMP4 into the ventricles inhibits proliferation in the SVZ, however it was not

shown whether this was a result of increased NSC quiescence (Lim et al., 2000). BMP7 and BMP4 have been shown to reach SVZ NSCs from the cerebrospinal fluid, where they diffuse into the intracellular space and are captured by fractones, finger-like basal membrane structures rich in extracellular matrix proteins such as laminins and collagens (Douet et al., 2012; Mercier and Douet, 2014). BMP4 and BMP7 signalling from fractones inhibits cell proliferation in the SVZ (Douet et al., 2012; Mercier and Douet, 2014). Therefore, although the specific effect on NSC quiescence has not been analysed, it is plausible that BMPs may promote NSC quiescence in the SVZ and warrants further investigation.

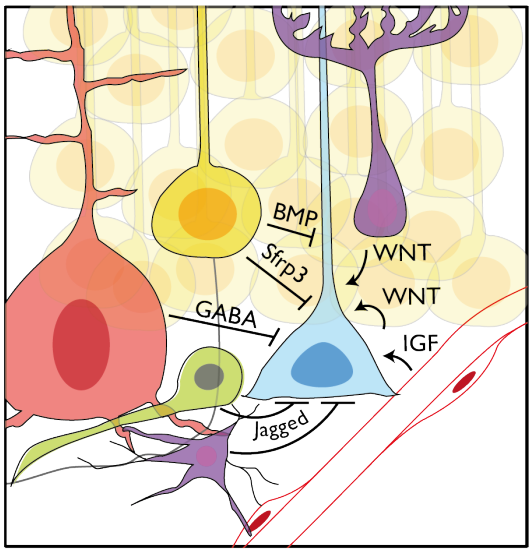

Figure 1.6. Sources of neural stem cell regulation in the hippocampal neurogenic niche.

SGZ neural stem cells (blue) receive regulating signals from their local niche in the dentate gyrus. Interneurons (red), granule neurons (yellow), progenitor cells (green) and astrocytes (purple) provide pro-quiescence signals, whilst the vasculature (blood vessel) and astrocytes provide pro-activating/proliferative cues. Modified from (Urban and Guillemot, 2014) with permission of the rights holder, Frontiers.

1.5 *In vitro* culture systems for studying adult NSCs

One of the ways in which adult neural stem cells were defined as stem cells, was by their ability to self-renew and generate neurons *in vitro* (Conti et al., 2005; Reynolds and Weiss, 1992; Roy et al., 2000). The ability to culture adult NSCs, including

following genetic modification or viral transduction, has proved to be a valuable tool to complement *in vivo* studies to precisely elucidate the extrinsic factors and intrinsic mechanisms regulating NSCs. Following dissection and dissociation of the dentate gyrus or SVZ, NSCs can be cultured in two ways, either as non-adherent floating neurospheres (Reynolds and Weiss, 1992) or as an adherent monolayer culture, normally on a substrate such as laminin (Ray et al., 1993). FGF2 was identified to be a crucial mitogen for the propagation of NSCs *in vitro* (Palmer et al., 1999), inducing stem cell maintenance and self-renewal, as has been reported for SVZ and SGZ NSCs *in vivo* (Mudo et al., 2009; Rai et al., 2007; Yoshimura et al., 2001). Epidermal growth factor (EGF) has also been used to induce proliferation and maintain NSCs in culture to great effect (Conti et al., 2005), although *in vivo* it has only been reported to regulate subventricular zone NSCs, which expressed EGF receptor in the active state (Aguirre et al., 2010), but there are currently no reports of SGZ NSCs being regulated by EGF *in vivo*, which means treatment of SGZ NSCs with EGF *in vitro* may generate a non-physiological state. *In vitro* cultures of adult neural stem cells can be treated with other recombinant niche proteins to modulate their activity or induce differentiation, allowing interrogation of the molecular regulation of these processes. Addition of BMP4 to the culture medium, for example, can induce a quiescent-like state of NSCs (Bonaguidi et al., 2008; Mira et al., 2010; Sun et al., 2011), and has been utilised to start to discover the intrinsic mechanisms regulating the quiescent neural stem cell state (Martynoga et al., 2013). These *in vitro* culture systems have also been used to show the interaction and cross-talk between different signalling pathways; FGF2 is required to maintain stemness and suppress astrocytic differentiation in the presence of BMP4, for example (Sun et al., 2011). While the *in vitro* system cannot fully reconstitute the *in vivo* niche, and therefore could result in NSCs responding in non-physiological ways, it still provides a highly tenable tool for discovering potential new mechanisms of NSC regulation. The number of cells that can be analysed in a single experiment vastly outnumber those that can be isolated directly from the adult niche, particularly as NSCs must be prospectively isolated by fluorescent activated cell sorting in order to generate a pure population, for transcriptional or epigenetic analyses. Technologies are improving, such that fewer or single-cells are required for analysis, however these experiments are labour intensive and costly, therefore a system which enables a quick, straightforward analysis of the effects of a factor or genetic manipulation is highly useful.

1.6 Intrinsic mechanisms regulating NSC quiescence

As discussed in Section 1.3.2, the quiescent stem cell state requires activation of many different categories of genes, which means there are likely intrinsic factors that induce the quiescence transcriptional programme. Moreover, the multiple different niche signals that modulate NSC activity need intrinsic factors to mediate their effects. The exact network of factors that regulate the quiescence-activation balance of adult NSCs is not fully understood, but several factors have been identified to mediate part of the programme controlling this balance.

1.6.1 TLX

TLX is an orphan-nuclear receptor that contributes to patterning of the telencephalon during embryonic development (Monaghan et al., 1995), and is also required specifically in the adult brain to maintain adult NSCs in an undifferentiated, proliferative state (Niu et al., 2011; Shi et al., 2004; Zhang et al., 2008). Overexpression of *Tlx* promotes neurogenesis and improves hippocampal functioning (Murai et al., 2014). The pro-proliferative effect of TLX is in part mediated by activating Wnt/β-catenin signalling (Qu et al., 2010). The induction of Wnt7a by TLX in cultured NSCs could induce the proliferation of co-cultured NSCs (Qu et al., 2010), suggesting it can regulate NSC proliferation in both an autocrine and paracrine manner. Interleukin-1beta (IL-1β), the most abundant pro-inflammatory cytokine in the brain, has been shown to directly inhibit TLX in hippocampal progenitors, suppressing their proliferation (Ryan et al., 2013), suggesting inhibition of TLX may mediate NSC quiescence.

1.6.2 MicroRNAs

MicroRNAs (miRNAs) are short (22-24 nucleotide) strands of non-coding RNAs, conserved from plants to humans, which negatively regulate mRNA gene transcripts by complementary base-pairing, inducing the cleavage or destabilisation of the mRNA (Fabian et al., 2010). A handful of miRNAs have been identified to regulate NSC activity, although most of their identified function concern promotion of neuronal differentiation (e.g. *miR-124*, *miR-132* (Kawahara et al., 2012)). *miR-9* is a neural-specific miRNA, conserved in *Drosophila*, zebrafish and mammals, and expressed in both embryonic and adult NSCs in the mouse (Kapsimali et al., 2007; Kawahara et al.,

2012). During development, *miR-9* suppresses the expression of genes implicated in neural stem cell maintenance and quiescence, such as Tlx and REST (Coolen et al., 2013; Packer et al., 2008; Zhao et al., 2009). In the adult zebrafish pallium, *miR-9* controls the balance between NSC quiescence and activation (Katz et al., 2016). The function of *miR-9* in adult murine NSCs is yet to be investigated but based on its function in other populations of NSCs, would be an interesting miRNA to investigate with regards to regulation of NSC quiescence.

1.6.3 Ascl1

Ascl1 (achaete scute like 1; Mash1) is a basic helix-loop-helix (bHLH) transcription factor, and part of the group of proneural proteins identified in *Drosophila* in the 1980's, which induce neural fate in mammalian embryonic progenitor cells (Guillemot, 2007; Guillemot and Hassan, 2017). The basic domain of bHLH transcription factors such as Ascl1 slots into the main groove of the DNA, and in this way mediates the binding of the TF to DNA, at specific hexanucleotide sequences, known as E-boxes (Bertrand et al., 2002). The HLH domain enables dimerization with other bHLH proteins, and Ascl1 requires heterodimerisation with E-protein binding partners in order to be stabilised, bind DNA and activate target gene expression (Imayoshi and Kageyama, 2014a; Sharma et al., 2015).

Ascl1 is expressed in the developing ventral telencephalon of mice, where it promotes the specification of progenitors into GABAergic neurons, as well as inducing embryonic progenitor cell proliferation (Bertrand et al., 2002; Castro et al., 2011; Imayoshi and Kageyama, 2014a). Ascl1 is also expressed in the outer radial glia of the developing neocortex in humans (Hansen et al., 2010), suggesting its function may be conserved in human embryonic neurogenesis. Ascl1 has multiple, context dependent functions promoting neural fate determination endogenously in embryonic progenitors, and also when overexpressed in astrocytes and fibroblasts Ascl1 can reprogram these cells into neurons (Berninger et al., 2007; Wapinski et al., 2013). Ascl1 also promotes the cell cycle of neural progenitors, as a result of its activation of target genes involved in cell proliferation, such as CyclinD1 (Castro et al., 2011; Urban et al., 2016). Despite its powerful neurogenic and pro-proliferative function during embryonic development, Ascl1 is dispensable for development of the DG (Galichet et al., 2008) and proliferation of progenitors in the postnatal DG (Andersen et al., 2014). This is surprising in light of

its recently discovered role in adult neurogenesis. Ascl1 is expressed in proliferating progenitors and a small proportion of active NSCs in the adult DG and SVZ (Kim et al., 2011), and its expression is absolutely required for activation of NSCs from quiescence, as conditional ablation in stem cells results in complete loss of activation and subsequent loss of neurogenesis in both niches (Andersen et al., 2014). In the absence of Ascl1, kainic acid-induced seizures are unable to induce neurogenesis (Andersen et al., 2014), indicating neurogenic niche signals can act at the earliest stage of the lineage, converging on Ascl1 to activate stem cells from quiescence.

The regulation of Ascl1 is still not fully understood, however it is known that Notch target genes Hes1 and Hes5 transcriptionally repress Ascl1 in embryonic NPCs to maintain an undifferentiated state (Imayoshi and Kageyama, 2014a). Interestingly, Ascl1 and other bHLH proteins have been demonstrated to oscillate in embryonic neural progenitors, and the oscillatory vs stable high vs stable low expression determines whether Ascl1 promotes cycling behaviour, neuronal differentiation or enables other fate determinants to dominate (respectively) (Imayoshi et al., 2013). Surprisingly, Ascl1 overexpression is also able to promote the differentiation of IPCs of the DG into oligodendrocytes, a cell type never normally generated by these cells (Jessberger and Gage, 2008), perhaps a result of its abnormally high and stable expression.

Ascl1 is also regulated post-translationally. Cyclin-dependent kinases can phosphorylate Ascl1 protein at multiple sites, preventing its ability to bind DNA and promote neuronal differentiation in embryonic NSCs (Ali et al., 2014). Akt signalling has been shown to regulate Ascl1 stability in the embryonic brain (Oishi et al., 2009), raising the possibility that IGF/Akt signalling could mediate its pro-proliferative effects by stabilising the activation factor Ascl1. Notch signalling, in addition to transcriptional repression of Ascl1, has also been shown to rapidly induce the degradation of Ascl1 at the protein level in cultured cancer cells (Sriuranpong et al., 2002). Ascl1 is also regulated at the protein level in RGLs in the adult DG, by the HECT domain E3 ubiquitin ligase Huwe1, which binds Ascl1 protein in active RGLs and targets it for proteasomal degradation (Urban et al., 2016). The reduction of Ascl1 protein levels in active RGLs is essential for their ability to switch off Ascl1-induced proliferation genes, and return to quiescence, and also to allow proliferating progenitors to progress towards neuronal differentiation (Urban et al., 2016). Protein-level regulation of Ascl1 in

RGLs is therefore crucial for maintaining the stem cell pool and allowing the proper progression of neurogenesis.

1.6.4 FoxO3

Most of the transcription factors involved in NSC activity promote the expression of genes involved in activation such as cell cycle genes, and quiescence is achieved by the inhibition of these factors. As previously discussed, IGF/Akt signalling can induce proliferation of NSCs in adult neurogenic niches. Part of the mechanism for this may be due to inactivation of the forkhead transcription factor FoxO3. FoxO3 has been identified as a 'quiescence factor' expressed in Sox2+ cells and required to maintain self-renewal of SGZ and SVZ neural stem cells, as FoxO3 ablation results in loss of the stem cell pool (Renault et al., 2009; Paik et al., 2009). IGF/Akt signalling phosphorylates FoxO3, causing it to be excluded from the nucleus, resulting in loss of FoxO3 activity (Tzivion et al., 2011) and therefore loss of NSC quiescence. Interestingly, the gene targets of FoxO3 have been shown to include genes involved in glucose metabolism and metabolic enzymes (Yeo et al., 2013). Metabolic changes can directly activate NSCs in adult neurogenic niches (Beckervordersandforth, 2017), raising the possibility that FoxO3 may induce quiescence via regulating NSC metabolism. Another potential mechanism of FoxO3-mediated quiescence is by competition with Ascl1 for DNA binding of target genes. ChIP-seq analysis has shown that FoxO3 shares many transcriptional targets with Ascl1 (Webb et al., 2013), suggesting when FoxO3 is in the nucleus, it acts as a repressor of Ascl1 target genes by physically blocking Ascl1 binding.

1.6.5 Pten

Upstream of Akt signalling, phosphatase and tensin homologue (Pten) is required to maintain quiescence of RGLs (Bonaguidi et al., 2011). Pten is a tumour suppressor, and has been shown to be crucial for quiescence and long-term maintenance of the stem cell pool, by supressing self-renewing symmetric divisions and by gating G0-to-G1 cell cycle entry in neural stem cells as well as other adult stem cells such as satellite cells (Bonaguidi et al., 2011; Groszer et al., 2006; Yue et al., 2017). Deletion of Pten in RGLs of the adult DG leads to activation from quiescence and an increase in symmetric self-renewal, however the subsequent differentiation of RGLs leads to

depletion of the pool over time (Bonaguidi et al., 2011). This is in contrast to Pten deletion in SVZ NSCs, where an expansion of the stem cell pool is not negated by increased differentiation, leading to a net increase in neurogenesis over time (Gregorian et al., 2009). Mechanistically, Pten dephosphorylates Akt, thereby inhibiting its activity including repression of FoxO3 (Song et al., 2012b).

1.6.6 Cell cycle proteins; p21, p27, p57

The entry into and exit from quiescence is dynamically regulated in concert with the cell cycle. Quiescent NSCs in *Drosophila* have different activation dynamics depending on the stage of the cell cycle in which they are arrested - G2 or G0 - and the entry into G2 quiescence involves the degradation of Cdc25 (Otsuki and Brand, 2018). Therefore, the regulation of cell cycle genes is likely to be intimately associated with the regulation of NSC quiescence and activation. The cyclin-dependent kinase inhibitors p27 and p57 are expressed in quiescent (Ki67 negative) Sox2-expressing and Nestin+GFAP+ RGLs in the adult DG, and p21 is expressed in NSCs in the adult SVZ, where they are reported to be required for long-term NSC maintenance and to maintain NSC quiescence by inhibiting the cell cycle (Andreu et al., 2015; Furutachi et al., 2013; Kippin et al., 2005; Marques-Torrejon et al., 2013; Porlan et al., 2013). Loss of p57 or p27 in RGLs of adult mice leads to a loss of RGL quiescence and subsequent increase in neurogenesis (Andreu et al., 2015; Furutachi et al., 2013), and p57 is reduced in the nuclei of RGLs in exercising mice, indicating it can be regulated by environmental neurogenic stimuli (Furutachi et al., 2013).

1.6.7 REST

Another factor identified to directly repress activation genes is the transcriptional repressor REST (repressor element 1-silencing transcription). REST functions in embryonic NSCs to repress the expression of neuronal genes (Ballas et al., 2005), and is expressed in quiescent and active NSCs of the adult DG where it is required to maintain NSCs in a quiescent and undifferentiated state (Gao et al., 2011; Mukherjee et al., 2016), partly via repression of *Ascl1* expression (Gao et al., 2011).

1.6.8 NFIX

Another transcription factor that can directly induce a quiescent neural stem cell state is NFIX. NFIX is highly expressed in quiescent adult hippocampal NSCs both *in vitro* and *in vivo*, and is bound to many active enhancers in BMP4-induced quiescent NSCs *in vitro* (Martynoga et al., 2013). Suppression of NFIX in the BMP4-induced quiescent culture model shows more than a third of the genes induced by BMP4 are also regulated by NFIX (Martynoga et al., 2013), regulating the expression of genes central to the quiescent cell state, including genes involved in cell junctions, cell adhesion and carbohydrate metabolism. Moreover, NFIX-null mice develop defects in RGL positioning and morphology in the SGZ, in addition to an increase in proliferation of NSCs (Martynoga et al., 2013), suggesting that cell adhesion and cell-contacts are important regulators of NSC quiescence.

1.6.9 Id proteins

The inhibitor of differentiation (Id) family of proteins play an important role in embryonic neurogenesis, by inhibiting the action of proneural bHLH transcription factors (Jung et al., 2010), and they are beginning to be identified as potential regulators of neural stem cell maintenance in adult neurogenic niches. I will therefore next describe what is currently known the expression, regulation and function of the Id proteins, particularly with their role in neurogenesis.

1.7 The Inhibitor of Differentiation proteins

1.7.1 Structure and conservation of Id proteins

Id proteins are evolutionarily conserved molecules, found in *Drosophila* to humans. There are four identified Id proteins in mammals, Id1-4, whilst *Drosophila* have just one, Extra macrochaetae (Emc). The defining feature of Id proteins is the HLH domain, which has extensive sequence homology between the four mammalian Ids, as well as the lack of DNA-binding domain, differentiating Ids from the bHLH transcription factors (Ling et al., 2014). The HLH domain mediates dimerization of the Ids with bHLH proteins. Due to the lack of DNA-binding domain in Id proteins, dimerization of Ids with bHLHs results in dominant-negative inhibition of bHLH function. Interestingly, there is

limited homology between the four Ids outside of the HLH domain, with 7-24% amino acid differences, which may reflect the surprising lack of redundancy between the factors (Patel et al., 2015) (Figure 1.7). Id4 is the longest protein out of the Id family, although only the first 2 out of 3 exons are protein coding; the 3rd exon is a 3'untranlsated region. Id4 is in fact the most divergent of the family, with many amino acid variations in the N- and C-terminal domains, suggesting it is in fact a remote homologue of Id1-3, and may have unique functions (Patel et al., 2015).

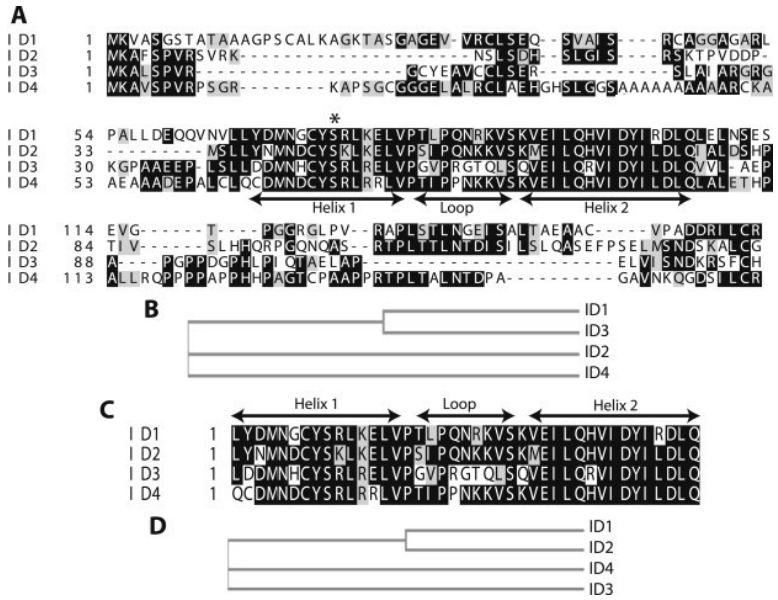

Figure 1.7. Conservation of Id1-4 protein sequence.

A. Protein sequence alignments for the four mammalian Id proteins. High level of conservation can be seen for the helix-loop-helix domains between the four Id proteins, whilst the alanine-rich N-terminal and proline-rich C-terminal domains are more divergent, particularly for Id4. Conserved residues are highlighted in black and grey. **B.** The divergence of Id4 in terms of full protein sequence can be seen by phylogenetic analysis. Id1 and Id3 are more closely related in terms of structural homology, while Id2 and Id4 are more diverged. **C.** Protein sequence alignment for only the HLH domain of Id1-4. **D.** The phylogenetic relationship based on just the HLH domain shows now that Id1 and Id2 are more closely related, whilst Id3 and Id4 are more diverged. Overall Id4 is the most diverged Id protein based on protein sequence. Reproduced from (Sharma et al., 2015) with permission of the rights holder, Elsevier.

1.7.2 Expression of Id proteins in embryonic and adult CNS

The Id genes and proteins have complex expression patterns and dynamics during embryonic development and in the adult mouse (Jen et al., 1997). Id knockout mice have provided some insight into the wide-reaching functions of Ids during development, with roles including (but not limited to) angiogenesis, heart development, mammary gland development, and haematopoiesis (Yuan et al., 2015). *Id2* mRNA is mostly ubiquitously expressed during development, which reflects the fact Id2 knockout mice have the most severe phenotype of all the Id KO mice (Yokota et al., 1999). During embryonic neurogenesis, Id1 and Id3 are expressed in dividing neuroblasts and have nearly overlapping expression patterns (Jen et al., 1997). This may confer redundancy, as the Id1 or Id3 single null mutants show no neural phenotype, whereas Id1/Id3 double knockout mice have smaller brains than littermates, likely as a result of premature neuronal differentiation, as well as altered glucose and lipid metabolism, and ultimately embryonic lethality (Lyden et al., 1999). *Id4* mRNA has a significantly different expression pattern than the other Ids during embryonic development, primarily expressed in the central nervous system, and complementary to the other Id genes (Jen et al., 1997). Id4 null mice present with growth retardation and premature neuronal differentiation, which results in the adult brain being severely reduced in size, with fewer neurons and glia (Ruzinova and Benezra, 2003). *Id4* expression is also observed in several adult human tissues including the brain, thyroid, testis and pancreas (Rigolet et al., 1998) and plays a central role in mammary gland development and ovary function in mice (Best et al., 2014; Dong et al., 2011). The divergent expression patterns of the four Ids during development may explain the lack of redundancy and different phenotypes in the single embryonic null mice (Yuan et al., 2015).

In the adult CNS, GFAP+ NSCs in the SVZ have been shown to highly express Id1, with expression decreasing in differentiating neuroblasts (Nam and Benezra, 2009). Id1 expression was found to be higher in TAPs, but lower in non-dividing quiescent NSCs, suggesting Id1 promotes a self-renewing stem cell identify in NSCs in the adult (Nam and Benezra, 2009). Id1 was also found to be expressed in RGLs in the DG, but it was not shown whether Id1 was higher in active or quiescent RGLs, and its function in RGLs was not explored (Nam and Benezra, 2009). Id3 expression is detected in a small population of proliferating cells in the DG, and highly expressed in neurospheres

derived from the hippocampus (Bonaguidi et al., 2008), however it was not directly assessed whether Id3 is expressed specifically in NSCs, nor was its function explored. In the SVZ, Id3 is expressed in almost all NSCs and proliferating progenitor cells (Bohrer et al., 2015). Id4 expression has not yet been reported in the adult neurogenic niches, however in single-cell RNAseq analysis of the transcriptional signature of quiescent-to-active NSCs in the DG, Id4 was shown to be the top most enriched gene in quiescent RGLs (Shin et al., 2015).

1.7.3 Regulation of Id expression

The expression of *Id1-4* is induced by BMP/Smad signalling in a variety of cell types (Lasorella et al., 2014; Ling et al., 2014). Id4 for example is a direct downstream target of BMP4 in neural progenitor cells (Samanta and Kessler, 2004). *Id* expression can also be induced by receptor tyrosine kinase signalling, including EGF and FGF2 (Lasorella et al., 2014). Notch signalling in murine embryonic stem cells has also been shown to induce the expression of the Id proteins (Meier-Stiegen et al., 2010). Id proteins are also highly regulated at the protein levels, and have a short half-life, with Id1-3 degraded by the ubiquitin-proteasome pathway (Bounpheng et al., 1999; Lasorella et al., 2014). Id4 can also be degraded via the ubiquitin-proteasome pathway, however it is less sensitive to this form of degradation, and it is not known which protein mediates its degradation (Bounpheng et al., 1999; Lasorella et al., 2014). Interestingly, Id1-3 have been shown to be inhibited by Id4 itself by heterodimerisation (Sharma et al., 2015), and Id4 may in fact promote E47 activity when the ratio of Id proteins favours Id4 (Sharma et al., 2015). The expression of Id genes and stability of the proteins is also affected in the context of cancer by a variety of mechanisms (Lasorella et al., 2014), highlighting the complexity of regulation of the Id genes.

1.7.4 Function of Id proteins

1.7.4.1 Inhibition of Class II bHLH factors and E-proteins by Id proteins

E-proteins were first identified as dimeric transcription factors that regulate the IgG enhancer in B cells, and found to bind to Ephrussi-box sequences of DNA (CANNTG), and hence termed E-proteins. *Drosophila* harbour a single E-protein, Daughterless (Da), whilst mammalian E-proteins consists of E12 and E47, generated by alternative

splicing of the *E2A* gene (also known as TCF3), E2-2 (TCF4), and HEB (TCF12). E-proteins are expressed in many different cell types and have a wide range of functions. E12 or E47 homodimers for example can inhibit proliferation by inducing the expression of CDKIs such as p15, p16, p21, p27 and p57. However, they are well known as functional heterodimer partners of the class II bHLH transcription factors, which includes MyoD in muscle stem cells, TAL1 in HSCs, and Ascl1in NSCs. It is thought that E-proteins stabilise bHLH monomers, and facilitate DNA-binding specificity of bHLHs, mediating their diverse tissue- and timing-specific activities. The Id proteins also function independently of E-proteins or bHLH inhibition. Id2 directly interacts with retinoblastoma (Rb) protein during development, inactivating Rb and subsequently enabling cell-cycle progression (Lasorella et al., 2000).

Despite the ability of Id proteins to inhibit class II bHLH TFs via direct binding of the HLH domain, it is thought that they predominantly bind E-proteins, thereby out-competing class II bHLHs for their heterodimerisation partner and rendering them unable to bind their DNA targets (Duncan et al., 1992) (Figure 1.8). It is certainly true that Id1 has a higher binding affinity for E-proteins than bHLH transcription factors (Ruzinova and Benezra, 2003).

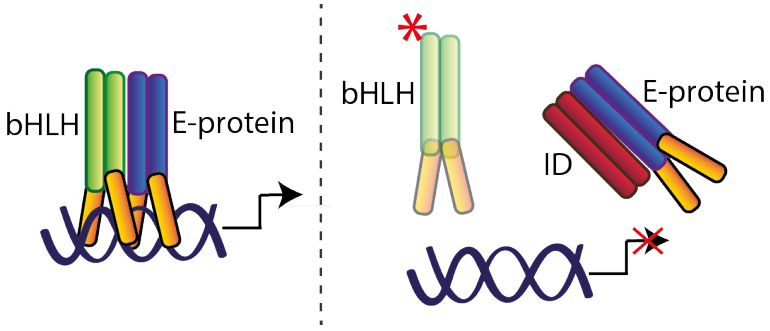

Figure 1.8. Protein-protein interactions between IDs, Class II bHLHs and E-proteins

Left panel: In the absence of Id proteins, Class II bHLH proteins (green) and E-proteins (blue) heterodimerise via their HLH domains, mediating binding of bHLH factors to their target DNA via their DNA binding domains (orange) and activating gene expression. Right panel: When Id proteins (red) are expressed at a sufficient level, they sequester the E-proteins, leaving bHLH factors undimerised and unable to bind their target DNA, and targeted for ubiquitin-proteasomal mediated degradation (red asterisk).

1.7.4.2 The role of Id proteins in stem cell maintenance

The classical role of Id proteins is, as their name suggests, inhibiting the differentiation of stem cells. Ids also often promote stem cell proliferation, therefore are considered important factors for stem cell maintenance (Ling et al., 2014). As described above, Id proteins block E-protein function (Peverali et al., 1994), which in turn inhibits E-protein mediated differentiation (Ling et al., 2014). Id-mediated inhibition of E-proteins will also indirectly block the E-protein induction of CDKIs, thereby promoting cell cycle progression (Yuan et al., 2015). The Id proteins have been reported to regulate stem cell self-renewal in a number of different ways. Id1, Id2 and Id4 promote self-renewing proliferation of cortical NSCs, and inhibit their neuronal differentiation, via interfering with binding of NeuroD/E47 complexes to their DNA targets (Jung et al., 2010). Id1 and Id2 are also required for NSC self-renewal in the embryonic telencephalon, by repressing the expression of cell adhesion regulator *Rap1GAP*, thereby preventing the delamination and migration of progenitors from the ventricular surface (Niola et al., 2012). Id1, Id2 and Id3 expression at low levels maintain stemness of NSCs by sustaining expression of Hes1, by blocking Hes1 auto-repression (Bai et al., 2007). Moreover, Id2 and Id4 contribute to maintenance of the undifferentiated state of NSCs by suppressing oligodendrocyte commitment via inhibition of the bHLHs Olig1 and Olig2 (Samanta and Kessler, 2004). These studies demonstrate the variety of ways in which Id proteins can regulate stem cell maintenance.

Due to their regulation of stem cell maintenance and proliferation, Id proteins also play major roles in oncogenic pathways, and are overexpressed in many cancer cell types, including glioblastoma (Lasorella et al., 2014; Ling et al., 2014). Id1 for example, is required for glioma stem cell maintenance via to adherence to their vascular niche, by blocking E-protein induction of the *rap1gap* gene (Niola et al., 2013). Expression of all four Ids have been shown to be individually increased in separate studies of brain cancer tissue analyses (Lasorella et al., 2014), which highlights their powerful function in neural stem cell maintenance. Interestingly, Id3 and Id4 act as tumour suppressors in some circumstances (Wang and Baker, 2015). Id4 for example is epigenetically silenced in a wide variety of cancers (Patel et al., 2015), including glioblastoma (Martini et al., 2013). The expression of Id proteins in adult gliomas suggests they could be expressed in and have functional importance in regulating adult NSCs.

The function of the Id proteins has not been extensively explored in the adult neurogenic niches. As mentioned above, Id1 expression is specifically high in SVZ NSCs (Nam and Benezra, 2009), and ablation of Id1 and Id3 (but not Id1 alone) reduces the self-renewal capacity of the NSCs (Nam and Benezra, 2009). Id1 is also reported to be expressed by GFAP+ RGLs in the SGZ, although its function in SGZ NSCs has not yet been explored (Nam and Benezra, 2009). Id1 has, however, been demonstrated to be expressed mostly in quiescent NSCs of the adult zebrafish pallium, where it is sufficient and necessary to promote NSC quiescence (Rodriguez Viales et al., 2015). As in the embryonic brain, Id1 and Id2 have been demonstrated to repress the expression of *Rap1Gap* in NSCs of the postnatal SVZ, thereby promoting adhesion of the stem cells to their niche (Niola et al., 2012), a property that is vital for maintaining NSC quiescence (Ottone et al., 2014). Id3 is expressed in SVZ NSCs and progenitors downstream of BMP2 signalling, where it represses E47 to promote astrocytic differentiation of SVZ NSCs following injury but is indispensable for normal NSC and progenitor cell functioning (Bohrer et al., 2015).

Ascl1 is an essential transcription factor for activation of adult neural stem cells from quiescence and proliferation of progenitors (described in Section 1.7.3) and as a Class II bHLH transcription factor, is a prime target for negative regulation by Id proteins (Figure 1.8). Such negative regulation has been demonstrated to occur in embryonic neural progenitor cells (Shou et al., 1999) and in an *in vitro* culture system of neuroendocrine lung cancer cells, in which BMP2 induces the expression of Id1, which in turn outcompetes Ascl1 for its E-protein binding partner E47 (Vinals et al., 2004). Interestingly, this mechanism inhibits Ascl1 function not only by inhibiting its DNA binding, but also by destabilising Ascl1 and promoting its degradation (Vinals et al., 2004). The authors demonstrate that it is the balance of Id-to-E proteins that regulates Ascl1 activity and stability. Considering the central role for Ascl1 in adult NSC activity, and the emerging expression of Id proteins in neurogenic niches, it would be highly interesting to investigate whether this relationship exists in adult neural stem cells. This is particularly fascinating in light of a recent study using mathematical modelling, which suggests Id proteins can potentiate the transcriptional repression of Ascl1 in quiescent NSCs by blocking the auto-repression of Hes gene expression (Boareto et al., 2017), much like that which was observed in embryonic NSCs between Id1-3 and Hes1 (Bai et al., 2007).

1.8 Aims of the present work

Stem cells in adult tissues, including neural stem cells of adult neurogenic niches, must balance long-term production of progenitors while minimising the accumulation of genetic and metabolic damage, in order to maintain the stem cell pool. Excessive stem cell activation would result in premature exhaustion of the stem cell pool, whilst too little activation would result in a deficit of new-born cells for the tissue, impairing tissue homeostasis. Dynamic and stringent regulation of the switch between stem cell quiescence and activation is essential for the stem cell pool to appropriately respond to the demands of the tissue.

The discovery of neural stem cells in dedicated niches in the adult mammalian brain has revealed the prospect that the brain may have endogenous regenerative capabilities. This has exciting clinical potential, for example tapping into the pool of quiescent neural stem cells to regenerate hippocampal neurogenesis in neurodegenerative conditions, or understanding the niche signals required to sustain and differentiate transplanted stem cells. Similarly, delineating the environmental and systemic stimuli that regulate NSC activity, and how these change with age to increase NSC quiescence, could enable possibly simple treatments for mitigating age-related cognitive decline. A thorough understanding of the molecular regulation of NSC quiescence also has implications for the prognosis and treatment of brain cancer, due to the existence of cancer stem cells in gliomas, with similar molecular mechanisms regulating quiescence and proliferation to endogenous neural stem cells.

Several different extrinsic signals and intrinsic factors have been identified to regulate adult neural stem cell activity, however the precise regulation of NSC quiescence is not fully understood. Previous work from the Guillemot laboratory has identified the bHLH transcription factor Ascl1 as a crucial activation factor for NSCs in the SGZ (Andersen et al., 2014), and regulation of Ascl1 at the protein level is required to allow NSCs to return to quiescence (Urban et al., 2016). However, the molecular mechanism maintaining NSC quiescence is unclear. Therefore, the aim of my PhD research is to elucidate the molecular mechanisms regulating adult hippocampal neural stem cell (AHNSC) quiescence. Specifically, I aim to investigate AHNSC quiescence in the following ways:

1. Identify novel ‘quiescence factors’ involved in regulating adult hippocampal neural stem cell quiescence downstream of BMP4.
2. Investigate the mechanism by which these ‘quiescence factors’ regulate neural stem cell quiescence, particularly with regards to the regulation of Ascl1.
3. Determine which hippocampal niche signals regulate the newly-identified quiescence factors.

Chapter 2. Materials & Methods

2.1 Experimental model and subject details

2.1.1 Mouse models

All procedures involving animals and their care were performed in accordance with the guidelines of the Francis Crick Institute, national guidelines and laws. This study was approved by the Animal Ethics Committee and by the UK Home Office (PPL PB04755CC). Mice were housed in standard cages under a 12h light/dark cycle, with ad libitum access to food and water.

All experimental mice were of a mixed genetic background. Founder mice were bred to MF1 mice, and then backcrossed to littermates of the F1 generation. In order to generate mice with a hippocampal stem cell-specific, tamoxifen-inducible recombination, plus a YFP reporter of recombination, GLAST-CreERT2 (Slc1a3$^{tm1(cre/ERT2)Mgoe}$) (Mori et al., 2006) mice were crossed with Rosa26-floxed-stop-YFP (RYFP; Gt(ROSA)26Sor$^{tm1(EYFP)Cos}$) (Srinivas et al., 2001) mice. These mice were then crossed with our experimental strains:

Smad4flx (Smad4^{tm1Rob}) mice, originally reported by (Chu et al., 2004).
RBPJkflx (Rbpj^{tm1Hon}) mice, originally reported by (Han et al., 2002).
Ascl1Venus (Ascl1$^{tg1(venus)Rik}$) mice, originally reported by (Imayoshi et al., 2013).
Ascl1KiGFP (Ascl1^{tm1Reed}) mice, originally reported by (Leung et al., 2007).
Id4flx mice, originally reported by (Best et al., 2014).
Glast-CreERT2 mice were crossed with Gt(ROSA)26Sor$^{tm9(CAG-tdTomato)Hze}$ (tdTomato), originally reported by (Madisen et al., 2010).

Glast-CreERT2;Smad4flx;RYFP mice were crossed with Glast-CreERT2;RBPJk;RYFP mice in order to generate the quadruple transgenic Glast-CreERT2;Smad4flx;RBPJkflx;RYFP line.

Both male and female mice were used for all *in vivo* genetic studies. Experimental groups were a mix of animals from different litters for each particular strain. All mice were injected with tamoxifen at postnatal day 60 +/- 2, and brain tissue collected by transcardial perfusion at 2, 5, 10 or 30 days after the first injection.

2.1.2 Primary Cell Cultures

For the derivation of adult hippocampal stem cell lines, 7-8-week-old mice were sacrificed and the dentate gyrus dissected (previously described by Walker et al., 2013). Cultures were amplified as neurospheres for two passages before dissociation to adherent cultures. Cells were propagated in basal media (DMEM/F-12 + Glutamax (Invitrogen 31331-093) + 1x Neurocult Supplement (Stem Cell Technologies, 05701) + 1x Penicillin-Streptomycin (ThermoFischer Scientific, 15140)+ 2μg/mL Laminin (Sigma, L2020) + 20ng/mL FGF2 (Peprotech, 450-33) + 20ng/mL EGF (Peprotech, 315-09) + 5μg/mL Heparin (Sigma, H3393-50KU). Cells were incubated at 37°C, 5% CO_2.

The control adult hippocampal neural stem cell line (AHNSC line #5) was derived from a single male WT/RYFP mouse. AHNSC Ascl1Venus cell line was derived from a single male Ascl1$^{wt/Venus}$ mouse. Huwe1 is X-linked, therefore AHNSC Huwe1flx cell line was derived from a male Glast-CreERT2$^{wt/wt}$; Huwe$^{fl/Y}$;Rosa$^{YFP/YFP}$ mouse.

2.2 Method Details

2.2.1 Tamoxifen administration

To induce activation of CreERT2 recombinase, 2mg (57-67mg/Kg) of 4-hydroxytamoxifen (Sigma, H6278) was administered intraperitoneally (ip) to mice at postnatal day 60 (P60), at the same time each day for 5 consecutive days. For in situ hybridization experiments, Glast-CreERT2;tdTomato (Ai19) mice received a single injection at postnatal day 60 +/- 2, and brain tissue collected by transcardial perfusion 48h later.

2.2.2 Tissue preparation and immunofluorescence

Mice were transcardially perfused with phosphate-buffered saline (PBS) for 3mins, followed by 4% paraformaldehyde (PFA) in PBS for 12mins. Brains were post-fixed for 2hours in 4% PFA at 4°C and washed with PBS. Brains were coronally sectioned at a thickness of 40μm using a vibratome (Leica).

For *in situ* samples, mice were perfused with PBS for 3mins, followed by perfusion with 10% neutral buffered formalin (NBF) for 12mins. Brains were post-fixed in 10% NBF at room temperature for 16-32h, and then washed with and stored in 70% EtOH. Brains were paraffin embedded, and coronally sectioned at a thickness of 5μm.
Cultured cells were fixed with 4%PFA in PBS for 10mins at room temperature, and washed with PBS.
For immunofluorescence of tissue, samples were blocked with 10% normal donkey serum (NDS) in 1%Triton-PBS for 2hrs at room temperature with rocking. Fixed cells were blocked with 10%NDS in 0.1%Triton-PBS for 1hr at room temperature. Primary antibodies were diluted in 10%NDS in 0.1%Triton-PBS, and incubated with samples overnight at 4°C with rocking. The following day, samples were washed 3x 0.1%Triton-PBS, and then incubated with secondary antibodies diluted in 10%NDS in 0.1%Triton-PBS for 2hrs at room temperature with rocking. Following 3x 0.1%Triton-PBS washes, samples were incubated with DAPI 1:10,000 in 1:1 PBS:H_2O for 30mins at room temperature with rocking. Primary and secondary antibodies are listed Table 2.1

EdU was detected following secondary antibody incubation and 3x 0.1%Triton-PBS washes, using Click-iT™ EdU Alexa Fluor 647 Imaging Kit (Invitrogen, C10340), following manufacturer's instructions.

O-propargyl-puromycin (OPP), was detected following secondary antibody incubation and 3x 0.1%Triton-PBS washes, using Click-iT™ Plus OPP Alexa Fluor 647 Protein Synthesis Assay Kit (Invitrogen, C10458), following manufacturer's instructions.
For MitoTracker™ detection, the MitoTracker™ reagent fluoresces in the far-red spectrum without the need for detection, therefore samples were processed as normal without using far-red secondary antibodies.

For RNA staining with Pyronin Y (PY), following all antibody incubations and DAPI staining, cells were washed 1x in 50% PBS-H_2O. 10mM PY stock was diluted 1:10,000 in 50% PBS-H_2O and incubated on coverslips for 10mins at room temperature, followed by 2x 50%PBS-H_2O washes.

To immunostain for BrdU-labelled NSCs, the following steps were taken to prevent false detection of EdU by the anti-BrdU antibody (as described in (Liboska et al., 2012)). Following detection of EdU labelling with the Click-iT™ detection kit described above,

coverslips were washed 3x with PBS, followed by incubated with a non-fluorescent azide molecule (azidomethylphenylsulfide) diluted to the same concentration as the azide dye used for EdU detection, in the same buffer mix from the EdU Click-iT™ detection kit, for 30mins at room temperature. This should block any EdU that was not previously stained with the fluorescent azide. Coverslips were then incubated in 10mM sodium ascorbate plus 4mM copper(ii)sulphate for 10mins at room temperature. This treatment should cause oxidative damage to the DNA, generating gaps in which the Anti-BrdU antibody can bind its antigen. Next the coverslips were incubated with 20mM EDTA for 30mins at room temperature, then washed 3x with PBS. Finally, coverslips were incubated with Anti-BrdU antibody diluted in PBS without Triton, in the presence of Exonuclease iii, which further elongates the gaps in the DNA enabling the antibody to permeate the DNA to better detect BrdU.

To mount the immunostained samples, brain sections were arranged onto a slide in 50% PBS-H_2O, the PBS-H_2O carefully aspirated. Aqua Polymount (Polysciences, 18606) was applied to the edge of the samples and a glass coverslip carefully placed over the top in a manner to cover the samples with Aqua Polymount medium, and left in the dark to dry overnight at room temperature. For mounting fixed cells, a ‘dot’ of Aqua Polymount was applied to a glass slide and the coverslip carefully placed on top, cell-side down, and left in the dark to dry overnight at room temperature.

2.2.3 RNA *in situ* hybridization

For RNA *in situ* hybridization, the RNAscope® Multiplex Fluorescent Reagent Kit V2 (ACD Bio-Techne, 323110) was used with NBF fixed-paraffin embedded 5μm sections, and stained according to the standard company protocol. Target retrieval was performed for 15mins, and Protease Plus treatment was carried out for 30mins. For dual RNAscope®-immunofluorescence, following the development of HRP-C3 signal and wash steps, slides were washed in distilled H_2O, and washed 3x 5mins in 0.1%Triton-PBS at room temperature. Slides were then processed for immunofluorescence as described above (without “rocking”; reagents were incubated *in situ* on the slides). Probes and fluorophores and their dilutions are listed Table 2.1.

2.2.4 Microscopic analysis

All images were acquired using an SP5 confocal microscope (Leica). For cell culture immunofluorescence, 3 random regions of each coverslip were imaged with a z-step of 1μm. For adult tissue immunofluorescence, both left and right dentate gyri of every twelfth 40μm section along the rostrocaudal length of the DG were imaged, with a z-step of 1μm through the whole 40μm section. For quantification of %+ RGLs, at least 200 RGLs in each of at least 3 mice for each genotype were quantified.

RGLs were identified based on their characteristic morphology (nucleus in the subgranular zone, radial process projecting through the molecular layer) and positive labelling with GFAP and GFP in the case of Glast-CreERT2;RYFP recombined cells, or tdTomato positivity in the case of Glast-CreERT2;tdTomato recombined cells.

2.2.5 Cell treatments

For culturing adult hippocampal NSCs in proliferation conditions, cells were grown in basal media (DMEM/F-12 + Glutamax (Invitrogen, 31331-093)) + 1x N2 supplement (R&D Systems, AR009) + 1x Penicillin-Streptomycin (ThermoFischer Scientific, 15140) + 2μg/mL Laminin (Sigma, L2020) + 5μg/mL Heparin + 20 ng/mL, and supplemented with either 20ng/mL EGF (Peprotech, 315-09) plus 20ng/mL FGF2 (Peprotech, 450-33), or 20ng/mL FGF2 alone. NSCs were propagated in supplemented basal media in laminin-coated flasks until 80% confluent, at which point they were passaged or frozen down. For freezing, NSCs were detached from their flask using Accutase (Sigma, A6964), centrifuged and the pellet resuspended in 10% DMSO in fully supplemented basal media, and chilled slowly to -80°C before being transferred to liquid nitrogen for long-term storage.

In order to transition cells from basal media containing both 20ng/mL EGF and 20ng/mL FGF2, to 20ng/mL FGF2 alone, cells were grown in T75 flasks until 80% confluent in the presence of both EGF and FGF2, at which point the media was aspirated and replaced by fresh supplemented media containing only 20ng/mL FGF2. Cells were incubated at 37°C, 5% CO_2, for 2-3 days before passaging. Cells were passaged in the presence of FGF2-alone for at least two passages before being used for experiments, in order to allow the cells to adjust to the conditions and to select for the self-renewing stem cells.

To induce quiescence, cells were plated onto laminin-coated P6 well plates (200,000 cells/well) or onto laminin-coated coverslips (40,000 cells/well) in the presence of 20ng/mL EGF+FGF2 or 20ng/mL FGF2 alone and incubated overnight to allow cells to adhere. Media was replaced the next day with basal media plus 20ng/mL recombinant mouse BMP4 (R&D Systems, 5020-BP), and cultured for 72h at 37°C, 5% CO_2. For culturing NSCs long term in a quiescent state, $1x10^6$ cells were seeded into a laminin-coated T75 flask in the presence of 20ng/mL FGF2. 24hrs later the media was refreshed containing 20ng/mL FGF2 + 20ng/mL BMP4. The media was refreshed every 3 days to ensure continuous BMP4 signalling, and the cells were passaged 1:3 into a new T75 flask when necessary (around once per week) to avoid the cells becoming too dense.

To titrate the concentration of FGF2 in NSCs, cells were plated as described for inducing quiescence. Following overnight incubation to allow of adherence of cells to the culture dish/coverslip, the media was replaced with fresh basal media supplemented with either 20ng/mL, 10ng/mL, 5ng/mL or 2.5ng/mL FGF2, and cultured for 72h before lysing cells for RNA extraction (from P6 wells) or fixing cells on coverslips with 4% PFA for immunocytochemistry.

To titrate the concentration of BMP4 in NSCs, cells were plated as described for FGF2 titration, and then cultured in the presence of 20ng/mL FGF2 plus either 20ng/mL, 10ng/mL, 5ng/mL or 1ng/mL BMP4, for 72h. After this time cells were lysed from P6 wells for RNA extraction, and cells on coverslips fixed with 4% PFA for immunocytochemistry.

To test that BMP4-induced cells could reactivate and differentiate, NSCs treated with 20ng/mL BMP4 + 20ng/mL FGF2 for 72h were detached from their flask using Accutase (Sigma, A6964) and re-plated into laminin-coated P6 wells (200,000 cells/well) for RNA extraction, or onto laminin coated coverslips in P24 wells (40,000 cells/well) in the presence of EGF+FGF2 or FGF2 alone. Re-plated cells were cultured for 24h, 48h or 72h and then fixed with 4% PFA and processed for immunocytochemistry, or the cells lysed for RNA extraction.

In order to test the multipotency of NSCs following reactivation, reactivated NSCs were cultured on laminin-coated coverslips in P24 well plates at a density of 40,000 cells/well,

for 72h in 20ng/mL EGF + 20ng/mL FGF2 or 20ng/mL FGF2 alone, to allow for full reactivation. At this point the media was changed to basal media supplemented with 10ng/mL FGF2 and NSCs cultured for 48h. After 48h the media was changed once again to basal media supplemented with 2% foetal bovine serum (Invitrogen, 10270-106) without EGF or FGF2. NSCs were cultured for a further 72h, at which point the cells were fixed and processed for immunocytochemistry.

In order to label cells in S-phase, 0.5μL of 10mM EdU (Invitrogen, C10340) was added to the media of cells on coverslips in 500μL media in P24 wells and dispersed by swirling the plate, for a final concentration of 10μM. 10μM EdU was incubated with the cells for 1hr prior to fixation with 4% PFA, and then cells were processed for antibody staining and EdU detection as described in Section 2.2.2. For EdU/BrdU pulse-chase experiments described in Section 3.1.2, 10μM EdU or BrdU was added to the media on cells in P24 wells and incubated for 24h. To label nascent protein synthesis, cells on coverslips were incubated with 50μM O-propargyl-puromycin (OPP) in DMSO, for 1hr prior to fixation with 4% PFA, and then processed for antibody staining and OPP detection as described in Section 2.2.2. In order to label the mitochondria of NSCs in culture, cells on coverslips were incubated with 30nM MitoTracker™ reagent diluted in DMSO, for 1hr prior to fixation with 4% PFA.

To inhibit the proteasome, cells were grown on laminin-coated 10cm diameter dishes for 72h in supplemented basal media with either just 20ng/mL FGF2 or FGF2 + 20ng/mL BMP4. Cells were treated with either 10μM MG132 (Sigma, SML1135) or an equal volume of DMSO (Sigma), for 30, 60 or 120mins, at which point the cells were lysed and processed for Western blot as described in Section 2.2.10.

For experiments in which Notch signalling was inhibited in NSCs, cells were plated onto laminin-coated P6 wells at a density of 200,000 cells/well, or onto laminin-coated coverslips in P24 well plates at a density of 40,000 cells/well. Media was refreshed 24h later to either 20ng/mL FGF2 alone or FGF2 plus 20ng/mL BMP4, and incubated for a further 72h to induce quiescence in BMP4-treated NSCs. After this time, 1uM of the gamma-secretase inhibitor LY411575 (LY) in DMSO (diluted from a stock of 10mM), or an equivalent volume of DMSO without LY was added to the culture medium on the cells. NSCs were then incubated for a further 72h before being lysed or fixed for analysis.

2.2.6 Constructs, plasmid transfection and viral transduction

For overexpression of Id4, Id1 and GFP in quiescent NSCs, cells were first cultured in laminin coated T75 flasks in the basal media supplemented with 20ng/mL FGF2 and 20ng/mL BMP4, for 72h. At this point, cells were detached using Accutase and counted. $5x10^6$ cells in suspension were used per construct for nucleofection using the Amaxa mouse neural stem cell nucleofector kit (Lonza, VPG-1004) and Amaxa Nucleofector II (Lonza), using the program A-033, according to manufacturer's instructions. For overexpression of Id4, the 6μg of pCbeta-Id4-FLAG construct was used, a kind gift from M. Israel (Rahme and Israel, 2015), which expresses Id4 from a CMV promoter and also expresses an N-terminal FLAG tag. This construct did not contain a fluorescent reporter, therefore in order to FAC sort Id4-transfected NSCs, cells were co-transfected with 3μg pCAGGS-IRES-GFP construct. These two constructs were nucleofected in a 2:1 concentration of Id4:GFP in order to increase the likelihood that GFP+ NSCs were also Id4+. For Id1 overexpression, quiescent NSCs were nucleofected with 3μg of pcDNA3-mId1-Venus (Addgene, Item ID #20966; originally reported in Nam et al., 2009) which expresses Id1 from a CMV promoter and also expresses a fluorescent Venus tag. To generate control quiescent cells overexpressing GFP, BMP4-treated NSCs were nucleofected with 2μg pMax-GFP (Lonza, VPG-1004). Following nucleofection, NSCs were plated into laminin-coated 1x P6 well ($2.5x10^6$ cells/well are plated although many cells die following nucleofection) and onto 4x laminin-coated coverslips in P24 wells ($0.625x10^6$ cells/well), in basal media supplemented with 20ng/mL FGF2 and 20ng/mL BMP4 and incubated at 37°C, 5% CO_2. The media was refreshed 24hr later in order to remove the dead cells, and cells were incubated for a further 24h. At this point cells in P6 wells were lysed into 1mL TriZol for RNA extraction, and cells on coverslips were fixed in 4% PFA for immunocytochemical analysis.

For overexpression of E47 and GFP in active NSCs, cells were first cultured in laminin coated T75 flasks in the basal media supplemented with 20ng/mL FGF2 for 72h. At this point, cells were detached using Accutase and counted. $5x10^6$ cells were used per construct as described above. For E47 overexpression, an expression construct was generated previously in the Guillemot lab by cloning E47 into pCAGGS-IRES-GFP via the EcroRV/Xho1 insertion site. 10μg of this construct was used to nucleofect active NSCs. To generate control active cells overexpressing GFP, NSCs were nucleofected with 2μg pMax-GFP (Lonza, VPG-1004). Following nucleofection, NSCs were plated as

described above, in basal media supplemented with 20ng/mL FGF2 and incubated at 37°C, 5% CO_2. The media was refreshed after 24h and cells were collected 48hrs post-transfection as described above.

To delete Huwe1 in NSCs derived from Huwe1 floxed transgenic mice, Huwe1 floxed cells were plated onto laminin coated coverslips in P24 wells at a density of 40,000 cells/well in the presence of 20ng/mL FGF2. 24hrs after plating, the media was replaced with media supplemented with 20ng/mL FGF2, or in 20ng/mL FGF plus 20ng/mL BMP4, and cultured for 72h. After this time, either the media was replaced with fresh media containing either empty adenovirus (Adeno-empty) or adenovirus expressing Cre recombinase (Adeno-Cre) at a concentration of 100 multiplicity of infection (moi) or number of virus particles per cell. The media was refreshed 24hrs post-transduction, and cells were incubated for a further 6 days to ensure complete degradation of the very stable Huwe1 protein, at which point the cells were fixed with 4% PFA for immunocytochemical analysis.

In order to overexpress Id4 in active NSCs by adenoviral overexpression, cells were plated onto laminin-coated P6 wells (200,000 cells/well), or onto laminin coated coverslips in P24 wells (40,000 cells/well) in the presence of 20ng/mL FGF2, and cultured for 24h. Media was replaced with FGF2-supplemented basal media containing adenovirus expressing mouse Id4 (Ad-m-ID4, Vector Biolabs) which expresses Id4 from the CMV promoter, at a concentration of 100 moi. Media was refreshed 24h post-infection, and cells were cultured for a further 20h in the presence of 20ng/mL FGF2 before being collected for analysis.

To delete Id4 in NSCs derived from the Id4 floxed transgenic mouse line, Id4 floxed cells were plated onto laminin-coated P6 wells (200,000 cells/well), or onto laminin coated coverslips in P24 wells (40,000 cells/well) in the presence of 20ng/mL FGF2, or in 20ng/mL FGF plus 20ng/mL BMP4, and cultured for 72h. After this time, either the media was replaced with fresh media (non-transduced control) or with fresh media supplemented with FGF2 and/or BMP4 plus 100moi with empty adenovirus (Adeno-empty) or 100moi adenovirus expressing Cre recombinase (Adeno-Cre), to induce recombination of the floxed Id4 locus, thereby genetically deleting Id4. Media was refreshed 24h post-transduction, and the cells collected for analysis 24hrs later.

2.2.7 FAC sorting

FACS tubes were pre-coated with 5%BSA-PBS at 37°C for at least 30mins prior to sorting. Cells were detached from flasks using Accutase (Sigma) and centrifuged at 0.3RCF for 5mins. Cell pellets were re-suspended in 750μL recovery media (5%BSA-PBS + 20 ng/ml FGF + 1μg/mL Heparin). 1μL propidium iodide was added to cell suspensions to check for cell viability. Cells were sorted on a FACS Aria III machine, into recovery media. Both GFP positive and negative cells were recovered into separate tubes.

2.2.8 RNA extraction, cDNA synthesis and QPCR

For FACS experiments, cells were lysed using Qiagen lysis buffer. For all other experiments, cells were lysed by direct addition of 700-1000μL Trizol reagent to the culture dish. RNA was extracted using RNeasy® Mini Kit (Qiagen, 74104) or Direct-zol™ RNA MiniPrep Kit (Zymo Research, R2052), according to manufacturer's instructions.

cDNA was synthesised using the High Capacity cDNA Reverse Transcription Kit (Applied Biosystems, 4387406) following manufacturer's instructions. Gene expression level was measured using TaqMan Gene expression assays (Applied Biosystems) and quantitative real-time PCR carried out on a QuantStudio Real-Time PCR system (ThermoFisher). Gene expression was calculated relative to endogenous controls Gapdh and ActinB, and normalised to the expression of the control sample in each group, to give a ddCt value.

QPCR probes		
ACTB QPCR probe	Applied Biosystems	Cat# 4352933E
Mm03058063_m1 Ascl1	Applied Biosystems	Cat# 4331182
Mm01279269_m1 Dll1	Applied Biosystems	Cat# 4331182
GAPDH QPCR probe	Applied Biosystems	Cat# 4352932E
Mm00775963_g1 Id1	Applied Biosystems	Cat# 4331182
Mm00711781_m1 Id2	Applied Biosystems	Cat# 4331182
Mm00492575_m1 Id3	Applied Biosystems	Cat# 4331182
Mm00499701_m1 Id4	Applied Biosystems	Cat# 4331182

Table 1. List of probes used for QPCR gene expression analysis

2.2.9 RNA sequencing and analysis

RNA concentration was quantified using the Qubit dsDNA BR/HS Assay Kit. A KAPA mRNA HyperPrep Kit (for Illumina) (KAPA Biosystems, Wilmington, MA, USA) was used with 1000ng of RNA diluted to a final volume of 50µl. Each RNA sample was captured with 50µl of capture beads at 65°C for 2 min and 20°C for 5 min. For the second capture, 50µl of RNase free water was used at 70°C for 2 min and 20°C for 5 min. Captured RNA was subjected to the KAPA Hyper Prep assay: end-repair, A-tailing, and ligation by adding 11µl of Fragment, Prime and Elite Buffer (2X). To obtain a distribution of 200-300bp fragment on the library, the reaction was run for 6 min at 94°C. cDNA synthesis was run in 2 steps following manufacturer's instructions. The ligation step consisted of a final volume of 110 µL of the adaptor ligation reaction mixture with 60µL of input cDNA, 5 µL of diluted adaptor and 45µL of ligation mix (50µL of ligation buffer+ 10 µL of DNA ligase). The Kapa Dual-Indexed Adapters (KAPA Biosystems-KK8720) stock was diluted to 7µM (1.5mM or 7nM) to get the best adaptor concentration for library construction. The ligation cycle was run according to manufacturer's instructions. To remove short fragments such as adapter dimers, 2 AMPure XP bead clean-ups were done (0.63 SPRI and 0.7SPRI). To amplify the library, 7 PCR cycles were applied to cDNA KAPA HP mix. Amplified libraries were purified using AMPure XP. The quality and fragment size distributions of the purified libraries was assessed by a 2200 TapeStation Instrument (Agilent Technologies, Santa Clara, CA, USA).

Libraries were sequenced with Hiseq4000 (Illumina), 50-bp paired-end reads for sequencing proliferating vs quiescent NSCs; 75bp single-end reads for Id4/E47 overexpressing NSCs, with a depth of $30x10^6$ reads.

The quality of RNA sequence reads was evaluated using FastQC (version 0.11.2)(Andrews, 2010). Low quality reads and contaminants (e.g. sequence adapters) were removed using Trimmomatic (version 0.32) (Bolger et al., 2014). Sequences that passed the quality assessment were aligned to the mm10 genome using tophat2 (version 2.0.14) (Kim et al., 2013), with bowtie2 (version 2.1.0) (Langmead and Salzberg, 2012) or for the quiescent NSC RNAseq data set, Cufflinks (Trapnell et al., 2010). Transcript abundance level (transcript count) was generated using HTSeq (version 0.5.3p9) (Anders et al., 2015). The transcript counts were further processed using R software environment for statistical computing and graphics (version 3.4.0). Data

normalization, removal of batch effect and other variant was performed using EDASeq R package [(Risso et al., 2011) and RUVseq package (Remove Unwanted Variation from RNA-Seq package) (Risso et al., 2014). Differential expression was performed using edgeR R package (Robinson et al., 2010), using the negative binomial GLM approach, or for the quiescent NSC RNAseq data set, Cuffdiff (version 7) (Trapnell et al., 2013).

To determine genes upregulated by BMP4, Id4, Id1, E47 or GFP, thresholds were set for expression level in the treated sample at >=1 (FPKM or CPM), a significant log2 fold change of >=1, and a false discovery rate (FDR) of <=0.05 (Benjamini-Hochberg multiple testing correction). To determine down-regulated genes, the expression level in control samples was set at >=1 (FPKM or CPM); log2 fold change was set at <=-1, and a false discovery rate (FDR) of <=0.05 (Benjamini-Hochberg multiple testing correction). The BioVenn website (www.biovenn.nl) was used to visualise overlap of gene expression. For gene ontology analysis, gene lists were analysed using the online DAVID bioinformatics “Functional Annotation” tool (https://david.ncifcrf.gov/).

Processing of the raw RNAseq data for the Id4, Id1 and E47 over-expression data sets was performed by D. van den Berg and E. Mulugeta of the Department of Cell Biology, Erasmus MC, Rotterdam. Processing of all other RNAseq data sets was performed by S. Vaga at the Francis Crick Institute.

The list of cell cycle genes for Figure 5.3L was obtained from Qiagen, at the following web address https://www.qiagen.com/gb/resources/resourcedetail?id=0ee18e97-d445-4fd7-9aa4-0ef4bece124f&lang=en

2.2.10 Protein purification, Western Blot and Co-immunoprecipitation

For Western blot analysis of NICD, LY- or DMSO-treated NSCs cultured in P6 well plates were detached from their culture plastic with Accutase and the cell suspensions centrifuged at 2000rpm for 5mins at 4°C. The supernatant was then aspirated and the pellet re-suspended in 1x Laemmli sample buffer. Samples were then boiled at 90°C for 5mins, cooled and then sonicated 1min on/30sec off for 3mins. Samples were then spin for 5mins at 13,000rpm at room temperature, after which they were run on polyacrylamide gel at 120V, after which they were transferred onto a nitrocellulose membrane. Filters were then saturated with 5% BSA in TBS-Tween or 5% milk TBS-

Tween and incubated with the primary antibody overnight at 4°C under rotation. Detection was performed using ECL Western Blotting Reagents (Sigma, GERPN2106) according to manufacturer's instructions.

For Western blot analysis of Id1-4, Ascl1 and E47 in wildtype and Ascl1-Venus NSCs, and co-immunoprecipitation experiments, NSCs were cultured in 10cm diameter dishes, in either proliferation (20ng/mL FGF2) or quiescent (20ng/mL FGF2 + 20ng/mL BMP4) conditions for 72h. Media was refreshed after 40h to ensure constant BMP4 signalling. Cells were then washed with ice-cold PBS, and scraped in Lysis Buffer (ThermoFischer Scientific, 87788) + 1x Protease inhibitor cocktail (ThermoFischer Scientific, 87786) + 1 x EDTA (ThermoFischer Scientific, 87788) + 1x Phosphatase inhibitor cocktail (ThermoFischer Scientific, 78420). Cells were lysed at 4°C for 20min under rotation and then centrifuged at 13,000 RPM at 4°C for 20mins and the pellet discarded. The supernatant was analysed either by western blot or subject to immunoprecipitation. For western blot analysis, the supernatant was mixed with 1x Laemmli sample buffer (Sigma, S3401-10VL) and incubated at 95°C for 5 mins.

For immunoprecipitation experiments, antibodies were added to cell lysate supernatants and incubated at 4°C for 2 hours under rotation. As controls, mouse anti-V5-tag or rabbit anti-HA-tag antibodies were used under the same conditions. Sepharose coupled to protein G (Sigma, P3296) was blocked with 5% BSA-PBS for 2 hours at 4°C under rotation. After several washes with PBS, it was then added to the lysate-antibody suspension and incubated for 2 hours at 4°C under rotation. After this period, Sepharose beads were washed with lysis buffer 5 times, then suspended in an equal volume of Laemmli sample buffer and incubated at 95°C for 5 mins. Samples were run in polyacrylamide gel at 120V, after which they were transferred onto a nitrocellulose membrane. Filters were then saturated with 5% BSA in TBS-Tween or 5% milk TBS-Tween and incubated with the primary antibody overnight at 4°C under rotation. Detection was performed using ECL Western Blotting Reagents (Sigma, GERPN2106) according to manufacturer's instructions.

2.3 Quantification and Statistical Analysis

2.3.1 Quantification of immunofluorescence

To measure immunofluorescence intensity, the nucleus of each identified RGL was manually outlined based on DAPI staining, and the average pixel value of the channel of interest was measured using FIJI software. Every value was normalised to the background level measured in a negative nucleus in the same z-plane as each RGL. At least 200 RGLs in each of at least 3 mice were quantified for each protein. For *in vitro* IHC quantification, average pixel intensity for each channel was measured for the area of each nuclei, using FIJI software. For each experiment, at least 100 cells were quantified across at least 3 biological replicates. To generate the arbitrary units (A.U.) for both *in vivo* and *in vitro* IHC, all the values within a sample were made relative to the average of the control, and multiplied by 100. For quantification of RNAscope® staining, the number of 'dots' in each identified RGL nucleus were counted for each probe. In addition, the average pixel intensity in and around each RGL nucleus was measured for each probe, using FIJI. 100 RGLs were quantified across 5 mice. For analysis of Id4 and E47 nucleofected cells, Id4+ or GFP+(E47) cells were identified by immunostaining for Id4 or GFP respectively, and positive cells compared to negative, non-transfected cells within the same coverslip. Cell counts were done from at least 3 coverslips from 3 biological replicates.

For quantification of WB and IP assays, films were scanned and, if appropriate, subjected to band densitometry and quantification using Image J software. Each band value was normalised according to the background of the filter and its loading control.

2.3.2 Statistics

Statistical analyses were conducted using a two-sample unpaired t test assuming Gaussian distribution using Prism software. All error bars represent the mean ± SEM. Significance is stated as follows: $p>0.05$ (ns), $p<0.05$ (*), $p<0.01$ (**), $p<0.001$ (***), $p<0.0001$ (****). Statistical details of each experiment can be found in the figure legend. n represents number of independent biological repeats.

Target Molecule	Species	Procedure	Dilution	Company	Catalogue #
Actin	Rabbit	WB	1:1000	Sigma-Aldrich	A2066
Ascl1	Mouse	WB	1:500	BD Pharmingen	556604
Ascl1	Guinea pig	IHC	1:10,000	J. Johnson	n/a
Ccnd1	Rabbit	IHC	1:400	ThermoScientific	RM-9104
BrdU	Rat	IHC	1:1000	ABD Serotec	OBT0030CX
E47	Mouse	WB	1:200	Santa Cruz Biotechnology	E2A (Yae): sc-416X
E47	Mouse	IP	1:225	Santa Cruz Biotechnology	E2A (Yae): sc-416X
GFAP	Rat	IHC	1:500	Invitrogen	13-0300
GFP	Chicken	IHC	1:2000	Abcam	ab13970
GFP	Rabbit	WB	1:1000	Life Technologies	A11122
		IP	1:1000		
Id1	Rabbit	WB	1:500	Biocheck	BCH-1/#37-2
		IHC	1:1000		
Id2	Rabbit	IHC	1:1000	Biocheck	BCH-3/#9-2-8
Id3	Rabbit	WB	1:500	Biocheck	BCH-4/#17-3
		IHC	1:200		
Id4	Rabbit	WB	1:2500	Biocheck	BCH-9/#82-12
		IP	1:400		
		IHC	1:1000		
Ki67	Mouse	IHC	1:50	BD Biosciences	550609
Nestin	Mouse	IHC	1:100	Biolegend	656802
NICD	Rabbit	WB	1:1000	Cell Signaling	4147S
PDGFRa	Rat	IHC	1:500	Biosciences	558774
p-Smad1/5/8	Rabbit	IHC	1:500	Cell Signaling	9516
tdTomato	Goat	IHC	1:1000	Sicgen	ABB181-200
Tuj1	Rabbit	IHC	1:400	Covance	PRB-435P-100
S100β	Rabbit	IHC	1:500	Dako	Z0311
Sox2	Goat	IHC	1:100	Santa Cruz	Sc-17320
V5	Mouse	IP	1:1000	ThermoFisher Scientific	R960-25
Chicken IgG	Donkey	IHC-488	1:500	Jackson	703-545-155
Mouse IgG	Donkey	IHC-488	1:500	Jackson	715-546-151

Rat IgG	Donkey	IHC-488	1:500	Jackson	712-546-150
Rabbit IgG	Donkey	IHC-Cy3	1:500	Jackson	711-166-152
Mouse IgG	Donkey	IHC-Cy3	1:500	Jackson	715-166-151
Rat IgG	Donkey	IHC-647	1:500	Jackson	712-606-153
Goat IgG	Donkey	IHC-647	1:500	Jackson	705-605-147
Mouse IgG	Donkey	IHC-647	1:500	Jackson	715-606-151
Mouse IgG	Rabbit	WB-HRP	1:1000	Dako	P0161
Rabbit IgG	Goat	WB-HRP	1:1000	Dako	P0448

RNAscope® Probes	Dilution	Company	Catalogue #
Mm-Ascl1-C2	1:50 in probe diluent or C1-probe	ACD (Bio-Techne)	313291-C2
Mm-Mki67-C1	1:1	ACD (Bio-Techne)	416771
TSA® Plus fluorophores			
TSA® Plus fluorescein	1:1500	Perkin Elmer	PN NEL741001KT
TSA® Plus Cyanine 3	1:1500	Perkin Elmer	PN NEL744001KT

Table 2. Antibodies and *in situ* probes.

Chapter 3. Results 1

Due to the high complexity of the adult hippocampal neurogenic niche, and the lack of markers specific to the quiescent compartment, delineating the effects of a particular signal specifically on the quiescent RGLs is challenging *in vivo*. In order to overcome these challenges, a reductionist approach was required, namely an *in vitro* model of adult NSC quiescence. Such a model had previously been established by the Guillemot laboratory and other groups (Martynoga et al., 2013), whereby mouse embryonic stem cell-derived neural stem cells ('NS5' cells as reported in (Conti et al., 2005)) were reversibly induced into a quiescent-like state by culturing in the presence of BMP4. However, embryonic stem cell-derived and adult hippocampus-derived neural stem cells might have fundamental biological differences with regards to their response to extrinsic signals, due to their origin. Therefore, in this chapter I will describe the generation and characterisation of an *in vitro* model of adult hippocampus-derived neural stem cell (AHNSC) quiescence, first validating that the model resembles a quiescent NSC state, and comparing the new model using adult hippocampal NSCs to the older NS5-NSC quiescence model, by transcriptomic analysis. I will then describe how I further refined the mode of AHNSC quiescence by titrating the component factors, and analysed more closely the transcriptional signature of BMP4-induced AHNSC quiescence.

3.1 Development of an *in vitro* model of adult hippocampal stem cell quiescence

3.1.1 Deriving adult hippocampal neural stem cells

In order to generate an *in vitro* model of adult hippocampal NSC quiescence, the dentate gyri of adult mice (P50-P60) were dissected, and the cells dissociated and grown as neurosphere cultures (as described in (Walker and Kempermann, 2014)). Subsequent passaging steps selected for the self-renewing stem cells, while the post-mitotic neurons and glial cells were diluted out by the proliferating stem cells or simply died. Subsequently, the neurospheres were dissociated and plated onto laminin-coated flasks, generating adherent cultures of self-renewing NSCs (Figure 3.1). This protocol was already in development in the laboratory, and so I took the cultures to develop the quiescence model. Initially, the NSCs were cultured in the presence of both EGF and

FGF2, in order to maximise proliferation and survival, and replicating the conditions used for the maintenance of NS5 cells (Conti et al., 2005; Martynoga et al., 2013; Mira et al., 2010). BMP4 was used to induce quiescence of the AHNSCs, as it is described to induce quiescence of NS5 cells (Conti et al., 2005; Martynoga et al., 2013) and AHNSCs (Mira et al., 2010) (Figure 3.1).

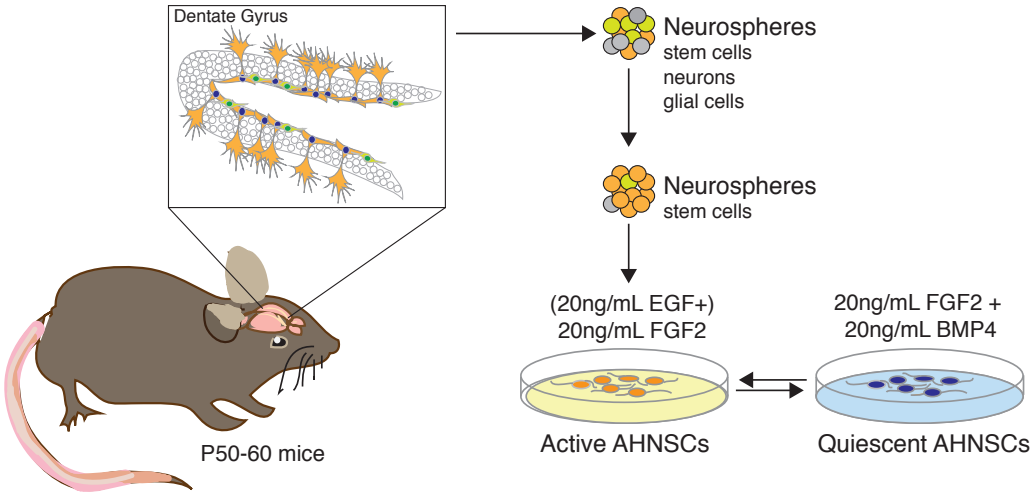

Figure 3.1. Scheme of *in vitro* model of adult-derived hippocampal neural stem cell quiescence

The dentate gyri of adult *wildtype* mice (P50-P60) were dissected, and the cells dissociated and grown as neurosphere cultures. Subsequent passaging steps selected for the self-renewing stem cells, while the post-mitotic neurons and glial cells were diluted out by the proliferating stem cells or simply died. Subsequently, the neurospheres were dissociated and plated onto laminin-coated flasks, generating adherent cultures of self-renewing adult hippocampal neural stem cells (AHNSCs). Active AHNSCs were cultured in FGF2 and (for early experiments) EGF, whilst addition of BMP4 (and removal of EGF) generates quiescent AHNSCs.

3.1.2 BMP4-treated AHNSCs can be induced into a reversible quiescent-like state

I first tested whether adult hippocampal NSCs derived in our lab could be induced by BMP4 into a quiescent-like state, by immunofluorescence staining for cell cycle markers Ki67 and CyclinD1, the activation factor Ascl1, and incorporation of the modified thymidine analogue EdU to label S-phase. Treating AHNSCs for 24h with

20ng/mL BMP4 in the presence of 20ng/mL FGF2 and withdrawal of EGF was already sufficient to cause a sharp decrease in the number of proliferating NSCs (Figure 3.2A-E). This initial suppression of proliferation was further decreased by 72h, by which time the percentage of proliferating cells had mostly stabilised, and remained at this low level throughout 7 days of BMP4 treatment (Figure 3.2A-E). I therefore chose 72h of exposure to BMP4 as a standard time to induce quiescence of AHNSCs in future experiments.

In addition to cell cycle exit, removal of EGF and addition of BMP4 resulted in the increased expression of GFAP, a characteristic marker of RGLs *in vivo* (Figure 3.2A). A true quiescent state should be a reversible cell cycle exit, a feature that distinguishes it from senescence or differentiation. To test whether BMP4-induced quiescence was reversible, and therefore a true quiescent state, I reactivated the BMP4-treated NSCs by plating them back into culture medium containing both EGF and FGF2 (without BMP4). Analysis by immunofluorescence shows that the percentage of NSCs positive for cell cycle markers Ki67 and EdU, and for activation factor Ascl1, are already back to the levels observed pre-BMP4 treatment by 48h after reactivation (Figure 3.2F, H-J). Interestingly, the %Ki67+ and %EdU+ NSCs at 48h and 72h post-reactivation exceeds those seen prior to BMP4-induced quiescence, which may reflect a synchronicity of the cells following coordinated reactivation. CyclinD1 expression was unique in its speed of recovery following reactivation, with %CyclinD1+ NSCs back to pre-BMP4 levels already by 24h post-reactivation (Figure 3.2K). This could be due to the fact CyclinD1 plays an important role in the early to mid-G1 phase of the cell cycle, and so its early expression may be required for the initial entry into the cell cycle from G0, or progressing through early G1.

The protocol used here to reactivate quiescent NSCs involved enzymatic dissociation of the cells from the culture plastic, and re-plating into proliferation conditions. This process causes disruption of the extracellular matrix and cell-cell contacts which may play important roles in regulating quiescence. I therefore tested whether quiescent NSC reactivation was solely dependent on BMP4 removal, by reactivating without dissociating the cells. Following 72h culture with BMP4, I washed the NSCs with dPBS (to ensure sufficient removal of BMP4) and pipetted fresh proliferation medium to the cells. 24h post-reactivation, the number of proliferating NSCs was similar to BMP4 conditions (Figure 3.2L), however by 4d post-reactivation proliferation markers Ki67,

CyclinD1 and EdU were expressed in a large proportion of the cells, as well as Ascl1 protein (Figure 3.2L). The expression of GFAP took longer to decrease in reactivated cells that were not dissociated, as can be seen 24h and 4d post-reactivation, although levels of GFAP had started to return to pre-BMP4 levels by 7d post-reactivation (Figure 3.2L). This is in comparison to dissociated cells in which GFAP levels are strongly reduced already by 48h post reactivation (Figure 3.2F, second panel). This indicates that removal of BMP4 and returning EGF is sufficient to reactivate cells from BMP4-induced quiescence and does not require disruption of the ECM or cell-cell contacts.

Quiescent NSCs *in vivo* are maintained in a quiescent state for long periods of time while still maintaining their stemness. It was important to investigate how well the *in vitro* system could model longer-term quiescence, in order to see if it could model a more physiological, long-term state of quiescence. Moreover, it was useful to test whether longer exposure to BMP4 would eventually cause differentiation or senescence. To this end, I tested whether the cells could be reactivated following 28 days in BMP4-induced quiescence. The percentage of NSCs positive for Ascl1, Ki67, CyclinD1 and EdU 72h after reactivation from long-term BMP4-induced quiescence were highly similar to those seen in reactivated cells after short-term quiescence (Figure 3.2.G-K). This suggests that NSCs do not change their identity if exposed to BMP4 plus FGF2 for at least 1 month, and therefore the *in vitro* system would be able to model more long-term regulation.

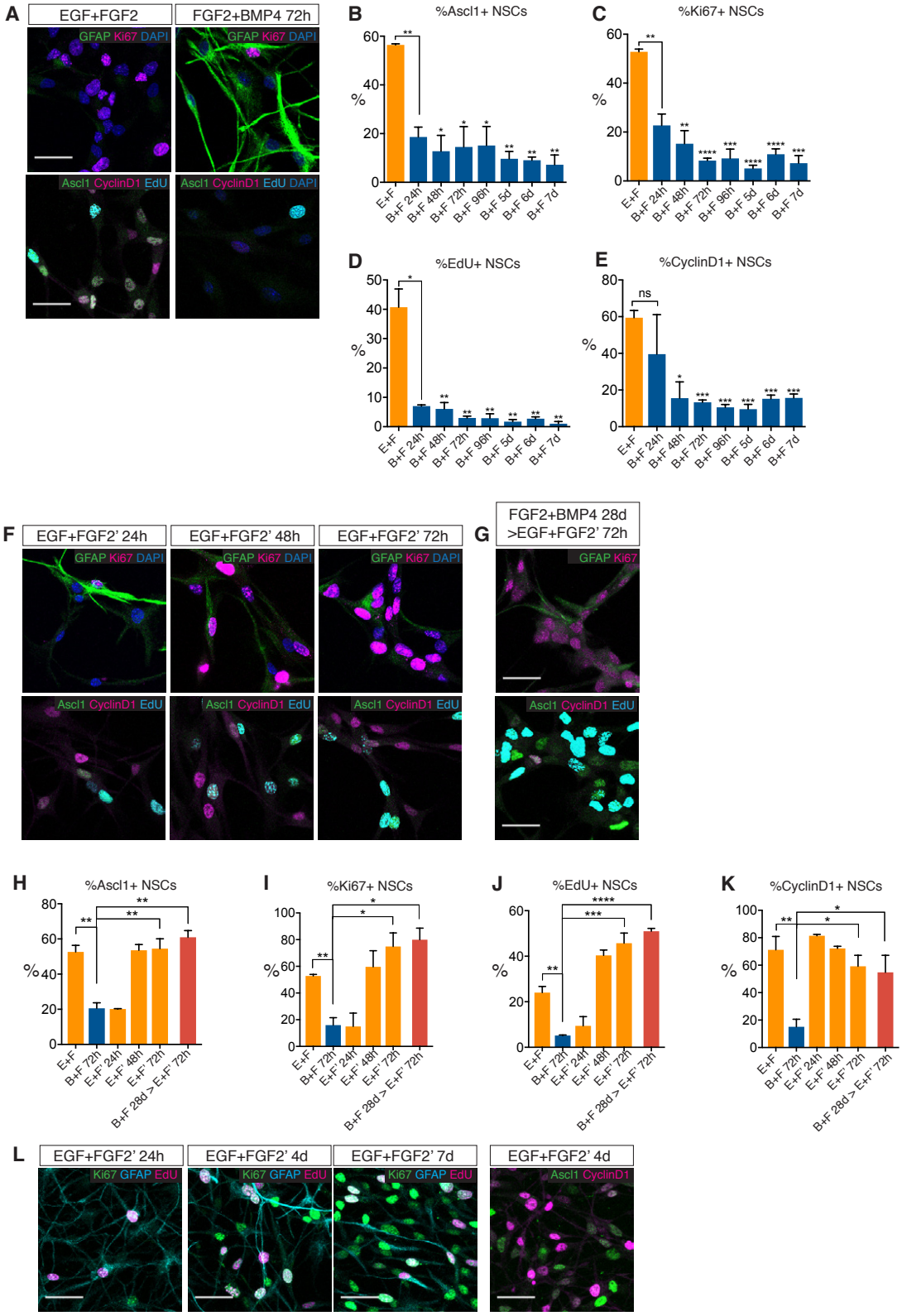

Figure 3.2. BMP4 induces reversible cell cycle exit in AHNSCs (legend next page)

Figure 3.2. BMP4 induces reversible cell cycle exit in AHNSCs

(A-E) Immunohistochemistry for cell cycle markers Ki67 and CyclinD1, activation factor Ascl1, and S-phase label EdU are decreased in AHNSCs by 72h BMP4 treatment and continually supressed for at least 7 days, as quantified in (B-E), whilst the RGL marker GFAP is increased upon BMP4 treatment (A). Abbreviations: E, EGF 20ng/mL; F, FGF2 20ng/mL; B, BMP4 20ng/mL.

(F-K) The effects of BMP4 are reversible, shown by increased immunofluorescence for Ki67, CyclinD1, Ascl1 and EdU incorporation by 48h post-reactivation (F) and quantified in (H-J). AHNSCs are able to reactivate from long-term (28 days) BMP4-induced quiescence (G, H-K).

(L) AHNSCs can be reactivated from quiescence without enzymatic dissociation of the cells from the culture plastic.

E, EGF; F, FGF2; B, BMP4. Scale bars, 30μm. Error bars represent the mean ± SEM. n=3 independent biological repeats for all data shown.

3.1.3 BMP4-induced quiescent AHNSCs maintain their multipotency

I next tested whether BMP4-induced quiescent NSCs maintain their multipotency, a key aspect of quiescence that distinguishes it from senescence or terminal differentiation. *In vivo*, RGLs are reported to have multipotency, with the capacity to differentiate into granule neurons and astrocytes (Bonaguidi et al., 2011), and can also generate oligodendrocyte precursor cells (OPCs) under conditions of high Ascl1 expression (Braun et al., 2015; Jessberger and Gage, 2008). Moreover NSCs *in vitro* have been shown to have trio-potentiality (Oh et al., 2014), therefore I tested for the expression of neuronal (Tuj1), astrocytic (GFAP and S100β) and OPC (PDGFRa) markers. Following 72h or 28d BMP4 treatment, I reactivated cells for 72h in the presence of EGF and FGF2, and subsequently exposed the cells to conditions which induce differentiation into glial and neuronal cells (scheme shown in Figure3.1.3A). In parallel I also differentiated cells directly from proliferation conditions, to determine if there were any differences in multipotency between reactivated NSCs and those that had not been exposed to BMP4 (Figure 3.3A). Many Tuj1+ neuronal cells were detected by IF following differentiation of all three populations of NSCs, as well as immunoreactivity for glial markers GFAP and s100β, and OPC marker PDGFRa (Figure 3.3B-D). Overall these initial results suggest that BMP4 can induce a reversible cell cycle arrest in adult hippocampal NSCs, without affecting their stemness as demonstrated by their ability to generate more differentiated neuronal, glial and

oligodendrocyte precursor-like cells. These features are central to defining the BMP4-induced state as 'quiescence' and distinguishing it from differentiation or senescence, and therefore indicate this can be a biologically relevant model of adult hippocampal NSC quiescence.

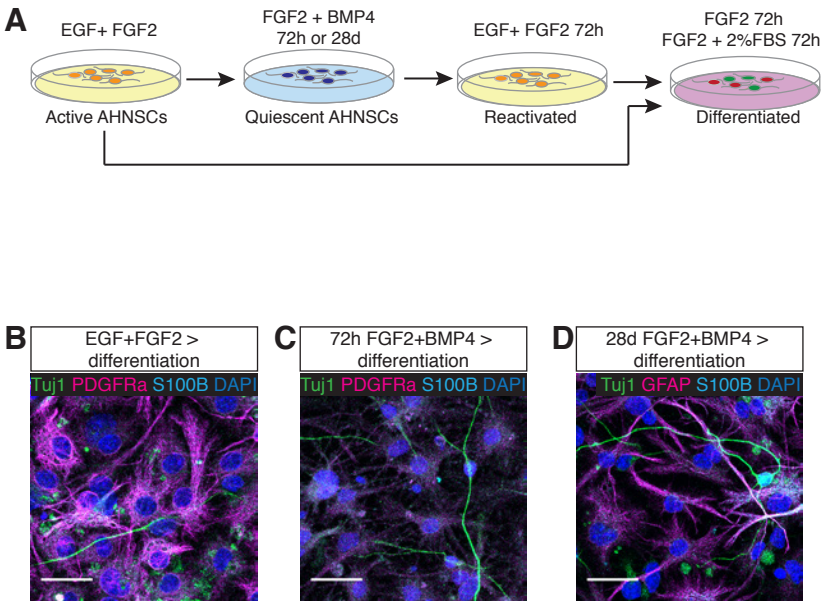

Figure 3.3. BMP4-induced quiescent AHNSCs retain their multipotency

(A) Scheme for the differentiation protocol of AHNSCs reactivated from quiescence. Active NSCs are induced to quiescence by either 72h or 28days BMP4 treatment. NSCs are then reactivated by culturing back in EGF+FGF2 for 72h, at which point EGF is removed and the concentration of FGF2 reduced for 48h, followed by replacement of FGF2 with 2% foetal bovine serum for 72h.

(B-D) Glial cells (S100β+, GFAP+) and Tuj1+ neurons can be generated from active AHNSCs as well as AHNSCs previously treated with BMP4 for 72h or 28days. Some cells could also be detected to express oligodendrocyte precursor cell marker PDGFRa. n=2 independent biological replicates.

3.1.4 BMP4-induced quiescent AHNSCs spontaneously enter the cell cycle and can re-enter quiescence

BMP4 treatment does not completely suppress the cell cycle of NSCs *in vitro*, as observed from the percentage of Ki67+ or EdU+ NSCs in the 7day BMP4-treatment time-course (Figure 3.2B-E). This could represent a low-level spontaneous entry of the cells into the cell cycle, which is interesting to study in more detail as it could inform on the dynamics of cycling NSCs, particularly how many times they divide and if they

return to quiescence. Alternatively, this cycling pool could represent a sub-population of cells 'resistant' to BMP4-induced quiescence, one which never exits the cell cycle. This hypothesis, if true, could be extended to suggest that the BMP4-induced NSCs are not truly reactivating from quiescence. The 'BMP4-resistant' cycling population of cells could be selected for upon reactivation, whilst the non-cycling cells never reactivate and are quickly out-competed. An immediate argument against this hypothesis is the fact I do not see an increase in the percentage of proliferating cells over time in BMP4 (Figure 3.2B-E), which would indicate a selective expansion of a subpopulation of cycling cells. However, to test this hypothesis more carefully, and also to analyse the cell cycle dynamics of NSCs in BMP4 conditions, I carried out an EdU pulse-chase paradigm, as shown in Figure 3.4A. I first labelled cells in S-phase by incorporation of the thymine analogue EdU for 24h, followed by a chase period of 18h. An 18h chase will allow for most cells that had just entered S-phase at the end of the 24h EdU incubation to progress through the cell cycle. After the chase period, the cells were fixed and immunostained for pan-cell cycle marker Ki67, which will label any cell currently in the cell cycle at the end of the experiment. This paradigm will tell me three things; firstly, how many cells enter S-phase within a 24h period (EdU+); secondly, how many of those cells re-enter the cell cycle (EdU+Ki67+), and thirdly how many cells exit the cell cycle and return to quiescence (EdU+Ki67-). By the end of the experiment, 43.77%±4.9 of the cells were EdU+ (Figure 3.4C), indicating just under half of all cells had gone through S-phase within a 24h period. Importantly, 16.81%±2.7 of NSCs were EdU+Ki67- ("only EdU+"), suggesting that many NSCs return to quiescence (Figure 3.4B,C). In addition, 7.42%±1.6 of the NSCs were Ki67+EdU- ("only Ki67+"), indicating that additional cells had entered the cell cycle after the EdU incorporation (Figure 3.4B,C). Together these data indicate BMP4-treated NSCs spontaneously and dynamically enter and exit the cell cycle, with some cells returning to quiescence and new cells, that had not previously cycled, entering the cell cycle. To investigate these dynamics in further detail, I extended the pulse-chase paradigm to include a 24h BrdU pulse with 18h chase (Figure 3.4D). Using the data generated from these labelling experiments, I measured the percentage of NSCs in the cycle states indicated in Table3.

Cell Cycle Label	Interpretation	% observed
Negative	Cells did not enter the cell cycle during the experiment	42.6 ± 4.6
EdU+ only	Cells divided, then entered quiescence for (at least) the following 60h	23.11 ± 5.0
BrdU+ only	Cells were quiescent for at least 24h, then divided, then entered quiescence for (at least) the following 18h	21.25 ± 1.5
Ki67+ only	Cells newly entering the cell cycle in the last 18h	2.63 ± 1.2
EdU+ BrdU- Ki67+	Cells divided, entered quiescence for at least 42h, then re-entered the cell cycle	1.96 ± 1.3
EdU+ BrdU+ Ki67-	Cells divided at least twice during the first 66h, then entered quiescence	2.54 ± 0.3
EdU- BrdU+ Ki67+	Cells did not divide until the BrdU pulse, and continue to cycle at the end of the experiment	4.46 ± 0.7
EdU+ BrdU+ Ki67+	Cells cycled throughout the experiment and continue to cycle at the end of the experiment	1.21 ± 0.6
Any combination of EdU/BrdU/Ki67	Represents the overall level of proliferation over 84h	57.4 ± 4.6

Table 3. Combinations of S-phase markers EdU and BrdU, and pan cell cycle marker Ki67 distinguish different cycling behaviours of the cells.
The percentage frequency with which each cell cycle label combination was observed is shown as the mean±SEM, n=3 independent biological replicates.

If the alternative hypothesis is correct and there is a small sub-population of cycling cells, then the expectation would be to see only 10% or so cells continuously cycling (EdU+BrdU+Ki67+), and none returning to quiescence (as they are insensitive to BMP4). In contrast, the results show that by the end of the experiment, nearly 60% of cells had entered the cell cycle, with 11.13%±1.7 NSCs actively cycling (Ki67+) at the final time-point (Figure 3.4E,F). Table 3 shows the percentage of cells observed for each 'cycle state'. Every combination of EdU, BrdU and Ki67 was observed (Figure 3.4G; Table 3). These data show that many NSCs dynamically enter and exit the cell cycle in BMP4 conditions over time, and importantly argues against a sub-population of BMP4-resistant cycling cells, because we see recruitment of previously non-cycling

cells into the cell cycle. This shows they had been induced to quiescence by BMP4, and subsequently spontaneously divided. Moreover, 48.86±2.0% of these cells then returned to quiescence, showing that even the dividing cells are sensitive to the effects of BMP4.

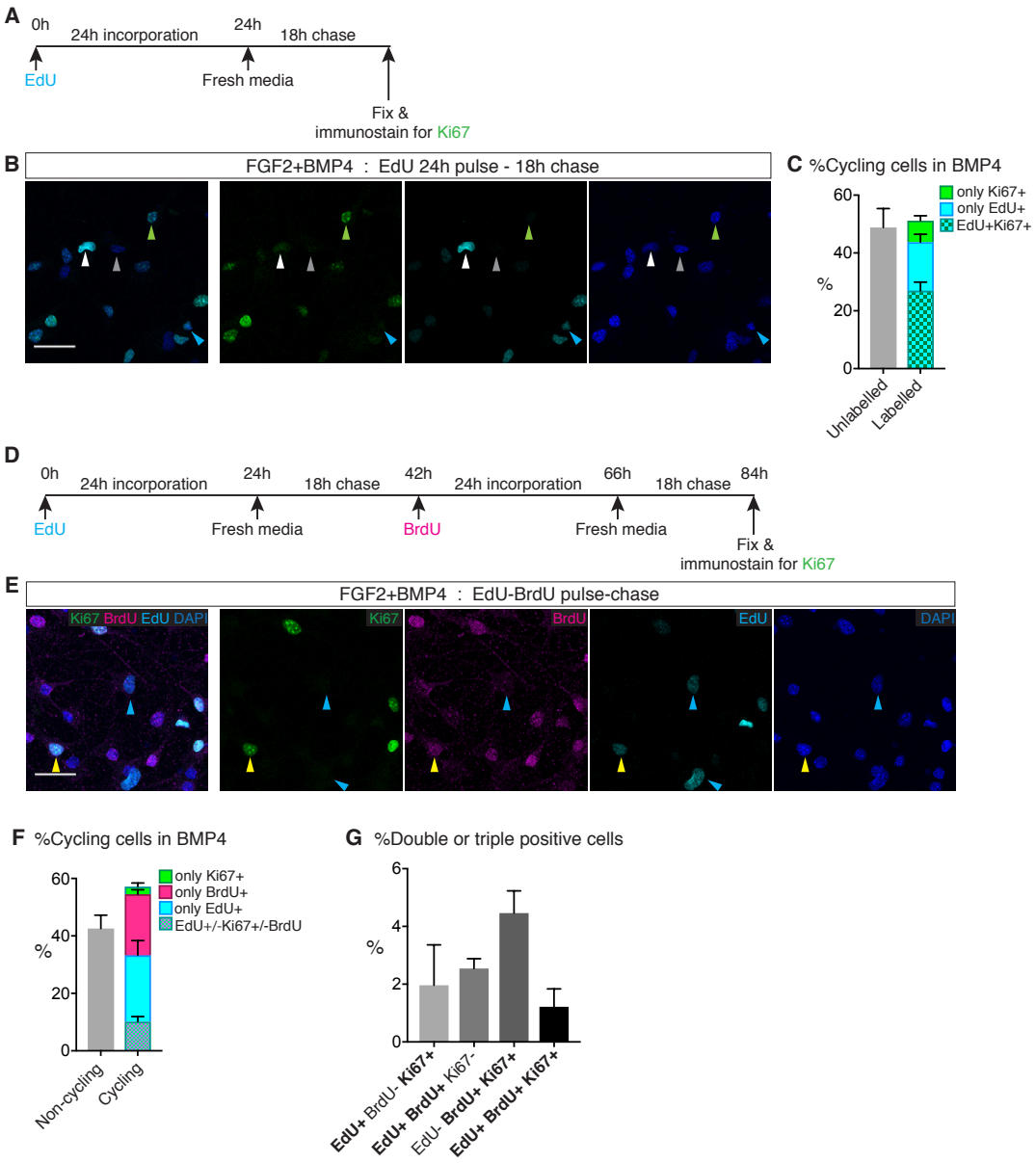

Figure 3.4. Analysis of cycling cells in BMP4-induced quiescence by EdU-BrdU pulse-chase

(A) Scheme of 24h EdU pulse followed by an 18h chase in AHNSCs in BMP4+FGF2 conditions, to label cells that have entered the cell cycle, and either remain cycling (EdU+Ki67+) or return to quiescence (EdU+Ki67-).

(B-C) 24h EdU labelling shows that around half of cells will cycle in a 42h period, with some cells returning to quiescence (EdU+Ki67-; blue arrow in (B)), some continuing to cycle (EdU+Ki67+; white arrow), and some cells newly entering the cell cycle at the end of the experiment (EdU-Ki67+; green arrow). The grey arrow in (B) shows a cell that remained quiescent during the experiment (EdU-Ki67-). n=2 independent biological repeats. 3 images analysed and at least 300 cells counted per condition.
(D) Scheme of EdU-BrdU pulse chase paradigm, with 24h pulses and 18h chases, to analyse the number of cells that enter and exit the cell cycle in BMP4-induced quiescence.
(E-G**)** More than half of the cells were labelled during the course of the experiment (F), with each combination of EdU/BrdU/Ki67 double or triple labelling being observed (Yellow arrow in E; G). Many cells re-entered quiescence following division (EdU+ only, blue arrow in (E); BrdU+ only) (F), and a small percentage of previously quiescent cells enter the cell cycle at the end of the experiment (Ki67+ only) (F). Scale bars, 30μm. Error bars represent the mean ± SEM. n=3 biological repeats.

3.2 BMP4 induces more quiescence-like features in AHNSCs than just cell cycle arrest.

Quiescence is more than simply cell cycle arrest, but involves the up- and down-regulation of many hundreds of genes to actively maintain a quiescent state and inhibit terminal differentiation (Codega et al., 2014; Coller et al., 2006; Liu et al., 2007; Shin et al., 2015). This includes changes in dynamics of RNA transcription, generally considered to be at lower levels, at least in quiescent yeast and HeLa cells (Gray et al., 2004; Kim and Sederstrom, 2015), as well as lower or more tightly regulated protein synthesis (Pereira et al., 2015). For example, deletion of Pten in haematopoietic stem cells results in stem cell depletion due to overactive protein synthesis (Signer et al., 2014). Tight regulation of protein synthesis may also be a hallmark of quiescent adult hippocampal neural stem cells, as aberrant activation of the mTorc1 pathway via deletion of Pten in RGLs also resulted in stem cell depletion (Bonaguidi et al., 2011). Similarly, aged hippocampal NSCs show dysfunctional lysosomal activity and increased protein aggregates, associated with an inability to activate from quiescence; restoration of their lysosomal function restores their ability to activate (Leeman et al., 2018). In addition to transcriptional and protein synthesis changes, quiescence is also accompanied by energetic changes. As described in Section 1.3, quiescent radial glial-like cells have characteristic mitochondrial distribution, (Beckervordersandforth, 2017),

and a predominantly glycolytic metabolism, with functional fatty acid oxidation which can directly regulate stem cell activity (Knobloch et al., 2013; Knobloch et al., 2017). Therefore, I investigated whether quiescent AHNSCs *in vitro* demonstrated the characteristic changes compared to active NSCs, in RNA and protein synthesis, mitochondrial distribution, and gene expression changes associated with the published "signature" of quiescence.

3.2.1 BMP4-induced quiescent AHNSCs have different metabolic, transcription and translation rates than active AHNSCs

I first investigated the changes to mitochondria in BMP4-induced quiescent AHNSCs, as a read-out of metabolic change. Incorporation of the mitochondrial marker MitoTracker™ clearly shows how the mitochondria in proliferating AHNSCs in the presence of EGF+FGF2 are abundant and tightly packed around the nucleus (Figure 3.5A, left panel). In contrast, in BMP4-induced quiescent AHNSCs, the mitochondria are spread out into the long processes, becoming elongated and separated (Figure 3.2.1A, right panel). This may reflect the different energetic demands of the two states; active NSCs have high energetic demands near the nucleus for DNA replication and mitosis, whereas quiescent NSCs need energy further from the nucleus, perhaps for localised transcription of transported RNAs, as occurs in neurons (Riccio, 2018). I also analysed the level of transcriptional activity using incorporation of the dye Pyronin Y (PY) which labels double-stranded RNA such as mRNA, thereby labelling nascent RNA transcription. The levels of PY were qualitatively slightly higher in EGF+FGF2 conditions then FGF2+BMP4 (Figure 3.5B), suggesting BMP4 treatment suppresses transcription in quiescent NSCs. Finally, I measured nascent protein production using incorporation of O-propargyl-puromycin (OPP), an alkyne analogue of puromycin which gets incorporated into newly synthesised proteins, and which has been shown to be enriched in active SVZ NSCs reflecting their high rate of protein translation compared to quiescent NSCs (Llorens-Bobadilla et al., 2015). The OPP is then detected using fluorescent Click-IT chemistry. The pattern of OPP incorporation in EGF+FGF2 conditions is mostly around the nucleus, and the overall levels of OPP incorporation is higher in active compared to quiescent NSCs (Figure 3.5C). Moreover, quiescent NSCs do not display the nuclear OPP staining, instead granules of OPP are dispersed throughout the cytoplasm (Figure 3.5C).

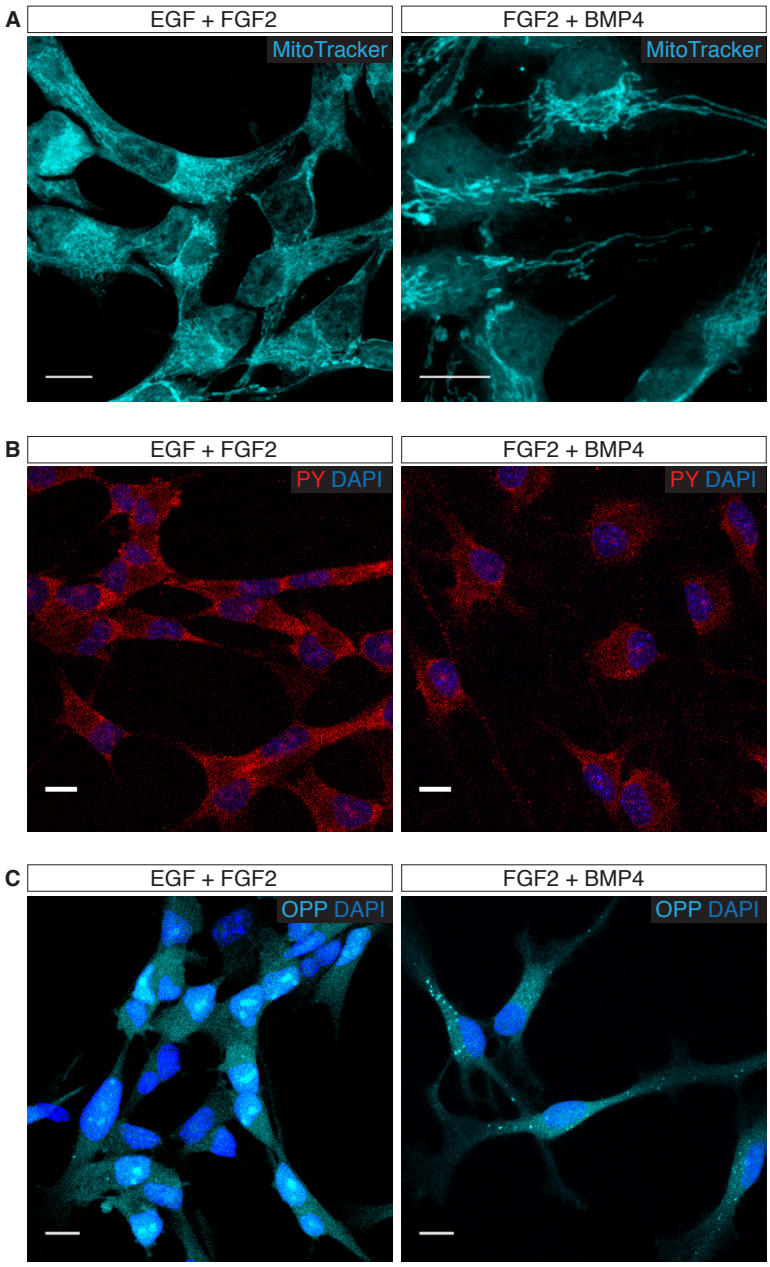

Figure 3.5. Analysis of mitochondria, RNA transcription and protein translation levels in AHNSCs.

(A) The mitochondria of active (EGF+FGF2) and quiescent (FGF2+BMP4) NSCs were labelled by incubation with 30nM MitoTracker™ Deep Red FM in the culture medium for 1 hour prior to fixation.

(B) Following fixation, active (EGF+FGF2) and quiescent (FGF2+BMP4) NSCs were stained with 1μM Pyronin Y, followed by DAPI staining, in order to visualise double stranded RNA.

Images shown are representatives of n=3 independent biological replicates.

(C) Detection of nascent protein synthesis was visualised by incubating active and quiescent NSCs with 50μM O-propargyl-puromycin (OPP) in the culture medium for 1 hour prior to fixation, followed by Click-IT detection and DAPI staining. Scale bars, 10μm.

3.2.2 Transcriptome-wide analysis reveals a quiescence "signature" of BMP4-treated AHNSCs

In order to further validate the *in vitro* model and also gain new insights into the transcriptional signature of quiescent AHNSCs, we performed RNA sequencing of active and quiescent AHNSCs. AHNSCs were cultured in the presence of either 20ng/mL EGF+ 20ng/mL FGF2 (active) or 20ng/mL FGF2+ 20ng/mL BMP4 (quiescent) for 72h, at which point cells were lysed and the RNA extracted. Samples from 3 independent biological repeats were collected and processed for RNA sequencing. Differential gene expression analysis revealed 1637 genes upregulated and 1456 genes downregulated in quiescent vs active NSCs. The genes most enriched in the quiescent state belonged to ontologies such as "cell adhesion", "cell-cell signalling", "cation transport" and "lipid catabolic process" (Figure 3.6A). These terms are highly characteristic of transcriptional signature associated with quiescent stem cells (Codega et al., 2014; Shin et al., 2015). Moreover, these ontologies were highly similar to those enriched in the BMP4-treated ES-NSCs (NS5 cells) from (Martynoga et al., 2013), as shown in Figure 3.6C. The genes downregulated in quiescent AHNSCs were mostly related to the arrest of the cell cycle, such as "cell cycle", "cell division", "DNA replication" as well as "RNA processing" (Figure 3.6B). Again, these ontologies matched closely to those downregulated in BMP4-treated NS5 NSCs (Figure 3.6D).

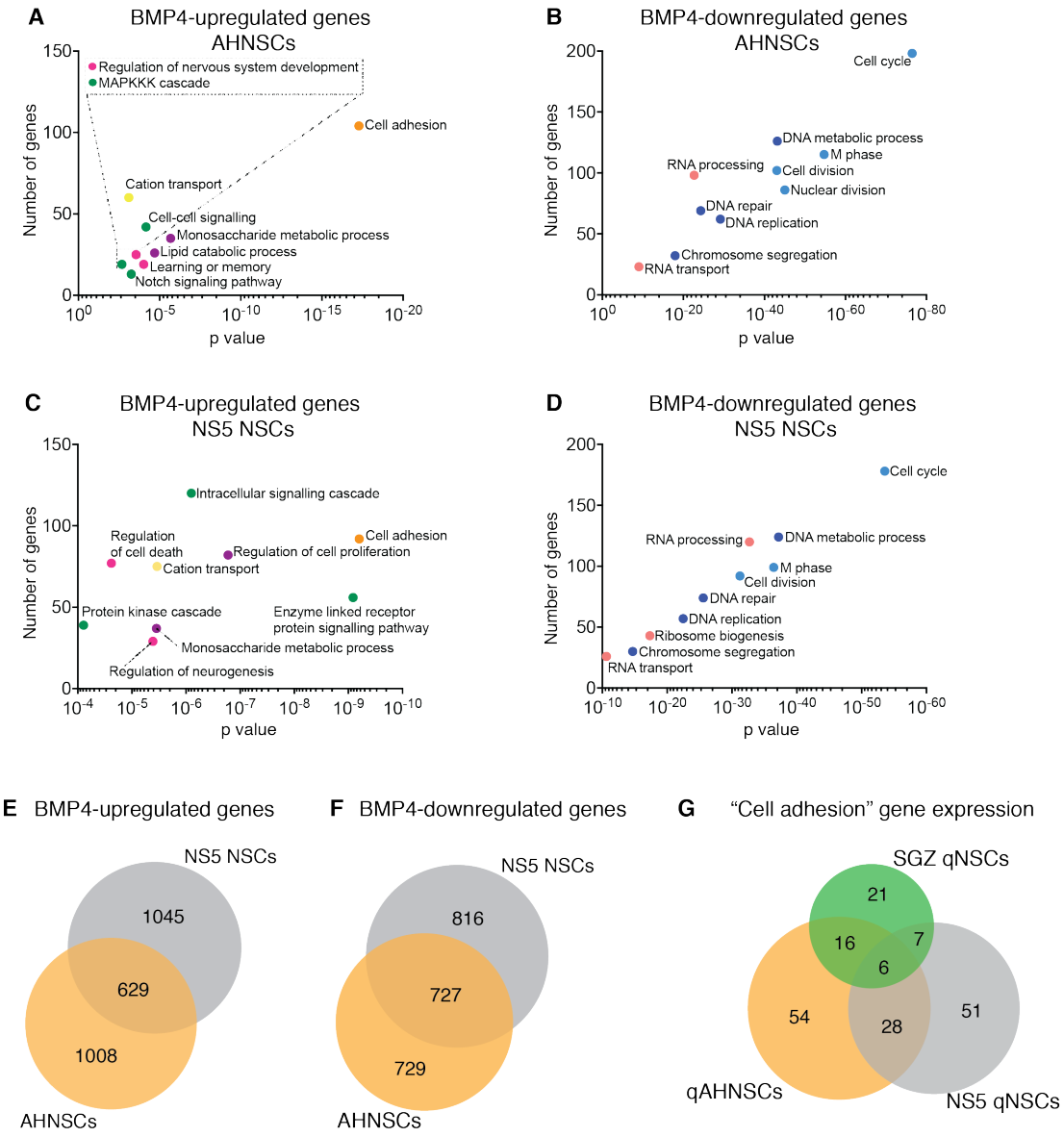

Figure 3.6. RNAseq analysis of active (EGF+FGF2) vs quiescent (BMP4+FGF2) AHNSCs and comparison with quiescent NS5-NSCs

(A,B) Graphs show the top gene ontologies for genes significantly up- or down-regulated in BMP4-induced quiescent AHNSCs.

(C-F) Around half of the genes significantly up- or down-regulated in quiescent AHNSCs are common with those genes regulated in quiescent ES-NSCs ("NS5" cells) (C, D), despite highly similar gene ontologies between the two quiescent cell types (E, F).

(G) Overlap of the genes within the "cell adhesion" ontology expressed in FACs isolated quiescent SGZ NSCs (Shin et al., 2015), quiescent AHNSCs and quiescent NS5 NSCs.

Interestingly, despite the ontologies of genes regulated by BMP4 being highly similar between the NS5 NSCs and AHNSCs, the overlap of actual genes was less than half for both up- and down-regulated genes (Figure 3.6 E,F), suggesting that specific genes within the shared ontology classes are different between the embryonic and adult NSCs. I investigated this further by looking at specific genes of the most significantly upregulated ontology, “Cell adhesion”, to see if there were adult hippocampal-specific genes being expressed in AHNSCs and not in NS5 NSCs. I overlapped the genes classified in the “cell adhesion” ontology in BMP4 treated NS5 cells with those for BMP4 treated AHNSCs, which again showed less than half of the specific “cell adhesion” genes are co-expressed in both types of NSCs (Figure 3.6G). I then overlapped these with the “cell adhesion” genes from a single cell RNAseq data set from RGLs FAC sorted from the adult SGZ, as a reference for adult hippocampal NSC-specific genes (Shin et al., 2015). I took the ‘top 1000 enriched genes’ in SGZ FAC sorted quiescent NSCs ((Shin et al., 2015) Supplementary Table S4), and ran it through gene ontology software to isolate the genes in the “cell adhesion” ontology. Out of 50 cell adhesion genes enriched in quiescent SGZ NSCs, 13 were also expressed by quiescent NS5 NSCs (26% of SGZ NSC genes), and 22 were expressed by quiescent AHNSCs (46% of SGZ NSC genes). Of those 22 genes, 16 were exclusively co-expressed in quiescent SGZ NSCs and AHNSCs, and not in NS5 NSCs (Figure 3.6G; genes listed in Table 4). These 16 genes were all expressed to some degree in adult hippocampal cells including RGLs (according to single cell expression data from www.linnarssonlab.org/dentate/). These data show that while there is not an exclusive overlap of genes expressed from SGZ NSCs with *in vitro* AHNSCs, the overlap is nearly double the overlap between SGZ NSCs and NS5 NSCs. This might reflect a more similar biological identity between the SGZ NSCs and the *in vitro* AHNSCs, which would make them a more reliable cell type for the *in vitro* quiescence model. In further support of the hypothesis that AHNSC have a greater “hippocampal stem cell” identity than NS5 NSCs, the ontology “Learning or memory” is specifically enriched in BMP4-treated AHNSCs, and not in NS5 NSCs (Figure 3.6A, C). The “Learning or memory” ontology includes genes associated with neurodegenerative diseases such as PARK2 (Parkinson’s disease); CLN3 (Batten disease); and APP, PSEN2 and APBB1 (Alzheimer’s disease), the dysfunction of which are associated with hippocampal neuron degeneration. These data could suggest AHNSCs have a “hippocampal” identity in addition to their neuronal stem cell properties, and suggest

they may model adult hippocampal NSC quiescence in culture more closely than NS5 NSCs.

Cell adhesion genes	
Expressed in both AHNSCs and SGZ RGLs	**Expressed in both NS5 NSCs and SGZ RGLs**
BCAN	CADM1
MEGF10	ATP1B2
NRCAM	CYR61
MFGE8	PDPN
NRXN1	HES1
NCAM2	NCAN
HEPACAM	ITGB5
LSAMP	CDH2
CTNND2	NEO1
DSCAML1	CD9
VCAM1	IGSF11
TTYH1	SORBS3
PCDH10	NLGN1
OMG	
NTM	
CDH11	

Table 4. Cell adhesion genes exclusively co-expressed in AHNSCs and SGZ RGLs, or NS5 NSCs and SGZ RGLs

3.3 Refining the *in vitro* model of AHNSC quiescence

3.3.1 Withdrawal of EGF and titration of FGF2 generates a more physiological model of AHNSC quiescence without affecting stemness.

A limitation of the model was the presence of EGF in the proliferation conditions, a potent mitogen and one which has been shown specifically to regulate SVZ NSCs (which express EGF receptor) but not SGZ NSCs (Doetsch et al., 2002; Gonzalez-Perez et al., 2009; Kuhn et al., 1997), therefore stimulation of AHNSCs with EGF in culture is artificial. In addition, the observed effects of BMP4 could in fact be intermixed

with effects of withdrawal of EGF, confounding the interpretation of the role of BMP4 in NSC quiescence. Therefore, I tested whether NSCs could be maintained in a self-renewing, proliferative state in FGF2 alone, and whether EGF withdrawal affected their stemness or self-renewal capacity. I first measured the proliferation levels of NSCs in the presence of both 20ng/mL EGF + 20ng/mL FGF2 compared to 20ng/mL FGF2 alone (Figure 3.7A-C), which showed that withdrawal of EGF resulted in about a 10% drop in the percentage of proliferating RGLs, identified by Ki67 and CyclinD1 immunoreactivity and incorporation of S-phase marker EdU. mRNA expression of *CyclinD1* was also decreased 2-fold following EGF withdrawal (Figure 3.7D), however this sharp decrease was not completely mirrored in the protein levels (Figure 3.7C), indicating the transcriptional change is not translating into a significant biological effect on the cell cycle. The sum of the results on NSC proliferation suggest that EGF with FGF2 induces the cell cycle more strongly than 20ng/mL FGF2 alone, but FGF2 alone is sufficient to keep NSCs self-renewing. To check that cells were not differentiating in conditions without EGF, I measured the mRNA levels of *Nestin*, a stem cell marker, which showed a 0.5-fold decrease following EGF withdrawal (Figure 3.7E), however *Nestin* is highly expressed in EGF+FGF2 conditions by RNAseq analysis (FPKM of 155.11), indicating the small drop in expression may not significantly affect the stem cell state. Transcript levels of *Dcx* (*doublecortin*), an immature neuron marker, measured by QPCR, appear to be strongly induced upon culturing in FGF2 alone (Figure 3.7F). However, according to FPKM levels in the RNAseq dataset, *Dcx* is not expressed in EGF+FGF2 conditions, therefore an increase in FGF2 alone still represents very low expression levels. *Ascl1* mRNA levels also increased 0.5-fold in the absence of EGF (Figure 3.7G), but average Ascl1 protein levels were not significantly affected by culturing cells in FGF2 without EGF (Figure 3.7H). AHNSCs could be passaged in the presence of 20ng/mL FGF2 without EGF for at least 18 passages, although beyond this point the cells would detach from the culture plastic more frequently, which could indicate higher levels of spontaneous differentiation and therefore loss of stemness. However, the proliferation of the stem cells was still good beyond passage 18, and as demonstrated through immunocytochemistry and gene expression analysis (carried out on passage 12-16 AHNSCs), AHNSCs cultured in 20ng/mL FGF2 without EGF do not demonstrate significant differentiation, supporting the decision to remove EGF entirely from the culture conditions in order to produce a more physiological culture medium.

Like EGF, FGF2 is a mitogen, but unlike EGF, FGF2 has been demonstrated to be present in the hippocampal niche *in vivo* and required for RGL maintenance (Kang and Hebert, 2015). FGF2 could not be withdrawn from the cell culture medium completely as it is reported to be crucial for hippocampal NSC survival and to prevent differentiation towards a neuronal fate, or, in the presence of BMP4 an astrocytic fate (Sun et al., 2011). However, RGLs in the hippocampal niche *in vivo* are likely to be exposed to a range of concentrations of FGF2, therefore I decided to titrate the concentration of FGF2 in the culture medium, to expose cells to a level that was perhaps more physiological. I titrated FGF2 to find the lowest concentration that could maintain stemness and self-renewal whilst preventing differentiation or cell death. I tested the original 20ng/mL FGF2, along with 10, 5 and 2.5ng/mL (Figure 3.7). The percentage of NSCs positive for cell cycle marker Ki67 and S-phase label EdU did not significantly vary across the concentrations of FGF2 (Figure 3.7A,B). Cell cycle protein CyclinD1 decreases with decreasing concentrations of FGF2 (although stabilises after 5ng/mL), and this is also reflected in the mRNA expression (Figure 3.7C,D). The average levels of Ascl1 protein measured by immunofluorescence intensity does not significantly change with decreasing FGF2 concentration (Figure 3.7H), although the mRNA levels measured by QPCR start to increase at concentrations lower than 10ng/mL and become more variable (Figure 3.7G), potentially suggesting the cells are moving towards differentiation. Transcript levels of stem cell marker *Nestin* are also decreased at 5 and 2.5ng/mL FGF2 (Figure 3.7E), again suggesting the NSCs may lose their stem identity with low levels of FGF2 signalling. Levels of *Dcx* transcript also increase strikingly in the lowest concentrations of FGF2 (Figure 3.7F), although as mentioned above, *Dcx* mRNA levels as measured by RNA sequencing were not detected in EGF+FGF2 conditions, and RNA sequencing on NSCs in 10ng/mL FGF2 alone (described in full detail in Section 3.4) show *Dcx* has an FPKM of 1.16, therefore even in 2.5ng/mL FGF2, *Dcx* is not expressed at very high levels. Even so, *Dcx* is induced in low concentrations of FGF2, suggesting NSCs may start to differentiate in low levels of FGF2 signalling. From a qualitative perspective, when observing the live cells in low concentrations of FGF2 in culture under the microscope, their morphology changed to become longer and thinner, with smaller, brighter nuclei, and with many more cells detaching from the plastic. Together these observations indicate that a concentration of FGF2 lower than 10ng/mL starts to induce differentiation of NSCs. Despite the observations that 10ng/mL FGF2 seemed sufficient to maintain NSCs in a self-renewing stem cell state, long-term passaging of NSCs with 10ng/mL FGF2

resulted in more spontaneous differentiation and higher numbers of cells detaching from the culture flask already by passage 16 compared to NSCs in 20ng/mL FGF2, indicating a faster loss of stemness than with 20ng/mL FGF2. Before making this final observation, I performed RNA sequencing of NSCs cultured for a low number of passages in 10ng/mL FGF2 (see Section 3.4). However, to ensure I was culturing AHNSCs in the best conditions for self-renewal and maintaining stemness over a longer period of time in culture, all other future experiments used 20ng/mL FGF2.

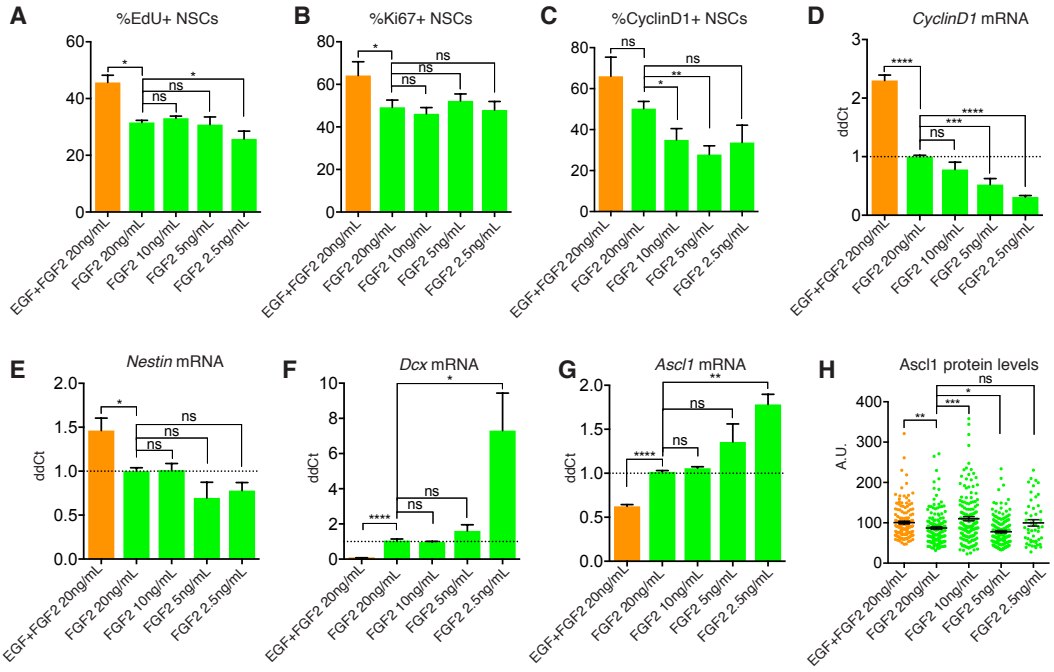

Figure 3.7. Withdrawal of EGF from active AHNSCs, and titration of FGF2

(A-C) Quantification of the fraction of EdU+, Ki67+ and CyclinD1+ NSCs following EGF withdrawal and titration of FGF2 concentration. NSC proliferation declines slightly following withdrawal of EGF, but is not strongly affected by lowering the concentration of FGF2. n=3

(D-G) QPCR analysis of *CyclinD1, Nestin, Dcx* (*doublecortin*) and *Ascl1* mRNA in EGF+FGF2 conditions, and titration of FGF2 alone. *CyclinD1* and *Nestin* decline following EGF withdrawal (D, E), and decrease in a dose-dependent manner in FGF2 titration. *Dcx* and *Ascl1* increase following EGF withdrawal (F, G) and are further upregulated in the lowest concentrations of FGF2. n=3

(H) Quantification of Ascl1 immunofluorescence levels (arbitrary units, A.U.) in NSCs in the presence of EGF+FGF2, or different concentrations of FGF2 alone. Ascl1 protein levels are not strongly affected by withdrawal of EGF or by FGF2 titration.

3.3.2 AHNSCs cultured in FGF2 alone can reversibly be induced into quiescence

Having chosen to remove EGF from the culture conditions, I re-tested whether the stem cells could be induced into a quiescent state by BMP4, and whether this was reversible. NSCs were passaged several times in the presence of FGF2 20ng/mL, and then cultured with the addition of 20ng/mL BMP4 for 72h. This resulted in a sharp decrease in the percentage of Ki67+ and EdU+ NSCs, along with an increase in GFAP immunoreactivity, as observed previously (Figure 3.8A-C). Importantly, NSCs could be quickly reactivated from BMP4-induced quiescence by plating cells back into media with FGF2 alone, with proliferation rates rebounding by 48h post-reactivation (Figure 3.8A-C). This reactivation was also not dependent on enzymatic dissociation of the cells, as when cells were reactivated without dissociation (as descried in Section 3.1) the number of Ki67+ and EdU+ cells were already increased to high levels by 48h post-reactivation (Figure 3.8D). These data strongly suggest that NSCs maintained in FGF2 alone can model BMP4-induced quiescence.

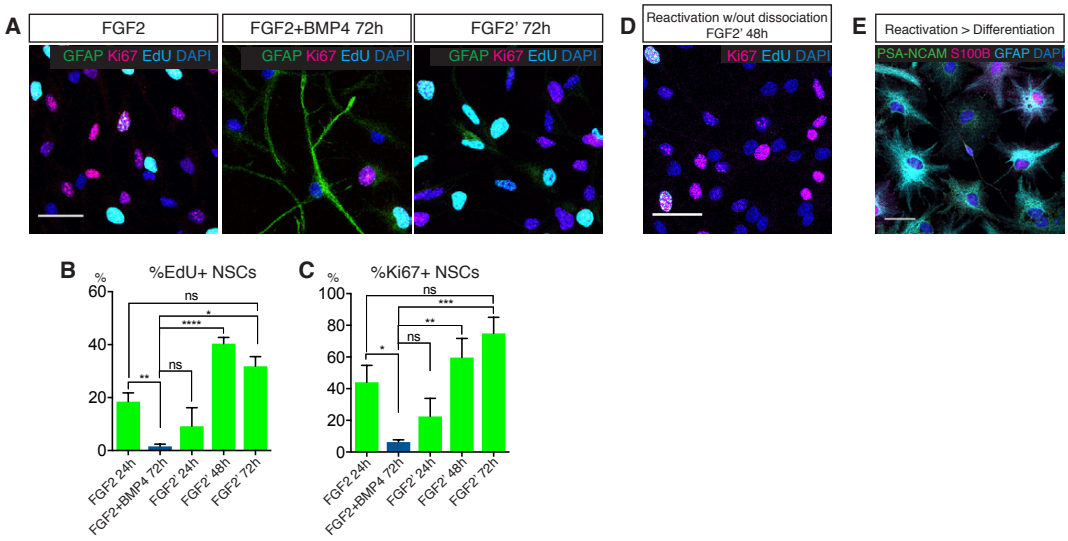

Figure 3.8. BMP4 induces reversible quiescence in AHNSCs propagated in FGF2 only

(A) Immunofluorescence for GFAP, Ki67, DAPI staining and EdU incorporation for NSCs propagated in FGF2 alone shows many proliferating NSCs, which is sharply reduced following 72h treatment with BMP4. NSCs are able to be fully reactivated from quiescence when BMP4 is withdrawn and cells are propagated in the presence of FGF2 alone, as shown by the many Ki67+ EdU+ NSCs.

(B, C) Quantification of the fraction of EdU and Ki67 positive NSCs, shown in (A). n=3.
(D) Immunostaining for Ki67 and EdU incorporation, plus DAPI staining, shows NSCs can reactivate without being dissociated from the culture plate, when BMP4 is withdrawn and cells are cultured in the presence of FGF2 alone.
(E) NSCs can be differentiated into neurons and glial cells having been propagated in FGF2 alone, induced into quiescence by BMP4 and then reactivated back into FGF2 alone. Scale bars, 30μm.

3.3.3 Titrating BMP4 induces different "depths" of quiescence

One purpose of developing an *in vitro* model of NSC quiescence is to test the effects of niche signals on NSC quiescence and examine their molecular mechanisms in more detail. *In vivo*, RGLs would potentially receive different concentrations of the various niche signals at different times, underpinning the dynamic regulation of their activity. It was important therefore to further develop the *in vitro* model to include a dynamic range of BMP4 concentrations. This would enable testing of potential activating signals, without BMP4 signalling overwhelming their effects. I therefore titrated BMP4 from 20ng/mL, to 10, 5, and 1ng/mL, and cultured the NSCs for 72h. Overall, the results show a dose curve for BMP4. Firstly, the expression of RGL marker *Gfap* shows a very clear dose-dependent upregulation with increasing concentration of BMP4, as does direct BMP4 target gene (and quiescence marker, discussed further in Section 3.4), *Id4* (Figure 3.9A,B). In contrast, cell cycle gene *CyclinD1* shows a BMP4 dose-dependent suppression (Figure 3.9C), as does the percentage of cells positive for the protein, as identified by IF (Figure 3.9E,Jiii). The percentage of Ki67+ NSCs is already strongly suppressed by 1ng/mL BMP4 compared to FGF2 alone, however there is still a dose-dependent decrease as BMP4 concentration increases (Figure 3.9F,Jiii). The percentage of cells incorporating EdU however is suppressed by 1ng/mL BMP4 and not further suppressed by higher concentrations (Figure 3.9G,Jiii). Interestingly, activation gene *Ascl1* expression is not significantly affected by BMP4 at any concentration (Figure 3.9D), but Ascl1 protein levels are suppressed in a dose-dependent manner (Figure 3.9H,Ji), an observation I will explore further in Chapter 4. Id4 protein level is also increased with increasing concentrations of BMP4 (Figure 3.9I,Ji). The morphology of cells in 1ng/mL BMP4 starts to resemble that of 20ng/mL BMP4 (Figure 3.9Jii) however the expression of GFAP protein is visibly lower in 1ng/mL BMP4 as compared to 20ng/mL (Figure 3.9Jii), reflecting the mRNA

expression levels (Figure 3.9B). These results show that 1ng/mL BMP4 is sufficient to induce cell cycle arrest in the majority of NSCs and morphological changes associated with BMP4-induced quiescence including slightly increased expression of GFAP protein, without strongly inducing or suppressing other genes. Therefore, 1ng/mL BMP4 could be used to model a “shallow” quiescence, in order to test the effects of activating signals on the cell cycle arrest aspect of quiescence, whilst 20ng/mL BMP4 induces a “deep” quiescence. Moreover, the other doses of BMP4 could be tested in concert with different concentrations of activating signal, to examine the relative strength of opposing signals on regulating NSC quiescence.

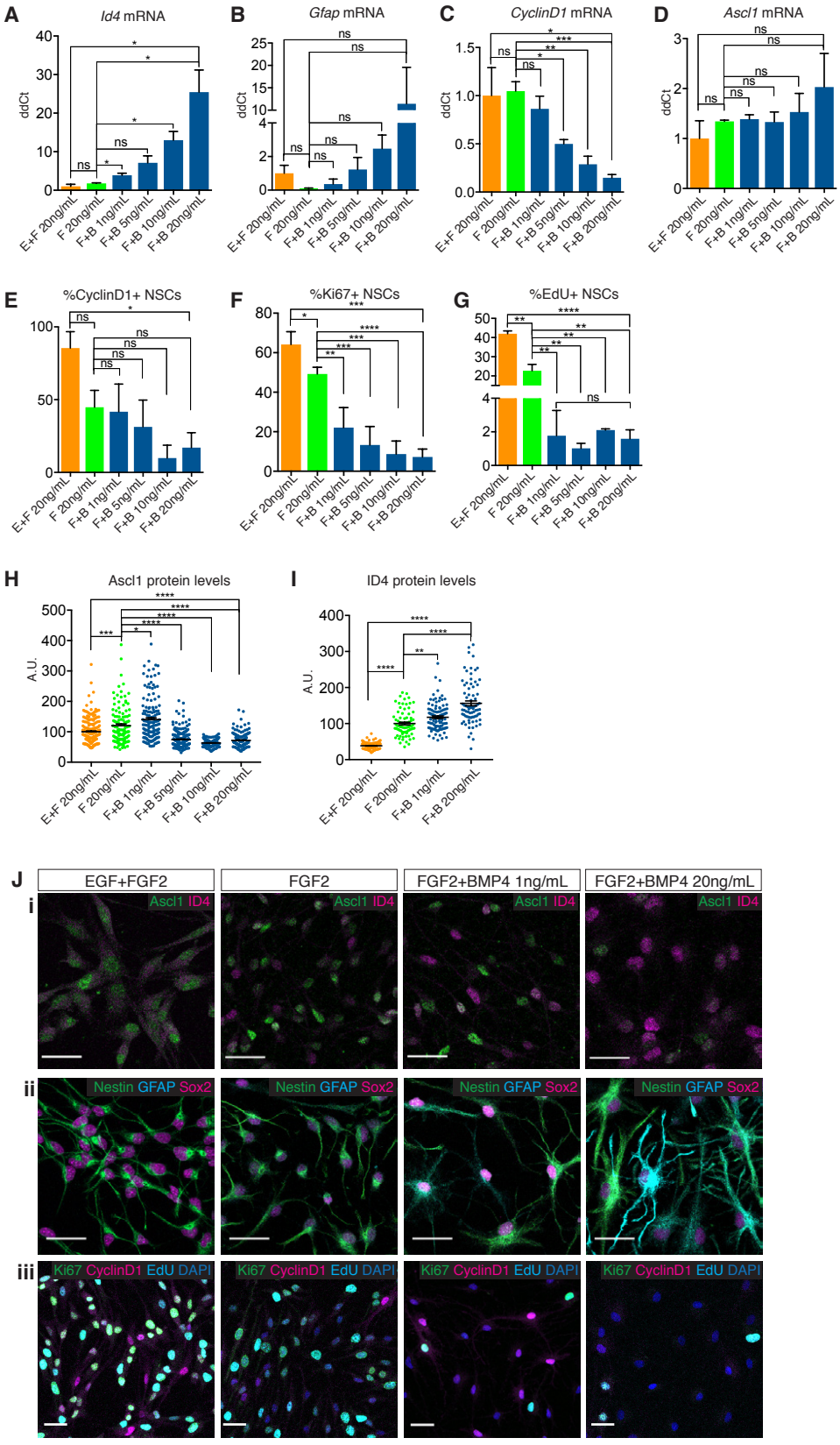

Figure 3.9. Titrating BMP4 induces quiescence in a dose-dependent manner (legend next page)

Figure 3.9. Titrating BMP4 induces quiescence in a dose-dependent manner
(A-D) QPCR analysis of the expression of *Id4, Gfap, CyclinD1* and *Ascl1* in NSCs treated with 20ng/mL EGF and 20ng/mL FGF2, FGF2 alone, or FGF2 plus BMP4 at 1ng, 5ng, 10ng or 20ng/mL (E: EGF, F: FGF2, B: BMP4). *Id4* and *Gfap* are induced and CyclinD1 repressed by BMP4 in a dose-dependent manner (A-C). Ascl1 mRNA expression is unaffected by BMP4 at any concentration (D). n=3, statistical analyses made using paired t-test (mean±SEM). p>0.05 (ns), p<0.05 (*), p<0.005(**), p<0.0005(***).
(E-G) Quantification of immunostaining for cell cycle markers CyclinD1, Ki67 and EdU incorporation in EGF+FGF2, FGF2 alone and FGF2+ 1-20ng/mL BMP4 (immunostaining shown in (Jiii)). The percentage of NSCs positive for CyclinD1 and Ki67 are reduced with increasing concentrations of BMP4. The percentage of EdU+ NSCs is suppressed by 1ng/mL BMP4 and is not further reduced by increasing concentrations. n=3
(H) Quantification of Ascl1 protein level, measured by immunofluorescence intensity (arbitrary units, A.U.) (immunostaining shown in (Ji)) shows Ascl1 is suppressed BMP4 in a dose-dependent manner.
(I) Quantification of Id4 protein level, measured by immunofluorescence intensity (arbitrary units, A.U.) (immunostaining shown in (Ji)). Id4 protein is induced by EGF withdrawal (FGF2 alone), and further induced by BMP4 in a dose-dependent manner.
(J) (i) Immunostaining for Ascl1 and Id4 in NSCs in EGF+FGF2, FGF2 alone, FGF2+BMP4 1ng/mL and FGF2+BMP4 20ng/mL (ii) Immunostaining for Sox2 and Nestin shows strong expression in NSCs in all conditions, suggesting they maintain their stemness in all conditions. GFAP is expressed at low levels in BMP4 1ng/mL and at high levels in BMP4 20ng/mL (iii) Immunostaining for Ki67, CyclinD1, EdU incorporation and DAPI shows proliferation decreases between EGF+FGF2 and FGF2, and with increasing concentration of BMP4. Scale bars, 30μm.

3.4 Transcriptome-wide analysis of the refined *in vitro* model shows BMP4-treated AHNSCs are quiescent

3.4.1 BMP4 treatment (and not EGF withdrawal) induces a quiescence transcriptional "signature" similar to *in vivo* quiescent NSCs

Having refined the *in vitro* model of NSC quiescence, I wanted to further investigate how well BMP4-induced NSCs modelled the transcriptional prolife of quiescent stem cells, both to validate the refined model and also to gain more knowledge about the genes specifically expressed in quiescent AHNSCs. We performed RNA sequencing

on AHNSCs treated with 10ng/mL FGF2, either alone or in the presence of either 1ng/mL or 20ng/mL BMP4 for 72h. At high concentrations, BMP4 regulates many hundreds of genes (1364 upregulated in 20ng/mL BMP4 vs FGF2; 933 downregulated) (Figure 3.10A,B). Gene ontology analysis showed that BMP4 strongly induces the expression of genes involved in “Cell adhesion”, “lipid metabolic process”, “Ion transport” and signalling pathways (such as Notch and Pi3k/Akt) (Figure 3.10A,B). These ontologies are highly associated with quiescence in stem cells (Shin et al., 2015) and reflect those found in quiescent NS5 cells (Figure 3.6C). The ontology “learning or memory” was also enriched in BMP4 treated AHNSCs, once again suggesting these NSCs may retain a transcriptional similarity to their *in vivo* origins in the dentate gyrus. The genes most downregulated by 20ng/mL BMP4 were mostly involved in “Cell cycle” and “Cell division” (Figure 3.10B), mirroring the results seen by IF and QPCR for cell cycle genes (Figure 3.9). An interesting difference between the ontologies enriched in the genes downregulated from FGF2 alone to BMP4, as compared to those downregulated from EGF+FGF2 to BMP4 (Figure 3.6B), is that there is a bigger variety of terms in the former, such as “Protein phosphorylation”, “Sterol biosynthetic process” and “Nervous system development”. This could indicate that the effect of removing EGF has a strong independent effect on cell cycle genes, which when combined with the effect of BMP4, enriches for cell cycle ontologies at the expense of the other BMP4-specific ontologies, further strengthening the reasoning for removing EGF from the *in vitro* system. I next compared the list of BMP4-upregulated genes with genes reported to be enriched in stem cells sorted directly from adult neurogenic niches. Specifically, I compared the 1364 genes in my dataset to the top 1000 genes enriched in FAC-sorted quiescent RGLs from the adult mouse dentate gyrus, identified by single-cell RNAseq, from the work of Shin and colleagues (Shin et al., 2015), and the genes enriched in FACS isolated quiescent SVZ NSCs by Codega and colleagues (Codega et al., 2014). Of the genes significantly upregulated by BMP4 in NSCs, 12.5% were also enriched in quiescent RGLs from the SGZ, and 23.7% were shared with quiescent SVZ NSCs (Figure 3.10C). Considering this analysis is comparing data gathered from stem cells isolated directly from the adult mouse brain versus stem cell cultures, from two different neurogenic niches, by different laboratories, and the raw data processed in different ways, it is striking that more than a third (36.3%) of the BMP4-induced genes are common with quiescent *in vivo* NSCs. Figure 3.10D shows the top 20 genes with the biggest fold-increase in BMP4-induced quiescent AHNSCs; genes that were also found to be enriched in quiescent RGLs *in*

vivo (Shin et al., 2015) are coloured green. Two of the other top "quiescence" genes identified by Shin et al., Id4 and Id3, were also strongly induced by BMP4 treatment (Figure 3.10C). Together these data strongly support the hypothesis that BMP4-induced AHNSCs model a state of quiescence with a high degree of similarity to quiescent RGLs of the adult dentate gyrus, and therefore is a biologically relevant system to further explore the regulation of SGZ NSC quiescence.

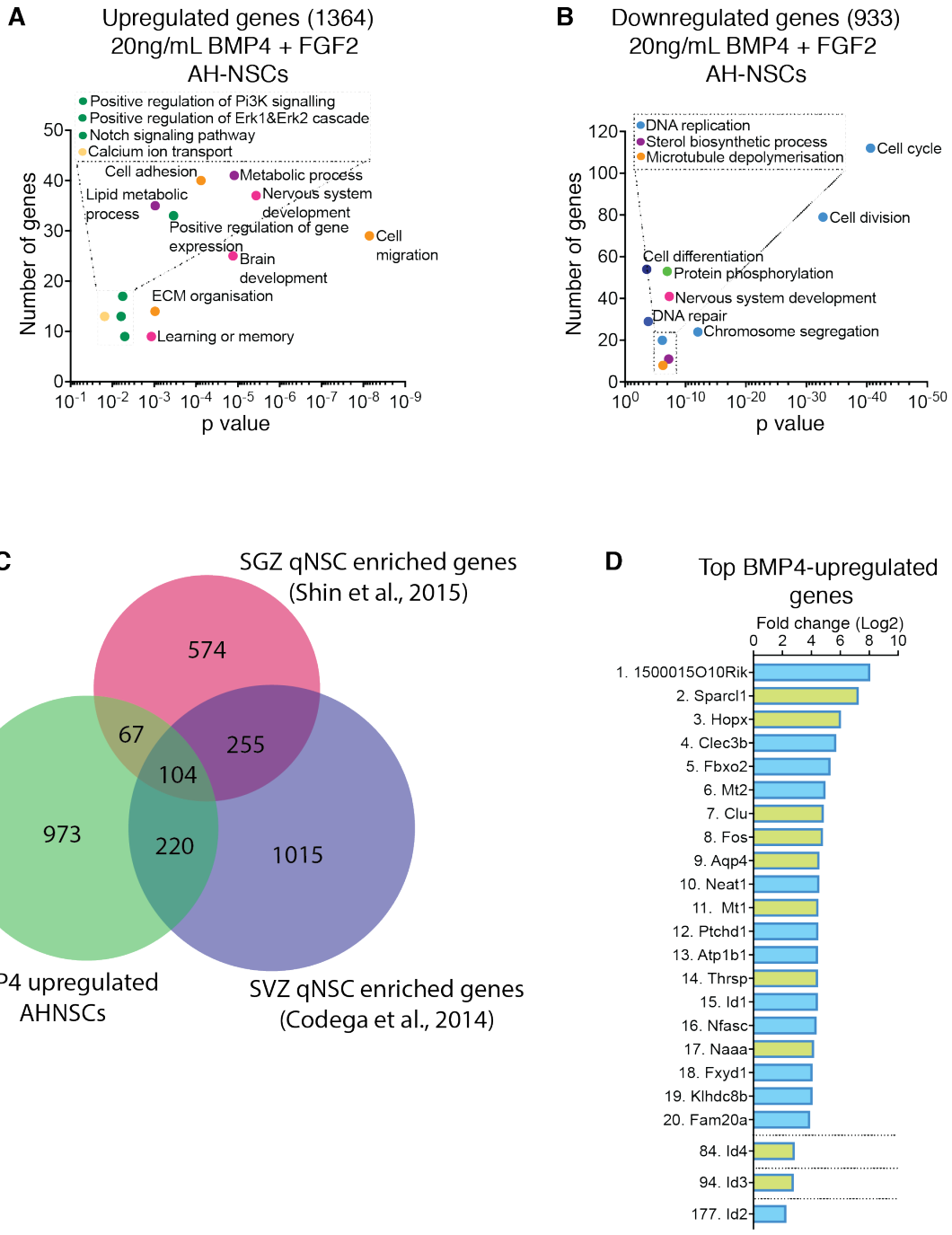

Figure 3.10. RNAseq analysis of active (FGF2 only) and quiescent (FGF2+BMP4) AHNSCs (legend next page)

Figure 3.10. RNAseq analysis of active (FGF2 only) and quiescent (FGF2+BMP4) AHNSCs

A list of genes differentially expressed between NSCs in FGF2 vs FGF2+BMP4 was generated, and split into significantly upregulated (FPKM expression in FGF2+BMP4 >=1, Log2 fold change >=1) and significantly downregulated (FPKM expression in FGF2 >=1, Log2 fold change <=-1). n=3 independent biological replicates.

(A-B) Gene Ontology terms associated with up- or down-regulated genes in FGF2+BMP4 20ng/mL 72h compared to NSCs in FGF2 alone. Shown for each term are the number of genes associated with the ontology, and its significance (p value). Dots are coloured based on their ontology terms - light blue: cell cycle/division; dark blue: DNA repair/replication; light green: Protein phosphorylation/modification; dark green: signalling, transcription; orange: adhesion/cytoskeleton; yellow: ion-related; pink: brain/nervous system related; purple: metabolism.

(C) Overlap of genes enriched (upregulated) in AHNSCs in FGF2+BMP4 conditions, with genes enriched in quiescent SGZ NSCs from Shin et al., 2015 (Supplementary Table S4, Top 1000 DOWN genes), and genes enriched in quiescent SVZ NSCs from (Codega et al., 2014) (Supplementary Table S1, "qNSC signature"). Numbers correspond to number of genes.

(D) The top 20 genes most enriched in FGF2+BMP4-treated NSCs compared to FGF2 alone are listed in order of fold change (FPKM expression in FGF2 >=1, Log2 fold change >=1). Green bars highlight genes also identified to be enriched in quiescent NSCs from (Shin et al., 2015) and (Codega et al., 2014). Also shown are Id4, Id3 and Id2 which are the 84th, 94th and 177th most expressed genes in BMP4, respectively.

3.4.2 "Shallow" and "deep" quiescent NSCs have specific transcriptional differences

As mentioned above, RGLs *in vivo* likely receive different concentrations of the various niche signals such as BMP. The level of BMP signalling they receive could dictate their response to other regulating signals, therefore it is useful to understand more about the biology of the stem cells in different concentrations of BMP4. To this end, I explored the dose-dependent transcriptional effects of BMP4 on NSCs by comparing RNAseq data generated from NSCs treated with 1ng/mL ("shallow" quiescence) vs 20ng/mL BMP4 ("deep" quiescence). Firstly, 20ng/mL BMP4 regulates far more genes than 1ng/mL BMP4 (1839 vs 254; Figure 3.11). There are some shared ontologies of genes upregulated in 1ng/mL and 20ng/mL BMP4, such as "Ion transport", "Lipid metabolic

process", "Pi3K signalling" and "Memory" (Figure 3.11A), and most of the upregulated genes overlap with those upregulated by 20ng/mL BMP4 (Figure 3.11C). However, the top enriched ontology in 20ng/mL BMP4 (and published NSC quiescent signatures (Codega et al., 2014; Shin et al., 2015)) "Cell adhesion" is not enriched in 1ng/mL BMP4 conditions, suggesting high doses of BMP4 are required to induce a full transcriptional "quiescence" profile. The downregulated genes however are more similar in ontology between the two concentrations of BMP4, mostly concerning "Cell cycle", and again most of the downregulated genes overlap with those downregulated by 20ng/mL BMP4 (Figure 3.11D), suggesting low dose of BMP4 mostly affects the cell cycle, which was also seen by analysis of proliferation markers (Figure 3.9). Overall, these results show that 1ng/mL BMP4 can partially induce the quiescence transcriptional programme, mostly regulating cell cycle genes, but it is not sufficient to induce the wide-scale transcriptomic changes seen with 20ng/mL BMP4, which more strongly correspond with the published data on quiescent NSCs (Codega et al., 2014; Shin et al., 2015). Lower concentrations of BMP4 may be useful in modelling a shallow state of quiescence from which the stem cells are more easily reactivated, as well as to determine the interaction of BMP with other niche signals such as Notch, which I will explore further in Chapter 5. The higher concentration of BMP4 induces a "deeper" state of quiescence and based on the analysis here may model more closely the quiescent state of adult RGLs *in vivo*.

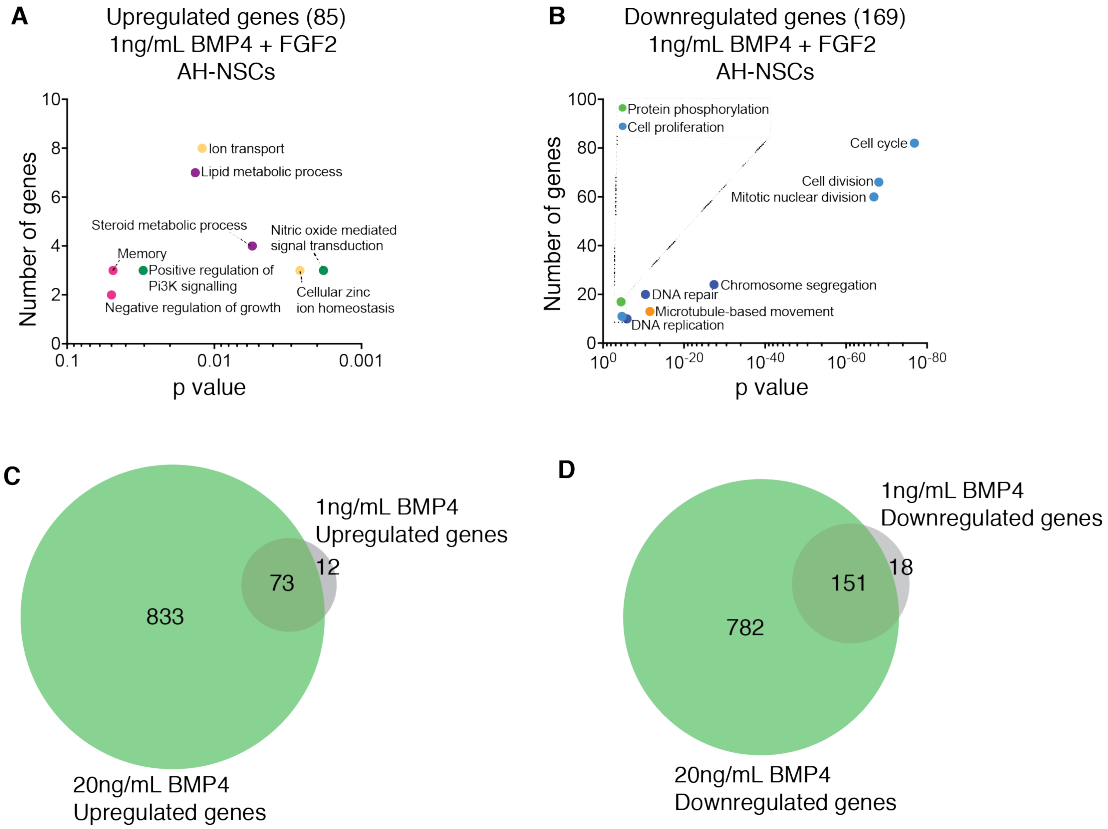

Figure 3.11. Comparison of 1ng/mL vs 20ng/mL BMP4 in quiescent AHNSCs by RNAseq

(A-B) Gene Ontology terms associated with up- or down-regulated genes in FGF2+BMP4 1ng/mL 72h compared to NSCs in FGF2 alone. Shown for each term are the number of genes associated with the ontology, and its significance (p-value). Dots are coloured based on their ontology terms - light blue: cell cycle/division; dark blue: DNA repair/replication; light green: Protein phosphorylation/modification; dark green: signalling, transcription; orange: adhesion/cytoskeleton; yellow: ion-related; pink: brain/nervous system related; purple: metabolism.

(C,D) Overlap of genes up- or down-regulated in 20ng/mL or 1ng/mL BMP4. Numbers correspond to number of genes.

Chapter 4. Results 2

Having developed an *in vitro* model of AHNSC quiescence that closely resembles many features of quiescent RGLs in the SGZ, as described in Chapter 3, I next sought to use this model to further investigate the molecular mechanisms downstream of BMP4-induced quiescence, by combining the *in vitro* model with investigating RGL quiescence *in vivo*. Previous work from our laboratory has identified Ascl1 protein to be expressed in a subset of active RGLs and a crucial activation factor for RGLs (Andersen et al., 2014), as well as being tightly regulated at the protein level by the E3-ubiquitin ligase Huwe1 (Urban et al., 2016). Moreover, in Chapter 3 I presented the interesting observation that BMP4 suppresses the levels of Ascl1 protein, but not *Ascl1* mRNA in quiescent NSCs (Figure 3.9D,H). These results raised the possibility that Ascl1 may be transcriptionally active in quiescent NSCs, but suppressed at the protein level. In light of these findings, I began my investigation of the regulation of RGL quiescence by further characterising Ascl1 expression in quiescent vs active RGLs. In this chapter, I will begin by presenting the unexpected findings of *Ascl1* mRNA expression in quiescent RGLs *in vivo*, focussing on the differences between the mRNA and protein expression, and confirming the *in vitro* model recapitulates these observations. I will then describe the identification of Id4 as a candidate regulator of Ascl1 protein stability downstream of BMP4 signalling, characterising its expression in RGLs *in vitro* and NSCs *in vivo*. Next, I will present the functional analysis of Id4 in NSCs *in vitro*, and the effects of Id4 conditional deletion *in vivo* on RGL quiescence. Finally, I will investigate whether Id4 expression is downstream of BMP/Smad signalling *in vivo*.

4.1 Ascl1 is expressed at the transcriptional level, but inhibited at the protein level, in quiescent NSCs *in vivo* and *in vitro*

4.1.1 Many more RGLs *in vivo* express *Ascl1* mRNA than Ascl1 protein

Ascl1 has been shown to be a crucial transcription factor for RGL activation, integrating niche signals to drive a transcriptional program to activate RGLs (Andersen et al., 2014). It has also been shown that negative regulation of Ascl1 stability by the E3 ubiquitin ligase Huwe1 is required to enable active RGLs to return to quiescence, by promoting the degradation of Ascl1 (Urban et al., 2016). However, considering Ascl1 levels are central to regulating RGL activation from quiescence, it had not been

examined whether Ascl1 protein is also regulated in quiescent RGLs, nor has the transcriptional expression of Ascl1 in RGLs been examined. Therefore, I investigated Ascl1 transcriptional levels in RGLs in adult mice, by examining the expression of GFP in P70 *Ascl1*^{KiGFP} mice in which the coding region of one allele of Ascl1 is replaced by the coding sequence for nuclear-localised GFP, downstream of the Ascl1 promoter. This means GFP+ RGLs report Ascl1 transcriptional expression. RGLs were identified by their expression of Glial Fibrillary Acidic Protein (GFAP), localisation of their nucleus in the subgranular zone of the DG, and the presence of a radial process extending towards the molecular layer. By monoclonal antibody immunostaining, Ascl1 protein is detected in a very small percentage of RGLs, representing the "active" fraction (Figure 4.1A; (Andersen et al., 2014)). Strikingly, *Ascl1* mRNA as reported by GFP immunoreactivity was found in the majority (82.3±3.8%) of RGLs, in stark contrast to the 1.9±0.3% RGLs positive for Ascl1 protein (Figure 4.1A,C) (IF and quantifications performed by N. Urban). I also used an independent readout of Ascl1 protein, the *Ascl1*^{Venus} mouse line, which expresses an Ascl1-Venus fusion protein and allows detection of lower levels of Ascl1 by GFP immunostaining (Figure 4.1B), levels which we were not able to detect using the monoclonal antibody (I will discuss further the issues of Ascl1 antibody staining in Section 4.4.3). Many more Ascl1+ RGLs were detected using Ascl1Venus fluorescence (50.5±10.5%) than monoclonal Ascl1 antibody immunoreactivity (Figure 4.1C), although quantification of the actual fluorescence levels showed many of the positive RGLs had very low levels of Venus (Figure 4.1D). Specifically, 72.4% of the RGLs measured had a Venus intensity less than the mean, indicating the majority of RGLs had low Ascl1Venus levels. Also, despite the higher percentage of Ascl1Venus+ RGLs than Ascl1KiGFP+ RGLs, still around 30% more RGLs expressed *Ascl1* mRNA (GFP) than Ascl1Venus (Figure 4.1C). Overall these data show many more RGLs express *Ascl1* mRNA than Ascl1 protein.

The levels of Ascl1 transcription in *Ascl1*^{KiGFP} mice (GFP immunostaining) were variable (Figure 4.1A,E,G), with some RGLs expressing high levels of GFP and others low levels. This could reflect an oscillatory expression of *Ascl1* transcription, similar to what has been observed for Ascl1 in embryonic NSCs (Imayoshi et al., 2013). A dynamic expression pattern of this kind could regulate the activation of RGLs, with higher Ascl1kiGFP levels representing RGLs that are closer to activation. To determine whether *Ascl1* transcription (GFP) levels correlated with other markers of activation, I

double-labelled RGLs for GFP and Ki67 (Figure 4.1E). Every Ki67+ RGL identified was also GFP+ (Figure 4.1F). However, 83.8±4.1% of Ki67- quiescent RGLs were also GFP+ (Figure 4.1F), indicating *Ascl1* mRNA is expressed in most quiescent RGLs. I next measured the GFP fluorescence intensity in Ki67+ (active) and Ki67- (quiescent) RGLs to see whether *Ascl1* is expressed at a higher level in active RGLs and at a lower level in quiescent RGLs. Figure 4.1G shows average GFP levels were not significantly different in active and quiescent RGLs. This shows that both active and quiescent RGLs express *Ascl1* mRNA, suggesting there is a negative regulatory mechanism functioning in most RGLs to suppress Ascl1 protein expression. Interestingly, the range of GFP intensity values was greater in quiescent compared to active RGLs. The dynamics of *Ascl1* transcription in RGLs *in vivo* has not been investigated, and it would be interesting to explore whether there is a functional significance to this expression pattern with regards to neural stem cell activity.

A caveat of using *Ascl1*^{KIGFP} mice to readout Ascl1 transcript levels is the stability of the GFP is not necessarily equivalent to the stability of Ascl1 protein, therefore GFP positivity may reflect a cell that had been transcribing Ascl1 in the past, but had shut it down by the time of analysis. In other words, *Ascl1*^{KiGFP} could be giving false positive results. Therefore, to more specifically examine *Ascl1* mRNA expression in RGLs *in vivo*, I performed fluorescent RNA *in situ* hybridization using the RNAscope® system (ACD/Biotechne) on brain sections from P60 mice, for both *Ascl1* and *Ki67*, followed by immunocytochemistry for GFAP. GFAP IHC allowed me to identify RGLs based on their immunoreactivity and morphology, and *Ki67* RNA staining enabled me to distinguish between active and quiescent RGLs. In addition, I also analysed *Ascl1* and *Ki67 in situ* in *GlastCre*^{ERT2}*;tdTomato (Ai9)* mice 48h after a single tamoxifen injection. These mice have a Cre reporter allele with a *loxP*-flanked STOP cassette, which allows for tdTomato expression following tamoxifen-induced Cre-mediated recombination. tdTomato clearly marks the morphology of recombined RGLs, allowing for more reliable identification of RGLs than GFAP IHC. Giving a single injection of tamoxifen induces sparse recombination in GLAST-expressing stem cells, allowing for the identification of individual recombined RGLs. I identified 93 RGLs across 5 mice, based on GFAP or tdTomato immunoreactivity and morphology, of which 20 were *Ki67*+, and 72 were *Ascl1*+. mRNA was detected as fluorescent ‘dots’ of varying sizes (Figure 4.1H,I). Every RGL positive for *Ki67* mRNA had at least 1 ‘dot’ of *Ascl1* mRNA (Figure 4.1H-J). Out of the *Ki67*- RGLs identified, 27.39% were negative for *Ascl1* mRNA,

however two thirds had at least one ‘dot’ of *Ascl1* mRNA, with many having far more, some with up to 17 detectable ‘dots’ (Figure 4.1J). This shows that Ascl1 is transcribed in quiescent RGLs *in vivo*, reflecting the results from quiescent NSCs *in vitro*. The average number of *Ascl1* mRNA ‘dots’ in *Ki67*- RGLs was 2.58±0.3, and was not significantly different from the average number in *Ki67*+ RGLs (3.95±0.8). mRNA ‘dots’ varied in size, with some having a stronger fluorescence signal than others, which could reflect differing amounts of RNA. Therefore, to determine whether there was a difference in *Ascl1* mRNA levels between active and quiescent RGLs that could be seen by differences in *Ascl1* fluorescence, I measured the fluorescence intensity of Ascl1 *in situ*, in the area within and around the nucleus of identified RGLs, following the boundary of GFAP or tdTomato immunofluorescence. Average fluorescence intensity of Ascl1 *in situ* was not significantly different between quiescent (*Ki67*-) and active (*Ki67*+) RGLs (86.51±3.6 vs 100±8.8 arbitrary units; Figure 4.1K), indicating *Ascl1* is transcribed at similar levels in both active and quiescent RGLs. This strongly suggests there is a mechanism regulating Ascl1 protein levels in RGLs *in vivo*.

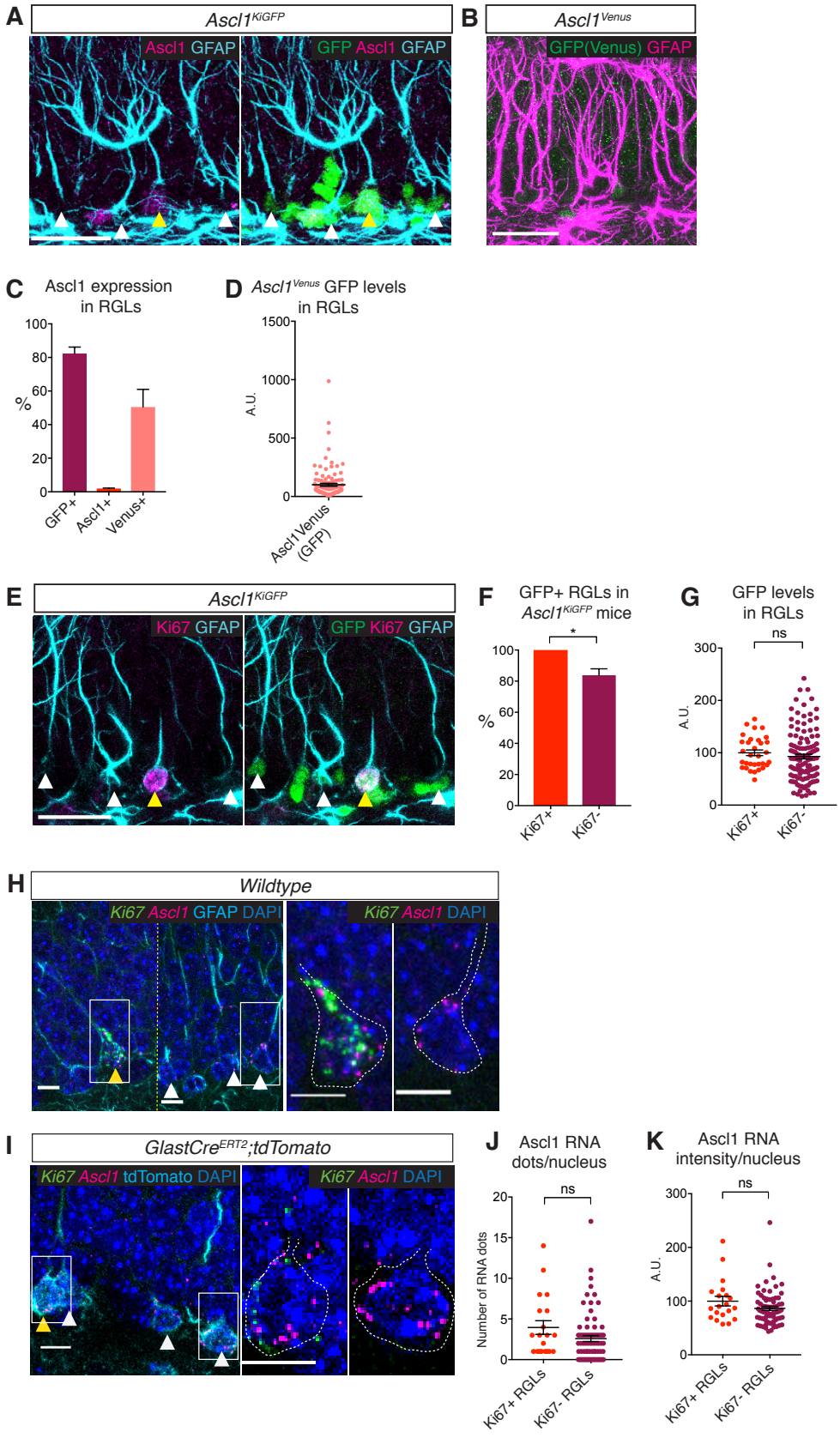

Figure 4.1. Ascl1 mRNA and protein expression in hippocampal RGLs (legend next page)

Figure 4.1. Ascl1 mRNA and protein expression in hippocampal RGLs

(A) Immunolabelling for Ascl1, GFAP and GFP in the subgranular zone (SGZ) of the dentate gyrus (DG) of *Ascl1*^{KiGFP} mice. White arrows indicate GFP+Ascl1- RGLs; yellow arrows indicate GFP+Ascl1+ RGLs. Scale bar, 30μm.

(B) Immunolabelling for GFAP and GFP(Ascl1-Venus) in adult *Ascl1*^{Venus} mice. Scale bar, 30μm.

(C) Quantification of percentage of GFP+ RGLs in *Ascl1*^{KiGFP} mice; Ascl1+ RGLs detected by monoclonal antibody staining; and Ascl1Venus+ RGLs in *Ascl1*^{Venus} mice. The widespread GFP expression in *Ascl1*^{KiGFP} mice indicates Ascl1 is transcribed in most GFAP+ RGLs. Venus immunostaining in *Ascl1*^{Venus} mice is detected in more RGLs than monoclonal antibody staining for Ascl1, likely due to the more sensitive and robust GFP antibody. n=3 mice.

(D) Quantification of the fluorescence levels of Ascl1Venus in *Ascl1*^{Venus} mice (detected by GFP immunostaining) shows a range of expression levels with the vast majority showing low levels of expression. n=1 representative mouse.

(E) Immunolabelling for GFP, Ki67 and GFAP in the SGZ of the DG of *Ascl1*^{KIGFP} reporter mice. White arrows indicate GFP+Ki67- RGLs; yellow arrows indicate GFP+Ki67+ RGLs. Scale bar, 30μm.

(F, G) Quantification of the data in (E). Most quiescent (Ki67-) RGLs express GFP and therefore transcribe *Ascl1* (F) and the average levels of GFP are not significantly different in quiescent and proliferating RGLs (G), indicating that Ascl1 is transcribed in both RGL populations. The range of GFP fluorescence levels is much higher in quiescent RGLs, suggesting they have a higher dynamic range of Ascl1 transcriptional activity, possibly reflecting an oscillatory expression. n=3 mice.

(H, I) RNA *in situ* hybridization by RNAscope® with an Ascl1 probe (magenta) and a Ki67 probe (green) and Immunolabelling for GFAP in wildtype mice, or tdTomato in *Glast-CreERT2;tdTomato* mice, to mark RGLs in the SGZ of the DG. To label RGLs with tdTomato, *Glast-CreERT2;tdTomato* mice were injected once at P60 with 4-hydroxytamoxifen, and analysed 48h later. White arrows indicate RGLs positive for Ascl1 RNA staining; yellow arrows show RGLs positive for both Ascl1 and Ki67 RNA. Magnifications of the RGLs marked by white boxes are shown on the right, highlighting an RGL positive for both *Ascl1* and *Ki67* RNA, and an RGL positive for only *Ascl1* RNA. Dotted lines show the outline of the GFAP or tdTomato signal. Scale bar, 10μm. n=5 mice.

(J, K) Quantification of the data in (H, I). Ascl1 RNA levels were quantified either by counting the number of RNA 'dots' per nucleus (J) and the intensity of the fluorescence signal per RGL nucleus (K). Ascl1 transcripts are found at a similar level in quiescent

(Ki67-) and proliferating (Ki67+) RGLs. 100 RGLs were quantified across n=5 mice. All statistical analyses were made using unpaired t-test (mean±SEM). p>0.05 (ns), p<0.05 (*).

4.1.2 Ascl1 protein, but not mRNA, is inhibited by BMP4-induced quiescence in AHNSCs *in vitro*

I next looked to see how Ascl1 mRNA and protein were expressed in active and quiescent AHNSCs *in vitro*, to see whether the observations *in vivo* could be recapitulated by the *in vitro* model. I repeated QPCR analysis of *Ascl1* mRNA levels in active (FGF2 20ng/mL) and quiescent NSCs (FGF2 20ng/mL +BMP4 20ng/mL, 72h), from cells that had been cultured for several passages in FGF2 alone (rather than immediately following EGF withdrawal, as for results shown in Chapter 1), which again showed no change between the two conditions (Figure 4.2A). I also analysed AHNSCs derived from adult *Ascl1*^{KiGFP} mice. GFP expression acts as a readout for Ascl1 transcriptional levels, so I performed immunocytochemistry for GFP in active and quiescent *Ascl1*^{KiGFP} AHNSCs in culture, which revealed many GFP+ cells in both active and quiescent conditions in a 'salt and pepper' pattern (Figure 4.2B), which could indicate an oscillatory expression dynamic, similar to the observation of Ascl1KiGFP staining *in vivo* and live imaging of Ascl1 transcription in embryonic NSCs (Imayoshi et al., 2013). Analysis of nuclear GFP fluorescence intensity in every cell revealed no significant difference in average intensity between active and quiescent AHNSCs (Figure 4.2C), further supporting the notion that BMP4 does not affect *Ascl1* mRNA expression. I next repeated immunofluorescence staining of Ascl1 protein in active and quiescent non-transgenic AHSNCs (Figure 4.2D), and measured the nuclear fluorescence intensity (Figure 4.2E), which showed BMP4 significantly supressed Ascl1 protein levels. This observation was confirmed by measuring Ascl1 protein levels in AHNSC lysates by Western blot (Figure 4.2F; Western blot performed by M. Masdeu), which showed a significant decrease in Ascl1 protein in quiescent AHNSCs. These results indicate Ascl1 is actively transcribed but repressed at the protein level in quiescent NSCs.

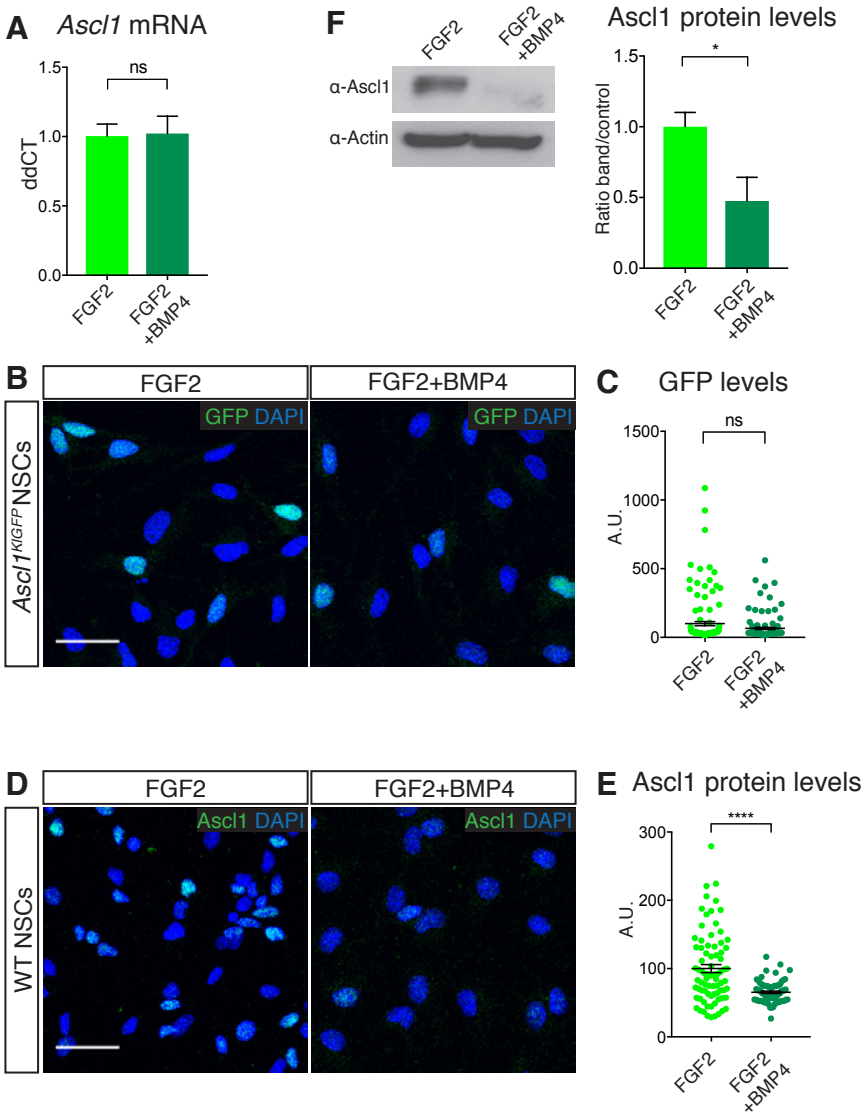

Figure 4.2. Ascl1 mRNA and protein expression in AHNSCs *in vitro*

(A) QPCR analysis of transcript levels of *Ascl1* in hippocampal-derived NSCs in active (FGF2) or quiescent (FGF2+BMP4 20ng/mL) conditions. Ascl1 mRNA levels are not changed between active and quiescent conditions.

(B) Immunocytochemistry for GFP and DAPI staining in active and quiescent NSCs derived from *Ascl1*^{KIGFP} mice. Scale bar, 30μm.

(C) Quantification of GFP levels shown in (B). The average fluorescence level (arbitrary units, A.U.) for GFP, which reports Ascl1 transcriptional activity, is not significantly different between active and quiescent NSCs. Data shown is from one representative experiment of n=3 independent biological replicates.

(D) Immunocytochemistry for Ascl1 and DAPI staining in FGF2- and FGF2+BMP4-treated NSCs. Scale bar, 30μm.

(E) Quantification of the data in (D). The levels of Ascl1 protein, measured by fluorescence intensity (A.U.) is expressed in a salt-and-pepper pattern in active NSCs, possibly reflecting an oscillatory expression, with many expressing high levels of Ascl1. Ascl1 protein is mostly undetectable in quiescent NSCs. Data shown is from one representative experiment of n=3 independent biological replicates.
(F) Western blot analysis and quantification of Ascl1, relative to Actin, in FGF2- and FGF2+BMP4-treated NSCs. BMP4 suppresses Ascl1 protein expression. n=3
All statistical analyses were made using unpaired t-test (mean±SEM). $p>0.05$ (ns), $p<0.05$ (*), $p<0.0001$(****).

4.1.3 Ascl1 protein is actively translated in NSCs *in vitro*

One hypothesis for why *Ascl1* mRNA but not protein is expressed in quiescent RGLs, is that *Ascl1* mRNA is transcribed into protein in quiescent RGLs, but is subsequently very rapidly degraded by the proteasome. This could be possible, due to the short 30-minute half-life of Ascl1 protein in active NSCs (Urban et al., 2016). An alternative hypothesis is that the mRNA is being transcribed but prevented from being translated, for example by microRNA-mediated translation inhibition (without mRNA destabilisation), or via the various other forms of translational regulation that exist in eukaryotic cells (reviewed by (Sonenberg and Hinnebusch, 2009)). Therefore, I tested whether Ascl1 protein was being actively translated in quiescent NSCs using the *in vitro* quiescence model, by inhibiting the proteasome and measuring Ascl1 protein levels by Western Blot. To inhibit the proteasome, I used MG132 which inhibits the function of the proteasome by covalently binding to the active proteolytic sites inside the proteolytic ß-ring domain, thereby inhibiting proteasomal degradation of ubiquitinated proteins. I induced quiescence in NSCs with BMP4, and then treated them with 10μm of the MG132 for 30, 60 and 120 minutes. Control quiescent NSCs were treated with an equal volume of DMSO for 30mins. Ascl1 protein is barely detectable in BMP4-induced quiescent NSCs (Figure 4.1F; Figure 4.3A DMSO control) however following MG132 treatment the protein is clearly detected and strongly increased compared to control (Figure 4.3A), indicating Ascl1 protein is actively transcribed in quiescent NSCs but rapidly degraded in a proteasome-dependent manner. Increased levels of Ascl1 protein were also observed in active NSCs treated with the proteasome inhibitor (Figure 4.3B), reflecting the dynamic regulation of Ascl1 and its short half-life (Urbán et al., 2016).

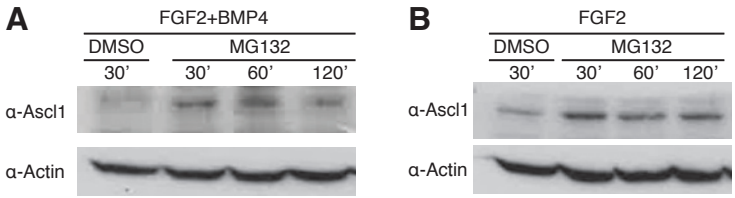

Figure 4.3. Ascl1 protein levels increase in AHNSCs following proteasomal inhibition

(A, B) Western blot analysis of Ascl1 in quiescent (FGF2+BMP4 10ng/mL) or active (FGF2) NSCs, after treatment with 10uM of the proteasome inhibitor MG132 for 30, 60 or 120 minutes. Ascl1 levels are undetectable in quiescent NSCs relative to Actin, however a clear band is observed following proteasomal inhibition (A). Ascl1 levels are also increased following proteasomal inhibition of active NSCs (B). n=1.

4.1.4 Proteasomal degradation of Ascl1 in quiescent NSCs is independent of Huwe1

As previously mentioned at the beginning of this chapter, our lab has shown that Ascl1 protein is targeted for degradation in active RGLs by the E3-ubiquitin ligase Huwe1 (Urban et al., 2016). I therefore tested whether Huwe1 was mediating the proteasomal degradation of Ascl1 in quiescent NSCs. I used AHNSCs derived from Cre-mediated Huwe1 knock-out mice (Huwe1$^{fl/Y}$; Urban et al., 2016) in order to conditionally delete Huwe1 (Huwe1^{cKO}) in AHNSCs *in vitro*. I transduced active and quiescent AHNSCs with either empty Adenovirus or Adenovirus expressing Cre-recombinase, to induce recombination of the floxed Huwe1 allele. I measured Ascl1 protein levels in Huwe1^{cKO} NSCs by immunofluorescence and found BMP4 was able to significantly suppress the levels of Ascl1 protein in the absence of Huwe1 (Figure 4.4A,B), indicating there is a Huwe1-independent mechanism acting in quiescent AHNSCs to promote the proteasomal degradation of Ascl1. This result agrees with the observation that Huwe1 is required *in vivo* to facilitate the return of proliferating RGLs to quiescence, but not required to maintain RGL quiescence itself (Urban et al., 2016).

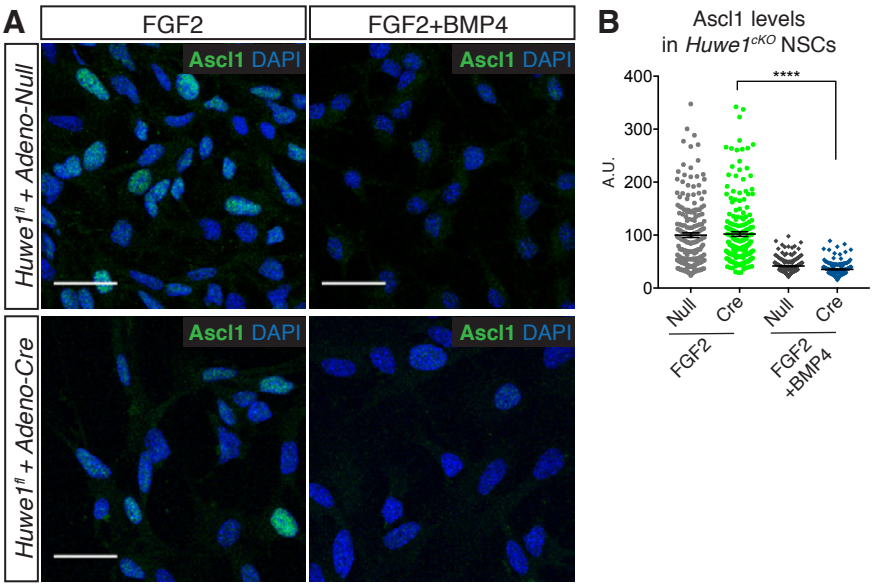

Figure 4.4. Inhibition of Ascl1 protein in quiescent AHNSCs is Huwe1-independent

(A) Immunostaining for Ascl1 and DAPI staining in NSCs derived from Huwe1-floxed mice, infected with either Adeno-empty or Adeno-Cre to induce recombination of the floxed alleles and delete Huwe1. Cells were fixed 6 days following adenoviral infection, in order to allow sufficient time for the very stable Huwe1 protein to degrade. Treatment with 72h BMP4 20ng/mL was able to suppress Ascl1 protein levels in both control and *Huwe1*^{cKO} cells. Scale bar, 30μm.

(B) Quantification of Ascl1 immunofluorescence shown in (A). Ascl1 levels (arbitrary units, A.U.) are significantly suppressed by BMP4 treatment even in the absence of Huwe1. n=1. Unpaired t-test (mean±SEM), p<0.0001(****).

4.2 Inhibitor of Differentiation 4 (Id4) is highly expressed in quiescent RGLs and NSCs, and anti-correlates with Ascl1 protein

4.2.1 Expression of the Id proteins *in vivo*

I next explored the potential mechanism regulating Ascl1 protein in quiescent RGLs. Id proteins have been described to negatively regulate bHLH transcription factors like Ascl1, by sequestering E-proteins, which are dimerization partners of Ascl1 and are required for the stabilisation of Ascl1 protein and DNA binding of its target genes (Shou

et al., 1999; Vinals et al., 2004). The RNAseq analysis of BMP4-induced quiescent NSCs showed the four *Id* genes *Id1-4* were strongly enriched in the quiescent state (Figure 3.10D). Id4 was also shown to be the most enriched gene in quiescent RGLs in the single cell RNAseq data generated from FAC sorted RGLs in adult mice (Shin et al., 2015). Therefore, I examined the expression of the four Id proteins in the SGZ of adult mice. Id1 is expressed in around half of all RGLs (52.2±4.4%; Figure 4.5A,B), whereas Id4 was found in 89.57±2.3% of all RGLs (Figure 4.5D,E). Id3 expression was found in a very small number of RGLs, and Id2 was expressed by granule neurons and not in RGLs (Figure 4.5I,J). Based on these expression patterns, Id1 and Id4 are the more likely candidates to be negatively regulating Ascl1 in quiescent RGLs. Interestingly, analysis of the protein level of Id1 or Id4 in quiescent (Ki67-) vs active (Ki67+) RGLs, quantified by fluorescence intensity of the immunostaining, showed that Id1 was enriched in active RGLs (Figure 4.5C), whereas Id4 was highly enriched in quiescent RGLs (Figure 4.5F). Moreover, immunostaining for Id4 in Ascl1Venus mice showed Ascl1Venus+ RGLs had lower levels of Id4 than Venus- RGLs (Figure 4.5G,H) suggesting an anti-correlation between Id4 and Ascl1. These data implicate Id4 as a key candidate for regulating Ascl1 protein in quiescent RGLs *in vivo.*

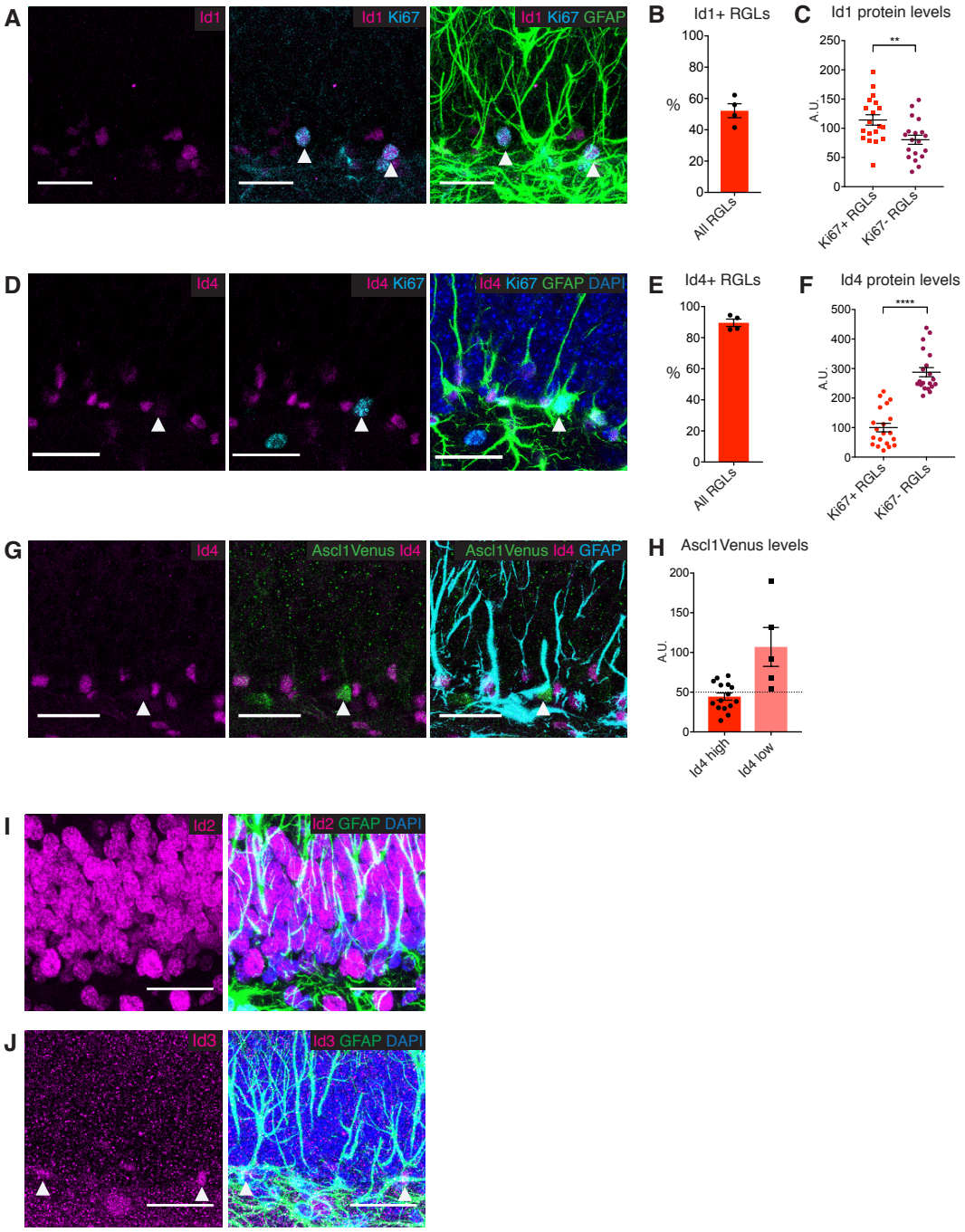

Figure 4.5. Protein expression of Id1, 2, 3 and 4 in the dentate gyrus

(A) Immunolabelling for Id1, Ki67 and GFAP in the dentate gyrus of adult mice. White arrows indicate GFAP+RGLs positive for both Id1 and Ki67. Scale bar, 30µm.

(B) Quantification of the percentage of Id1+ GFAP+ RGLs. n=4 mice.

(C) Quantification of Id1 protein levels, measured by immunofluorescence intensity (A.U.) in active (Ki67+) or quiescent (Ki67-) RGLs. Id1 levels are significantly higher in active RGLs. n=4 mice.

(D) Immunolabelling for Id4, Ki67 and GFAP in the dentate gyrus of adult mice. The white arrow indicates a GFAP+RGL positive for Ki67 and negative for Id4. Scale bar, 30μm.
(E) Quantification of the percentage of Id4+ GFAP+ RGLs. n=4 mice.
(F) Quantification of Id4 protein levels, measured by immunofluorescence intensity (A.U.) in active (Ki67+) or quiescent (Ki67-) RGLs. Id4 protein is strongly enriched in quiescent RGLs. n=4 mice.
(G) Immunolabelling for Id4, Ascl1Venus (GFP) and GFAP in the dentate gyrus of adult *Ascl1*^{Venus} mice. The white arrow indicates a GFAP+RGL positive for Ascl1Venus and negative for Id4. Scale bar, 30μm.
(H) Quantification of the immunofluorescence levels of Ascl1Venus in RGLs with high or low levels of Id4. Ascl1Venus levels are much higher in Id4 low RGLs, compared to Id4 high. The dotted line indicates the threshold for Ascl1Venus positivity. n=1 representative mouse.
(I, J) Immunofluorescence for GFAP and Id2 (I) or Id3 (J) plus DAPI staining in the DG of adult mice. Id2 is expressed in granule neurons, while Id3 is expressed in astrocytes and very small number of RGLs. White arrows indicate Id3+ GFAP+ RGLs. Scale bar, 30μm.

4.2.2 Id4 is the most enriched Id protein in quiescent AHNSCs *in vitro*, and anti-correlates with Ascl1

I returned to the *in vitro* model of AHNSC quiescence to see whether Id4 was enriched in BMP4-induced quiescence. I had already observed that Id4 was upregulated upon BMP4 treatment compared to EGF+FGF2 conditions (Figure 3.9A,I). I repeated the QPCR for *Id4*, along with *Id1-3*, in cells cultured in FGF2 alone and FGF2+BMP4, which showed all four Id genes were upregulated upon 72h BMP4 treatment, with *Id4* showing the biggest fold-change (Figure 4.6A). I next analysed the protein levels of the four Ids by immunocytochemistry (Figure 4.6E-H). Each Id protein had some degree of expression in active NSCs, and quantification of the fluorescence intensity showed Id2 and Id3 were not changed following BMP4 addition, whereas Id1 and Id4 were strongly upregulated at the protein level in quiescent NSCs (Figure 4.6B). Moreover, the pattern of Id2 and Id3 in quiescent NSCs was fairly uniform, whereas Id1 and Id4 had a salt and pepper expression pattern (Figure 4.6E-H), much like Ascl1, which could indicate a dynamic regulation and allow for the expression of Ascl1 protein in those cells where Id1/4 is lower expressed. Western blotting for Id1, Id3 and Id4 confirmed the upregulation of Id1 and Id4 by BMP4 (Figure 4.6C) (the antibody for Id2 did not work

for Western blot; Western blots performed by M. Masdeu). The fold increase for Id4 protein is quantified in Figure 4.6D, showing significant upregulation by BMP4. Id1 and Id4 therefore presented as promising candidates for regulating Ascl1 protein in quiescent NSCs, with Id4 being the top candidate based on its expression *in vivo*. I next analysed the co-expression of Ascl1 and the Id proteins by immunofluorescence (Figure 4.6E-L). Ascl1 is expressed at low levels in a small percent of quiescent NSCs, and so I measured the fluorescence intensity of Ascl1 and each Id protein, and plotted the values against each other. Pearson correlation coefficient analysis showed a positive correlation between Ascl1 and Id1, Id2 and Id3 (Figure 4.6I-K), whereas for Id4 the correlation coefficient was close to 0. When I inputted the thresholds for Id4 and Ascl1 positivity (determined by background fluorescence, marked by dotted lines on graph 4.6L), I saw that no quiescent NSC was positive for both Ascl1 and Id4; where Id4 levels were higher, Ascl1 was low or negative, and in the few cells that express detectable Ascl1, Id4 levels were below the threshold to be considered positive. This mutually exclusive expression pattern reflects the pattern of Id4 and Ascl1Venus *in vivo*, and may be indicative of Id4 functioning to suppress Ascl1 levels.

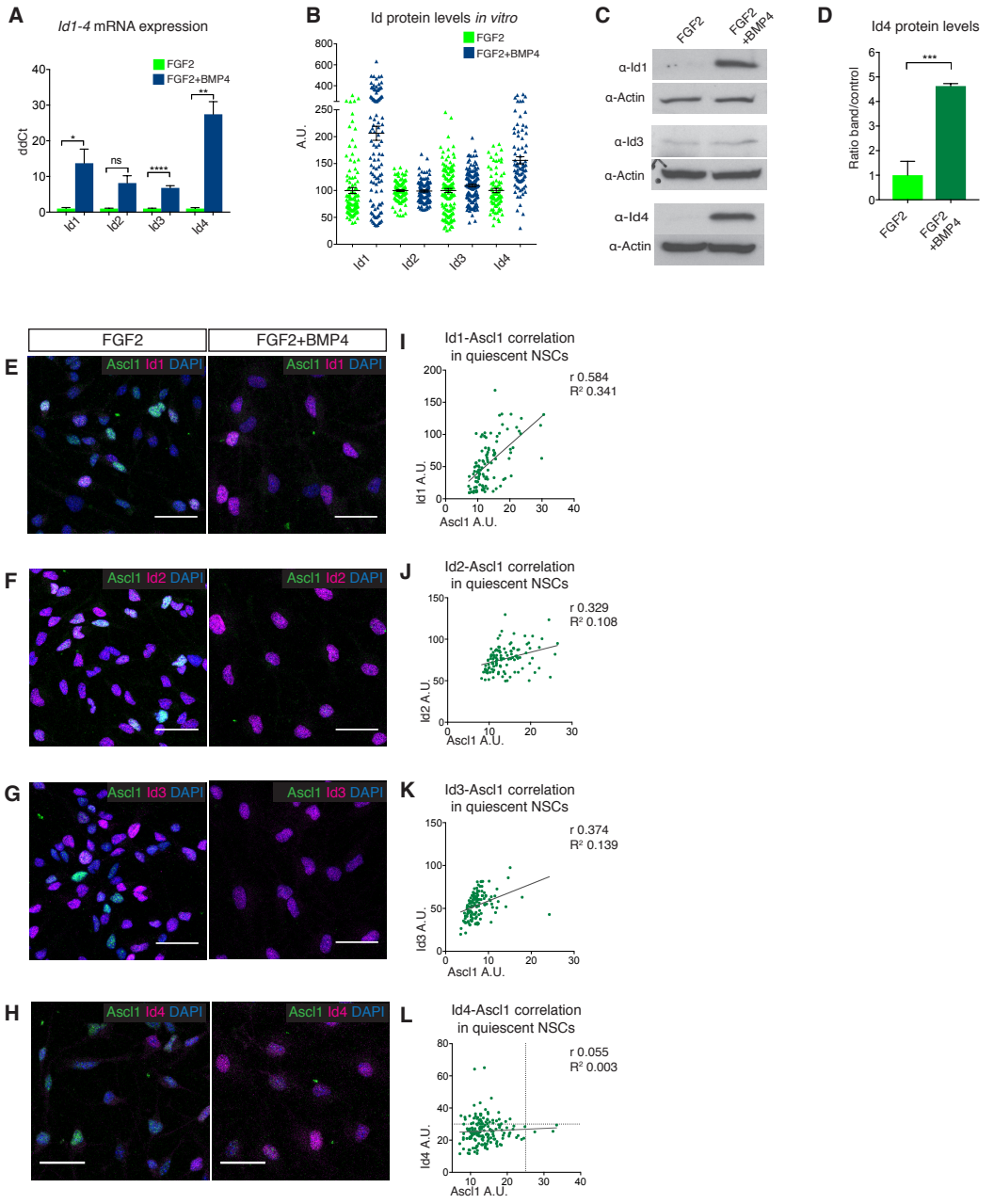

Figure 4.6. Expression of Id1-4 in AHNSCs *in vitro*

(A) QPCR analysis of the expression levels of *Id1-4* in active (FGF2) and quiescent (FGF2+BMP4 20ng/mL) NSCs *in vitro*. n=3 for Id1,3 and 4. n=2 for Id2.

(B) Quantification of immunofluorescence levels (A.U.) of Id1-4 in active (FGF2) and quiescent (FGF2+BMP4 20ng/mL) NSCs *in vitro*. n=3. At least 100 cells were quantified.

(C) Western blot analysis of Id1, Id3 and Id4 in active (FGF2) and quiescent (FGF2+BMP4 20ng/mL) NSCs *in vitro*. Id2 antibody was unable to detect any signal, with high background.

(D) Quantification of Id4 protein levels as determined by Western blot. n=3.

(E-H) Immunolabelling of Id1, Id2, Id3 or Id4 with Ascl1 and DAPI staining in active and quiescent NSCs. Scale bar, 30μm.
(I-L) Plots of Ascl1 immunofluorescence vs Id1,2,3 or 4 immunofluorescence per nuclei, measured from the immunostainings shown in (E-H). Shown are the correlation coefficients (r) and coefficient of determination (R^2) for Ascl1 with each Id protein. Ascl1 is positively correlated with each Id protein except for Id4.

4.2.3 E-proteins are expressed in hippocampal NSCs and interact with Ascl1 and Id4 *in vitro*

Before further investigating the function of Id4 in relation to Ascl1 in quiescence, I needed to examine the expression of the third player in the Id-bHLH dynamic, the E-proteins, which in mammals are E47, E12, E2-2 and HEB. The inhibitor of differentiation proteins are well known to regulate bHLH transcription factors by sequestering the bHLH dimerization partners, E-proteins, rendering the bHLH factor unable to bind DNA and activate its target genes. When Ascl1 is monomeric, it is highly unstable and rapidly targeted for degradation (Vinals et al., 2004). At this stage, we hypothesised that the degradation of Ascl1 protein in quiescent RGLs was caused by the high levels of Id4 sequestering the E-protein dimerization partners of Ascl1. I therefore examined the expression of the genes encoding the E-proteins, *Tcf3* (the mRNA of which is alternately spliced to produce E47 or E12 protein), *Tcf4* (encoding E2-2) and *Tcf12* (encoding HEB) from the RNAseq data of active vs quiescent NSCs described in Chapter 3. FPKM values for the three *Tcf* genes show all three are expressed in NSCs *in vitro*, with slightly lower expression in quiescent NSCs (Figure 4.7A). I also examined their expression in the database of single cell RNAseq gene expression generated by the Linnarsson lab from FAC sorted adult DG cells, which show all three *Tcf* genes are expressed in RGLs, with *Tcf4* being the most highly expressed (http://linnarssonlab.org/dentate/), although none are expressed at high levels, especially when compared to Id4 expression, suggesting that expression of the E-proteins is a limiting factor in the stability of Ascl1 protein. I next examined whether the protein product of these genes was detectable in NSCs *in vitro*. E47 protein is expressed in both active and quiescent NSCs *in vitro*, shown by Western blot (Figure 4.7B; Western blots performed by M. Masdeu). Attempts were made to measure the levels of the other E-proteins, but commercial antibodies tested were unable to detect any protein. I next investigated whether E47 binds to Ascl1 and Id4 in NSCs *in vitro*. The Ascl1Venus cell line was used here, as the mouse monoclonal antibody against

Ascl1 does not work well for Western blot, in contrast to the very strong and consistent signal for GFP (Ascl1Venus). The Ascl1Venus fusion protein is reported to have similar expression as endogenous Ascl1 and Ascl1Venus transgenic mice show normal development (Imayoshi et al., 2013), suggesting the fusion protein functions comparably to endogenous Ascl1. In active NSCs, immunoprecipitation for E47 was able to pull down GFP (Ascl1), whereas no Id4 co-immunoprecipitated with E47 or Ascl1 (GFP) in this condition (Figure 4.7C, lanes 1 and 5), although this may reflect the low expression of Id4 in FGF2 conditions. In contrast, in quiescent NSCs, E47 was able to pull down Id4 (lane 5), and Id4 could pull down E47 (lane 8), whereas no Id4-Ascl1 co-IP was detected, although again this may simply reflect the low levels of Ascl1 in quiescent NSCs, meaning there is no protein to IP in the first place. However, when Ascl1Venus (GFP) was immunoprecipitated in quiescent NSCs, a band was detected using the GFP antibody (Lane 7), suggesting there is still some Ascl1 in quiescent conditions to IP, which would suggest Id4 and Ascl1 do not dimerise. We would expect that in conditions of high Id4 (quiescence), E47 and Ascl1 do not dimerise, as Id4 is sequestering all the E-protein. However, Ascl1-E47 co-IP is also observed in quiescent NSCs (lane 7) (Figure 4.7C). This could reflect that Id4 is not able sequester all the E-protein away, leaving some to bind with Ascl1, but not enough to stabilise high levels of Ascl1 protein. This makes sense with regards to the immunostaining of Ascl1 in BMP4-treated NSCs; even though there is a very strong suppression, some cells do have detectable Ascl1. A mouse anti-V5 tag antibody was used as the negative control; V5 is never expressed in cells unless genetically modified, therefore the antibody will only detect background for mouse species of antibody. The negative control showed no co-IP of any of the proteins, and each protein was able to be detected by Western blot for its own IP (Figure 4.7C, lanes 3,4,7,8) (Co-IPs and Western blots performed by M. Masdeu). Overall, these results confirm that Ascl1-E47 heterodimers exist in active NSCs, and Id4-E47 dimers are present in quiescent NSCs. It could therefore be inferred that Id4 is sequestering E47 from Ascl1 in quiescent conditions, promoting unstable monomeric Ascl1.

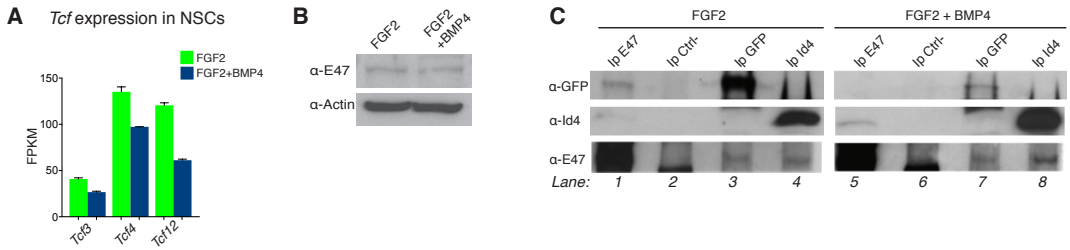

Figure 4.7. E-protein expression and co-immunoprecipitation of E47, Id4 and Ascl1 in AHNSCs *in vitro*

(A) The expression of the *Tcf3, 4* and *12* are shown as Fragments per Kilobase per Million reads (FPKM) from RNA sequencing of active and quiescent NSCs. All three *Tcf* genes are expressed in both conditions, slightly higher in active than quiescent NSCs.

(B) Western blot analysis for *Tcf3* gene product E47, which shows it is expressed at the protein levels in both active and quiescent NSCs.

(C) Immunoprecipitation of the Ascl1 dimerisation partner E47 from FGF2- and FGF2+BMP4-treated NSCs, followed by western blot analysis of GFP(Ascl1Venus) and Id4. E47 co-immunoprecipitates with GFP in FGF2 conditions but with Id4 in FGF2+BMP4 conditions. Mouse anti-V5 antibody was used for the negative control.

4.3 Functional analysis of Id4 *in vitro* reveals its role in maintaining quiescence of NSCs

4.3.1 Over-expression of Id4 in active NSCs *in vitro* suppresses Ascl1 protein, and induces cell cycle arrest

The results so far suggest Id4 may function to maintain quiescence by inhibiting and downregulating Ascl1 protein, via sequestration of its E-protein binding partners. To test this functionally, I nucleofected active AHNSCs with Id4 expressed from a pcBeta plasmid, with a CMV promoter and an N-terminal FLAG tag (pcBeta-Id4-nFLAG) (Figure 4.8A). Nucleofected NSCs were then incubated for a further 48h in the presence of FGF2, and then analysed. The hypothesis is that in active NSCs, Ascl1 is heterodimerised with the E-protein E47, and able to bind the E-box sites in its target genes to activate transcription. However, over-expression of Id4 will cause E47 to be preferentially dimerised to Id4, leaving Ascl1 monomeric and therefore 1) unable to bind DNA to activate transcription of its target genes, and 2) rapidly targeted for degradation (Figure 4.8B). After 48h transfection, the

efficiency of transfection was 33.75±4.2%, measured by the very strong immunoreactivity for overexpressed Id4; endogenous Id4 was undetectable due to the very high levels of exogenously expressed Id4 (Figure 4.8C,D). By measuring the fluorescence intensity of Ascl1 immunostaining in Id4+ vs Id4- NSCs, I observed a highly significant reduction in Ascl1 protein level in Id4 over-expressing NSCs (Figure 4.8C,E). This suggests Id4 may be mediating the BMP4-induced suppression of Ascl1 protein in AHNSCs, although Id4 is expressed at a higher level by overexpression, compared with BMP4-induced Id4, and so the effect observed here could also be a result of artificially high levels of Id4. I confirmed that Id4 overexpression was not affecting *Ascl1* mRNA expression by QPCR (Figure 4.8F) from RNA extracted from FAC sorted, nucleofected NSCs (described below in Section 4.3.2). Id4 overexpression also partially induced cell cycle arrest in NSCs; the percentage of Ki67+ NSCs was significantly reduced from 50.81±5.7% in Id4- NSCs to 29.7±2.9% in Id4+ NSCs (Figure 4.8G,H), and the percentage of NSCs in S-phase marked by EdU incorporation during a 1 hour pulse prior to fixation, was also decreased, although not significantly (22.03±4.6% in control NSCs, 13.19±2.7% in Id4+ NSCs; Figure 4.8I,J). I independently validated these findings by over-expressing Id4 in active NSCs via transduction of an Id4-expressing Adenovirus. I transduced cells in FGF2 with either 100moi (multiplicity of infection; number of viral particles per cell) Adeno-empty virus, as a control, or Adeno-Id4 at 100moi, and analysed the cells after 20h. After this time, Ascl1 protein levels were decreased in Id4-overexpressing NSCs compared to control NSCs, quantified by immunofluorescence intensity (Figure 4.8K-M). The percentage of cells positive for EdU following a 1 hour pulse prior to fixation, was also decreased in Adeno-Id4 transduced cells compared to Adeno-empty transduced. Together these results support the hypothesis that Id4 contributes to the reduced levels of Ascl1 protein and to the reduced levels of proliferation in quiescent NSCs. However, the Adenovirus over-expression experiment was n=1, and therefore must be repeated before strong conclusions can be drawn.

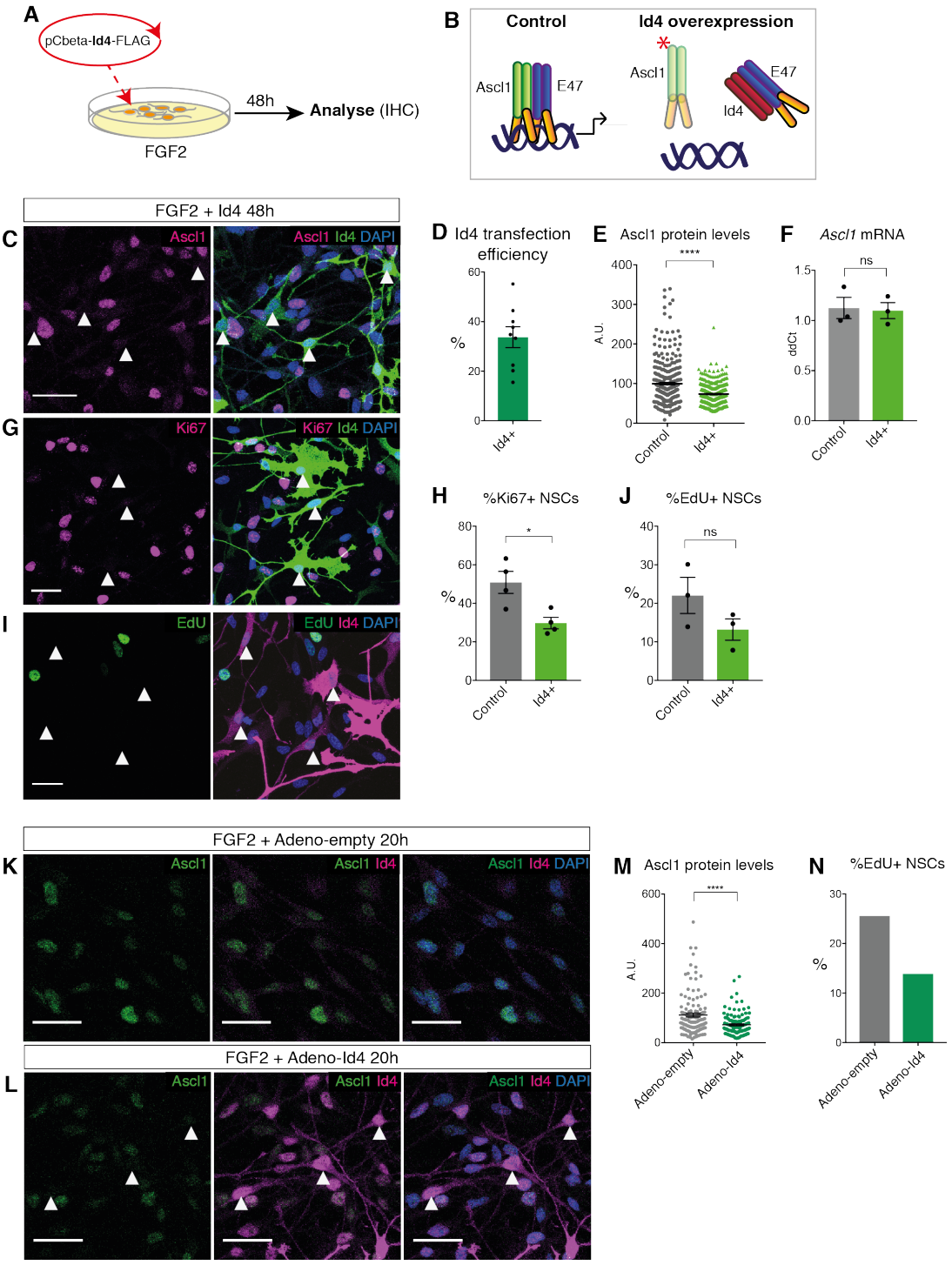

Figure 4.8. Over-expression of Id4 in active AHNSCs *in vitro*

(A) Experimental design for the overexpression of Id4 in active NSCs, via nucleofection of a pCbeta-Id4-NFLAG expression construct. NSCs were analysed 48h after nucleofection. (B) Scheme showing the hypothesis for the effect of Id4 overexpression. In control active NSCs, Ascl1 is heterodimerised to E47, and able to bind DNA and activate transcription of its target genes. When Id4 is overexpressed, it sequesters E47, leaving Ascl1 undimerised.

In its monomeric form, Ascl1 is unable to bind DNA and activate transcription, and is also highly unstable and quickly targeted for degradation (red star).
(C) Immunostaining for Ascl1 and Id4 and DAPI in active NSCs 48h-post Id4 nucleofection. The high levels of Id4 overexpression can be seen from the strong green immunolabelled cells. White arrows show the low or absent levels of Ascl1 in Id4-overexpressing NSCs. Scale bar, 30μm.
(D) The percentage of Id4+ NSCs amongst all NSCs was quantified to give a transfection efficiency. n=8 from 4 independent biological repeats.
(E) Quantification of the data shown in (C). Ascl1 protein levels are significantly reduced in active NSCs over-expressing Id4. n=4
(F) Ascl1 mRNA levels are unaffected by Id4 overexpression, measured by QPCR. n=3
(G, I) Immunostaining for Ki67 (G) or EdU (I) with Id4 and DAPI staining in active NSCs 48h-post Id4 nucleofection. White arrows indicate Id4+ NSCs negative for Ki67 or EdU. Scale bar, 30μm.
(H, J) Quantification of the data shown in (G, I). The percentage of NSCs positive for Ki67 or EdU is reduced when Id4 is overexpressed. n=4 for H, n=3 for J.
(K, L) Immunolabelling of Ascl1, Id4 and DAPI staining in active NSCs transduced with either control adenovirus (Adeno-empty, upper panel) or adenovirus expressing Id4 (Adeno-Id4, lower panel). A concentration of 100 multiplicity of infection (moi) i.e. 100 viral particles per cell, was used and NSCs were analysed 20h post-infection. White arrows indicate Id4-overexpressing NSCs with undetectable levels of Ascl1. Scale bar, 30μm. n=1
(M) Quantification of the data shown in (K,L). Ascl1 protein levels were significantly suppressed in Adeno-Id4 infected NSCs. n=1
(N) The percentage of EdU+ NSCs was reduced in NSCs infected with Adeno-Id4 vs control adenovirus. n=1

4.3.2 Over-expression of Id4 in active NSCs *in vitro* induces transcriptional changes associated with quiescence

To determine how much of the BMP4-induced quiescence programme was mediated by Id4, I examined the global transcriptional effect of Id4-overexpression in active NSCs, by RNAseq of Id4-transfected NSCs. In order to isolate transfected cells, I needed to co-transfect a GFP-expressing plasmid (pCAGGS-IRES-GFP) alongside pCbeta-Id4-nFLAG, which does not express a fluorescent protein. Active NSCs were nucleofected with either pCAGGS-IRES-GFP alone or in combination with pCbeta-Id4-FLAG in a ratio of 1:2 (GFP:ID4) to ensure GFP+ NSCs were likely to also be Id4+ in

co-transfected cells. NSCs were incubated in FGF2 for 48h following nucleofection, FAC sorted for GFP+ NSCs, and RNA extracted for RNAseq analysis (Figure 4.9A). In order to confirm the transfected NSCs received both the GFP and Id4 plasmids together, I immunostained co-transfected cells for both GFP and Id4, and analysed their co-localisation (Figure 4.9B), which showed a high degree of co-expression. I quantified this by plotting the A.U. fluorescence value for GFP and ID4 in each cell against each other, which showed a positive correlation (Figure 4.9C) suggesting FAC sorted GFP+ NSCs are highly likely to also be transfected with Id4, and therefore will provide a clean population of transfected NSCs for RNAseq analysis. To control for the overexpression of GFP, active NSCs were transfected with the same GFP-expressing construct in parallel to those transfected with Id4 (Figure 4.9A), and FAC sorted and processed for RNAseq. Differential gene expression analysis was performed on mRNA sequenced from GFP+ (control) versus Id4+(GFP+) NSCs. This analysis revealed Id4 regulates a large number of genes; over-expression induced the expression of 806 genes, and inhibited the expression of 823 (Figure 4.9D). The ontology of genes upregulated by Id4 include “Cell adhesion”, “Metabolic process”, and “Anion transport” (Figure 4.9E), ontologies also seen enriched in BMP4-induced quiescence (Figure 3.6A), suggesting Id4 may contribute to regulating a large subset of “quiescence” genes. Much like with BMP4-induced quiescence, the ontologies of genes downregulated by Id4-overexpression centre mostly on cell cycle processes (Figure 4.9F), reflecting the effect of Id4-overexpression on cell cycle arrest (Figure 4.8G-J), and again suggesting Id4 may mediate part of BMP4-induced cell cycle arrest. Direct comparison of the genes regulated by Id4 and BMP4 showed a large overlap (Figure 4.9G) with 44.2% of BMP4-regulated genes also regulated by Id4. The ontologies of the commonly up- and down-regulated genes unsurprisingly show the common quiescence signature ontologies, including “cell adhesion”, signalling pathways and cell cycle regulation (Figure 4.9H,I). Together these results show Id4 can regulate a large part of BMP4-indcued quiescence, although the majority of the BMP4-induced genes are induced by other factors downstream of BMP4.

Finally, I examined the effect of Id4 overexpression on specific Ascl1 target genes, to see whether the suppression of Ascl1 protein levels by Id4 corresponds to a suppression of Ascl1 activity. Indeed, the Counts Per Million of all 10 Ascl1-target genes examined, including *Dll1*, *Skp2*, *Birc5*, *Egfr*, and *Rrm2* (identified by ChIP-chip for Ascl1, in embryonic mouse telencephalon (Castro et al., 2011)) showed significant

downregulation in Id4-overexpressing active NSCs compared to GFP-expressing active NSCs (Figure 4.9J; grey bars control, green bars Id4). Moreover, Id4-overexpression was sufficient to downregulate these genes to very similar levels as BMP4+GFP-treatment alone (Figure 4.9J, blue bars). The only Ascl1 target gene that was not regulated in the same way by Id4 as BMP4, was *Fbl*, which was significantly downregulated by Id4 but not BMP4. Id4 also regulated many cell cycle genes to a similar extent as BMP4, such as CyclinB1 and CyclinE1 (Ccnb1, Ccne1; Figure 4.9K). Even CyclinD2, which is in fact significantly upregulated by BMP4 treatment, is also trending towards upregulation by Id4. Overall, these data indicate Id4 is responsible for regulating a significant proportion of the transcriptional programme induced by BMP4 in quiescent NSCs, specifically the suppression of Ascl1 target genes. This is likely an indirect result of the suppression of Ascl1 protein by Id4. Moreover, Id4 appears to regulate more than just the cell cycle status of NSCs, as evidenced by the upregulation of genes involved in cell adhesion, phosphorylation and signalling pathways. These data suggest Id4 is central to the regulation of adult NSC quiescence.

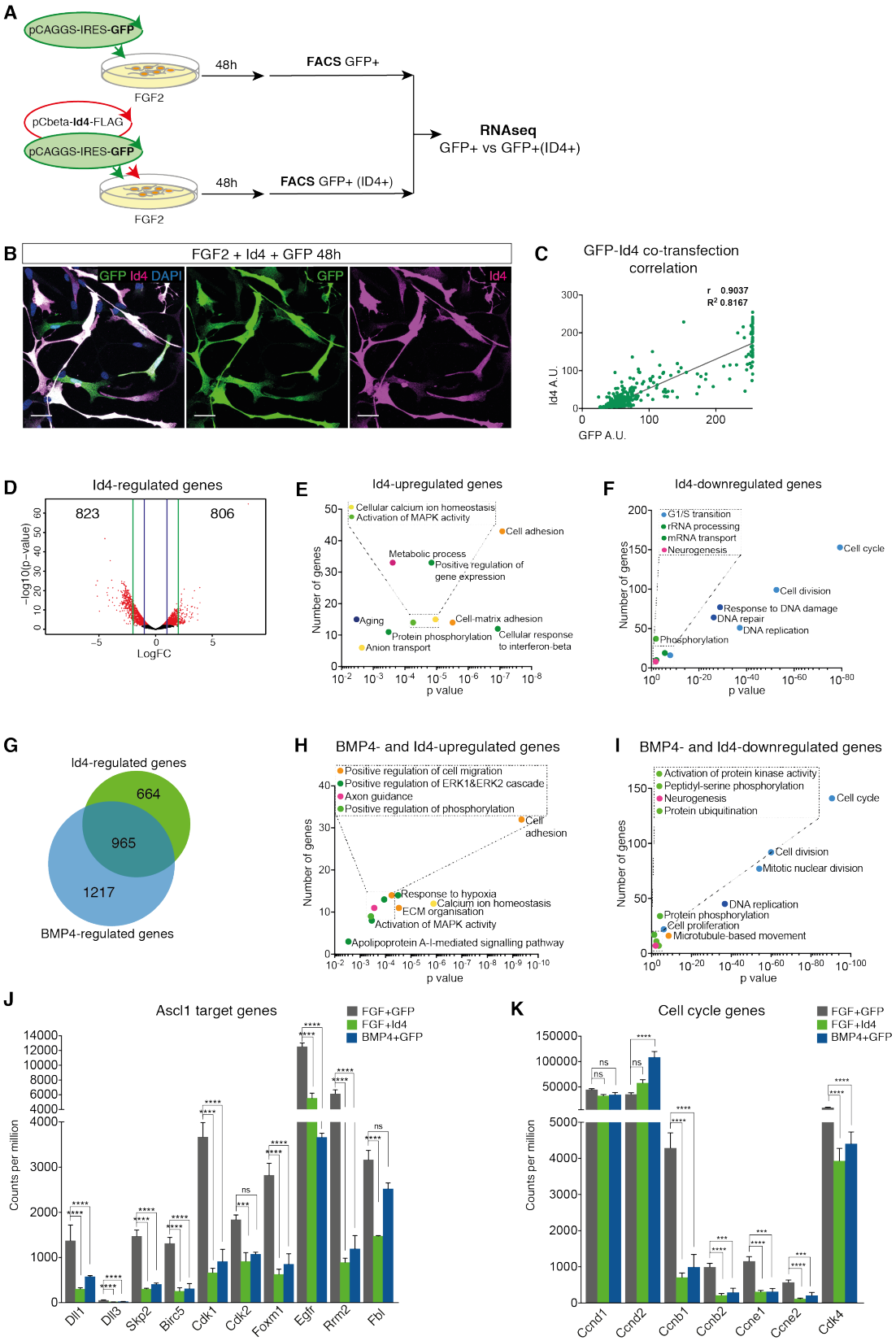

Figure 4.9. RNAseq analysis of Id4 over-expression in active AHNSCs *in vitro* (legend next page)

Figure 4.9. RNAseq analysis of Id4 over-expression in active AHNSCs *in vitro*

(A) Experimental design for overexpressing Id4 in active NSCs followed by Fluorescence Activated Cell Sorting (FACS). Active NSCs were nucleofected with either pCAGGS-IRES-GFP alone or in combination with pCbeta-Id4-FLAG in a ratio of 1:2 (GFP:ID4) to ensure GFP+ NSCs are likely to also be Id4+ in co-transfected cells. NSCs were incubated in FGF2 for 48h following nucleofection, FAC sorted for GFP+ NSCs, and RNA extracted for RNAseq analysis.

(B) Immunostaining for GFP and Id4, and DAPI staining in NSCs nucleofected with both GFP and Id4 constructs, showing a high level of co-transfection.

(C) Quantification of data shown in (B). The immunofluorescence level of GFP is highly correlated with Id4 in co-transfected cells, with a correlation coefficient of 0.9037. The coefficient of determination (0.8167) shows the data closely fit the regression line. n=360 cells from one biological repeat.

(D) Volcano plot of genes regulated by Id4 overexpression in active NSCs.

(E,F) Gene ontology terms associated with up- or down-regulated genes in active NSCs overexpressing Id4 compared to GFP-nucleofected NSCs. Shown for each term are the number of genes associated with the ontology, and its significance (Log10 p-value). Dots are coloured based on their ontology terms - light blue: cell cycle/division; dark blue: DNA repair/replication; light green: Protein phosphorylation/modification; dark green: signalling, transcription; orange: adhesion/cytoskeleton; yellow: ion-related; pink: brain/nervous system related; purple: metabolism; navy blue: organism-wide process.

(G) Overlap of Id4-regulated and BMP4-regulated genes.

(H, I) Gene ontology terms associated with up- or down-regulated genes in both Id4-overexpressing and BMP4-treated NSCs. Ontologies are coloured based on categories described above.

(J) Expression of Ascl1 target genes, shown as counts per million (CPM) from RNAseq analysis of active NSCs nucleofected with GFP or Id4, and quiescent NSCs nucleofected with GFP. Every Ascl1 target is significantly suppressed by Id4 overexpression, and to a very similar extent to BMP4 treatment. n=3 independent biological replicates.

(K) Expression of cell cycle genes, shown as counts per million (CPM) from RNAseq analysis of active NSCs nucleofected with GFP or Id4, and quiescent NSCs nucleofected with GFP. Id4 regulates cell cycle genes to the same extent as BMP4, strongly downregulated several genes. n=3 independent biological replicates.

Unpaired t-test was used for all statistical analyses (mean±SEM), $p>0.05$ (ns), $p<0.001$(***), $p<0.0001$(****).

4.3.3 Over-expression of Id1 can induce cell-cycle arrest but does not suppress Ascl1 protein

The effect of Id4 on NSCs is highly suggestive of a specific role for Id4 in regulating quiescence, however it could also be an effect of high expression levels of any Id protein, and the over-expression of another Id protein could have the same effects. Id1 is expressed in quiescent NSCs *in vitro* and RGLs *in vivo*, and even though it is observed to be enriched in active RGLs *in vivo*, this correlation cannot rule out a role in regulating quiescence. Therefore, to both test whether Id4 is unique in its regulation of quiescence, and whether Id1 specifically plays a role in quiescence, I over-expressed a pCDNA-mId1-Venus construct, which drives Id1 and a Venus tag from a CMV promoter, in active NSCs via nucleofection, and analysed the effects 48h later (Figure 4.10A). I first analysed Ascl1 protein levels in Id1-overexpressing cells (Venus+). Quantification of Ascl1 fluorescence intensity in Id1Venus- and Id1Venus+ NSCs showed a very small decrease of Ascl1 in Id1-overexpressing cells (Figure 4.10B), with the average levels only declining from 98.54±3.2 A.U. to 88.9±2.8 A.U (Figure 4.10C), with many more Ascl1 strong positive NSCs than observed when Id4 is overexpressed (Figure 4.8E). This suggests the effect of Id4-overexpression on Ascl1 protein levels is a specific function of Id4, rather than a general effect of high Id protein levels. Id1 over-expression suppressed the cell cycle of NSCs to a similar degree as Id4 overexpression (Figure 4.10G-J). The percentage of Ki67+ NSCs decreased from 56.49±6.0% in Venus- cells to 33.97±2.2% in Venus+ cells (Figure 4.10D,E), while the percentage of EdU+ NSCs decreased from 27.09±5.3% to 18.5±4.6% (Figure 4.10F,G). Id1-overexpression in active NSCs induces cell cycle arrest to a similar degree as Id4-overexpression suggesting it could contribute to BMP4-induced quiescence when expressed at high levels.

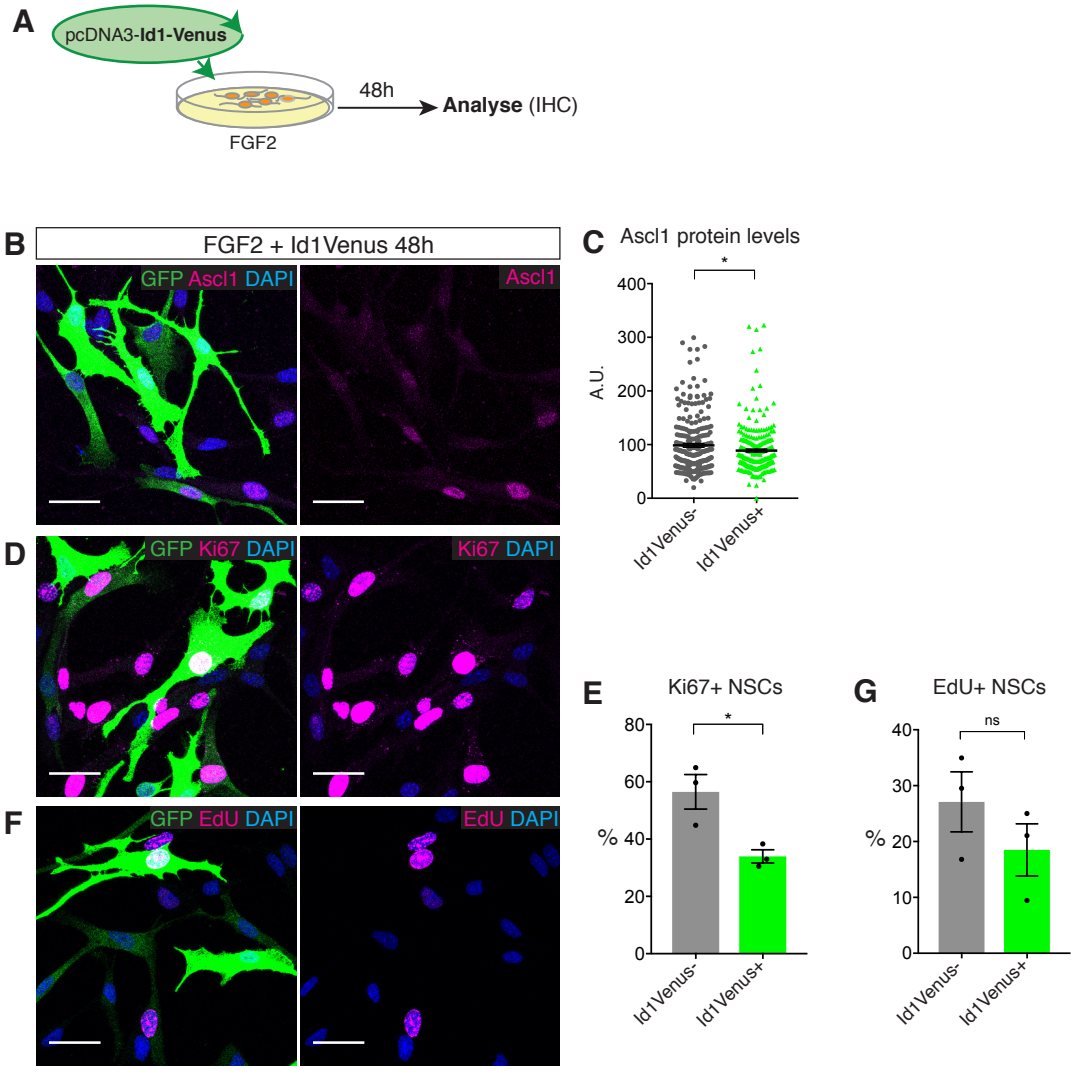

Figure 4.10. Over-expression of Id1 in active AHNSCs *in vitro*

(A) Experimental design for overexpressing Id1 in active NSCs. NSCs cultured in FGF2 were nucleofected with pCNDA3-Id1-Venus, cultured for a further 48h, at which time they were analysed.

(B) Immunostaining for GFP (Venus) and Ascl1, and DAPI staining, shows a reduction of Ascl1 in some Id1-expressing NSCs. Scale bar, 30μm.

(C) Quantification of the data in (B). Immunofluorescence levels of Ascl1 protein (arbitrary units, A.U.) are mildly suppressed in Id1-overexpressing NSCs compared to non-transfected NSCs. n=3 independent biological replicates.

(D, E) Immunostaining for Ki67 in Id1-transfected NSCs is reduced relative to non-transfected NSCs, quantified in (E). n=3. Scale bar, 30μm.

(F, G) Detection of EdU incorporation (1-hour pulse) shows fewer EdU+ Id1-transfected NSCs compared to non-transfected NSCs, quantified in (F). n=3 independent biological replicates. Scale bar, 30μm.

4.3.4 Id1 only induces a small subset of the quiescence transcriptional signature, and does not regulate Ascl1 target genes

To further compare the effect of Id1 vs Id4 over-expression, I FAC sorted Venus+ NSCs, and performed RNA sequencing, comparing the gene expression to FGF2+GFP nucleofected NSCs (Figure 4.11A). Id1 was only able to regulate the expression of a relatively small number of genes, with 359 upregulated and 83 downregulated by Id1-overexpression (Figure 4.11B), which is far fewer genes than either BMP4 or Id4-overexpression (Figure 4.11C). This suggests Id4 is specific in its induction of a large proportion of the BMP4-induced quiescence 'programme'. Despite the difference in number of genes regulated, most of the genes regulated by Id1 are common with BMP4-regulated and/or Id4-regulated genes (Figure 4.11C). Moreover, the ontologies of genes up- or down-regulated by Id1 are highly similar to those seen for BMP4 and Id4, such as "Cell adhesion" ion-related and signalling-related for upregulated genes, and "Cell cycle" for downregulated genes (Figure 4.11D,E). However, when I looked specifically at direct Ascl1 target genes, none were regulated by Id1 overexpression (Figure 4.11F), nor were most specific cell cycle genes that were previously shown to be strongly downregulated by BMP4 and Id4 (Figure 4.9K), apart from CyclinB1 (Figure 4.11G). These results show that Id1 has a very minor contribution to the quiescent state induced by BMP4, and the effects of Id4 over-expression demonstrate the specific function of Id4. Moreover, unlike Id4, Id1 does not strongly negatively regulate Ascl1 protein and as a result, does not repress activation or cell cycle genes associated with Ascl1 transcriptional activity. Overall these results suggest Id4 has a specific function in the BMP4-induced quiescent state in NSCs due to a unique role (at least in comparison to Id1) of inhibiting and downregulating Ascl1 protein.

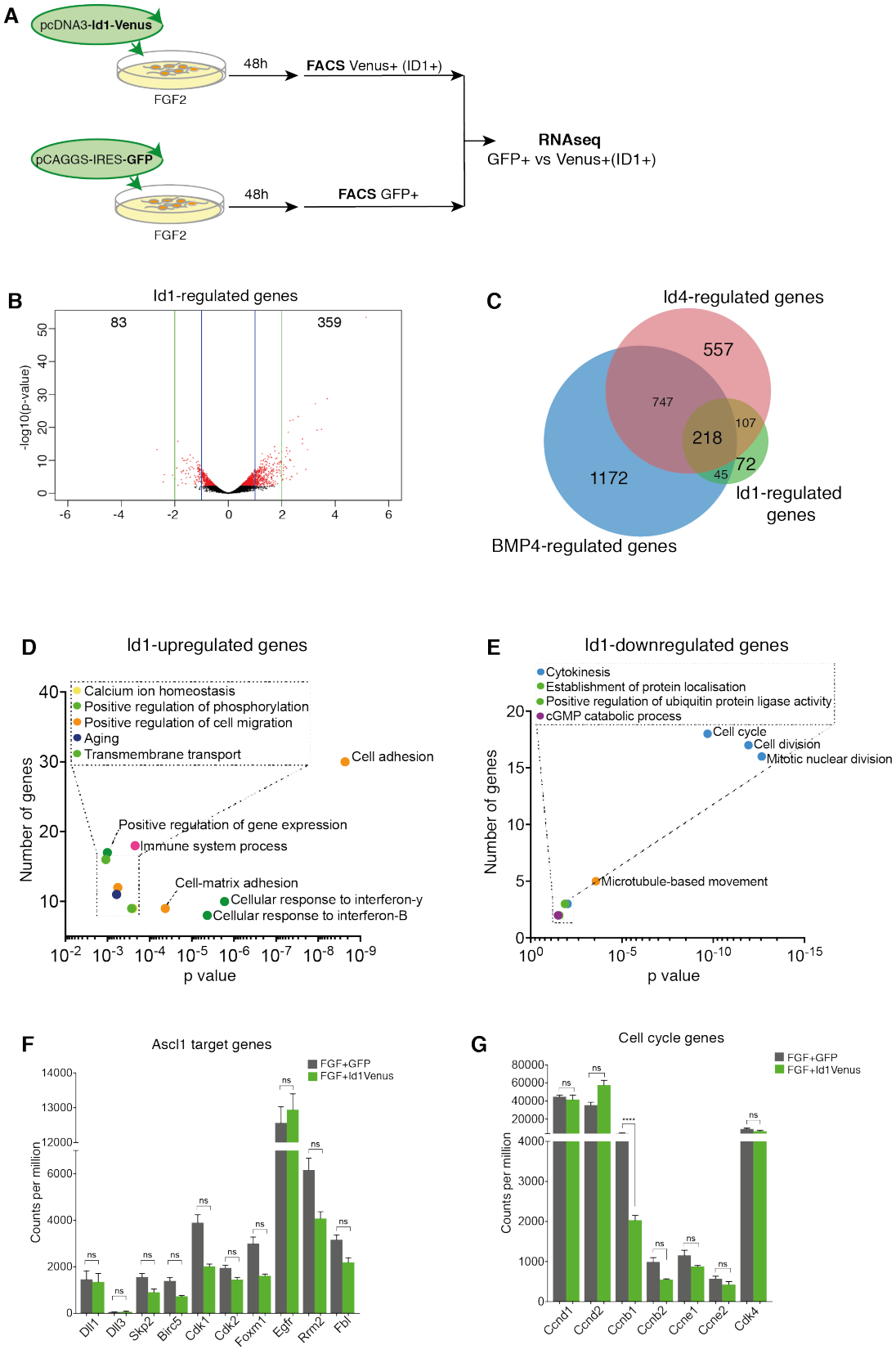

Figure 4.11. RNAseq analysis of Id1 over-expression in active AHNSCs *in vitro* (legend next page)

Figure 4.11. RNAseq analysis of Id1 over-expression in active AHNSCs *in vitro*
(A) Experimental design for overexpressing Id1 in active NSCs followed by Fluorescence Activated Cell Sorting (FACS). Active NSCs were nucleofected with either pCAGGS-IRES-GFP or pCDNA3-Id1-Venus. NSCs were incubated in FGF2 for 48h following nucleofection, FAC sorted for GFP+ NSCs, and RNA extracted for RNAseq analysis.
(B) Volcano plot showing genes regulated by Id1 overexpression in active NSCs.
(C) Overlap of genes regulated by Id4-overexpression, Id1-overexpression or BMP4-treatment.
(D, E) Gene ontology terms associated with up- or down-regulated genes in Id1-overexpressing NSCs compared to GFP-transfected NSCs. Ontologies are coloured based on categories described above.
(F) Expression of Ascl1 target genes, shown as counts per million (CPM) from RNAseq analysis of active NSCs nucleofected with GFP or Id1. None of the Ascl1 target genes were significantly regulated by Id1. n=3 independent biological replicates.
(G) Expression of cell cycle genes, shown as counts per million (CPM) from RNAseq analysis of active NSCs nucleofected with GFP or Id1. Id1 only regulates CyclinB1 (Ccnb1), and does not affect the expression of any other cell cycle gene analysed. n=3

4.3.5 Inactivating Id4 in quiescent NSCs stabilises Ascl1

Expression of Id4 is sufficient to inhibit Ascl1 protein levels and induce a quiescent-like state in active NSCs. To determine whether it is also required to maintain quiescence in BMP4-induced NSCs, I re-reintroduced the binding partner of Ascl1 via nucleofection of an E47-expression plasmid, into BMP4-induced quiescent NSCs (Figure 4.12A). In this way, Id4 (and the other Id proteins) were inhibited as high levels of E47 “mops up” the Ids, and the remaining E47 that is not bound to Id4 would be able to dimerize with Ascl1, stabilising Ascl1 and enabling it to bind to its target DNA (Figure 4.12B). 48h after transfection of quiescent NSCs with pCAGGS-E47-GFP, many cells were GFP+, with a transfection efficiency of 31.05±5.2 (Figure 4.12C). Comparison of Ascl1 protein levels in GFP+ and GFP- NSCs showed an increase in the mean fluorescence intensity as well as more Ascl1 bright NSCs, in E47 over-expressing cells (Figure 4.12D,E). This increase occurred without affecting *Ascl1* mRNA levels (Figure 4.12F); in fact, *Ascl1* mRNA trended towards downregulation in E47-overexpressing NSCs. The mRNA here was obtained through FAC sorting nucleofected cells, discussed in more detail

below in Section 4.3.6. This observation suggests E47 is able to re-stabilise Ascl1 protein in conditions where BMP4 is high. In addition to the effect on Ascl1, E47-overexpression also resulted in an increase in the fraction of Ki67+ and EdU+ cells in the GFP+ population compared to the GFP- (Figure 4.12G-I), suggesting E47 is counteracting the cell cycle arrest induced by BMP4/Id4, potentially as a direct result of re-stabilisation of Ascl1 protein.

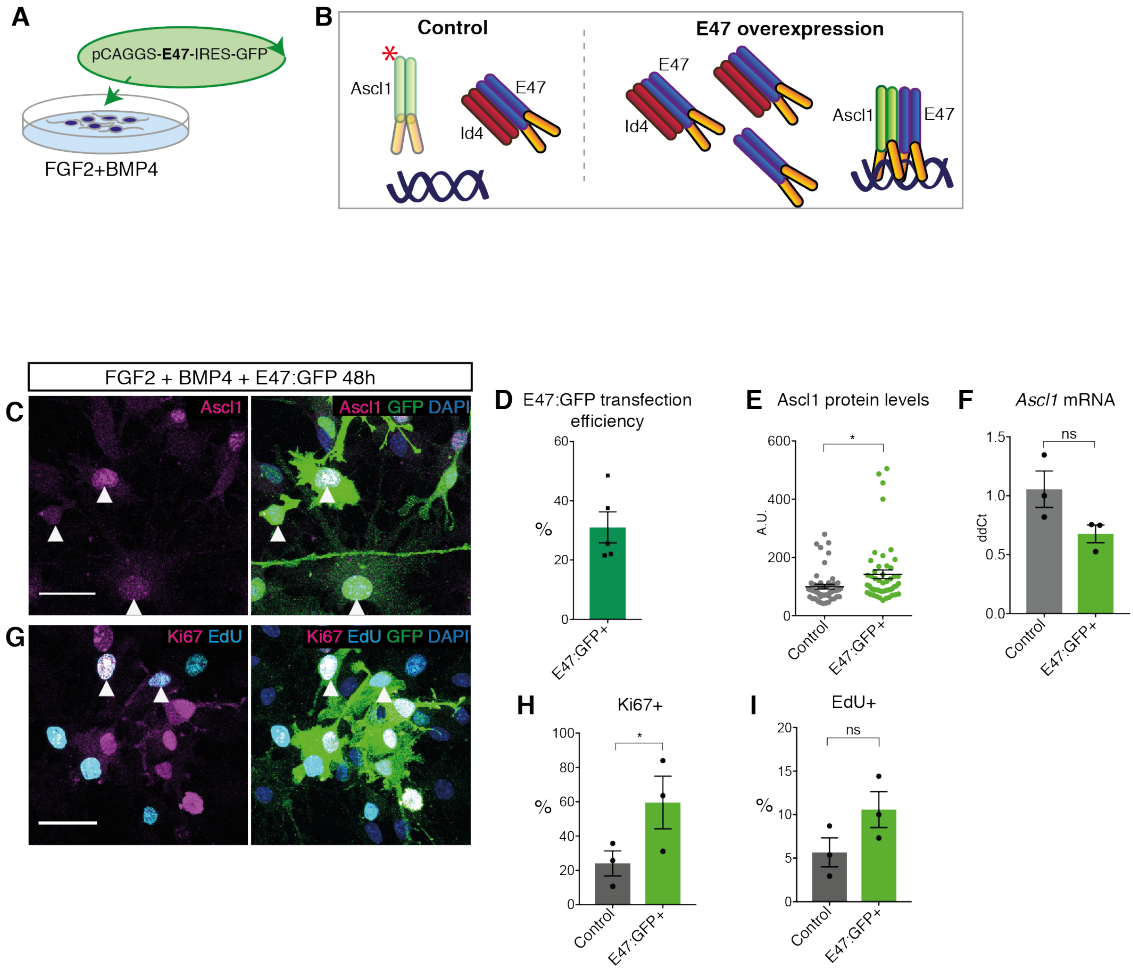

Figure 4.12. Over-expression of E47 in quiescent AHNSCs *in vitro*

(A) Experimental design for overexpressing E47 in quiescent NSCs. NSCs cultured in FGF2+ 20ng/mL BMP4 for 72h, were nucleofected with pCAGGS-E47-IRES-GFP, cultured for a further 48h in the presence of FGF2+BMP4 20ng/mL, after which point they were analysed.

(B) Scheme showing the hypothesis for the effects of E47 overexpression in quiescent NSCs. In control cells, in the presence of FGF2 and 20ng/mL BMP4, Id4 expression is high and sequesters the E-protein binding partner of Ascl1, resulting in its inactivity and

degradation. Following E47 overexpression, Id4 is mopped up, and excess E47 is free to dimerise with newly transcribed Ascl1, stabilising it and enabling its transcriptional activity.
(C) Immunostaining for Ascl1, GFP and DAPI staining in quiescent NSCs transfected with E47 for 48h. Scale bar, 30μm.
(D) The percentage of GFP(E47)+ NSCs within each sample was quantified to determine the transfection efficiency. n=5 images from 4 independent biological repeats.
(E) Quantification of Ascl1 immunofluorescence levels (A.U.) shows Ascl1 is significantly increased in E47-overexpressing quiescent NSCs. n=1 representative of 4 biological repeats.
(F) QPCR analysis of Ascl1 mRNA levels in control and E47-transfected NSCs. n=3 independent biological replicates.
(G-I) Immunostaining and quantification of %Ki67+ and %EdU+ NSCs in control and E47-transfected NSCs. Both Ki67 and EdU are increased in E47-overexpressing quiescent NSCs. Control cells are non-transfected (GFP-) NSCs within the transfected sample. n=3 independent biological replicates. Scale bar, 30μm.

4.3.6 Inactivating Id4 in quiescent NSCs restores the function of Ascl1

E47 overexpression should induce gene expression changes associated more with the active state, than quiescent, due to the fact it should block Id4-mediated inhibition of Ascl1. Moreover, if E47 is able to re-stabilise Ascl1 protein in BMP4 conditions and restore its function as a transcription factor, we should also see an upregulation of Ascl1 target genes. To test both of these hypotheses, I FAC sorted GFP+ NSCs from BMP4-induced E47:GFP transfected NSCs, or as a control, quiescent NSCs transfected with just GFP, and performed RNA sequencing on the GFP+ sorted cells (Figure 4.13A). E47 overexpression significantly induced the expression of 1768 genes, and downregulated 619 genes (Figure 4.13B), as compared to the gene expression in BMP4+GFP NSCs. Comparison of the genes induced by E47 with those downregulated by BMP4 (i.e. genes enriched in the active state), showed a large overlap, with 40.65% the genes downregulated by BMP4 also induced by E47 (Figure 4.13C). Gene ontology analysis showed these commonly regulated genes are mostly involved in the cell cycle, as well as “negative regulation of Notch signalling”, which is interesting considering the reported role for Notch signalling in maintaining quiescence of hippocampal RGLs, as described in Section 1.5.2.2. I looked specifically at the subset of known Ascl1 target genes (previously discussed in Section 4.3.1), to see

whether stabilisation of Ascl1 protein by E47 overexpression results in restoration of its function. Indeed, every gene had a trend towards upregulation, with significant upregulation observed for *Dll1*, *Dll3*, *Birc5* and *Rrm2* (Figure 4.13E). This shows that replenishing the binding partner of Ascl1 in conditions of high Id4 expression is sufficient to re-stabilise Ascl1 protein and restore its function, whilst also resulting in a reversal of the quiescent-like state (specifically cell cycle arrest), potentially as a direct result of Ascl1 transcriptional activity.

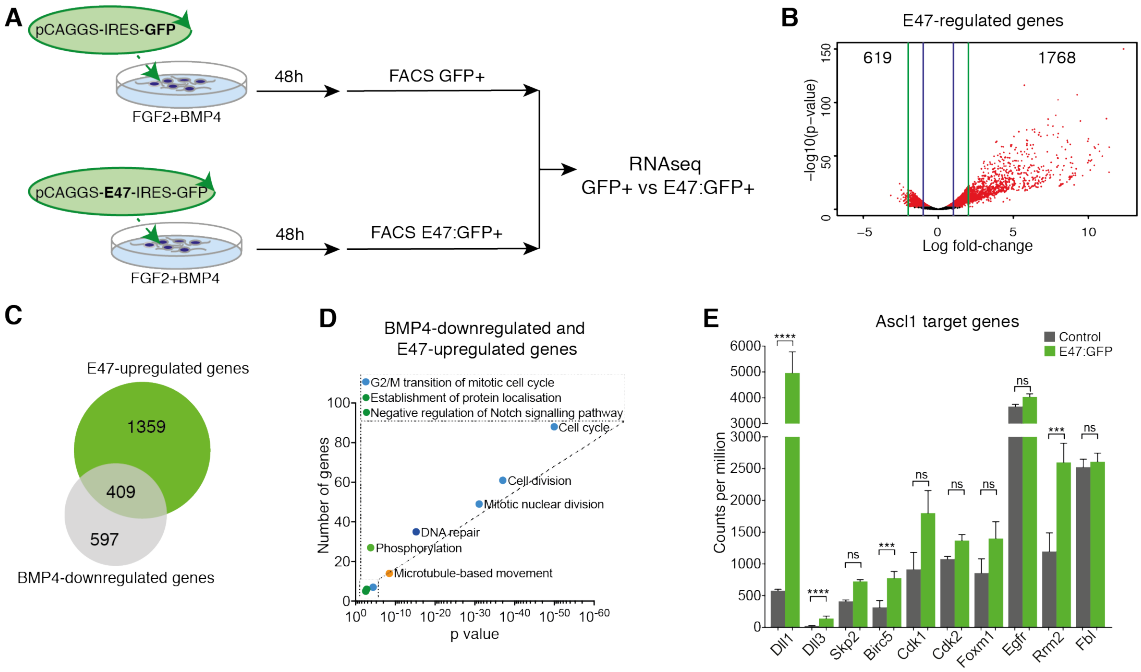

Figure 4.13. RNAseq analysis of E47 over-expression in quiescent AHNSCs *in vitro*

(A) Experimental design for overexpressing E47 in quiescent NSCs followed by Fluorescence Activated Cell Sorting (FACS). Quiescent (FGF2+BMP4 20ng/mL) NSCs were nucleofected with either pCAGGS-IRES-GFP or pCAGGS-E47-IRES-GFP. NSCs were incubated in FGF2+BMP4 for 48h following nucleofection, FAC sorted for GFP+ NSCs, and RNA extracted for RNAseq analysis.

(B) Volcano plot showing the genes significantly regulated by E47 overexpression.

(C) Overlap of genes up-regulated by E47 overexpression, and genes downregulated by BMP4 treatment (i.e. genes associated with the active state).

(D) Gene ontology terms associated with genes down-regulated by BMP4 and up-regulated by E47 overexpression. Ontologies are coloured based on categories described above.

(E) Expression of Ascl1 target genes, shown as counts per million (CPM) from RNAseq analysis of quiescent NSCs nucleofected with GFP (Control) or E47. Several Ascl1 target

genes were significantly upregulated following 48h E47-overexpression, and several trended towards upregulation. n=3 independent biological replicates.

4.3.7 Loss of Id4 in NSCs results in increased Ascl1 protein levels but does not prevent cell cycle arrest in BMP4-induced quiescence

To inactivate Id4 via an alternative method, NSCs were derived from the Cre-inducible Id4flx mouse line, whereby adenovirus-mediated expression of Cre recombinase in these NSCs induces recombination of loxP sites flanking exons 1 and 2 of the Id4 gene, which represents the entire coding region (exon 3 represents a 3' untranslated region) (Figure 4.14A). However, immunostaining for Id4 in both non-transfected NSCs in FGF2 and FGF2+BMP4 conditions showed no Id4 signal (Figure 4.14B,C), and unsurprisingly no signal was detected in quiescent NSCs transduced with Adeno-empty or Adeno-Cre virus (Figure 4.14D,E). QPCR for *Id4* mRNA extracted from these cells also suggested that these cells had lost expression of Id4 sometime during the derivation process (Figure 4.14F), although the probe used to detect Id4 spanned exon boundary 2-3, and so the ability of the taqman QPCR probe to detect its target mRNA may have been impaired by the loxP sites. Nevertheless, the immunocytochemistry was highly suggestive that Id4 expression was very low or gone in these cells and concurrently the levels of Ascl1 were much higher in BMP4-treated Id4flx NSCs (Figure 4.14C) than observed previously for non-transgenic AHNSCs (Figure 4.6H). This further supports the idea that Id4 can mediate the BMP4-induced suppression of Ascl1 protein. The loss of Id4 did not affect the ability of BMP4 to induce cell cycle arrest, shown by a reduction in the number of Ki67+ and EdU+ NSCs (Figure 4.14G) 72h after BMP4. One possible explanation for this is compensation by the other Id proteins which are still highly expressed in Id4KO NSCs (Figure 4.14I). Moreover, I have shown Id1 can induce cell cycle-related quiescence without affecting Ascl1 protein levels (Section 4.3.4). *Id1* mRNA expression was increased 2-fold in Id4KO NSCs compared to wildtype NSCs (Figure 4.14H), in both FGF2 and FGF2+BMP4 conditions. Id1 protein levels were not significantly increased compared with wildtype NSCs, but these data suggest that the high expression of Id1-3 may mediate a part of BMP4-induced cell cycle arrest.

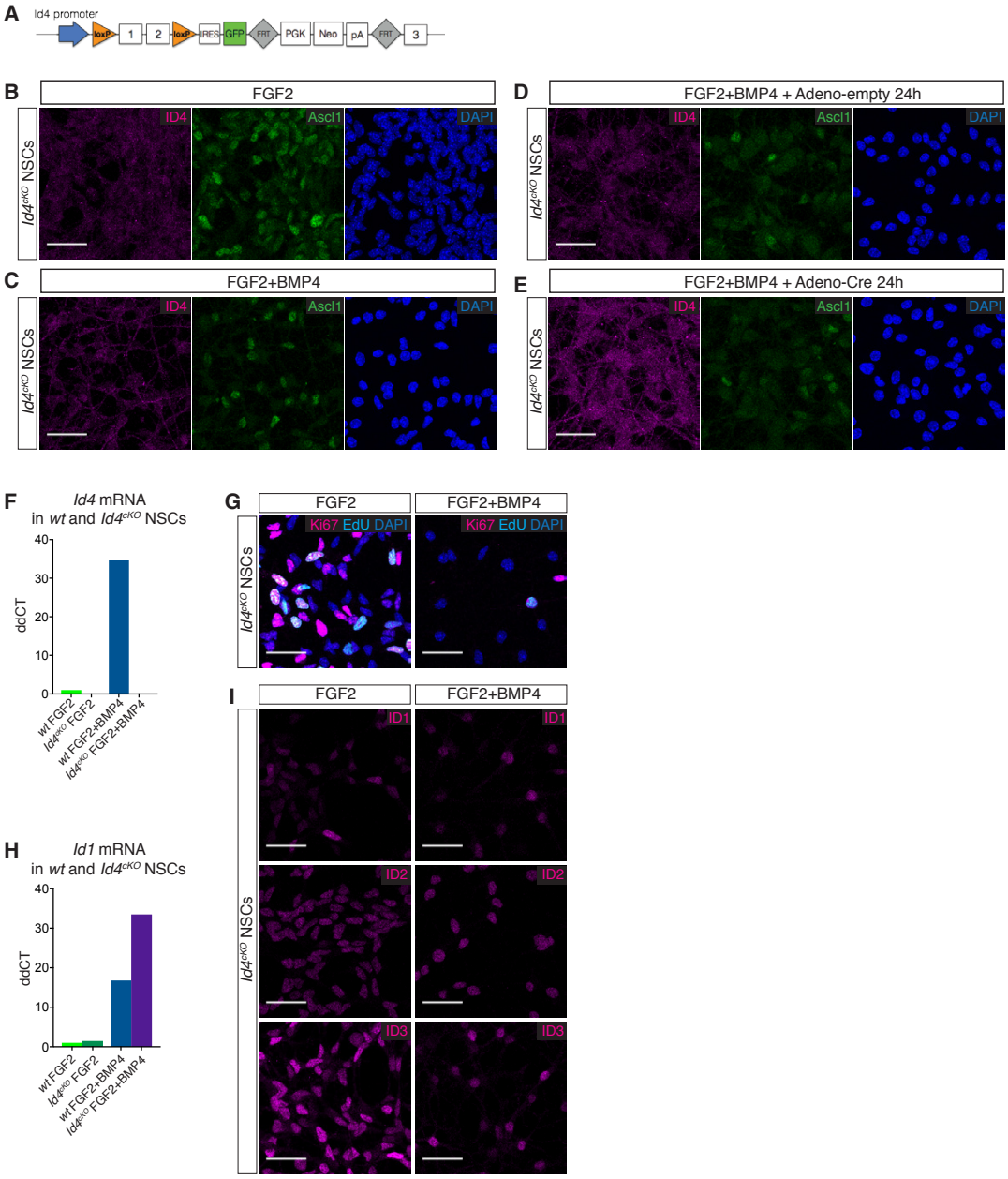

Figure 4.14. Expression of Id-4 and Ascl1 in AHNSCs derived from Id4flx mice

(A) Structure of the Id4 floxed allele in the *Id4*^{cKO} mice, from which the *Id4*^{cKO} NSC line was derived.

(B, C) Immunostaining for Id4 and Ascl1 and DAPI staining in *Id4*^{cKO} NSCs cultures in FGF2 or FGF2+BMP4. Id4 is undetectable in either condition. Ascl1 protein levels are high even in quiescent *Id4*^{cKO} NSCs. Scale bar, 30μm.

(D, E) Immunostaining for Id4 and Ascl1 and DAPI staining in quiescent *Id4*^{cKO} NSCs cultures transduced with either control adenovirus (Adeno-null) or adenovirus expressing

Cre-recombinase (Adeno-Cre), in order to delete the floxed exons of Id4. Id4 protein levels are undetectable in both conditions, and Ascl1 levels are unaffected by transduction with Adeno-Cre virus. Scale bar, 30μm.
(F) QPCR analysis of *Id4* mRNA levels in active and quiescent wildtype and $Id4^{cKO}$ NSCs. *Id4* mRNA is undetectable in $Id4^{cKO}$ NSCs. n=1.
(G) Immunostaining for Ki67 and EdU incorporation in active and BMP4-treated $Id4^{cKO}$ NSCs. Scale bar, 30μm.
(H) QPCR analysis of *Id1* mRNA levels in active and quiescent wildtype and $Id4^{cKO}$ NSCs. *Id1* mRNA is upregulated in $Id4^{cKO}$ NSCs compared to wildtype NSCs. n=1.
(I) Immunostaining for Id1, Id2 and Id3 in active and BMP4-treated $Id4^{cKO}$ NSCs. Scale bar, 30μm.

4.4 Id4 maintains quiescence of RGLs *in vivo*

4.4.1 Acute conditional deletion of Id4 *in vivo* activates RGLs from quiescence

Overall the functional analysis of Id4 *in vitro* strongly indicates Id4 can 1) suppress Ascl1 protein levels and 2) induce a quiescent-like state. I therefore investigated whether Id4 is important for maintaining quiescence of RGLs *in vivo*. I utilised the Id4flx transgenic mouse line described in Section 4.3.7, crossed to $GLASTCre^{ERT2}$*;Rosa26-EYFP* mice, in order to conditionally delete Id4 in GLAST-expressing stem cells via tamoxifen-induced Cre-mediated recombination. The Cre is fused to mutated hormone-binding domains of the estrogen receptor, and is activated by binding of the ligand OHT (4-hydroxytamoxifen) which results in translocation to the nucleus where it recombines the loxP-flanked Id4 exons. These mice also carry the Rosa26-EYFP allele, in which a floxed PGK-neo cassette containing a tpA stop sequence, and an enhanced yellow fluorescent protein gene, are inserted in the Gt(ROSA)26Sor locus. Upon tamoxifen-induced recombination, the STOP sequence is floxed out, enabling expression of YFP and identification of recombined cells by YFP fluorescence. Adult P60 mice, either homozygous for the floxed Id4 locus ($Id4^{cKO}$ mice), or wildtype for Id4 (control mice), were injected with tamoxifen once a day for 5 days, and analysed on the 5th day (Figure 4.15A). These mice were housed in the animal facility of collaborators E. Huillard and B. Rocamonde at the Institute du Cerveau et de la Moelle Epinière (ICM) in Paris, and required travelling to their institute in order to perfuse mice for

analysis, which meant the number of mice were very limiting for these experiments (discussed further in Section 4.4.3 below). Immunostaining for Id4 showed the protein was completely lost in every YFP+ cell after 5 days of tamoxifen (Figure 4.15B). As a result of Id4 deletion, the number of Ascl1+YFP+GFAP+ RGLs was increased almost 3-fold, from 6.0±0.6% in control mice to 15.0±2.1% in *Id4*^{cKO} mice, in mice analysed immediately after 5 days of tamoxifen treatment (Figure 4.15D). Ascl1 protein levels, measured by fluorescence intensity, were also significantly increased in *Id4*^{cKO} mice (Figure 4.15E). This indicates Id4 normally functions to suppress Ascl1 protein in RGLs. To test whether this had an effect on the proliferation of RGLs, I measured the fraction of Ki67+ YFP+GFAP+ RGLs, which increased from 5.1±1.1% in control mice to 12.3±1.9% in *Id4*^{cKO} mice (Figure 4.15F, G). Overall, these results show Id4 is required to maintain quiescence of RGLs, potentially via suppression of Ascl1 protein. It is interesting that despite the fact Id4 is expressed in the majority of RGLs, and the deletion is complete in *Id4*^{cKO} mice, only a fraction of RGLs activate following Id4 deletion, potentially indicating compensatory mechanisms.

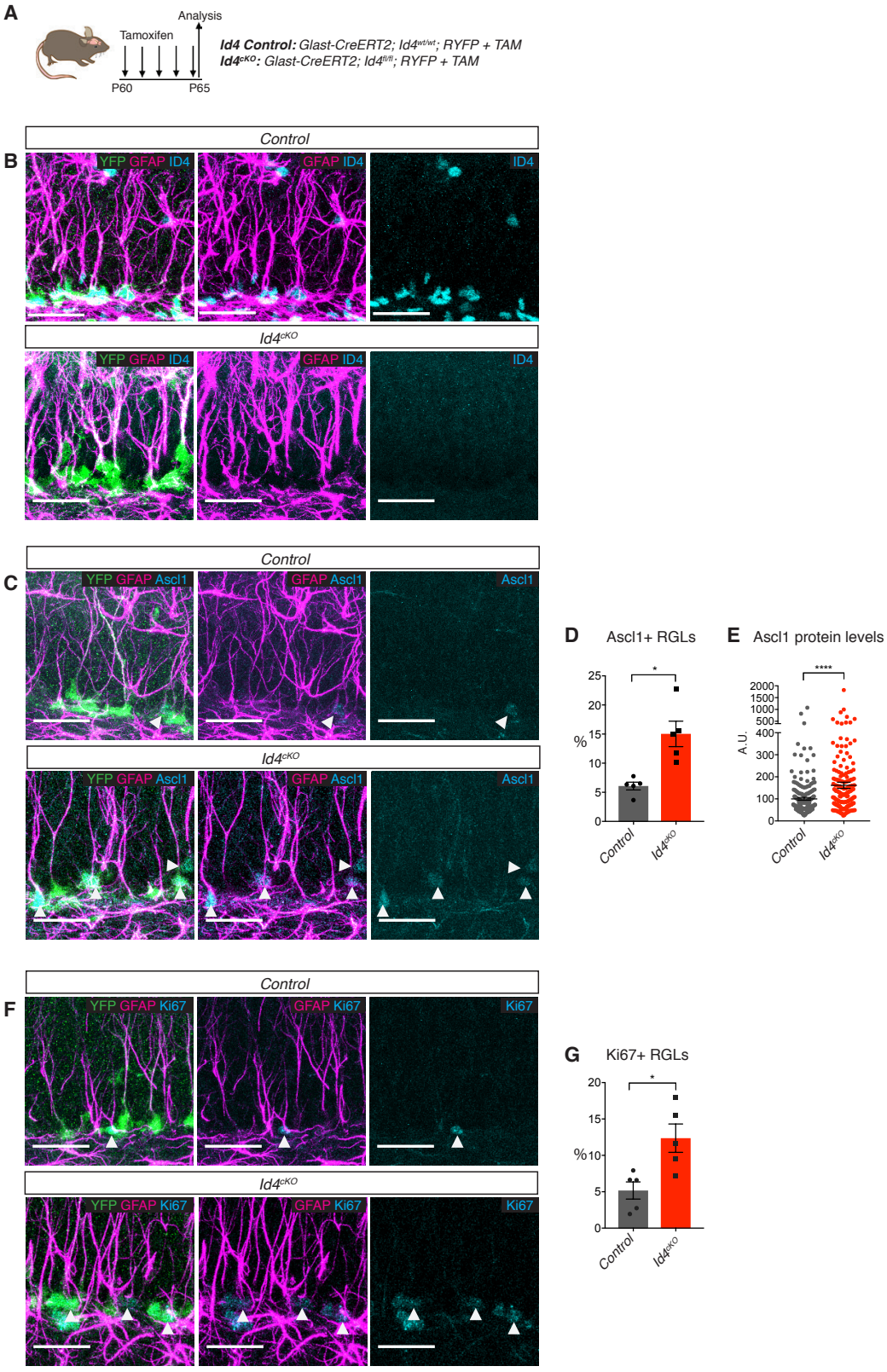

Figure 4.15. Effects of acute conditional deletion of Id4 from RGLs in the adult hippocampus (legend next page)

Figure 4.15. Effects of acute conditional deletion of Id4 from RGLs in the adult hippocampus

(A) Experimental design for the deletion of Id4 from RGLs in adult (P60) *Id4*^{cKO} mice. Mice either wildtype (*control*) or homozygous floxed (*Id4*^{cKO}) for the Id4 locus were treated with tamoxifen for 5 days, and analysed immediately after.

(B) Immunolabelling of YFP, GFAP and Id4 shows complete elimination of Id4 protein from YFP+GFAP+ RGLS in *Id4*^{cKO} mice after 5 days of tamoxifen. Scale bar, 30μm.

(C) Immunolabelling of YFP, GFAP and Ascl1 in control and *Id4*^{cKO} mice following tamoxifen-induced deletion of Id4. White arrows indicate Ascl1-positive RGLs. Scale bar, 30μm.

(D) Quantification of percentage Ascl1+ RGLs, from the data shown in (C). Loss of Id4 in RGLs results in increased numbers of Ascl1+ RGLs. n=5

(E) Quantification of Ascl1 protein immunofluorescence levels (A.U.) in YFP+GFAP+ RGLS in control or *Id4*^{cKO}. n=5 mice.

(F) Immunostaining of YFP, GFAP and Ki67 Ascl1 in control and *Id4*^{cKO} following 5days of tamoxifen treatment. White arrows indicate Ki67-positive RGLs. Scale bar, 30μm.

(G) Quantification of the data shown in (F). Loss of Id4 results in an increase in the fraction of proliferating RGLs. n=5 for both control and *Id4*^{cKO}

Unpaired t-test was used for all statistical analyses (mean±SEM), $p<0.05$ (*), $p<0.0001$(****).

4.4.2 The effects of conditional Id4 deletion from RGLs are lost after 30 days

In accordance with the hypothesis that compensatory mechanisms may be supressing the effects of acute Id4 deletion, one month after Id4 deletion (Figure 4.16A), the effect on Ascl1 and proliferation is lost, with no difference observed in %Ascl1+ or %Ki67+ RGLs between control and *Id4*^{cKO} mice (Figure 4.16B-E). I first analysed Ascl1 expression by immunofluorescence and found no strong difference in the percentage of Ascl1+ YFP+GFAP+RGLs between *cKO* (4.39%) and *control** mice (3.14±0.8%) (Figure 4.16B,C). However strong conclusions cannot yet be drawn from this data, due to a lack of P90 *Id4*^{cKO} mice and lack of the same kind of control mouse used for acute Id4 deletion; control (*control**) mice in this case are homozygous Id4 floxed mice which were not treated with tamoxifen, as opposed to mice wildtype for Id4 with tamoxifen treatment (Figure 4.15A). The reason for the lack of data here is due to differences in

perfusion technique and issues with antibodies against Ascl1 for immuno-detection, which I will discuss further in the Section 4.4.3 below. In addition, I also analysed levels of RGL proliferation of *control* (Id4 wildtype plus tamoxifen), *control** (Id4 floxed without tamoxifen) and *Id4*^{cKO} mice treated with tamoxifen for 5 days and analysed 30 days later (Figure 4.16D,E). Quantification of Ki67+ YFP+GFAP+RGLs in the three conditions showed no significant difference between %Ki67+ RGLs in *control* (3.63±0.89%) and *Id4*^{cKO} mice (5.49±0.8%), and only a small significant increase between *control** mice (2.80±0.3%) and *Id4*^{cKO} mice. Moreover, there was no difference in %Ki67+ RGLs between the two sets of control mice, indicating both are suitable as controls.

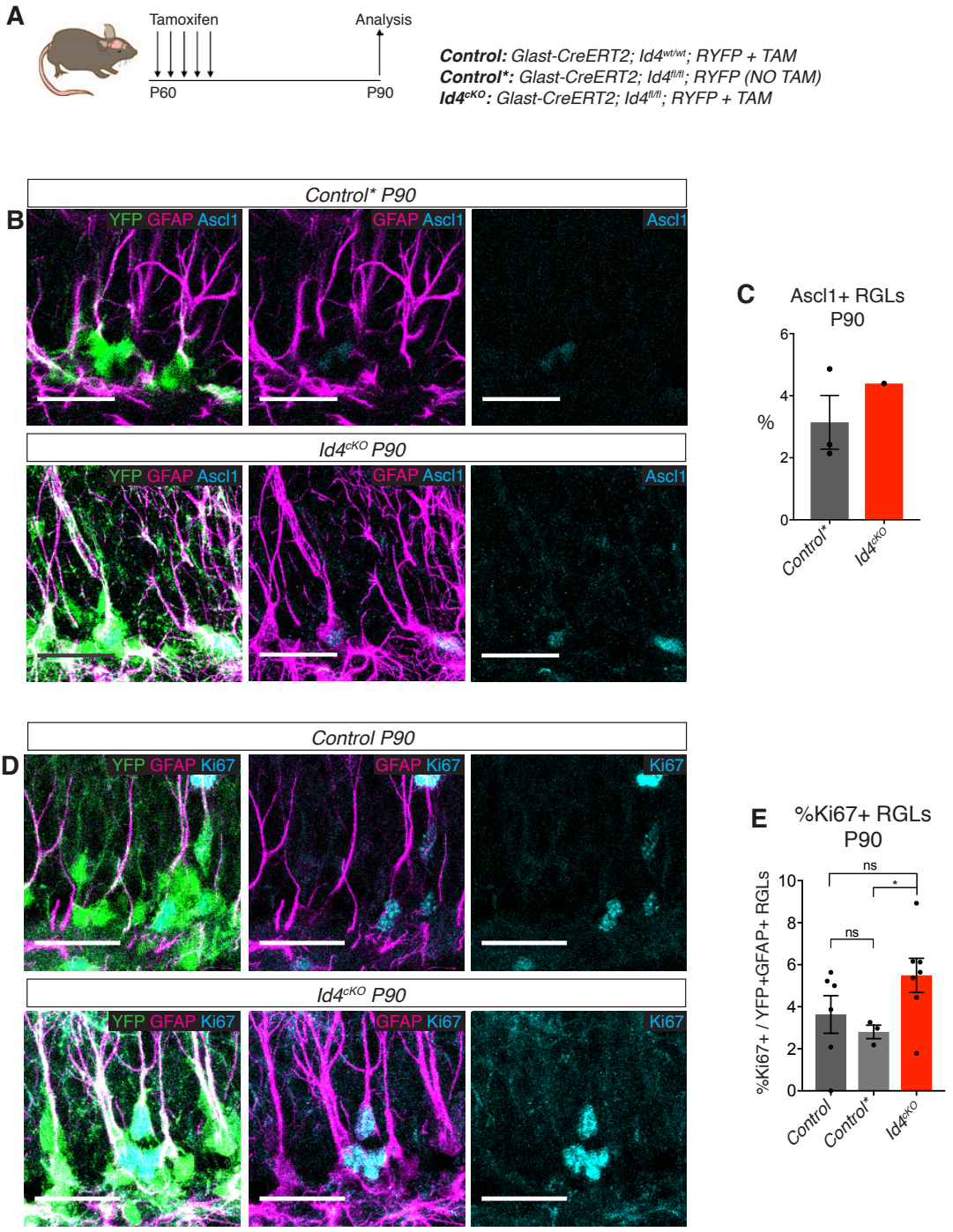

Figure 4.16. Long-term effects of Id4 deletion on RGL activity and Ascl1 protein level

(A) Experimental design for analysis of RGLs 1 month after Id4 deletion in adult (P60) *Id4*^{cKO} mice. Mice either wildtype (*control*) or homozygous floxed (*Id4*^{cKO}) for the Id4 locus were treated with tamoxifen for 5 days, and 30 days later (P90).

(B) Immunolabelling of YFP, GFAP and Ascl1 in control and *Id4*^{cKO} mice 30 days after tamoxifen administration. Control mice in this case are mice homozygous for the floxed Id4 allele, without tamoxifen treatment. Scale bar, 30μm.
(C) Quantification of the percentage of Ascl1+ YFP+GFAP+RGLs in control and *Id4*^{cKO} mice 30 days after Id4 deletion. Control mice in this case are mice homozygous for the floxed Id4 allele, without tamoxifen treatment. n=3 for control and n=1 for *Id4*^{cKO}.
(D) Immunolabelling of YFP, GFAP and Ki67 in control and *Id4*^{cKO} mice 30 days after tamoxifen administration. Scale bar, 30μm.
(E) Quantification of the percentage of Ki67+ YFP+GFAP+RGLs in control and *Id4*^{cKO} mice 30 days after Id4 deletion. n=6 for both control *Id4*^{cKO} mice.
Unpaired t-test was used for all statistical analyses (mean±SEM), p>0.05 (ns).

4.4.3 Perfusion technique and Ascl1 antibody species affects Ascl1 protein detection

Despite showing data for Ascl1 immunostaining for just three *control** mice and one *Id4*^{cKO} mouse at P90, many *control* and further *Id4*^{cKO} P90 mice were perfused and stained. These samples were perfused by collaborators who were already analysing the Id4 floxed mouse line and kindly sent samples to our lab. However, they used a different perfusion technique to that of the Guillemot lab, resulting in very difficult antibody detection of Ascl1, the detection of which is very sensitive to fixation. Moreover, they had routinely used the Guinea pig anti-Ascl1 antibody, produced by the lab of Jane Johnson, whereas the Guillemot lab used a monoclonal mouse anti-Ascl1 antibody generated in-house (also available commercially, BD Pharmingen, #556604). All P65 samples analysed and presented in Section 4.4.1 were from mice perfused by myself of N. Urbán, and stained with mouse-anti Ascl1. Shown in Figure 4.17Ai are examples of staining with the Guinea pig anti-Ascl1 antibody in *control* P90 mice perfused by collaborators, which gave very high levels of background in these samples, particularly in the granule neurons indicating non-specific staining, rendering it very difficult to identify Ascl1 positive cells. However, the detection of Ascl1 was challenging in these samples also when using the mouse anti-Ascl1 antibody, producing high non-specific background staining (Figure 4.17Aii). We therefore decided to perfuse mice ourselves to avoid differences in Ascl1 detection. This greatly improved the sensitivity of Ascl1 detection for both Guinea pig- and mouse-anti Ascl1 antibodies, as show in Figure 4.17B. However, there were not enough mice to perfuse

and analyse at P90 and generate a full data set. This is why we used some Id4 homozygous floxed mice without tamoxifen treatment as controls (*control**), as we lacked Id4 wildtype mice the most. Despite the high levels of background observed when using the Guinea pig anti-Ascl1 antibody, in some samples the detection was very clear, and I tended to detect more Ascl1+ cells, which raised the question of whether the Guinea pig antibody was more sensitive than the mouse anti-Ascl1, when used on samples perfused in the appropriate manner. Moreover, I have demonstrated that there are many RGLs expressing *Ascl1* mRNA via *Ascl1*^{KiGFP} reporter mice and *Ascl1* RNA *in situ* (Section 4.1.2), and more Ascl1+ RGLs can be detected using the *Ascl1*^{Venus} mouse line than with monoclonal antibody staining (Section 4.1.2), suggesting there may be significant issues with sensitivity of the mouse anti-Ascl1 antibody and raising the requirement for a better antibody. Therefore, I investigated whether there was a significant difference between the sensitivity of the Guinea pig- and mouse-anti Ascl1 antibodies in *control* and *Id4*^{cKO} samples perfused by myself or N. Urbán. I first quantified the fraction of Ascl1+ YFP+GFAP+RGLs in P65 control and *Id4*^{cKO} mice, which showed significantly more Ascl1+ RGLs were detected with the Guinea pig antibody in control samples (Figure 4.17C), however there was no difference in *Id4*^{cKO} mice between the detection of Ascl1 using the mouse or Guinea pig antibody. This meant the increase in the percent of Ascl1+ RGLs between control and *Id4*^{cKO} was significant when using the mouse antibody, but not when using the Guinea pig antibody. A similar pattern emerged when analysing P90 samples with both antibodies, with a trend (although not significant) towards a higher percentage of Ascl1+ RGLs in *control** samples stained with the Guinea pig antibody (Figure 4.17D). Again, this higher sensitivity of the Guinea pig antibody was not seen in *Id4*^{cKO} P90 samples, although only 1 mouse was available to analyse here (Figure 4.17D). Direct comparison of the percentage of Ascl1+ RGLs in every mouse that had been stained with both Ascl1 antibodies highlighted some instances where the values were very different, although on average the difference between the two antibodies was not significant (Figure 4.17E). As a final investigation into the sensitivity of each Ascl1 antibody, I compared the percentage of Ascl1+ RGLs with the percentage of Ki67+ RGLs quantified within each mouse. Ki67 is expressed in activated RGLs, following Ascl1 expression, therefore Ki67 and Ascl1 immunostaining should correlate fairly closely. In this way, I can identify if one of the Ascl1 antibodies is detecting more or less positive RGLs than expected. Plotting the data from control and *Id4*^{cKO} P65 and P90 mice against each other shows a very strong positive correlation

between %Ascl1+ and %Ki67+ RGLs, with an r value of 0.8708 (Figure 4.17F). No sample stained with either antibody deviates strongly from the regression line. Overall these data suggest that while there are issues with low sensitivity of the mouse anti-Ascl1 antibody, the Guinea pig anti-Ascl1 has only a marginally higher sensitivity, and it also potentially gives greater non-specific background staining, such as in the granule neurons (Figure 4.17A). It is worth using both antibodies in the future to confirm quantifications of Ascl1 immunostaining, however these data indicate that the use of mouse anti-Ascl1 in data presented here is reliable.

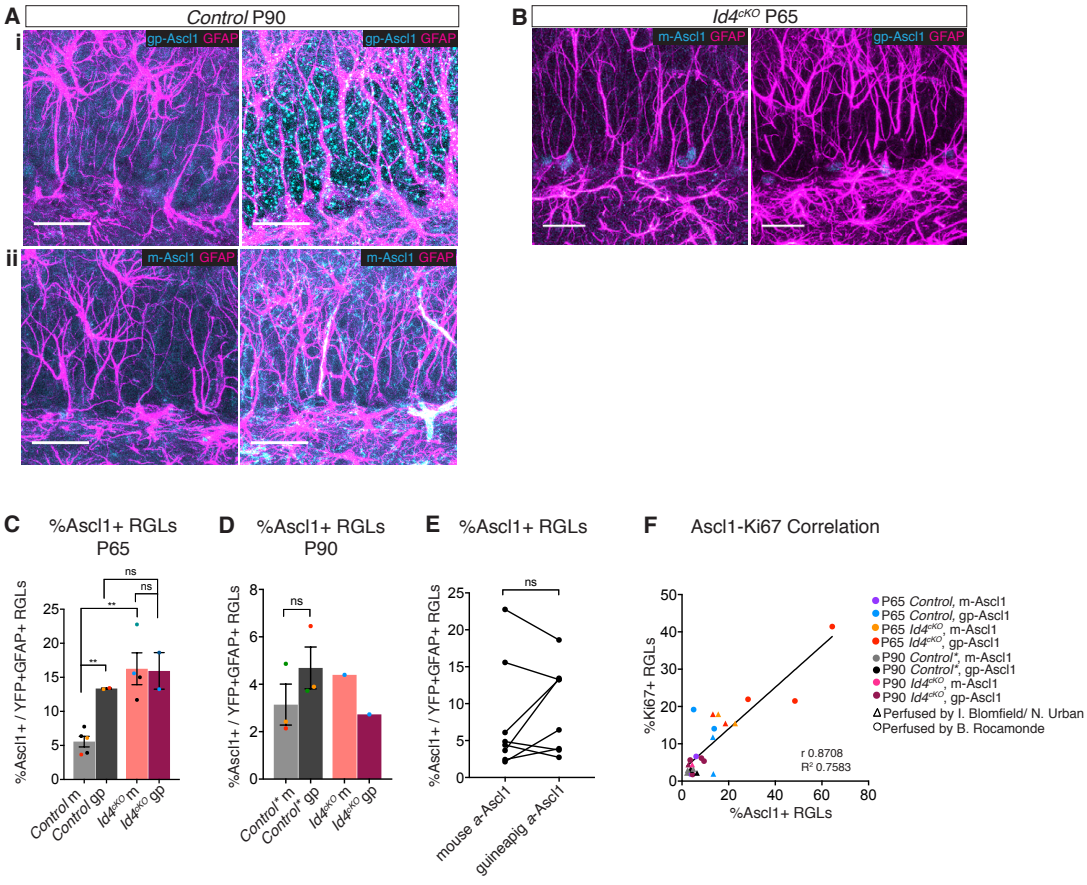

Figure 4.17. Analysis of perfusion method and antibody on Ascl1 immunodetection

(A) P90 *control* Id4 floxed mice, perfused by collaborator B. Rocamonde, were immunostained for GFAP and Ascl1 using either the guinea-pig (i) or mouse (ii) anti-Ascl1 antibody. Scale bars, 30μm.

(B) Immunostaining for GFAP and Ascl1, using either the mouse or Guinea pig anti-Ascl1 antibody, in a P65 *Id4*^{cKO} mouse perfused by N. Urbán. Scale bars, 30μm.

(C) Quantification of the %Ascl1+ YFP+GFAP+RGLs detected with either the mouse or Guinea pig anti-Ascl1 antibody, in P65 control and *Id4*^{cKO} mice perfused by myself or N. Urbán. Data points are coloured to identify the same mouse stained with each antibody.
(D) Quantification of the %Ascl1+ YFP+GFAP+RGLs detected with either the mouse or Guinea pig anti-Ascl1 antibody, in P90 control* (Id4 homozygous floxed, without tamoxifen) and *Id4*^{cKO} mice perfused by myself or N. Urbán. Data points are coloured to identify the same mouse stained with each antibody.
(E) Direct comparison of the %Ascl1+ RGLs detected with either mouse or Guinea pig anti-Ascl1 antibody within each sample.
(F) Correlation of the %Ascl1+ RGLs with the %Ki67+RGLs within each sample, from all P65 and P90 control and *Id4*^{cKO} mice, stained with either Guinea pig or mouse anti-Ascl1. Linear regression and correlation analysis show a strong positive correlation between Ki67 and Ascl1 immunoreactivity.
Unpaired t-test was used for all statistical analyses (mean±SEM), p>0.05 (ns), p<0.01 (**).

4.4.4 Id1 and Id3 are upregulated in response to Id4 deletion

Returning to the effect of Id4 deletion, I investigated further the loss of phenotype 30 days post-tamoxifen. Compensation by the other Id proteins could explain the loss of effect on proliferation. In line with this hypothesis, I observed a dramatic increase in the expression of Id1 and Id3 in the DG of *Id4*^{cKO} mice, both 5 days and 30 days post-tamoxifen. The percentage of Id1+ RGLs in *Id4*^{cKO} mice increased 5 days after tamoxifen, from 51.82±10.3 in control to 88.02±3.1 in *Id4*^{cKO} (Figure 4.18A,B). This increase was maintained at 30 days post-tamoxifen (42.79±1.9 in control, 74.16±1.0 in *Id4*^{cKO}; Figure 4.18C, D). Id1 is normally found to be enriched in active, rather than quiescent RGLs (Section 4.2.2), so might not be expected to be able to compensate for Id4, a quiescence factor. However, we have seen that overexpression of Id1 in active NSCs *in vitro* can induce partial quiescence (Section 4.3.3), so its higher-than-normal expression levels following Id4 deletion *in vivo* may facilitate compensation for the suppression of proliferation. Id3+ RGLs increased very highly following Id4 deletion, both 5 days and 30 days post-tamoxifen (Figure 4.18E,F). I have not investigated the molecular function of Id3 in NSCs, nor have I quantified its levels in active vs quiescent RGLs, however it is reasonable to hypothesise that upregulation of Id3 in *Id4*^{cKO} RGLs could also potentially mediate the compensatory effect observed. It would be highly

interesting to investigate the role of Id1 and Id3 in RGL quiescence and activation further.

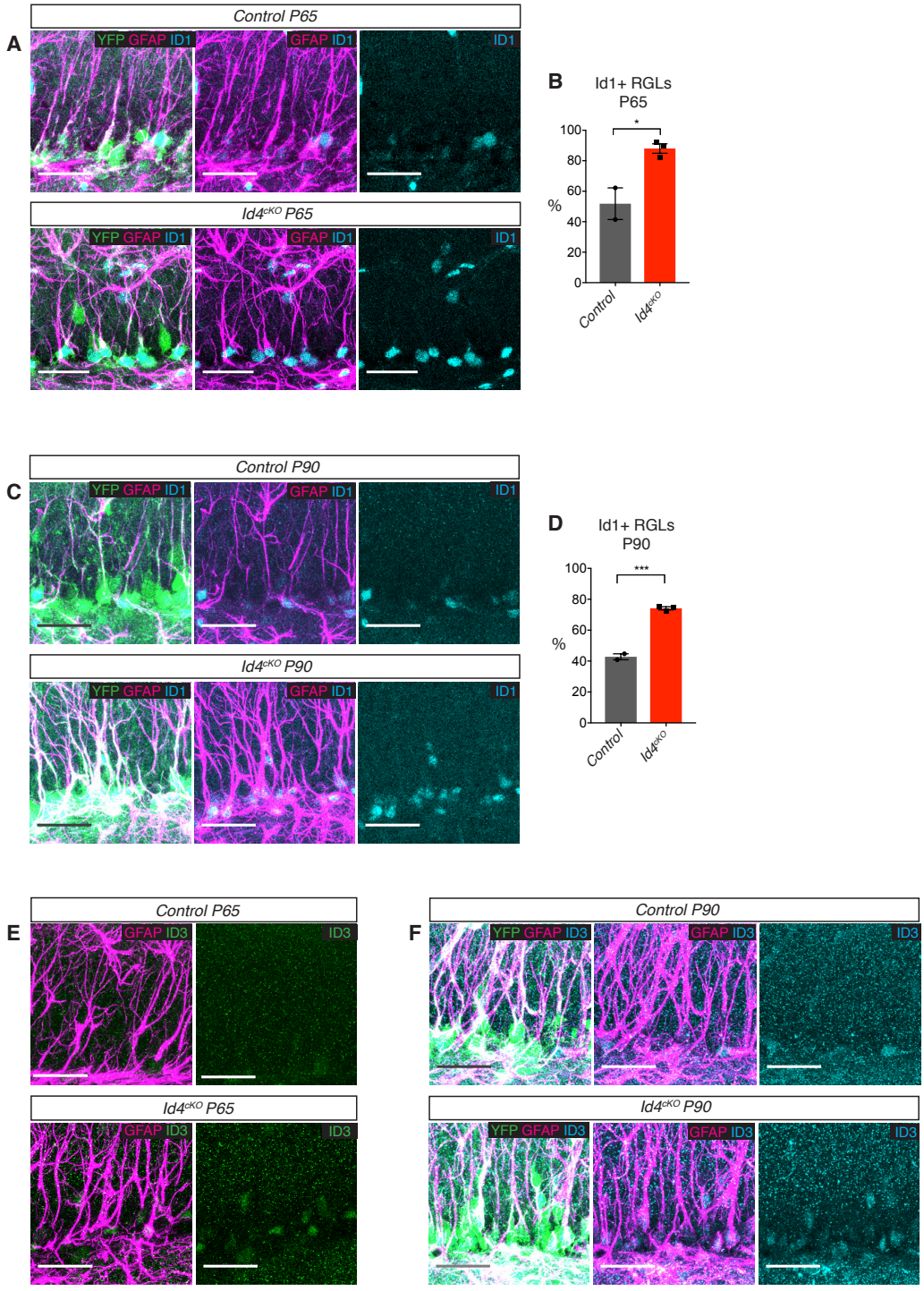

Figure 4.18. Effects on Id1 and Id3 expression following acute and long-term conditional deletion of Id4 from RGLs (legend next page)

Figure 4.18. Effects on Id1 and Id3 expression following acute and long-term conditional deletion of Id4 from RGLs

(A) Immunostaining of YFP, GFAP and Id1 in control and *Id4*^{cKO} following 5 days of tamoxifen treatment (P65). Scale bar, 30μm.

(B) Quantification of percentage Id1+ YFP+GFAP+RGLs, from the data shown in (A). Loss of Id4 in RGLs results in increased numbers of Id1+ RGLs. n=2 for control and n=3 for *Id4*^{cKO}.

(C) Immunostaining of YFP, GFAP and Id1 in control and *Id4*^{cKO} 30 days after tamoxifen treatment (P90). Scale bar, 30μm.

(D) Quantification of percentage Id1+ YFP+GFAP+RGLs, from the data shown in (C). The percentage of Id1+ RGLs is increased 30days post-Id4 deletion. n=2 for control and n=3 for *Id4*^{cKO}.

(E) Immunostaining of GFAP and Id3 in control and *Id4*^{cKO} following 5 days of tamoxifen treatment (P65). The number of Id3+ RGLs is visibly increased in *Id4*^{cKO} mice compared to control mice. Scale bar, 30μm.

(F) Immunostaining of YFP, GFAP and Id3 in control and *Id4*^{cKO} 30 days after tamoxifen treatment (P90). The increased number of Id3+ RGLs in *Id4*^{cKO} mice is sustained even 30 days after Id4 deletion. Scale bar, 30μm.

Unpaired t-test was used for all statistical analyses (mean±SEM), $p<0.05$ (*), $p<0.001$(***).

4.5 Id4 expression is independent of Smad4 *in vivo*

Having identified Id4 as a key regulator of RGL quiescence, I next asked what signalling pathways regulate Id4 *in vivo*. Due to the strong regulation of Id4 by BMP4 in AHNSCs *in vitro*, and due to the fact that Ids are induced by BMP in embryonic neural progenitor cells (Samanta and Kessler, 2004), I began by investigating the effect of BMP/Smad signalling on Id4 in RGLs *in vivo.* I utilised a transgenic mouse line containing floxed Smad4 alleles, which when crossed with *GlastCre*^{ERT2}*; Rosa26-EYFP* mice, would allow me to conditionally delete Smad4 in adult RGLs. Smad4 deletion should block BMP signalling, as it is a common effector of the pathway, integrating signalling via phosphorylated Smads1/5/8 as well as phosphoSmad2/3.

4.5.1 Smad signalling is active in a small number RGLs *in vivo*, in the presence or absence of Smad4

BMP-Smad signalling has previously been reported to be active in many cells in the DG, including stem cells (Bonaguidi et al., 2008; Colak et al., 2008; Mira et al., 2010), so I confirmed this by performing immunostaining for pospho-Smad1/5/8 in adult brain sections from either control or *Smad4*^{cKO} mice (Figure 4.19A). I was able to identify a small number of pSmad1/5/8+ RGLs in both control and *Smad4*^{cKO} mice (Figure 4.19B), suggesting both that BMP/Smad signalling is active in some adult RGLs and that Smad4 deletion in RGLs does not affect signalling upstream. However, the number of pSmad1/5/8 RGLs detected was far less than the number of Id4+ (or Id1+) RGLs, suggesting pSmad detection here is not sensitive enough, or that Id4 expression can be independent of pSmad1/5/8 signalling. Poor detection of pSmad1/5/8 may be the more likely case, as detection using a different pSmad-1 antibody by Mira et al., 2010 show high levels of pSmad-1 staining in the DG, including in Sox2+ RGLs; the results I obtained closely reflected the staining seen by Colak et al., 2008, who used the same pSmad1/5/8 antibody I used. It is therefore likely that BMP-Smad signalling is active in RGLs in the adult DG, and could induce Id4 expression.

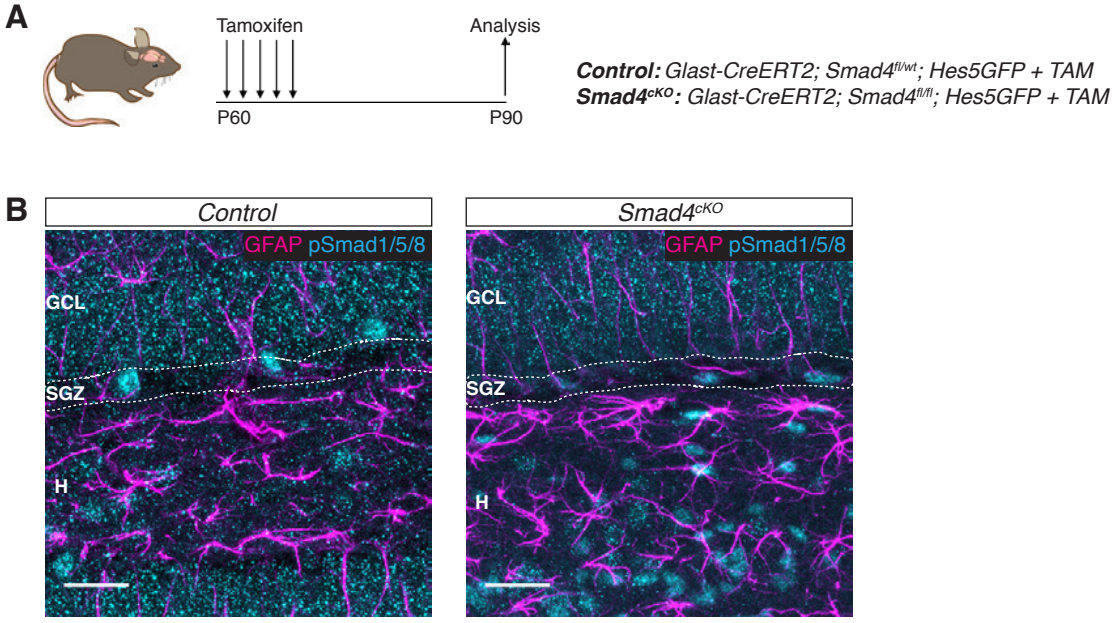

Figure 4.19. Expression of phospho-Smad1/5/8 in the dentate gyri of control and *Smad4*^{cKO} mice (legend next page)

Figure 4.19. Expression of phospho-Smad1/5/8 in the dentate gyri of control and *Smad4^{cKO}* mice

(A) Experimental design for the deletion of Smad4 from RGLs in adult (P60) *Smad4^{cKO}* mice. Mice either wildtype (*control*) or homozygous floxed (*Smad4^{cKO}*) for the Smad4 locus were treated with tamoxifen for 5 days, and analysed 30 days later (P90).
(B) Immunostaining for GFAP and phospho-Smad1/5/8 in the dentate gyrus of control and *Smad4^{cKO}* 30days post-tamoxifen treatment. pSmad1/5/8 staining is found in hilar (H) astrocytes, as well as some GFAP+ RGLs. The subgranular zone (SGZ) is identified by the white dotted lines. GCL: granule cell layer. Scale bar, 30μm.

4.5.2 Conditional deletion of Smad4 *in vivo* does not affect Id4 expression or RGL activation

I next asked whether Id4 expression in RGLs is dependent upon BMP/Smad4 signalling. I conditionally deleted Smad4 in RGLs of adult mice, and analysed brain sections of control and *Smad4^{cKO}* mice (Figure 4.20A) either 5 days (Figure 4.20Ai) or 30 days (Figure 4.20Aii) following tamoxifen administration. Surprisingly, 5 days after Smad4 deletion, the percentage of YFP+GFAP+ RGLs expressing Id4 was not significantly changed (97.11±0.9% in control vs 99.48±0.5% in *Smad4^{cKO}*) (Figure 4.20B,C), and in fact the level of Id4 protein was increased, measured by fluorescence intensity (average of 100.7± 4.1 A.U. in control vs 129.8± 4.5 A.U. in *Smad4^{cKO}*) (Figure 4.20C). The percentage of Id4+ RGLs was also not significantly changed 30 days following Smad4 deletion (89.85±4.5% in control vs 79.92±2.7% in *Smad4^{cKO}*) (Figure 4.20D). Smad4 deletion did however strongly suppress the levels of Id1 protein in YFP+GFAP+ RGLs, both 5 days post-tamoxifen (17.73±3.6% in control vs 6.86±0.7% in *Smad4^{cKO}*) and 30 days post-tamoxifen (52.59±3.4 in control vs 5.96±1.4% in *Smad4^{cKO}*) (Figure 4.20E-G). This shows that the deletion of Smad4 was functional, and highlights yet again the difference between Id4 and the other Ids. The increase in Id4 expression may reflect the reduction of Id1, which may negatively regulate Id4 to a small degree. Further to the effect on Id protein expression, I examined whether Smad4 deletion affected RGL activation, by quantifying the percentage of Ascl1+ or Ki67+ YFP+GFAP+ RGLs. 5 days post-tamoxifen neither Ascl1 nor Ki67 were significantly changed (Figure 4.20H-K). This again indicates Id1 does not strongly regulate RGL quiescence when Id4 expression is high. More surprisingly these results

show that Id4 expression is independent of Smad4-mediated BMP signalling in RGLs *in vivo*.

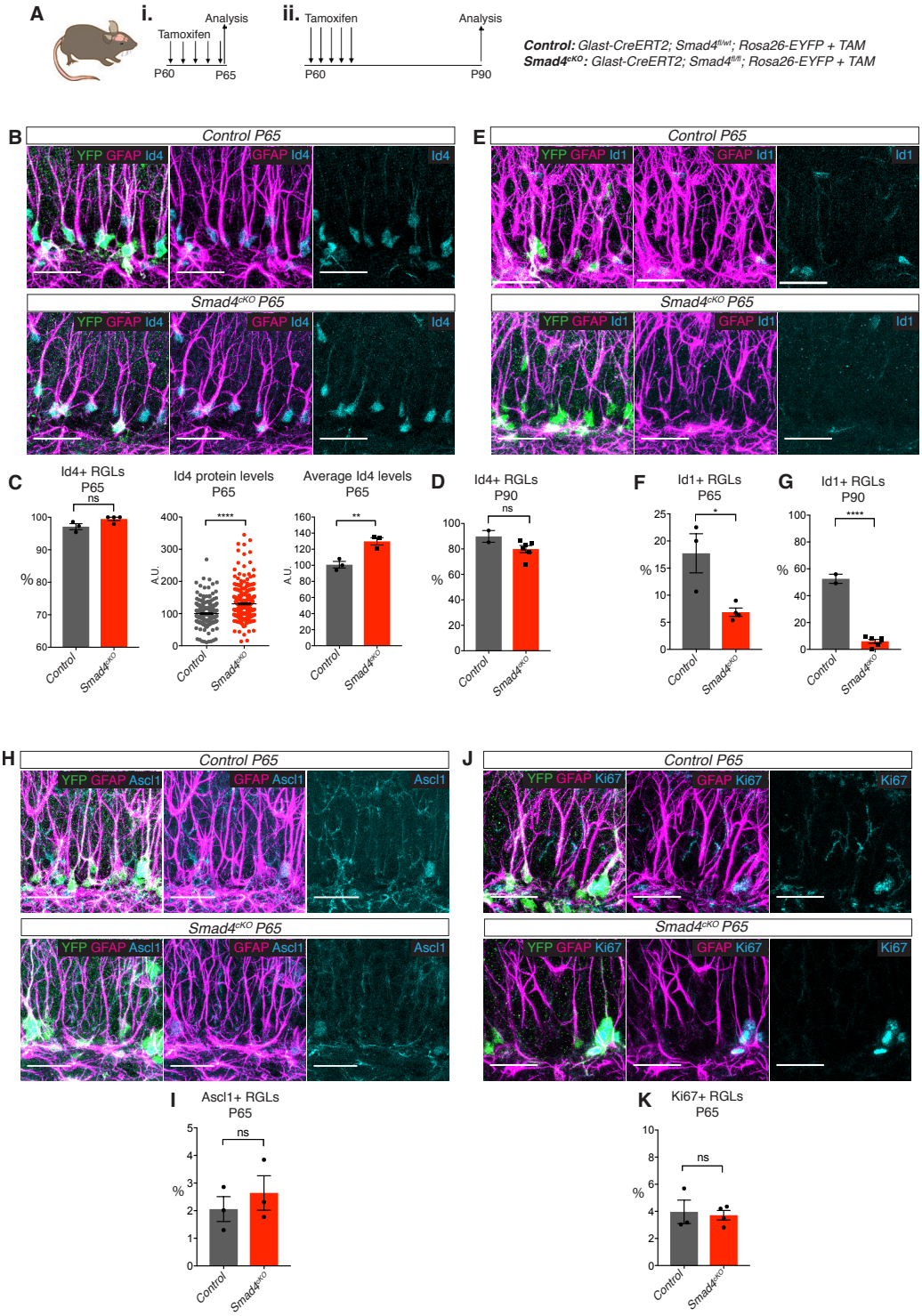

Figure 4.20. Effects of acute and long-term conditional deletion of Smad4 from RGLs (legend next page)

Figure 4.20. Effects of acute and long-term conditional deletion of Smad4 from RGLs

(A) Experimental design for the deletion of Smad4 from RGLs in adult (P60) *Smad4*^{cKO} mice. Mice either wildtype (*control*) or homozygous floxed (*Smad4*^{cKO}) for the Smad4 locus were treated with tamoxifen for 5 days, and (i) analysed immediately or (ii) 30 days later (P90).

(B) Immunolabelling of YFP, GFAP and Id4 shows Id4 protein is still expressed in YFP+GFAP+ RGLS in *Smad4*^{cKO} mice after 5 days of tamoxifen, at similar levels to control mice. Scale bar, 30μm.

(C) Quantification of Id4 levels shown in (B). The percentage of YFP+GFAP+ RGLs positive for Id4 was unchanged between control and *Smad4*^{cKO} mice after 5 days of tamoxifen. Id4 protein levels as measured by immunofluorescence intensity (A.U.) was significantly increased in *Smad4*^{cKO} mice compared to control, and the average fluorescence levels were also increased in *Smad4*^{cKO} mice. n=3 for control and n=4 for *Smad4*^{cKO}.

(D) The percentage of Id4+ YFP+GFAP+ RGLs was not changed between control and *Smad4*^{cKO} mice 30 days after tamoxifen treatment (P90). n=2 for control and n=6 for *Smad4*^{cKO}.

(E) Immunolabelling of YFP, GFAP and Id1 shows Id1 protein is reduced in YFP+GFAP+ RGLS in *Smad4*^{cKO} mice after 5 days of tamoxifen, compared with control mice. Scale bar, 30μm.

(F) Quantification of Id1 levels shown in (B). The percentage of YFP+GFAP+ RGLs positive for Id1 was strongly reduced in *Smad4*^{cKO} mice after 5 days of tamoxifen treatment. n=3 for control and n=4 for *Smad4*^{cKO}.

(G) The percentage of YFP+GFAP+ RGLs positive for Id1 was also strongly reduced in *Smad4*^{cKO} mice 30 days after tamoxifen administration. n=2 for control and n=6 for *Smad4*^{cKO}.

(H) Immunolabelling of YFP, GFAP and Ascl1 shows little difference in Ascl1 immunostaining between control and *Smad4*^{cKO} mice after 5 days of tamoxifen treatment. Scale bar, 30μm.

(I) Quantification of the data shown in (H). The percentage of YFP+GFAP+ RGLs positive for Ascl1 was 2.05±0.4% in control mice and 2.64±0.6% in *Smad4*^{cKO} mice after 5 days of tamoxifen treatment, and therefore not significantly changed. n=3 for both control and mutant mice.

(J) Immunolabelling of YFP, GFAP and Ki67 shows similar numbers of Ki67+ RGLs between control and *Smad4*^{cKO} mice after 5 days of tamoxifen treatment. Scale bar, 30μm.

(K) Quantification of the data shown in (J). The percentage of YFP+GFAP+ RGLs positive for Ki67 was unchanged between control (3.96±0.8%) and *Smad4*^{cKO} (3.71±0.3%) mice after 5 days of tamoxifen treatment. n=3 control mice and n=4 for *Smad4*^{cKO} mice. Unpaired t-test was used for all statistical analyses (mean±SEM), p>0.05 (ns), p<0.05 (*), p<0.01 (**), p<0.0001(****).

4.5.3 Conditional deletion of Smad4 in AHNSCs *in vitro* does not affect Id4 protein level, but does lead to a loss of Id1 and Id3

The following experiment shows only a single repeat, and is therefore preliminary data. However, the results suggest an interesting divergence between the different Id proteins and their regulation by Smad4 signalling, therefore I present them here as an insight for the results obtained *in vivo* in the *Smad4*^{cKO} mice. In order to examine the effects on all Id proteins following Smad4 deletion in AHNSCs, I utilised an adult hippocampal neural stem cell line derived from the Smad4flx mice described in Section 4.5.2 (line derived by N. Urbán). Normal AHNSCs in active and quiescent conditions have the capacity to signal via the BMP/Smad pathway, due to the expression of *Smad1-5* seen in the RNA sequencing data, as well as the expression of the BMP receptors *Bmpr1a*, *Bmpr1b* and *Bmpr2*, and the expression of BMP ligands such as *Bmp1*. Therefore, deletion of Smad4 in these cells could have a functional consequence, particularly in light of the report that hippocampal NSCs exposed to the BMP agonist Noggin *in vitro* show increased proliferation (Mira et al., 2010). Smad4flx AHNSCs were cultured in either proliferation conditions (20ng/mL FGF2 plus 20ng/mL EGF; these cells were derived directly into FGF2+EGF conditions and utilised for experiments prior to being transitioned into FGF2-alone) or quiescent conditions (20ng/mL BMP4 + 20ng/mL FGF2, 72h). Cells were then transduced with 100moi adenovirus expressing either GFP or Cre-recombinase to induce recombination of the floxed Smad4 alleles, and the cells cultured for 4 days to allow time for the remaining Smad4 protein to be degraded. At this point, cells were collected and either fixed for immunocytochemistry, or RNA extracted. I first checked the expression of targets of BMP/Smad signalling *Id1*, *Id3* and *Id4* by QPCR (ddCT are shown relative to the expression in proliferating AHNSCs transduced with Adeno-GFP, to show the change in expression upon BMP4 treatment). In quiescent conditions, *Id1*, *Id3* and *Id4* were all downregulated at the mRNA level following Smad4 deletion, with a fold-change of 2.0, 9.8 and 2.6 respectively (Figure 4.21A-C), indicating BMP4-induced expression of these three *Id* genes is mediated in part by Smad4, and *Id3* is the most strongly

regulated Id gene by Smad4 signalling. It also suggests there is another signal present in the *in vitro* culture system capable of inducing Id gene expression. I next examined the protein levels of Id1-4, to determine how Id protein levels were affected following Smad4 deletion. I immunostained for all four Id proteins in quiescent Smad4flx NSCs, transduced with either Adeno-GFP or Adeno-Cre, and quantified the fluorescence intensity of each protein per nucleus. Smad4 deletion in proliferating AHNSCs results in a strong decrease in the protein levels of Id1 (Figure 4.21D, I) and Id3 (Figure 4.21F, K), whereas Id2 protein levels are very slightly increased in *Smad4*^{cKO} cells (Figure 4.21E, J), and Id4 protein levels are unchanged (Figure 4.21G, L). These results highlight a differential induction of the four Ids by BMP/Smad4 signalling, particularly for Id4, for which the protein level is sustained despite a decrease in mRNA expression following Smad4 deletion. These data also corroborate the observations that Smad4 deletion in RGLs *in vivo* results in a loss of Id1 protein but not Id4. Finally, I also checked Ascl1 protein levels, to see whether a reduction in Id1-3 protein affected Ascl1 levels. Ascl1 protein levels were significantly increased in *Smad4*^{cKO} AHNSCs (Figure 4.21H, M) suggesting either that Id proteins other than Id4 contribute to the negative regulation of Ascl1 protein levels, or that Smad4 signalling can directly suppress Ascl1 expression.

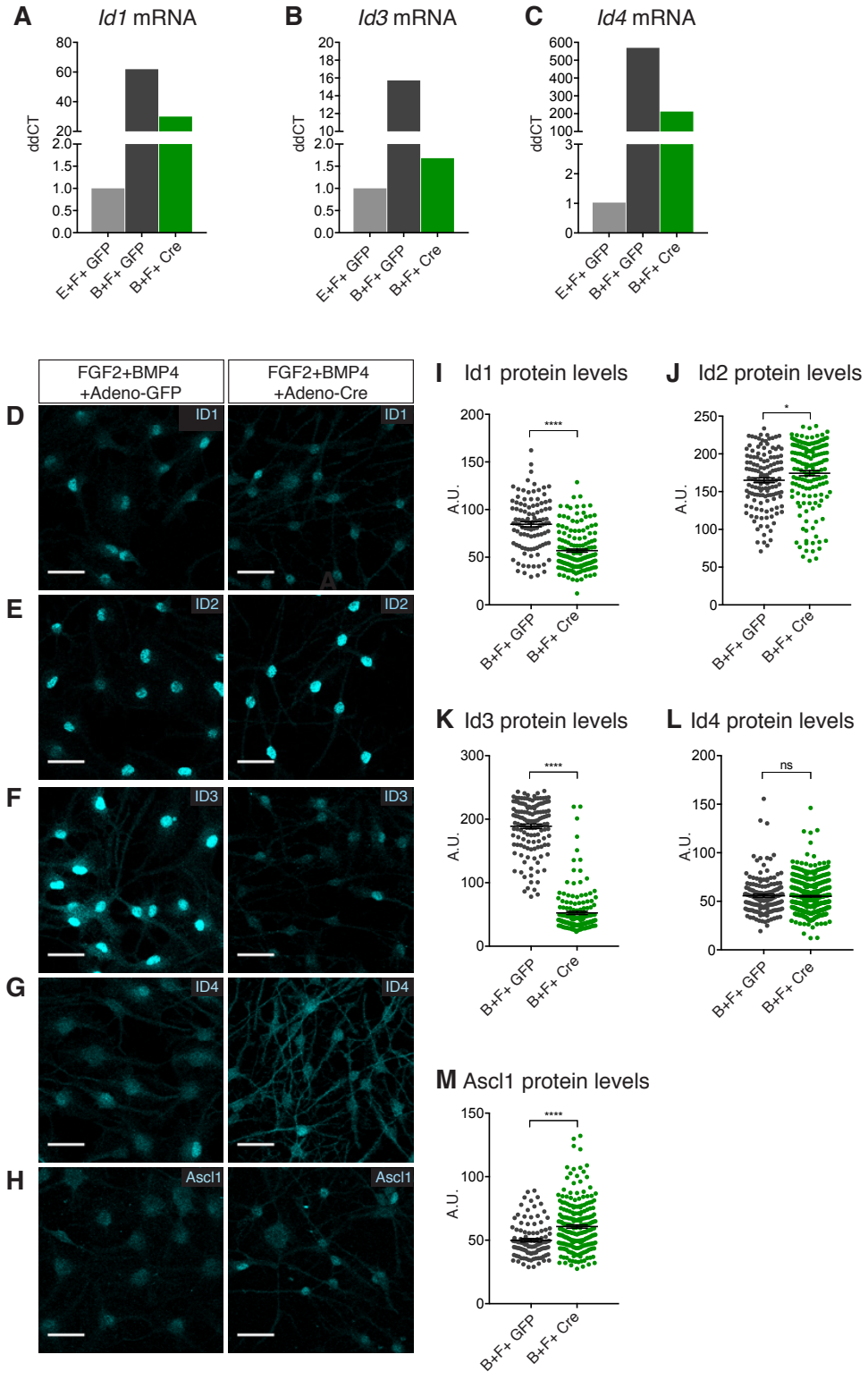

Figure 4.21. Analysis of Id levels in AHNSCs derived from Smad4flx mice

(A-C) QPCR analysis of *Id1, Id3* and *Id4* mRNA levels in Smad4flx AHNSCs, in BMP4-induced quiescent conditions (20ng/mL BMP4 + 20ng/mL FGF2, 72h), transduced with either 100moi Adeno-GFP or Adeno-Cre virus for 4 days. ddCt shown are relative to the

relative expression of each gene in Smad4flx AHNSCs in proliferation conditions (20ng/mL EGF + 20ng/mL FGF2) transduced with 100moi Adeno-GFP for 4 days. n=1.
(D-G) Immunostaining for Id1, Id2 Id3 and Id4 in BMP4-induced quiescent Smad4flx AHNSCs, transduced either 100moi Adeno-GFP or Adeno-Cre virus for 4 days. Scale bar, 30 μm.
(I-L) Quantification of the immunofluorescence intensity (arbitrary units, A.U.) of the staining shown in (D-G). Error bars shown mean±SEM, $p>0.05$ (ns), $p<0.05$ (*), $p<0.0001$(****).
(H) Immunostaining for Ascl1 in BMP4-induced quiescent Smad4flx AHNSCs, transduced either 100moi Adeno-GFP or Adeno-Cre virus for 4 days. Scale bar, 30 μm.
(M) Quantification of the immunofluorescence intensity (arbitrary units, A.U.) of Ascl1 staining shown in (H).
Error bars shown mean±SEM, $p<0.0001$(****). E, EGF; F, FGF2; B, BMP4.

Chapter 5. Results 3

The neurogenic niche in the adult dentate gyrus provides a source of multiple different signals that have the potential to regulate adult neural stem cell quiescence and activation. Delineating the effects of these signals specifically on stem cell activity is important for linking together the changes in the niche which often occur as a result of a change in behaviour or global biology of the organism, to the behaviour of the stem cells. BMP signalling has been reported to be active in the dentate gyrus, and acts to maintain quiescence of adult RGLs. As I have shown it also induces quiescence of NSCs *in vitro*. Notch signalling has also been shown to be required to maintain RGL quiescence (Ables et al., 2010; Basak et al., 2012; Ehm et al., 2010). However, it is yet to be examined how these two niche factors interact to regulate quiescence. Therefore, in the following chapter I will examine the interplay of Notch and BMP signalling on the quiescent state. Moreover, having identified Id4 as an important factor for maintaining quiescence of adult RGLs, I will investigate whether Notch signalling regulates Id4 expression *in vivo*.

5.1 Modulating Notch signalling has different effects in different concentrations of BMP4

5.1.1 Notch signalling is active in NSCs *in vitro*

I first turned to the *in vitro* model of quiescence in order to investigate the role of Notch signalling specifically in the regulation of stem cell quiescence and Id4 expression, and how Notch interplays with BMP4 signalling. Notch signalling can have different effects in different contexts, and the different Notch receptors are reported to differently regulate RGL quiescence. It therefore may regulate active and quiescent NSCs differently. Moreover, RGLs *in vivo* are likely to receive differing concentrations of the various niche signals; it is plausible that the balance of BMP, Notch and other niche signals is highly relevant for stem cell regulation. Therefore, I tested the role of Notch in three different concentrations of BMP4; the “active” proliferating state with AHNSCs in the presence of FGF2 (and EGF for experiments done early in my PhD) with no BMP4; “shallow” quiescence with 1ng/mL BMP4; and “deep” quiescence with 20ng/mL BMP4 (scheme shown in Figure 5.1.1A). I blocked Notch signalling in the three NSC states by treating AHNSCs with either DMSO as a vehicle control, or a gamma-secretase

inhibitor (GSI) LY411575 (hereafter referred to as LY) which blocks the cleavage of the intracellular domain (NICD) of Notch receptors1, 2 and 3, preventing NICD-mediated Notch-target gene activation ((Alunni et al., 2013); Figure 5.1B). I first checked the endogenous level of Notch signalling in the three NSC states, to check whether blocking Notch would have a functional effect. The three Notch receptors *Notch1, 2* and *3* were all expressed in the three NSC states, as shown by FPKM values from RNAseq (Figure 5.1C) and QPCR relative expression (Figure 5.1D). All three receptors were expressed at similar levels in all three states, indicating Notch signalling could potentially be induced in NSCs in each state. I next measured the expression levels of the Notch target genes *Hes1*, *Hes5* and *Hey1*, by both FPKM from the RNAseq data set and by QPCR relative expression levels. All three targets were expressed in all three states, with *Hes5* having the highest expression of the three genes, indicating Notch signalling is active in active and quiescent NSCs. Interestingly, *Hes5* expression was increasingly suppressed by increasing BMP4 concentration (Figure 5.1E,F), suggesting BMP4 may inhibit Notch signalling at high concentrations. Overall these results suggest Notch signalling may be functional in active and quiescent NSCs *in vitro*, and this model can therefore be used to test its function in regulating quiescence.

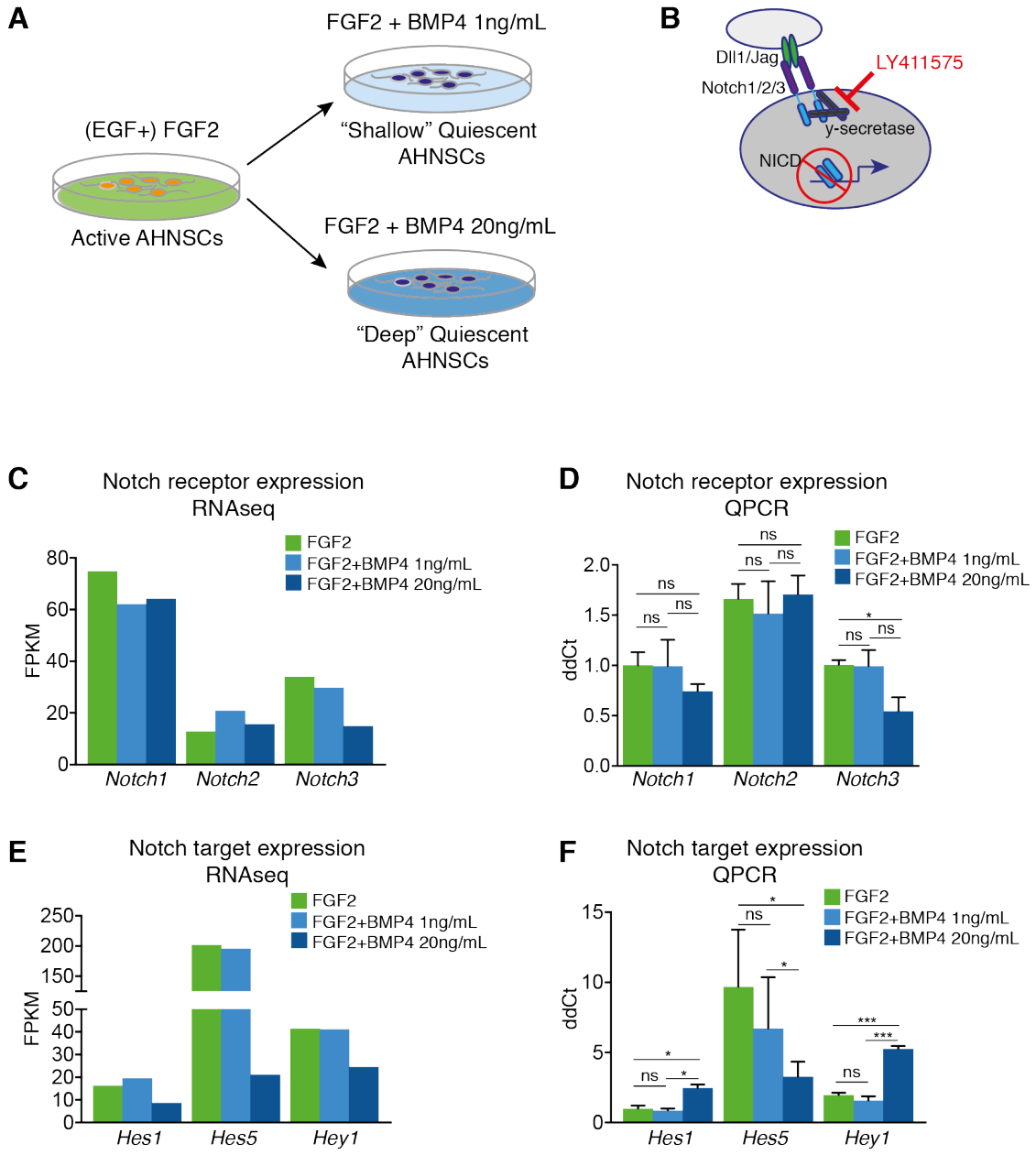

Figure 5.1. Scheme for inhibiting Notch signalling and expression of Notch components in AHNSCs *in vitro*

(A) Scheme showing the treatment of NSCs to induce three different states of activity or quiescence. "Active" NSCs are propagated in the presence of 20ng/mL FGF2 (plus 20ng/mL EGF for a small number of earlier experiments). "Shallow" quiescence is induced by treating active NSCs with 1ng/mL BMP4 for 72h, and "Deep" quiescence is induced with 20ng/mL BMP4 for 72h.

(B) Scheme of Notch signalling, inhibited by the y-secretase inhibitor (GSI) LY411575. Notch receptors 1, 2 and 3 are activated via binding of their ligands Dll1 or Jagged presented on neighbouring cells, promoting a conformational change of the receptor. This

allows for cleavage by ADAM metalloproteases, followed by proteolytic cleavage of the Notch intracellular domain (NICD) via the y-secretase enzyme. NICD then enters the nucleus and binds to the DNA of its gene targets in a complex with DNA-binding protein CSL, thus activating transcription. The GSI LY411575 inhibits y-secretase mediated cleavage of NICD, thus preventing activation of Notch target genes.
(C) The expression of the *Notch receptors 1,2* and *3* are shown as Fragments per Kilobase per Million reads (FPKM) from RNA sequencing of active, shallow and deep quiescent NSCs. All three receptors are expressed in all three conditions at similar levels, with *Notch1* showing the highest expression. *Notch3* is slightly suppressed in “deep” quiescence.
(D) Quantitative PCR for *Notch1,2* and *3*, from mRNA extracted from active, shallow and deep quiescent NSCs, confirms the expression levels observed in the RNAseq data, although here suggests the expression levels for all three receptors are similar in all conditions, in contrast to the higher levels of *Notch1* observed in the RNAseq data. The ddCt values shown are relative to the expression of internal control genes GAPDH and ActinB, and then relative to the expression of *Notch1* in active NSCs.
(E) The expression of the Notch target genes *Hes1, Hes5* and *Hey1* are shown as Fragments per Kilobase per Million reads (FPKM) from RNA sequencing of active, shallow and deep quiescent NSCs. All three genes are expressed in all three conditions. *Hes5* has the highest expression of the three, however is downregulated in “deep” quiescence.
(F) Quantitative PCR for *Hes1, Hes5* and *Hey1,* from mRNA extracted from active, shallow and deep quiescent NSCs, confirms the expression levels observed in the RNAseq data. The ddCt values shown are relative to the expression of internal control genes GAPDH and ActinB, and then relative to the expression of *Hes1* in active NSCs.

5.1.2 Active Notch signalling is required for low-level proliferation of quiescent NSCs, independent of Id4 and Ascl1

I next tested whether treatment with LY could block Notch signalling in NSCs. “Active” AHNSCs (in the presence of EGF and FGF2) and “deep” quiescent AHNSCs were treated with either 1uM, 10uM or 20uM LY, or an equal volume of DMSO as a control, for 72h after which cell lysates were extracted to perform Western blot for the Notch1 intracellular domain (N1ICD). 72hr was chosen in order to allow time for any cleaved NICD to be recycled, and to give time for the cells to enter/exit the cell cycle, as with BMP4 treatment. N1ICD was strongly detected in both active and quiescent NSCs, further demonstrating that Notch signalling is active in these conditions. Treatment with LY, even at the lowest concentration (1uM), was sufficient to completely block the

cleavage of the Notch1 receptor and the production of NICD (Figure 5.2A), as compared to the control samples, in both active and “deep” quiescent AHNSCs. I therefore chose 1uM LY to inhibit Notch in AHNSCs for future experiments. I next checked the expression level of Notch target gene *Hes5* in active, “shallow” and “deep” quiescent NSCs treated with either 1uM LY or an equal volume of DMSO. QPCR for *Hes5* in LY treated NSCs showed that Notch inhibition in active or “shallow”-quiescent NSCs could strongly suppress Notch signalling (Figure 5.2B). Interestingly, LY could not suppress *Hes5* expression in the “deep” quiescent NSCs, suggesting high levels of BMP4 signalling may be able to induce *Hes5* expression. This is paradoxical to the observation in Section 5.1.1 that increasing concentration of BMP4 suppresses Hes5 expression (also seen in Figure 5.1B). It could be that BMP4 simultaneously inhibits endogenous Notch signalling whilst also inducing some Notch target genes such as Hes5, albeit less strongly than Notch can induce them. I will explore this further in Section 5.1.3. Concurrent to the suppression of *Hes5*, LY treatment led to the upregulation of *Ascl1* mRNA (Figure 5.2C). This would be expected, because Ascl1 is suppressed at the transcriptional level by Hes1/5 (Imayoshi and Kageyama, 2014b) Moreover, the upregulation of *Ascl1* was less marked in “deep” quiescence compared to “shallow” quiescence (Figure 5.2C), which could reflect the sustained expression of *Hes5* in the presence of high levels of BMP4 plus GSI (Figure 5.2B). Notch1 signalling is reported to be important for maintaining quiescence of RGLs *in vivo*, therefore I measured the proliferation rate of LY-treated cells by immunostaining for cell cycle markers Ki67 and CyclinD1, and incorporation of S-phase marker EdU. Notch inhibition did not affect the proliferation of active NSCs (Figure 5.2D-F, green bars; Gi), likely reflecting the fact they are already proliferating at a high rate. Notch inhibition also did not significantly affect the proliferation of shallow quiescent NSCs, although there was a trend towards lower proliferation rates (Figure 5.2D-F, light blue bars; Gii). Most surprisingly, LY treatment of deeply quiescent NSCs induced an even deeper state of quiescence as shown by significant reduction of the fraction of EdU+, Ki67+ and CyclinD1+ NSCs (Figure 5.2D-F, dark blue bars; Giii). I checked whether this was due to changes in the levels of Ascl1 and Id4. *Id4* expression was not significantly affected by LY in deeply quiescent NSCs, although was upregulated in active and shallow-quiescent NSCs (Figure 5.2H). Id4 protein was mildly increased in active and shallow-quiescent NSCs following Notch inhibition, as measured by fluorescence intensity from immunostaining (Figure 5.2J), corresponding with the observed increase in mRNA expression (Figure 5.2H). Id4 levels were mildly decreased in LY-treated deep-

quiescent NSCs (Figure 5.2J,N) and the shift to lower fluorescence levels with LY treatment can be seen when plotted as a histogram of intensity (Figure 5.2K). Therefore, Notch appears to suppress Id4 expression in the presence of low BMP4, but higher concentrations of BMP4 can overcome this suppression to induce Id4. This shows the decrease in proliferation of “deep” quiescent NSCs following Notch inhibition cannot be explained by changes in Id4 levels *in vitro*. Moreover, despite the higher or normal levels of Id4 protein (Figure 5.2 J), Ascl1 protein levels were increased in all three conditions treated with LY (Figure 5.2L) and the shift towards higher Ascl1 levels in LY-treated deeply-quiescent NSCs can be seen clearly in a histogram of Ascl1 fluorescence intensity (Figure 5.2M). This is likely a result of increased *Ascl1* transcription following Notch inhibition (Figure 5.2C). Increased Ascl1 protein levels would be expected to lead to increased proliferation, however the opposite is observed, suggesting Notch may regulate other pathways that induce proliferation in the presence of BMP4, independent of Ascl1. There may potentially be a compensatory effect by other Id proteins, as *Id1* expression is upregulated following LY-treatment, only in quiescent NSCs (Figure 5.2I). However, I have not quantified whether Id1 protein is significantly upregulated in LY-treated quiescent NSCs. Overall these results suggest an interesting dynamic between Notch and BMP4 signalling at different levels in NSCs *in vitro*, whereby Notch is able to modulate the levels of Hes5, Ascl1, and Id4 when BMP4 is absent or low. In contrast, in high concentrations of BMP4, Notch has less of an effect on the transcription of these factors, but more strongly affects the low level of proliferation. These results may be explained by a potential effect of Notch on the oscillations of Ascl1, Id4 and Hes5 protein, which I will discuss further in Section 6.

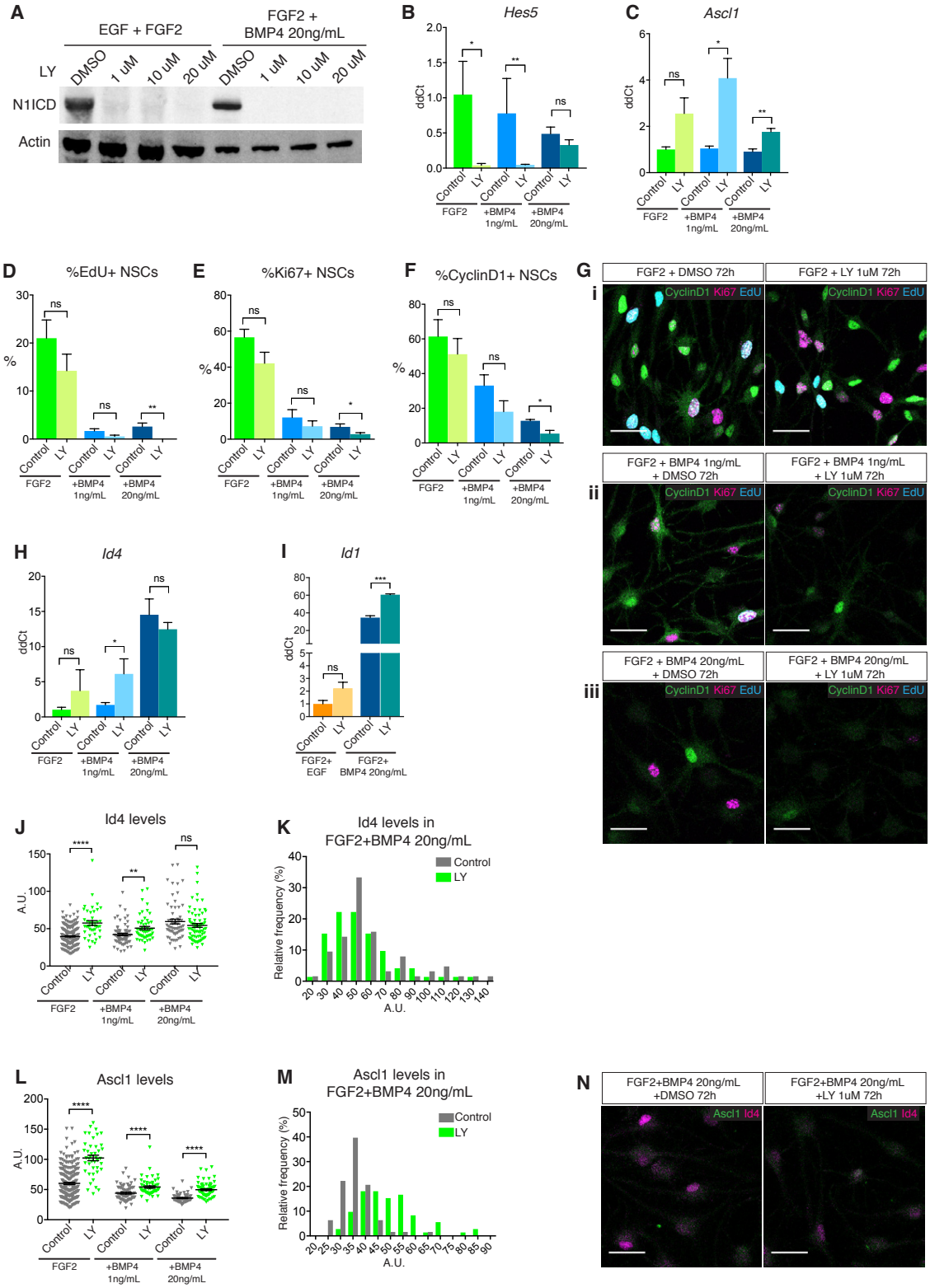

Figure 5.2. Effects of inhibiting Notch signalling in active and quiescent AHNSCs *in vitro* (legend next page)

Figure 5.2. Effects of inhibiting Notch signalling in active and quiescent AHNSCs *in vitro*

(A) Western Blot analysis of Notch1 intracellular domain (N1ICD) and Actin in NSCs in EGF+FGF2 ("active") or FGF2+BMP4 20ng/mL ("deep" quiescent) conditions, treated for 72h with either DMSO or 1uM, 10uM or 20uM of the y-secretase inhibitor LY411575. N1ICD can be strongly detected in both active and deep quiescent NSCs, and is completely lost upon treatment with all concentrations of LY.

(B) QPCR analysis of *Hes5* expression in active, shallow and deep quiescent NSCs, treated for 72h with either 1uM LY or an equivalent volume of DMSO (control). n=3.

(C) QPCR analysis of *Ascl1* expression in active, shallow and deep quiescent NSCs, treated for 72h with either 1uM LY or an equivalent volume of DMSO (control). n=3.

(D) Quantification of the percentage of NSCs that have incorporated the S-phase marker EdU during a 1hour pulse, in control (DMSO) or Notch-inhibited (1uM LY) active, shallow and deep quiescent NSCs. n=3.

(E) Quantification of the percentage of NSCs positive for Ki67 immunostaining, in control or (1uM LY) Notch-inhibited active, shallow and deep quiescent NSCs. n=3.

(F) Quantification of the percentage of NSCs positive for CyclinD1 immunostaining, in control (DMSO) or Notch-inhibited (1uM LY) active, shallow and deep quiescent NSCs. n=3.

(G) Immunostaining for Ki67, CyclinD1, and EdU in deep quiescent NSCs treated with either DMSO (control) or 1uM LY. Scale bar, 30μm.

(H) QPCR analysis of *Id4* expression in active, shallow and deep quiescent NSCs, treated for 72h with either 1uM LY or an equivalent volume of DMSO. n=3.

(I) QPCR analysis of *Id4* expression in NSCs in EGF+FGF2 ("active") or FGF2+BMP4 20ng/mL ("deep" quiescent) conditions, treated for 72h with either 1uM LY or an equivalent volume of DMSO (control). n=3.

(J) Immunofluorescence intensity (arbitrary units, A.U.) of Id4 in the nuclei of NSCs are plotted for active, shallow and deep quiescent NSCs, treated for 72h with either 1uM LY or an equivalent volume of DMSO (control). n=3.

(K) Histogram plot of the immunofluorescence intensity values for Id4 in deep quiescent NSCs in DMSO (control) or 1uM LY, shown in (J). LY-treated NSCs have a lower percentage of nuclei with Id4 A.U. values above 80.

(L) Immunofluorescence intensity (A.U.) of Ascl1 in the nuclei of NSCs are plotted for active, shallow and deep quiescent NSCs, treated for 72h with either 1uM LY or an equivalent volume of DMSO (control). n=3.

(M) Histogram plot of the immunofluorescence intensity values for Ascl1 in deep quiescent NSCs in DMSO (control) or 1uM LY, shown in (J). LY-treated NSCs have a higher percentage of nuclei with Ascl1 A.U. values above 40.
(N) Immunohistochemistry for Ascl1 and Id4 in deep quiescent NSCs treated with DMSO or 1uM LY for 72h. Scale bar, 30μm.
Unpaired t-test was used for all statistical analyses (mean±SEM), $p>0.05$ (ns), $p<0.05$ (*), $p<0.01$(**), $p<0.001$(***), $p<0.0001$(****). All repeats were independent biological replicates.

5.1.3 Notch regulates different genes depending on the level of BMP4 signalling

To further understand the interaction of Notch and BMP signalling in regulating NSC quiescence, I performed RNA sequencing of active (20ng/mL FGF2), “shallow” quiescent (20ng/mL FGF2 + 1ng/mL BMP4) and “deep” quiescent (20ng/mL FGF2 + 20ng/mL BMP4) NSCs treated for 72h with DMSO or 1uM LY. A transcriptome-wide analysis allowed me to identify potential pathways that Notch regulates in the presence of no, low or high BMP4, to help explain the effects seen on proliferation. The first striking observation was that Notch regulates far more genes in active and shallow quiescent NSCs (1722 and 1738 genes, respectively), than in deep quiescence (427 genes) (Figure 5.3A,B). This could suggest that high concentrations of BMP4 can induce Notch target genes, or that high levels of BMP signalling suppress Notch and therefore Notch inhibition would have little effect in this condition. This ties in with the observation made in Figure 5.2B, that 20ng/mL BMP4 inhibits the QPCR expression of Hes5 compared to active and shallow quiescent NSCs, but also induces Hes5, as Notch inhibition does not affect Hes5 in this condition. I looked further into this by analysing the FPKM expression of Notch target genes Hes1, Hes5 and Hey1 in active, shallow quiescent and deep quiescent NSCs treated with DMSO or LY (Figure 5.3C-D). I found consistently for all three notch target genes that 20ng/mL BMP4 suppressed their expression compared to active and shallow quiescent NSCs in control conditions (Figure 5.3C-D, grey bars). LY treatment strongly suppressed all three Notch targets in active and shallow quiescent NSCs. However, LY did not affect the expression of Hes1, Hes5 or Hey1 in the presence of 20ng/mL BMP4, indicating BMP4 actually induces these genes. Overall it appears that in high concentrations, BMP4 acts redundantly with Notch signalling, suppressing its signalling and inducing its target genes (at least in the case of Hes1, Hes5 and Hey1) albeit less strongly than Notch. In

further support of this notion, the genes regulated by Notch in deep quiescence are mostly unique to that state, whereas the majority of genes regulated by Notch in active NSCs are also regulated in shallow quiescent NSCs (Figure 5.3A,B). This implies that BMP signalling is regulating Notch target genes in deep quiescence but not in shallow quiescence or active NSCs, therefore Notch inhibition affects more genes in the latter two conditions. To see more broadly the categories of genes that were regulated by Notch, I analysed the ontologies of genes significantly up- or down-regulated by LY treatment in active, shallow and deep quiescent NSCs. Interestingly, cell cycle genes were strongly upregulated by Notch inhibition in active and shallow quiescence (Figure 5.3F,H). This concurs with the reported role for Notch in maintaining quiescence *in vivo* (Ables et al., 2010; Ehm et al., 2010; Kawaguchi et al., 2013; Ottone et al., 2014), however it does not translate to an actual increase in proliferation in the *in vitro* system (Figure 5.2D-G). Genes downregulated following Notch inhibition in active and shallow quiescent NSCs are highly enriched for “Lipid metabolic process”, “Cell adhesion”, and “Oxidation-reduction process” (Figure 5.3G,I), indicating Notch may regulate quiescence by modulating metabolism or adhesion of NSCs to the niche, both of which have been reported to regulate NSC quiescence *in vivo* ((Knobloch et al., 2013); adhesion shown to regulate SVZ NSCs, but not for SGZ NSCs yet, i.e. (Kazanis et al., 2010; Ottone et al., 2014)). “Protein phosphorylation” ontologies are found in both up- and down-regulated samples in all conditions, suggesting Notch may dynamically regulate phosphorylation (Figure 5.3F-K). In contrast, inhibiting Notch signalling in deep quiescent NSCs does not significantly regulate any cell cycle genes (Figure 5.1.3L) perhaps due to the fact BMP4 already strongly suppresses cell cycle genes. Instead, genes associated with “Negative regulation of Wnt signalling” are upregulated, whilst “Erk1/2 cascade” and “NFkB activity” are downregulated following Notch inhibition, suggesting it may be regulating various mitogenic signalling pathways in high levels of BMP4. As for active and shallow quiescent NSCs, “Cell adhesion” and lipid metabolism genes are also regulated in deep quiescence by Notch, indicating Notch signalling may play an important role in regulating these aspects of NSC biology. Overall these results suggest Notch plays an important role in regulating metabolism of NSCs, protein phosphorylation, and maintaining quiescence of NSCs in lower concentrations of BMP4. However, higher concentrations of BMP4 simultaneously suppress Notch signalling and incudes Notch target genes. Both Notch and BMP signalling are required to maintain the stem cell population in the DG in adult mice, therefore it is rational that they can both induce stemness/quiescence genes, and act

redundantly. However, it appears that their effects may change depending on the concentration of each signal. The role of Notch in deeply quiescent NSCs is subtler, perhaps regulating other signalling pathways, such as Wnt or MAPK, that could help to maintain the low-level proliferation of NSCs, or by modulating the activity of proteins via phosphorylation, or by regulating adhesion or metabolism, indirectly affecting quiescence.

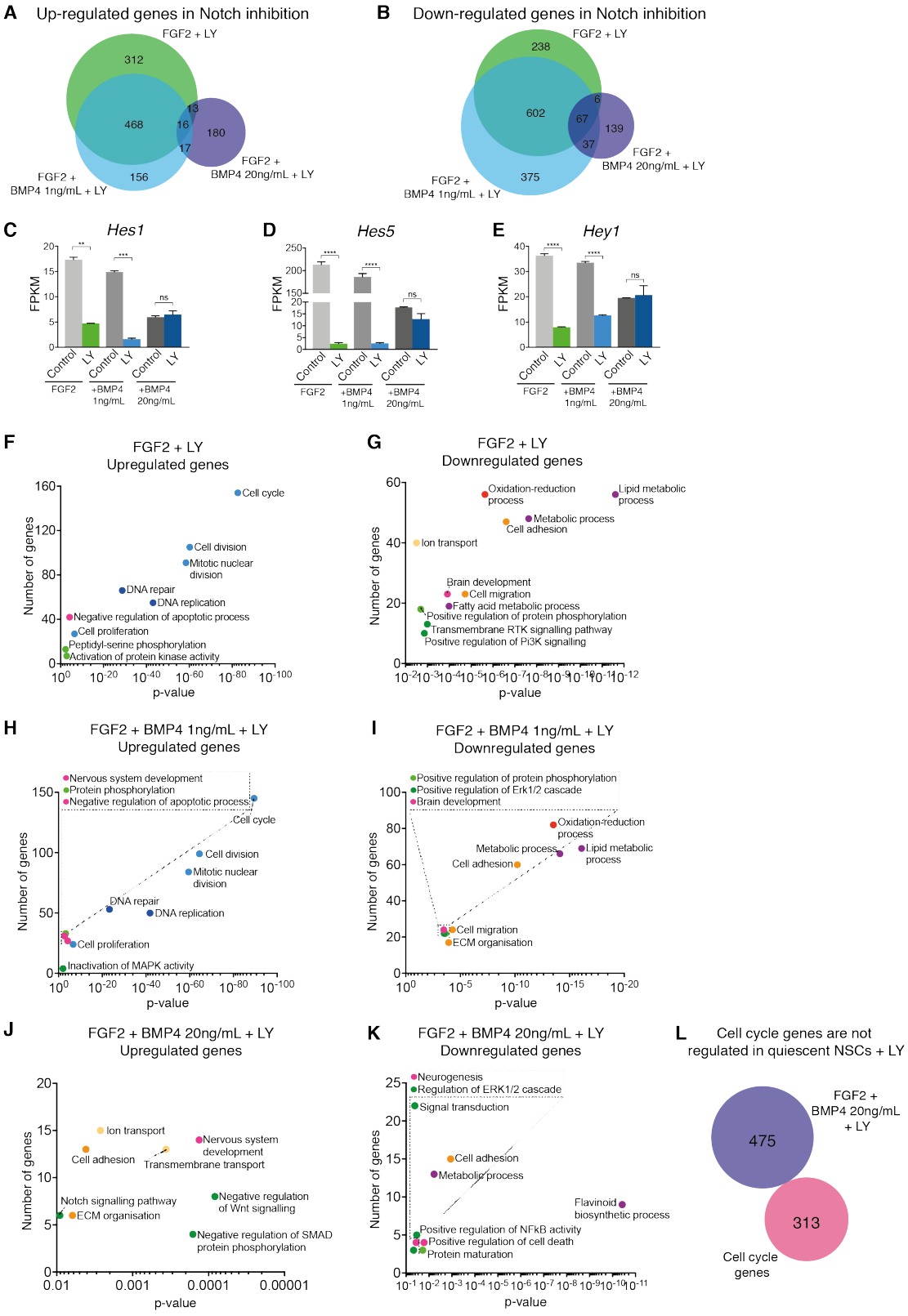

Figure 5.3. RNAseq analysis of active, shallow quiescent and deep quiescent AHNSCs following Notch inhibition (legend next page)

Figure 5.3. RNAseq analysis of active, shallow quiescent and deep quiescent AHNSCs following Notch inhibition

(A-B) Overlap of genes significantly up- or down-regulated following 72h 1uM LY treatment, as compared to DMSO control samples, in “active” (FGF2), “shallow” quiescent (FGF2+BMP4 1ng/mL) and “deep” quiescent (FGF2+BMP4 20ng/mL) NSCs. Upregulated genes were determined by a significant Log2-fold change greater than 1, and with a minimum expression of 1 FPKM in LY-treated NSCs. Down-regulated genes were determined by a significant Log2-fold change less than -1, and with a minimum expression of 1 FPKM in DMSO-treated NSCs.

(C-D) Expression of Notch target genes *Hes1*, *Hes5* and *Hey1* in NSCs treated with DMSO or 1uM LY for 72h, measured by RNA sequencing. Expression values are shown as FPKM from 3 biological repeats.

(F-K) Gene Ontology terms associated with genes up- or down-regulated in active, “shallow” quiescent or “deep” quiescent NSCs treated with 1uM LY for 72h, compared to DMSO-treated control NSCs. Shown for each term are the number of genes associated with the ontology, and its significance (Log10 p-value). Dots are coloured based on their ontology terms - light blue: cell cycle/division; dark blue: DNA repair/replication; light green: Protein phosphorylation/modification; dark green: signalling, transcription; orange: adhesion/cytoskeleton; yellow: ion-related; pink: brain/nervous system related; purple: metabolism; red: oxidation/reduction.

(L) Overlap of genes regulated in LY-treated “deep” quiescent NSCs and cell cycle genes (list from Qiagen.com.) None of the 313 cell cycle genes are regulated by Notch in “deep” quiescent NSCs.

3 independent biological repeats were processed for RNA sequencing.

5.2 Investigating the effect of Notch signalling on Id4 *in vivo*

Manipulating Notch signalling *in vitro* has produced contradictory data to the role of Notch reported for RGLs *in vivo*, however there are many caveats for the *in vitro* model (discussed in Section 6), and I saw a small effect of inhibiting Notch signalling on Id4 expression. I was therefore interested to examine whether Notch signalling induces Id4 expression in RGLs *in vivo*, which could explain part of the molecular mechanism by which Notch maintains RGL quiescence. The use of LY *in vitro* results in indiscriminate inhibition of all Notch receptors. I used a similar approach *in vivo*, via conditional deletion of RBPJk, the downstream effector of Notch signalling. Loss of RBPJk will result in a block of all Notch signalling. I crossed mice with a floxed RBPJk allele to the

*GlastCre^{ERT2}; Rosa26-EYF*P mice, in order to conditionally delete RBPJk specifically in RGLs of adult mice.

5.3 Notch-RBPJk signalling is not required to maintain Id4 expression in RGLs

In order to examine whether Notch-RBPJk signalling is required for Id4 expression in RGLs *in vivo*, RBPJk control or floxed (*RBPJk^{cKO}*) mice were treated with tamoxifen for 5 days to induce Cre-mediated recombination in RGLs, and then analysed 5 days later (P70), in order to allow time for the stable RBPJk protein to degrade (Andersen et al., 2014) (Figure 5.4A). Immunostaining for Id4 did not show any striking difference between control and *RBPJk^{cKO}* mice (Figure 5.4B). The fraction of Id4+ YFP+GFAP+ RGLs was reduced to a small degree in *RBPJk^{cKO}* mice (89.83±1.6% in control vs 81.92±1.6% in *RBPJk^{cKO}* mice), however the Id4 fluorescence intensity per RGL nucleus was not changed between control and *RBPJk^{cKO}* mice (Figure 5.4C). Notch signalling therefore may be able to induce Id4 to a small degree in RGLs *in vivo*, as was observed *in vitro*, but it is not required for Id4 expression. RBPJk deletion does lead to a large increase in the fraction of Ascl1+ and Ki67+ RGLs (Figure 5.4D,E), as has previously been reported (Andersen et al., 2014), likely due to the loss of the transcriptional suppression of *Ascl1* by Notch/Hes1/5 (Imayoshi and Kageyama, 2014b). Interestingly, loss of RBPJk also resulted in a large increase in the number of Id1+ RGLs (Figure 5.4F). These results suggest that Notch signalling is not the main signal inducing of Id4 expression in the DG, and also suggests the maintenance of RGL quiescence by Id4 can be bypassed by Notch inhibition, perhaps as a result of the large increase in Ascl1 expression.

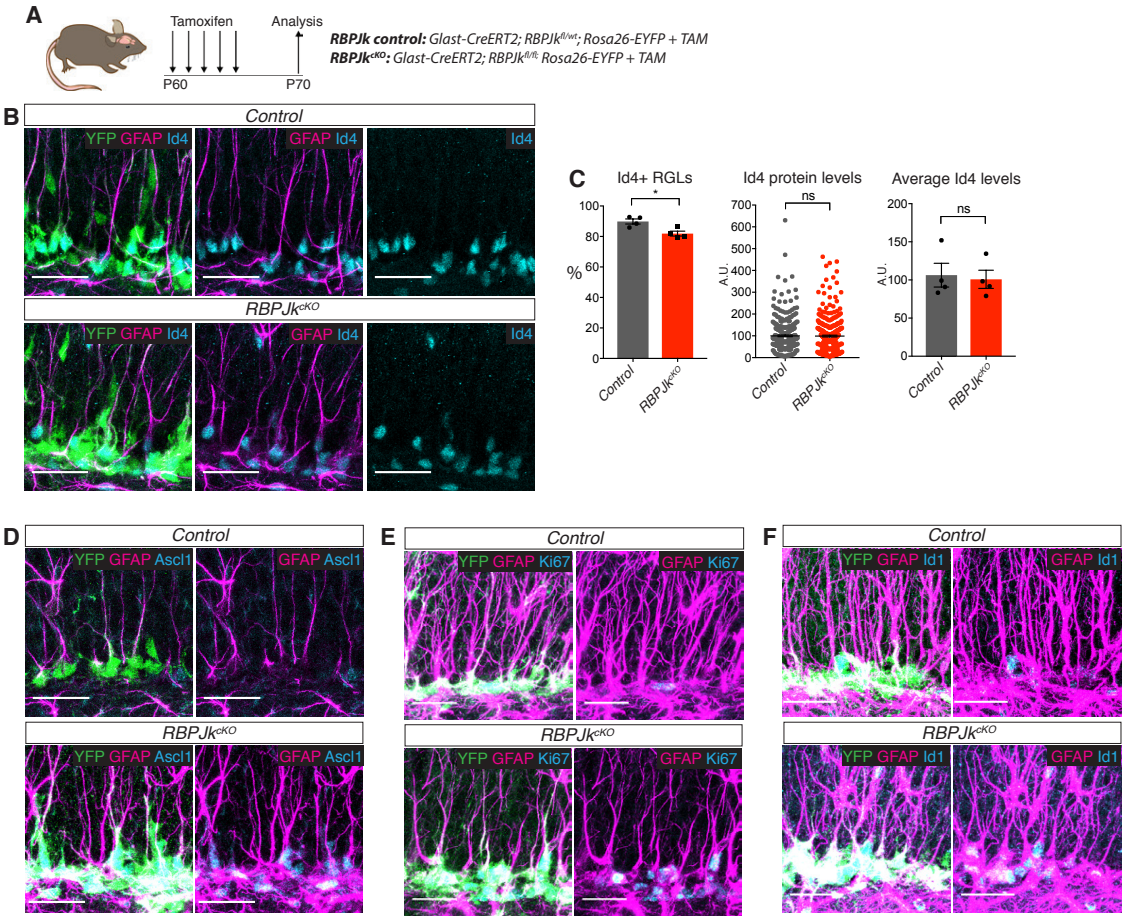

Figure 5.4. Effects of acute deletion of Notch effector RBPJk in RGLs

(A) Design of the experiment for deleting RBPJk from RGLs of the adult hippocampus using *RBPJk*^{cKO} mice.

(B) Immunolabelling for YFP, GFAP and Id4 in the DG of *RBPJk*^{cKO} and control mice 10 days after the first tamoxifen administration. Scale bar, 30µm.

(C) Quantification of the data in (B). The number of Id4 expressing RGLs is mildly decreased, while the levels of Id4 are not significantly different in the absence of Notch-RBPJk signalling. Unpaired t-test (mean±SEM), p>0.05 (ns), p<0.01 (**), p<0.0001 (****). n=4 for both control and mutant mice.

(D-F) Immunolabelling for YFP, GFAP and either Ascl1, Ki67 or Id1 in the DG of *RBPJk*^{cKO} and control mice 10 days after the first tamoxifen administration. Scale bar, 30µm.

5.4 Id4 expression in RGLs is independent of both Notch and BMP signalling *in vivo*

Considering the fact that both BMP and Notch are reported to be important signalling pathways for the maintenance of RGL quiescence, and that neither alone are required to induce Id4 expression, I asked whether there is redundancy between Notch and BMP in the regulation of Id4. To this end, I generated *GlastCre^{ERT2};Smad4-floxed;RBPJk-floxed;Rosa26-EYFP* mice (*RBPJk^{cKO};Smad4^{cKO}* mice), in which both Notch and BMP signalling will be conditionally inactivated in RGLs in adult mice.

5.4.1 Double RBPJk-Smad4 conditional deletion does not strongly affect Id4 expression in RGLs

I treated *RBPJk^{cKO};Smad4^{cKO}* mice with tamoxifen for 5 days, and then 5 days later (P70) analysed the mice (Figure 5.5A), to allow time for both Smad4 and RBPJk proteins to be degraded. The fraction of Id4+ YFP+GFAP+ RGLs was reduced, but not significantly, in double cKO mice (90.59±3.5% in control vs 79.48±6.7% in *RBPJk^{cKO};Smad4^{cKO}*), and the fluorescence levels were also mildly decreased (Figure 5.5C). However, this decrease in Id4 was similar to that observed for the single *RBPJk^{cKO}* mice, suggesting this is mostly a result of loss of Notch. The fraction of Ascl1+ RGLs was increased in the *RBPJk^{cKO};Smad4^{cKO}* mice (Figure 5.5D), again likely as a result of the loss of Notch rather than Smad4. The results suggest that there is not redundancy between BMP-Smad4 and Notch-RBPJk with regards to Id4 expression, however both signals can regulate Id4 expression in a small way. I also examined the effect on Id1 and Id3 protein expression in the double cKO mice. Id1 protein levels are increased in RGLs of *RBPJk^{cKO};Smad4^{cKO}* mice (Figure 5.5 E), similar to the increase in Id1 protein observed in *RBPJk^{cKO}* mice (Figure 5.4F). Id3 protein levels were not noticeably affected by deletion of both RBPJk and Smad4 (Figure 5.5F), suggesting Id3 may be regulated by different signals in a similar way to Id4. It is therefore highly interesting to investigate the regulation of Id4 further, to determine which of the many niche signals converge with Notch and BMP4 to induce Id4, thereby promoting the degradation of Ascl1 and maintaining NSC quiescence.

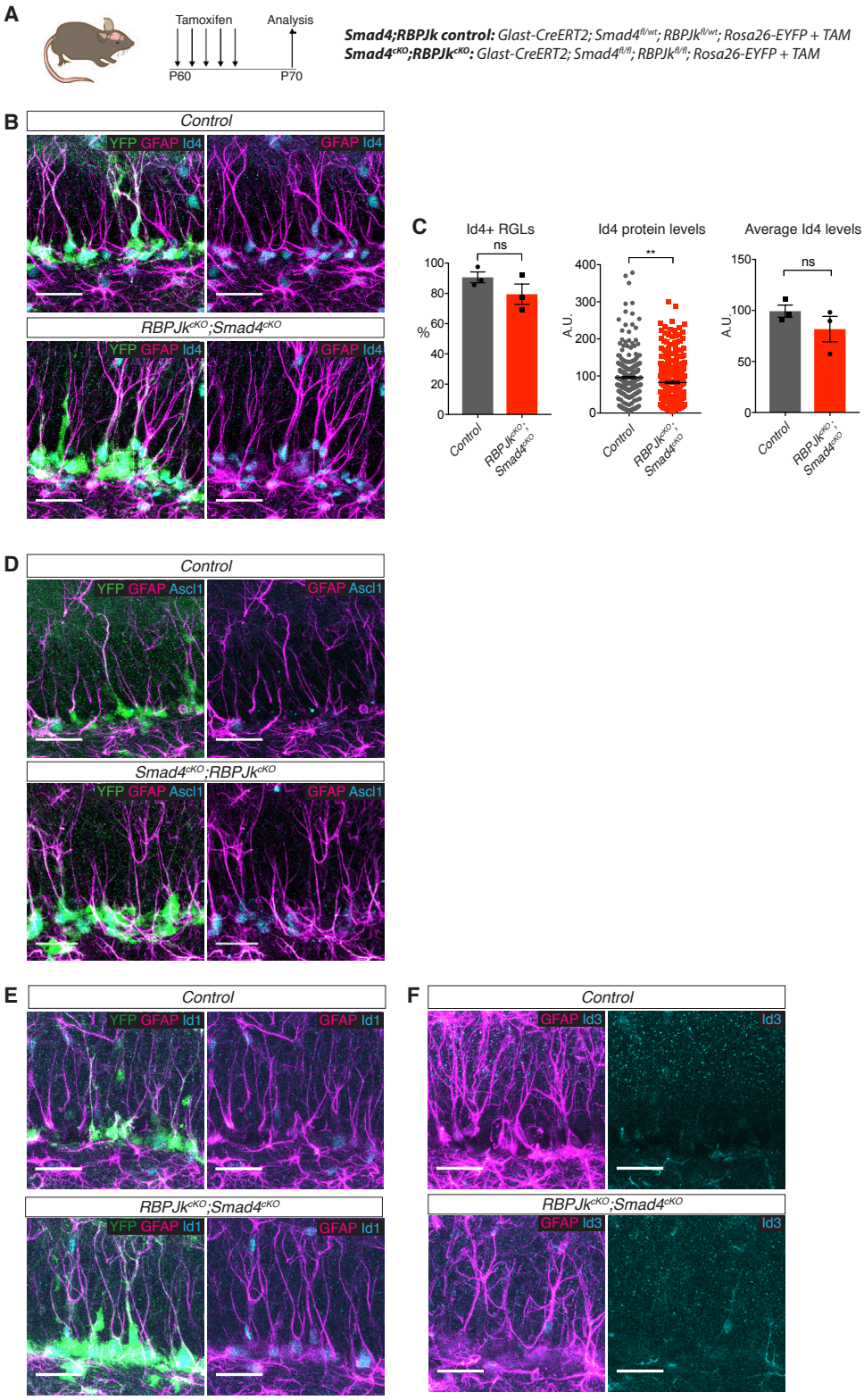

Figure 5.5. Effects of acute deletion of both Smad4 and RBPJk in RGLs

(A) Design of the experiment for inactivating both BMP and Notch pathways in hippocampal RGLs. Both RBPJk and Smad4 are deleted using 5 days of tamoxifen

administration to *Smad4*^{cKO}*;RBPJk*^{cKO} mice, and analysed 10 days after the first tamoxifen injection to ensure the elimination of RBPJk protein.
(B) Immunolabelling for YFP, GFAP and Id4 in the DG of *Smad4*^{cKO}*;RBPJk*^{cKO} and control mice 10 days after the first tamoxifen administration. Scale bar, 30μm.
(C) Quantification of the data in (B). The percentage of Id4 expressing RGLs is mildly, but not significantly, decreased in *Smad4*^{cKO}*;RBPJk*^{cKO} mice. The levels of Id4 protein, measured by fluorescence intensity, is significantly decreased in *Smad4*^{cKO}*;RBPJk*^{cKO} mice, although the change in average levels does not reach significance. Unpaired t-test (mean±SEM), $p>0.05$ (ns), $p<0.01$ (**). n=3 for both control and mutant mice.
(D) Immunolabelling for YFP, GFAP and Ascl1 in RGLs of *Smad4*^{cKO}*;RBPJk*^{cKO} and control mice following tamoxifen treatment. Scale bar, 30μm.

Chapter 6. Discussion

The work presented here has highlighted that a classical mechanism for stem cell regulation - the dominant negative regulation of bHLH transcription factors by Id proteins - exists in a novel stem cell population, the neural stem cells of the adult hippocampal neurogenic niche. I have investigated the molecular mechanisms central to controlling the maintenance of adult hippocampal stem cell quiescence, by building upon an *in vitro* model of BMP4-induced quiescence that had been previously utilised by our laboratory to investigate quiescence of embryonic stem cell-derived NSCs (Martynoga et al., 2013). Using this technique in combination with *in vivo* analysis, I have identified firstly that the activation factor Ascl1 is unexpectedly expressed in many quiescent RGLs, and that the inhibitor of differentiation protein Id4 is enriched in quiescent RGLs and can mediate Ascl1 protein degradation to maintain a quiescent stem cell state. Interestingly, the loss of Id4 in RGLs may be compensated by Id1 and/or Id3, which is particularly fascinating in light of the fact they appear to be negatively regulated by Id4. Finally, I investigated the niche signals upstream of Id4, uncovering a complex situation in which it seems likely multiple or non-canonical signals induce Id4 expression in the hippocampal niche. By investigating the molecular regulation of the quiescent NSC state specifically, this work both provides a deeper understanding of the homeostatic regulation of NSC activity, as well as generating insight into the mechanistic changes that may occur in NSCs in age-related cognitive decline, neurodegenerative disease, and glioma stem cells, potentially leading to novel therapies.

In this chapter, I will present a discussion of my results, exploring the implications in the context of the field of adult neurogenesis and adult stem cell research. I will also suggest improvements of this work, as well as propose future experiments to address the remaining questions generated by the data generated here.

6.1 An *in vitro* model of adult hippocampal neural stem cell quiescence

The adult hippocampal stem cell niche is a complex environment, with many cell types regulating the activity of NSCs via direct cell contacts or secreted signalling molecules.

This means it is difficult to directly test the function of a gene or signal on a specific cell type within the niche, without indirectly affecting activity and signalling elsewhere. This is particular true of RGL quiescence, a stem cell state not fully understood or characterised. Therefore, there was a strong requirement for a tractable, reductionist system for investigating the complex molecular regulation of adult hippocampal NSC quiescence. I therefore built upon work by Mira and colleagues (Mira et al., 2010), and our lab (Martynoga et al., 2013), to develop an *in vitro* model of quiescence, using cells derived specifically from the adult dentate gyrus, in order to generate a biologically relevant method for studying the molecular regulation of this particular population of cells (Figure 3.1).

6.1.1 BMP4-treated adult hippocampal neural stem cells robustly model RGL quiescence

Treatment with BMP4 was able to strongly but reversibly suppress the proliferation of adult hippocampal neural stem cells (AHNSCs), without affecting their multipotency, although I did not quantify the proportion of neurons, astrocytes or oligodendrocytes generated from AHNSCs differentiated either directly from an active state, versus following reactivation from quiescence. Treatment with BMP4 could potentially affect the propensity of AHNSCs to differentiate into the different subtypes.

Interestingly, a small proportion of AHNSCs were still proliferating in BMP4-induced quiescence, even after 7 days of BMP4 exposure (Figure 3.2). The percentage of Ki67+ and EdU+ NSCs in BMP4 conditions was very similar to the percentage of Ki67+ or EdU+ RGLs observed in the DG of P60 mice (around 8% and 2% respectively (Andersen et al., 2014; Urban et al., 2016)). This could suggest BMP4-treated AHNSCs *in vitro* represent the whole population of quiescent and active RGLs *in vivo*, with similar mechanisms regulating spontaneous cell cycle entry and return to quiescence. It also highlights that quiescent NSCs are not senescent, rather appear to be poised to activate as soon as the appropriate activating signals are received. This could be why CyclinD1 expression increases so rapidly following re-activation (Figure 3.2); CyclinD1 is an early cell cycle gene that induces G1 progression, therefore would be a primary responder to an activation signal. CyclinD1 is also a known target of Ascl1 (Andersen et al., 2014; Castro et al., 2011), and could mediate activation induced by Ascl1.

The cycling AHNSCs in BMP4-induced quiescence were likely a result of spontaneous entry of the population of cells into the cell cycle. However, they could also represent a subpopulation of NSCs that were refractory to BMP, and not induced to quiescence. If this was true, the reactivation of AHNSCs from BMP4-induced quiescence could in fact represent the expansion of NSCs that were never quiescent. I therefore employed an EdU-BrdU pulse-chase paradigm, combined with Ki67 expression in order to identify whether the same cells were repeatedly dividing, or if new cells entered the cell cycle, as well as to see whether some cycling cells returned to quiescence. I was able to observe all combinations of label incorporation, including cells that had returned to quiescence having previously divided, as well as the recruitment of cells into the cell cycle that had not previously divided. These results suggest the cycling cells in BMP4-induced quiescence represent a population-level spontaneous entry into the cell cycle. Moreover, I observed many cells that were negative for pan cell cycle marker Ki67, suggesting they are in a true G0 state, as opposed to a paused or elongated G1 state.

As described in Section 1.5.2, adhesion to the niche and cell-cell contacts can directly regulate NSC quiescence. I therefore demonstrated that BMP4-induced quiescent AHNSC can reactivate without disrupting their extracellular matrix and cell-cell contacts, therefore proving it was the removal of BMP4 that led to reactivation. AHNSCs reactivated without enzymatic dissociation from their culture plastic took longer to reactivate, which could be because BMP is sequestered by the ECM (Sedlmeier and Sleeman, 2017), causing BMP signalling to be maintained even after the cells are washed and cultured in only proliferation media. However, it could also be because disrupting cell adhesion and cell-cell signalling shuts down quiescence signals such as Notch, enabling a faster exit from quiescence. This highlights the importance of cell-cell contacts and adhesion in NSC regulation, and suggests the *in vitro* model is able to functionally recapitulate this regulation.

BMP4-induced quiescent AHNSCs were also able to very quickly reactivate and differentiate following 1month in the quiescent state (Figure 3.2). It could have been expected that the longer the cells were exposed to BMP4, the deeper the state of quiescence, perhaps due to epigenetic modifications, and therefore would take longer to reactivate after a month of BMP4 exposure compared to 3 days. This phenomenon has been observed in fibroblasts induced to quiescence by contact-inhibition (Kwon et

al., 2017). However, AHNSCs were able to reactivate as quickly after 1 month of BMP4 as 3 days (Figure 3.2). It is possible that AHNSCs need a longer exposure to BMP4 to induce epigenetic changes that affect the rate of reactivation. Alternatively, it is likely there are other factors in the cell culture medium that promote NSC activation, such as insulin, which could maintain BMP4-treated AHNSCs in a more readily activated state, even after long-term BMP4 exposure. It would be interesting to try and remove these factors from the media, or provide other pro-quiescence signals such as GABA (Song et al., 2012a), to test whether AHNSCs are harder to reactivate after long periods in a deep quiescence. This could potentially model the mechanisms that cause hippocampal RGLs to become more quiescent and difficult to activate with increasing age, providing insights into possible interventions for the age-related decline in neurogenesis.

6.1.2 Modulating extrinsic factors *in vitro* generates different NSC states

EGF and FGF2, as well as BMP4, actively regulate AHNSCs *in vitro*. Culturing the cells in the presence of EGF seemed to induce a more intermediate progenitor-like cell identity. It has not been reported that EGF signalling regulates RGLs in the dentate gyrus, however AHNSCs *in vitro* are capable of responding to EGF. It became apparent that removal of EGF from the media induced many transcriptional changes in AHNSCs that were previously assumed to be BMP4-specific. I therefore refined the model to eliminate EGF completely, and showed that 20ng/mL FGF2 alone was sufficient to maintain a self-renewing stem cell state. Modulating the levels of these factors can functionally affect the stem cells, and I have shown that titrating the concentration of BMP4 allowed us to induce different depths of quiescence in AHNSCs. By treating cells with 1ng/mL or 20ng/mL BMP4, we were able to induce a ‘shallow’ and ‘deep’ state of quiescence, respectively. RNA sequencing analysis of the transcriptional response of AHNSCs in shallow vs deep quiescence showed many more genes are regulated by high concentrations of BMP4, compared with low concentrations. This has implications for potentially modelling more accurately the physiological level of BMP4, as well as enabling a better understanding of the cross-regulation of BMP with other niche signals. Moreover, part of the heterogeneity of RGLs observed *in vivo* could be due to the cells receiving different levels of signals, including BMP, therefore titrating the concentrations of these factors *in vitro* could allow us to better understand the source of RGL heterogeneity.

6.1.3 BMP4-treated AHNSCs model multiple features of neural stem cell quiescence

Quiescence is more than a cell cycle state, rather characterised by specific energetic and metabolic profiles, as well as by the expression of a transcriptional 'signature' of quiescence (Beckervordersandforth et al., 2017; Bracko et al., 2012; Cheung and Rando, 2013; Codega et al., 2014; Morizur et al., 2018; Shin et al., 2015). Qualitative analysis of transcription and translation, as well as the pattern of mitochondria in active and quiescent AHNSCs, demonstrated the clear differences between the two states. The pattern of nascent protein synthesis in quiescent AHNSCs, as visualised by OPP staining, showed localisation to small puncta in the cytoplasmic processes (Figure 3.5D). This could suggest protein synthesis occurs in locally in quiescent NSC processes, which is reminiscent of the export and local translation of mRNA in the axons of neurons (Riccio, 2018), which highlights an interesting similarity between quiescent RGLs and post-mitotic neurons, and some aspects of their regulation could be shared. The mitochondria in quiescent AHNSCs were larger and more tubular than in active AHNSCs (Figure 3.5A), a difference which has been observed for RGLs and IPCs *in vivo* (Beckervordersandforth et al., 2017). The intensity of Pyronin Y staining was also lower in BMP4-treated compared to active AHNSCs (Figure 3.5B), potentially reflecting reduced transcriptional activity, which is suggested to be a feature of quiescent stem cells (Cheung and Rando, 2013). These qualitative measures support the notion that BMP4 can induce a state of quiescence in AHNSCs that is biologically similar to other quiescent stem cells and RGLs *in vivo*, therefore further supporting the use of this model to investigate the molecular regulation of adult hippocampal NSC quiescence.

Analysis of the transcriptional changes that occur in AHNSCs upon BMP4 treatment provided further evidence that multiple aspects of the quiescent state were acquired in these cells with BMP4. The ontologies of genes induced by BMP4 treatment highly reflected those identified in 'signatures' of quiescent neural stem cells, including "cell adhesion", "cell-cell signalling" and metabolism ontologies (Figure 3.6). Overlapping the top enriched genes in quiescent adult NSCs with BMP4-treated AHNSCs showed a high degree of overlap (Figure 3.6). These results strongly suggest that adult hippocampal-derived NSCs treated with BMP4 acquire a state of quiescence highly

representative of quiescent adult NSCs *in vivo*, suggesting that using this model to investigate the molecular regulation of quiescence will generate meaningful and biologically relevant results, expediting the costly and time-consuming *in vivo* analysis. Comparison of the transcriptional signatures in AHNSCs and NS5 NSCs demonstrated that there are many transcriptional differences between adult-derived NSCs and embryonic stem cell-derived NSCs (Figure 3.6), including the presence of the 'learning and memory' ontology (comprised of genes involved in adult neurogenic processes and diseases) exclusively in BMP4-treated AHNSCs, justifying the use of adult hippocampal-derived NSCs to specifically model adult hippocampal NSC quiescence.

An issue with this culture system was in determining whether the cells cultured *in vitro* were definitely neural stem cells, and not reactive astrocytes. The two populations would be very similar, both being astrocytic-like cells expressing GFAP and GLAST, with an ability to activate, self-renew and generate neuronal progenitors. Astrocytes have been shown to become mitotically active *in vivo* in conditions of inflammation or injury (Liddelow and Barres, 2017). Moreover, deriving cells from the DG or striatum and subsequently culturing them in the presence of BMP4 is a common protocol for culturing astrocytes *in vitro,* therefore it could not be immediately ruled out that the AHNSCs used here were in fact reactive astrocytes. However, the cells had impressive self-renewal properties, and the transcriptional profile of AHNSCs so closely resembled adult NSCs isolated from the hippocampus and SVZ, including absence of several known markers of adult astrocytes, that it strongly suggests the cells cultured here are neural stem cells. Moreover, maintaining FGF2 in the culture medium is known to inhibit the differentiation of NSCs into astrocytes (Sun et al., 2011), therefore the presence of FGF2 provides a culture condition more permissive for maintenance of neural stem cell identity. A full comparison of the transcriptomes of AHNSCs and prospectively isolated astrocytes would provide a stronger picture of whether AHNSCs are indeed true NSCs and distinct from reactive astrocytes.

6.1.4 Future uses of the *in vitro* model of AHNSC quiescence

Establishing a reliable and robust *in vitro* model of adult hippocampal NSC quiescence has opened up the possibility of investigating many aspects of the molecular regulation of NSC quiescence and activation. The model could be used in the future to investigate other signalling pathways either already implicated or novel in the regulation of NSC

quiescence. Delineating the mechanisms by which Wnt, Shh, and GABA regulate quiescence for example could generate highly interesting insights, particularly for understanding the cross-talk of these signals with BMP and each other. Moreover, the *in vitro* system allows for the generation of huge numbers of cells for a single experiment, therefore analyses which require large volumes of cellular material could be achieved using the culture system, such as investigating the epigenetic changes that occur in quiescence, or probing the protein-protein interactions by mass spectrometry. The culture system would also allow for relatively easy live cell imaging We are able to reproduce the *in vitro* model of quiescence using NSCs derived from transgenic reporter mice (such as the *Ascl1*^{KiGFP} and *Ascl1*^{Venus} mice reported here). This is especially advantageous, as these lines could be used to image endogenous transcriptional and protein dynamics, both of which have been shown in this thesis to be important for regulating NSC activity. Long-term culture of AHNSCs in the presence of BMP4 and other factors is possible, and could generate insights into the changes that occur in NSCs with age. There is also huge scope to further develop the model beyond a 2-D homogenous monolayer. Co-culture with other niche cells is a technique already widely used and would be easily applied to this *in vitro* system, to further investigate the mechanisms by which niche cells regulate NSC activity. RGLs are also a highly polarised cell type and this morphology has been linked to differential signal reception by different subcellular compartments (Urban and Guillemot, 2014). In other words, the characteristic morphology of RGLs may be required to receive distinct regulatory signals, and may result in asymmetric distribution of signalling components which could have functional consequences for quiescence and activation (Urban and Guillemot, 2014). It would therefore be very interesting to test whether the polarised morphology of RGLs can be recapitulated *in vivo*, by utilising cell culture substrates micro-patterned with factors that promote polarised morphology, or 3-dimensional culture systems, both of which have been used for other stem cells in culture (Griessinger et al., 2014; Joo et al., 2015; McKee and Chaudhry, 2017). Finally, the hypothesis that RGLs exist in either a resting or dormant quiescent state (Urban et al., 2016) has raised the intriguing question as to what mechanisms dictate the difference between these two states. Dormant RGLs are difficult to identify *in vivo*, due to the fact identification relies on absence of proliferation markers in EdU-retention assays. By definition, dormant NSCs are those that have never activated, therefore the current culture system of AHNSC quiescence presented in this thesis very likely represents the resting state of RGLs, and cannot model the dormant state. Despite this limitation, the

in vitro system of adult hippocampal neural stem cell quiescence presented here can enable the investigation of molecular mechanisms regulating multiple aspects of hippocampal NSC biology, providing an invaluable tool to complement more complex and time consuming *in vivo* analysis.

6.2 The unexpected expression of *Ascl1* in quiescent RGLs

6.2.1 Ascl1 mRNA is expressed in quiescent NSCs, but suppressed at the protein level

The *Ascl1*^{KiGFP} mouse line was originally used to investigate the transcriptional regulation of *Ascl1* in SGZ RGLs *in vivo*, but led to the surprising discovery that *Ascl1* may be expressed in more than 80% of RGLs in the adult mouse DG (Figure 4.1). Considering only around 8% of RGLs are proliferating at any given time (Andersen et al., 2014; Urban et al., 2016), this suggested that many quiescent RGLs express *Ascl1*, and was confirmed by combination *in situ* hybridisation of *Ascl1* and *Ki67* with immunocytochemistry for RGL markers. This was surprising both because Ascl1 is an activation factor, and also because Ascl1 protein was only detected in a tiny fraction of RGLs (Figure 4.1), suggesting Ascl1 is post-transcriptionally suppressed in quiescent hippocampal NSCs. The *in vitro* model of AHNSC quiescence similarly showed *Ascl1* expression in BMP4-indcued quiescence but suppressed levels of Ascl1 protein, again confirming the *in vitro* system can closely model *in vivo* RGL quiescence (Figure 4.2). By utilising the model, we were able to show that Ascl1 protein is indeed expressed in quiescent conditions, but rapidly degraded in a proteasomal-dependent manner (Figure 4.3), suggesting a quiescence factor actively inhibits Ascl1 at the protein level in quiescent NSCs.

An interesting observation was that the range of intensities for nuclear GFP in quiescent RGLS in the *Ascl1*^{KiGFP} mice was far greater than for active RGLs (Figure 4.1). The RGLs with high GFP intensity could reflect a peak of *Ascl1* transcription, prior to Ascl1 translation and activation, thereby identifying RGLs that may be close to activation, or would activate if the inhibitory factor regulating Ascl1 protein is simultaneously repressed. The range in GFP intensities might also reflect oscillations of *Ascl1* transcription. Oscillatory expression has been observed for Ascl1, Hes1 and Olig2 in embryonic NSCs (Imayoshi et al., 2013) therefore Ascl1 expression might also

oscillate in RGLs to dynamically regulate RGL activation. Live imaging of hippocampal stem cells *in vivo* expressing GFP reporters has been recently achieved (Pilz et al., 2018), therefore it might be possible to live-image RGLs in *Ascl1*^{KiGFP} mice, to observe in real-time whether Ascl1 transcription oscillates, and whether peaks of transcription corresponds to stem cell activation. A limitation of the *Ascl1*^{KiGFP} reporter is that the GFP may not have the same protein dynamics as *Ascl1* mRNA, and so may not be a true readout of *Ascl1* transcriptional dynamics.

The Notch target genes Hes1 and Hes5 are known transcriptional repressors of Ascl1. Both Hes genes are expressed in hippocampal NSCs (Ehm et al., 2010; Lugert et al., 2010) therefore it would be predicted that they inhibit Ascl1 transcription in RGLs. However, the fact that I observed *Ascl1* mRNA in most RGLs analysed (Figure 4.1) indicates that Hes proteins do not fully repress transcription of *Ascl1* in these cells. However, *Ascl1* expression is strongly enhanced when the Notch effector *gene* RBPJk is deleted (Figure 5.4D), suggesting that the Notch-RBPJk-Hes pathway partially represses *Ascl1* and maintains *Ascl1* expression at low levels. Therefore, there appears to be a multi-level regulation of Ascl1 in RGLs, both transcriptionally and translationally, reflecting the importance of regulating Ascl1 and RGL activation. This is logical, as aberrant activation would result in fast exhaustion of the stem cell pool, as observed in mice with conditional deletion of RBPJk in RGLs (Ehm et al., 2010).

As described in Section 4.4.3, detecting Ascl1 protein in adult mouse tissue by monoclonal antibody immunostaining is challenging, and can be very easily affected by tissue fixation. The expression of Ascl1Venus fusion protein in RGLs of the *Ascl1*^{Venus} transgenic mouse line indicates that more RGLs express Ascl1 protein than are detected by immunostaining (Figure 4.1B,C). It would be worth investigating whether different fixation techniques could improve monoclonal antibody detection of Ascl1, such as using a lower percentage PFA for perfusions, or by post-fixing tissue sections from flash-frozen fresh brain samples. The latter would allow for very precise fixation conditions, which could enable us to identify the ideal fixation conditions for Ascl1 immunodetection. We could also utilise the *Ascl1*^{Venus} transgenic mouse line more frequently, however the fusion protein might not always behave exactly like endogenous Ascl1, therefore improving Ascl1 immunodetection would be the ideal course of action.

Overall, these results strongly suggested the existence of a post-translational regulator of Ascl1 expressed in quiescent NSCs. Huwe1 is an E3-ubiquitin ligase which had already been identified and characterised by our lab to be a post-translational regulator of Ascl1 in SGZ RGLs *in vivo* (Urban et al., 2016). However, Huwe1 did not appear to be required to maintain RGL quiescence *in vivo* (Urban et al., 2016) therefore we hypothesised an alternative post-translational mechanism regulates Ascl1 in quiescent RGLs or BMP4-treated AHNSCs. To confirm that Huwe1 was dispensable for BMP4-mediated repression of Ascl1 protein levels, I conditionally deleted Huwe1 in AHNSCs derived from Huwe1flx mice. In the absence of Huwe1, BMP4 treatment was still able to suppress Ascl1 protein levels, detected by immunostaining (Figure 4.4). This experiment requires repeating and further confirmation of loss of Huwe1 protein and Ascl1 protein levels by Western blot analysis. However, the results complement the *in vivo* data that Huwe1 prevents active RGLs from returning to quiescence, but does not result in the activation of quiescent RGLs (Urban et al., 2016), implying that a second, Huwe1-independent mechanism negatively regulates Ascl1 protein stability in quiescent NSCs.

These data imply that rather than being in a state of cellular ‘shut-down’, quiescent RGLs are in fact actively transcribing and translating, and poised to activate. This is supported by the report that quiescent RGLs express many different cell-signalling components, suggesting they are receiving and actively processing multiple cues from the niche (Shin et al., 2015). By actively transcribing and translating an activation factor, RGLs only require the inhibition of one factor, the post-translational regulator inhibiting Ascl1 protein, in order to leave quiescence. Suppression of said protein could be achieved rapidly by phosphorylation for example, targeting it for degradation. This dynamic state may represent the ‘resting’ state of RGLs, which are quiescent but with a high propensity to activate quickly (Urban et al., 2016). It would be interesting to see whether the dormant population of RGLs do not actively transcribe or translate Ascl1 protein, which could explain their dormancy despite inhabiting the same niche environment – therefore potentially receiving similar activating cues – as resting RGLs. Alternatively, dormancy could be a result of stabilising the inhibitor of Ascl1. Factors involved in dynamic regulatory networks often have short half-lives, to facilitate rapid modulation of the network. This is true of Ascl1 which has a reported half-life of around 30 minutes in embryonic NSCs (Gillotin et al., 2018; Urban et al., 2016). In this thesis, I have presented Id4 as the candidate for regulating Ascl1 protein in quiescent RGLs,

and in support of the hypothesis that this regulatory network consists of dynamically regulated proteins with short half-lives, Id4 has also been reported to have a short half-life of around 1 hour (in 3T3-L1 cells) and be degraded following ubiquitination (Bounpheng et al., 1999). Interestingly, Id4 has been shown to be less sensitive compared to the other Id proteins to proteasomal degradation (Bounpheng et al., 1999), suggesting it is uniquely regulated at the protein level. It would be intriguing to identify dormant and resting RGLs using an EdU retention assay, and use *in situ* hybridisation to determine whether there is a difference in Ascl1 mRNA levels between dormant and resting cells. Moreover, it would be interesting to measure the stability of Id4 in dormant vs resting cells. However, this would be far more challenging as it would require either live imaging of Id4 expression dynamics in these cells, or prospective isolation of dormant RGLs. Specific isolation of dormant and resting RGLs has so far not been attempted, however it could be possible by use of a *Ki67Cre^{ERT2};tdTomato* transgenic mouse line. Inducing recombination in these mice would enable labelling of resting RGLs with tdTomato, while dormant RGLs could be isolated based on their negativity for tdTomato in combination with the GFP/YFP reporter expression of GFAP or GLAST. Once isolated, Ascl1 mRNA expression could be measured, and it might be possible to analyse the protein stability of Id4, by culturing cells in the presence of the protein synthesis inhibitor cycloheximide, or by Western blot analysis of Id4 ubiquitination.

6.3 Identification of Id4 as a candidate for regulating Ascl1 protein in quiescence

6.3.1 Id4 is a marker of quiescent RGLs

Analysis of protein expression *in vivo* showed that Id4 is highly expressed in RGLs in the DG, and co-staining with Ki67 showed Id4 is enriched in quiescent RGLs (Figure 4.5). In contrast, Id1 was shown to have higher expression in active (Ki67+) RGLs. The difference between Id1 and Id4 expression suggests an interesting dichotomy in the function of these two Ids. Id1 is perhaps functioning as a more classical Id protein, promoting stem cell self-renewal, as in embryonic stem cells (Romero-Lanman et al., 2012). This is contrast however to the reported role for Id1 in promoting quiescence of SVZ NSCs (Niola et al., 2012), which could either reflect a context-dependent function for Id1, or differences in the regulation of NSCs between the SVZ and SGZ. Id4 is the

most diverged Id protein at the sequence level (Figure 1.7), and could therefore regulate SGZ RGLs differently to Id1. Id3 is also expressed in the DG, albeit in few cells, however it would be interesting to fully characterise and quantify Id3 expression, especially in combination with Ascl1 and proliferation markers, to determine if it is enriched in active RGLs, as was shown by Bonaguidi and colleagues (Bonaguidi et al., 2008). This would be particularly useful in light of the upregulation of Id3 in the DG following conditional Id4 deletion (discussed further below in Section 6.3.3.2). It would also be interesting to immunostain combinations of Id proteins, to determine if there is co-expression; unfortunately, the antibodies against Id proteins used here are all raised in rabbit, preventing co-immunostaining.

6.3.2 Id4:E47 interaction is observed in quiescent AHNSCs

Based on the reports in the literature that Id proteins inhibit bHLH proteins predominantly indirectly by interacting with E-proteins (Duncan et al., 1992), I checked to see whether E-proteins were expressed in SGZ RGLs *in vivo* and AHNSCs *in vitro*. Our RNA sequencing data from active and quiescent AHNSCs showed that *tcf3*, *tcf4* and *tcf12*, the genes encoding E2A, E2-2 and HEB respectively, were all expressed in both conditions (Figure 4.7). Western blot analysis for E47 (splice variant of E2A) confirmed the expression of the protein in both active and quiescent AHNSCs. Western blots for the other E-proteins were attempted, however we did not manage to find reliable antibodies to detect them. The E47 antibody, whilst sufficient for Western blot detection of the protein, does not work for immunocytochemistry, therefore I was unable to confirm the expression of E47 in RGLs in the adult DG. However, the publically available single cell RNAseq datasets of adult mouse dentate gyrus generated by the Linnarsson lab (linnarssonlab.org/dentate/) shows the expression of all three *tcf* genes in subsets of RGLs. This is promising evidence that Id4 and E-proteins could interact in RGLs, mediating the inhibition of Ascl1 protein. We also demonstrated in BMP4-induced quiescent AHNSCs *in vitro* by co-immunoprecipitation (Co-IP), that Id4 and E47 do indeed physically interact in the quiescent state (Figure 4.7C), therefore potentially preventing binding of E47 and Ascl1, causing Ascl1 to be unable to bind its target DNA and ultimately targeted for degradation. Id4 is expressed at a low level in active AHNSCs, so might be expected to also interact with E47 in this condition, however no interaction was detected. Whilst this cannot confirm the two proteins do not interact in active AHNSCs, it may indicate that the relative levels and

stoichiometry of Id4, E47 and Ascl1 are important for dictating the balance of interactions. The levels of Id4 in active AHNSCs may be too low to sequester E47 from Ascl1.

An unexpected interaction was observed between Ascl1 (GFP/Ascl1Venus) and E47 in BMP4-induced quiescent conditions. Our hypothesis suggests BMP4-induced Id4 protein levels should be high enough to block all Ascl1:E47 interaction in BMP4 conditions, thus resulting in Ascl1 protein degradation and maintenance of quiescence. However, although Ascl1 protein is strongly suppressed in the presence of BMP4, it is not completely absent. Similarly, BMP4-treated AHNSCs still proliferate at a low frequency, which could be a result of residual and possibly functional levels of Ascl1 protein in BMP4 conditions. We could test this hypothesis, by knocking down Ascl1 in quiescent AHNSCs, and examining whether further reduction of Ascl1 results in a further reduction in proliferation. If so, a small amount of Ascl1:E47 interaction could be expected to be detected in quiescent conditions.

Perhaps the Ascl1 protein detected in quiescent conditions is non-functional, and despite some level of interaction with E47, is still targeted for degradation. It has been recently demonstrated that long poly-ubiquitin chains can be detected on Ascl1 when it is targeted for E3-ubiquitin ligase mediated degradation, whilst short ubiquitin chains are observed when it is in the nucleus bound to chromatin and not degraded (Gillotin et al., 2018). Analysis of the poly-ubiquitin chains on Ascl1 by Western blot in quiescent AHNSCs could reveal whether the low levels of Ascl1 protein are in fact non-functional and on their way to be degraded.

The observed interaction between Ascl1 and E47 could also be an artefact created by the Ascl1Venus fusion protein. We utilised the *Ascl1*^{Venus} stem cell line, as the monoclonal antibody against Ascl1 was not sensitive enough to sufficiently pull down or detect Ascl1 in the Co-IPs, unlike the much more sensitive anti-GFP antibody which detects the Ascl1Venus (GFP) fusion protein. In spite of the report that the expression of the reporter is similar to endogenous Ascl1 during development (Imayoshi et al., 2013), it is possible that the fusion protein affects the endogenous binding properties of Ascl1, creating stronger Ascl1:E47 interactions which Id4 cannot overcome. The levels of endogenous Ascl1 in non-transgenic AHNSCs could be boosted by treatment with the proteasome inhibitor MG132, enabling detection using the monoclonal antibody

and avoiding the need to use *Ascl1*^{Venus} AHNSCs. However, blocking the proteasome would also increase the levels of the Id and E-proteins as well, which could affect the relative levels of these players, causing them to interact in a different way than they would at endogenous levels in quiescent AHNSCs.

These limitations of Co-IP analysis of protein-protein interactions in AHNSCs is in addition to the fact it is not a quantitative measure; we cannot know whether there is more Id4:E47 than Ascl1:E47 in quiescent conditions, we can only know if the interaction is detected. Therefore, the much more sensitive and unbiased analysis by mass spectrometry could be necessary, and certainly highly informative, to identify and quantitatively measure the relative levels of interaction between the Id proteins, E-proteins and Ascl1 in AHNSCs.

6.3.3 The function of Id4 in adult hippocampal NSCs

6.3.3.1 Id4 induces cell cycle exit, Ascl1 protein degradation and subsequent inhibition of Ascl1 target genes in vitro

The *in vitro* model of AHNSC quiescence has proved highly useful in testing the function of Id4. Overexpression of Id4 from a pCbeta-Id4-FLAG construct in active AHNSCs was able to suppress the cell cycle and Ascl1 protein levels (Figure 4.8), suggesting Id4 is sufficient to induce quiescence, and inhibit Ascl1 protein. Moreover, the inhibition of Ascl1 protein by Id4 overexpression led to a decrease in Ascl1 target gene expression, confirming the inhibition of Ascl1 function (Figure 4.9). It would be useful to further confirm that Id4 causes increased protein degradation of Ascl1 by testing the half-life of Ascl1 in Id4-overexpressing vs control AHNSCs. Moreover, we could directly test whether Id4-induced quiescence is dependent on Ascl1 degradation, by overexpressing stabilised Ascl1 along with Id4. Similarly, the hypothesis that Id4 mediates Ascl1 degradation by sequestering its E-protein binding partners could be directly tested by seeing whether overexpression of E47 can rescue the effects of Id4 overexpression. This was technically already achieved by overexpression of E47 in BMP4-treated AHNSCs (discussed below), however there is the possibility that BMP4 induces other factors involved in the inhibition of Ascl1:E47, therefore directly overexpressing Id4 and E47 in active AHNSCs would rule out the effects of other BMP4 targets.

Our *in vitro* overexpression experiments also revealed that Id4 regulates a significant proportion of the BMP4-induced quiescence transcriptional profile, suggesting Id4 is a major effector of BMP4-induced quiescence (Figure 4.9). This was in stark contrast to the effects of Id1 overexpression, which regulated only a fraction of the genes induced by BMP4 (Figure 4.11). Interestingly, overexpression of Id1 was sufficient to partially suppress the cell cycle of active AHNSCs, to a similar extent as Id4 over-expression. However, in contrast to Id4, Id1 overexpression did not strongly affect Ascl1 protein or function, as measured by Ascl1 target gene expression. Id1 is required to maintain quiescence of SVZ NSCs by promoting adherence to the niche (Niola et al., 2012), therefore high expression levels of Id1 in AHNSCs could promote quiescence. One caveat for the direct comparison of the genes regulated by Id1 vs Id4-overexpression is that the two Ids were overexpressed from different plasmid backbones. Expression of genes in different plasmid backbones can be quite different, therefore the differences observed between Id1 and Id4 overexpression could simply be a result of different levels of overexpression.

Nevertheless, Id4 is able to partially induce quiescence of AHNSCs. This is very similar to another transcription factor identified by our group to regulate quiescence of embryonic-stem cell derived NSCs, NFIX (Martynoga et al., 2013). Both NFIX and Id4 are able to regulate a similar proportion of the genes induced by BMP4, therefore it would be interesting to compare the genes regulated by each factor, to see if they regulate common or independent aspects of NSC quiescence.

In order to inactivate Id4 protein activity, I overexpressed E47 in BMP4-treated AHNSCs, providing the binding partner of Ascl1 in excess of Id proteins, which resulted in re-stabilisation of Ascl1 protein, subsequent activation of Ascl1 target genes, and increased proliferation of BMP4-treated AHNSCs (Figure 4.12-13). This result indicates that Id4 induces quiescence via destabilisation of Ascl1 protein, by sequestering its E-protein binding partner and rendering it unable to bind DNA and targeted for degradation. A potential problem with using E47 specifically to inactive Id4, as opposed to other E-proteins, is that E47 preferentially homodimerises (Sharma et al., 2015), which means overexpression would very likely result in activation of E47 target genes in addition to heterodimerising with Ascl1. This may explain the very high number of genes regulated by E47 overexpression observed in the RNA sequencing data (Figure

4.13). Nevertheless, overexpressing E47 was still able to counteract the inhibition of Ascl1 by BMP4/Id4.

A more direct examination of the function of Id4 in BMP4-induced quiescence would be direct knockdown. We attempted this by deriving an adult hippocampal stem cell line from the Id4flx mice, in order to acutely delete Id4 in BMP4 conditions. However, Id4 had become genetically silenced during the derivation process, resulting in a Id4 null cell line. Id4 null AHNSCs were still able to be induced into quiescence by BMP4 (Figure 4.14), suggesting the other Ids (or other factors) could also mediate BMP4-induced cell cycle exit. Interestingly, Ascl1 protein levels were higher in Id4 null AHNSCs compared to non-transgenic AHSNCs, and Ascl1 protein was maintained at this high level even in the presence of BMP4 (Figure 4.14). This suggests a unique role for Id4 in mediating Ascl1 protein degradation, as well as raising the possibility that Id1-3 could block the activity of Ascl1, thereby inducing quiescence, without affecting its protein stability.

The effect of overexpressing Id1 in AHNSCs has raised the question of whether the other Id proteins can also regulate Ascl1 stability and quiescence, especially in light of the fact all the Id proteins are expressed in BMP4-treated AHNSCs. Therefore, overexpression of Id2 and Id3 in active AHNSCs would be a worthwhile experiment, followed by measurement of Ascl1 protein levels and stability, as well as cell proliferation rates and RNAseq to generate a full picture of Id-protein regulation of NSC quiescence.

6.3.3.2 The function of Id4 in adult hippocampal RGLs in vivo

The combination of the expression pattern of Id4 *in vivo*, along with the functional *in vitro* experiments, strongly suggested Id4 has a unique function in regulating quiescence of RGLs in the adult mouse DG, specifically by negatively regulating Ascl1 protein levels. I directly tested this by conditionally deleting Id4 in RGLs in the adult mouse hippocampus, via Cre-mediated recombination of the floxed exons 1 and 2 of the Id4 alleles in GLAST-expressing stem cells. Acute deletion resulted in a modest increase in the fraction of RGLs positive for Ascl1 protein and cell cycle marker Ki67, as well as increased Ascl1 protein levels across all RGLs (Figure 4.15), indicating Id4 functions to suppress Ascl1 protein levels and maintain quiescence of adult

hippocampal neural stem cells. However, it was curious that the observed effect of Id4 deletion was not bigger, considering its strong and widespread expression in quiescent RGLs. One possible explanation could be due to the limitations of the Ascl1 monoclonal antibody, as I discussed in Section 6.2.2., meaning it may have not been detecting all of the Ascl1 protein expressed by the RGLs *in vivo*. However, an argument against this hypothesis is the concurrently modest increase in Ki67. Presumably increased expression of Ascl1 would induce activation of RGLs and entry into the cell cycle, directly resulting in Ki67 expression. Therefore, if Id4 deletion resulted in greater de-repression of Ascl1 than observed because I was under-detecting Ascl1, I should still observe a bigger fraction of proliferating RGLs. Alternatively, increased levels of Ascl1 protein in quiescent RGLs may not directly result in cell cycle entry and Ki67 expression. One way to distinguish this would be to co-immunostain Ascl1 and Ki67 in the DG of $Id4^{cKO}$ mice; if co-expression is observed, we can conclude that the effect of loss of Id4 on Ascl1 protein levels and RGL quiescence is in fact modest.

An alternative and perhaps more likely explanation, is that redundancy exists between the other Id proteins and Id4, resulting in compensation by the other Ids following Id4 deletion. The enrichment of Id1 in active RGLs *in vivo* would not immediately implicate it as a compensatory factor for Id4, and the functional investigation of Id1 *in vitro* suggests this Id protein may not strongly suppress Ascl1 protein levels. Id1 has also recently been shown to have a role in the activation of hematopoietic stem cells upon stress signals (Singh et al., 2018). However, when over-expressed at high levels in AHNSCs *in vitro*, Id1 was able to repress the cell cycle. Moreover, Id1 protein levels were highly increased in RGLs immediately following Id4 deletion (Figure 4.15). It is plausible that in the context of higher-than-normal expression levels, Id1 function shifts to suppress the cell cycle, and could therefore mediate a possible compensatory effect for Id4 deletion. Id3 protein levels are also dramatically increased following acute Id4 deletion (Figure 4.15). I had not examined which cell types express Id3 in normal conditions, so I therefore do not know whether Id3 is more enriched in quiescent or active RGLs, nor had I tested the function of Id3 in AHNSCs *in vitro*. However, much like Id1, higher-than-basal levels of Id3 protein may confer a redundancy with Id4 function, providing another possible explanation for why the effect of Id4 deletion is not more severe. The upregulation of Id1 and Id3 following Id4 deletion is in itself a fascinating result, suggesting another function of Id4 is to actively repress the other Id

proteins (I did not check Id2 protein levels in RGLs in *Id4*^{cKO} mice) something which has been observed at the mRNA level for *Id1*, *Id2* and *Id3* in the telencephalon of Id4null embryos (Yun et al., 2004). Repression of Id1-3 by Id4 has also been suggested by a study which overexpressed recombinant Id1-4 in lung cancer cells; the authors showed Id4 can physically interact with Id1-3, and has a higher affinity for Id1 than E47, meaning Id4 blocks the inhibition of E-proteins by Id1-3 (Sharma et al., 2015). It is not clear whether physical interaction between Id4 and the other Ids could result in suppression of their protein levels, but possible mechanisms include Id4 sequestering the E-proteins from the other Ids, preventing E-protein-mediated stabilisation of Id1-3 (Lingbeck et al., 2005), thereby exposing Id1-3 to cytoplasmic E3 ubiquitin ligases, which target them for degradation.

Due to the difficulties in obtaining enough *Id4*^{cKO} mice 30days post-tamoxifen and good quality Ascl1 immunostaining (discussed in Sections 4.4.1, 4.4.3 and 6.2.2), data is lacking to determine the long-term effects of Id4 deletion in *Id4*^{cKO} mice. The fraction of YFP+Ki67+ RGLs is still mildly increased 30days post-tamoxifen, but the difference is only significant compared to *Id4*$^{fl/fl}$ mice that were not injected with tamoxifen (*control**), whereas the difference between tamoxifen-injected *Id4*^{cKO} and *Id4*$^{wt/wt}$ (*control*) mice was not significant (Figure 4.16). As discussed above, the other Id proteins may compensate for Id4 in *Id4*^{cKO} mice, resulting in loss of the phenotype by P90. It will be very interesting to see whether Ascl1 protein levels are still significantly increased at P90 in *Id4*^{cKO} mice, despite the proliferation rates returning to control levels (Figure 4.16). It is possible that the suppression of Ascl1 protein is a unique function of Id4, so while Id1 and Id3 - which are still highly upregulated at P90 in *Id4*^{cKO} mice – could compensate for maintaining RGL quiescence, they cannot fully suppress Ascl1 protein levels. Rather, they may directly inhibit cell cycle progression, or perhaps could interfere with DNA binding of Ascl1, thereby blocking its transcriptional activity without affecting its protein stability. This mechanism is plausible, based on the observation discussed above that Id4 null AHNSCs can be induced into quiescence by BMP4, despite the lack of Id4 and high Ascl1 protein levels. It would be very interesting in the future to conditionally delete Id4 along with Id1 and/or Id3 in SGZ RGLs, to determine whether these other Ids can functionally compensate for Id4.

A thorough examination of the fate of *Id4*^{cKO} RGLs would also be useful, in determining the broader function of Id4 in SGZ neurogenesis. For example, do *Id4*^{cKO} RGLs

become exhausted? Quantification of the total numbers of RGLs at P90 or later should be carried out to answer this question. Is neurogenesis increased, with respect to the number of newborn neurons, in *Id4*^{cKO} mice? My thesis research focussed on the regulation of stem cell quiescence, therefore I did not investigate broader neurogenesis, however it would be interesting to discover whether Id4 could mediate neurogenic stimuli. Alternatively, perhaps *Id4*^{cKO} RGLs are differentiating into oligodendrocytes? Id4 deletion increases the levels of Ascl1 in RGLs, and Ascl1 overexpression in RGLs has been shown to induce oligodendrocytic differentiation, despite RGLs generating only neuronal precursors in basal conditions (Jessberger and Gage, 2008). Therefore, staining for oligodendrocyte precursor markers would be useful to determine whether Id4 is required to maintain neuronal fate of RGLs.

The modest effect of Id4 deletion could reflect a role for Id4 beyond maintaining RGL quiescence in homeostasis. Id4 might also function downstream of neurogenic stimuli, regulating RGL quiescence in response to environmental inputs or injury. This could be investigated by testing *Id4*^{cKO} mice with a neurogenic stimulus, such as exercise or kainic acid-induced mild seizures. The absence of Id4 may result in much greater levels of activation upon stimulation in *Id4*^{cKO} mice compared to control mice, revealing Id4 as a brake to prevent RGL over-stimulation. This is a plausible hypothesis, considering the reported role for Id4 as a tumour suppressor including in glioblastoma (Martini et al., 2013).

The Notch target genes, Hes1 and Hes5, are bHLH transcription factors with roles in neural stem cell maintenance and differentiation, and as bHLH factors they are can also be regulated by Id proteins. Hes proteins auto-repress their own expression, by binding to their own promoters, and Id proteins can inhibit this auto-repression when expressed at low levels, by binding the HLH domain of Hes proteins, reducing their capacity to bind DNA. Id4 therefore may play a dual role in maintaining RGL quiescence, firstly by partially stabilising Hes protein expression and thereby maintain a mild repression of *Ascl1* transcription, and secondly by sequestering the E-protein binding partners of Ascl1, causing the remaining low levels of Ascl1 to be degraded.

Having begun collaborative experiments with our colleagues at the ICM in Paris, using the Id4flx mice, I discovered that the transgene containing the floxed Id4 allele also contained a GFP reporter construct, outside of the loxP sites (structure of the

transgene is shown in Figure 4.14A). We realised this could cause a major issue for our analysis, due to the fact we use a YFP reporter of Cre-mediated recombination. Immunostaining for YFP would also detect the GFP induced by Id4 expression, which would still be active following recombination (unless Id4 protein is necessary for its own expression), as the loxP sites surround exons 1 and 2, but not the Id4 promoter. However, we reasoned that the complete ablation of Id4 observed by immunostaining following tamoxifen administration in *Id4*^{cKO} mice (Figure 4.14B) would mean that all GFP+RGLs analysed, whether Id4GFP+ or Rosa26YFP+, would all lack Id4 protein, therefore could be included in our analysis. To further verify that Id4 ablation was definitely comprehensive enough to justify continuing to analyse these mice, I checked Id4 immunostaining in *Id4*^{cKO} mice 30 days post-tamoxifen, and did not observe any Id4+GFP+ cells, although I did not quantify this. This is important to quantify if lineage tracing experiments were to be carried out, for example, as this relies on identification of recombined cells that would not necessarily express Id4 anymore, therefore there would be no way to be sure whether Id4 was deleted in the first place. For future experiments, it would be better to cross the Id4flx mice to a strain harbouring a reporter of recombination in a different fluorophore than GFP; for example, our lab is currently breeding GlastCre^{ERT2};Id4flx;tdtomato mice, ensuring recombined cells (tdTomato+) can be differentiated from Id4 expressing-GFP+ cells.

6.4 Hippocampal niche signals other than canonical BMP and Notch regulate Id4 expression

Many lines of evidence pointed to induction of Id4 in RGLs by BMP signalling in the DG. There is literature evidence for BMP-induced Id4 expression in neural progenitor cells, in addition to the powerful induction of Id4 by BMP4 in the *in vitro* model of AHNSC quiescence presented here, as well as the reported increase in BMP signalling in the DG with age and concurrent increase in RGL quiescence. If Id4 is a direct target of BMP signalling in the hippocampal niche, Id4 could be responsible for mediating the age-related increase in BMP and decline in RGL activity (Yousef et al., 2015b). However, we were surprised to observe no decrease in Id4 expression following conditional Smad4 deletion, and in fact a slight increase in protein levels (Figure 4.20). Deletion of Smad4 was sufficient to strongly reduce the expression of Id1 in SGZ RGLs, indicating the Smad4 was definitely ablated, and that it is functional in RGLs.

Interestingly, RGLs did not activate following Smad4 deletion, further highlighting the observation that Id1 does not maintain quiescence of RGLs, in contrast to Id4. A possible explanation for the lack of effect on Id4 is that BMP signalling does induce Id4, but in a Smad-independent mechanism. In my introduction, I described the different studies which have identified Smad-independent BMP signalling, such as by BMP-induced p38/MAPK signalling (Section 1.5.2.9). Alternatively, Smad4 deletion may be compensated by the expression of a cofactor, such as Trim33. Redundancy of Smad4 by Trim33/Tif1γ has been observed in the developing forebrain (Falk et al., 2014).

The preliminary *in vitro* data generated from the neural stem cell line derived from Smad4flx mice, corroborated the results observed *in vivo* (Figure 4.21). Loss of Smad4 in BMP4-induced quiescent AHNSCs led to a reduction in Id1 and Id3 protein levels, but did not affect Id4 protein expression, suggesting Id4 is induced by alternative pathways more strongly than Smad4-mediated induction. It would be interesting to examine the levels of Id3 in *Smad4*^{cKO} mice, to see whether it is similarly regulated by Smad4 *in vivo* as *in vitro*.

Notch signalling was another promising candidate to regulate Id4 expression in the DG. Notch has been shown to induce the expression of Id proteins in embryonic stem cells (Meier-Stiegen et al., 2010), and is required to maintain quiescence of SGZ NSCs (as described in Section 1.5.2.2). However, similar to Smad4, inhibition of Notch signalling by the conditional ablation of the transducer RBPJk in RGLs only very mildly reduced Id4 protein levels, but not significantly (Figure 5.4). Id1, however, was strongly induced following RBPJk deletion, raising the possibility that Notch maintains quiescence by suppressing Id1 expression. This suggests Id1 expression is important for stem cell self-renewal, a function which has already been observed for Id1 in embryonic stem cells and mammary stem cells (Romero-Lanman et al., 2012; Shin et al., 2015). This hypothesis also complements the observation that Id1 is enriched in active RGLs (Figure 4.5F). Alternatively, the increase in Id1 expression could be an indirect result of the increase in Ascl1 expression in *RBPJk*^{cKO} mice; Id1 has been shown to be a transcriptional target of Ascl1 in the embryonic telencephalon (Castro et al., 2011), therefore upregulation of Ascl1 could result in a concurrent upregulation of Id1 and subsequent proliferation of RGLs.

Considering neither BMP/Smad4 nor Notch/RBPJk signalling alone was necessary to induce Id4 expression, it was highly plausible that both signals redundantly induce Id4 *in vivo*, therefore compensate for each other in the single conditional mutants. However, conditional deletion of both pathways in RGLs still did not affect Id4 levels, with the observed increase in Ascl1 protein and RGL proliferation likely a primary effect of RBPJk deletion (Figure 5.5).

Overall, there is still much to be discovered regarding the regulation of Id4 by the hippocampal niche. As I have mentioned, non-canonical BMP signalling may be responsible, which would explain the strong induction of Id4 by BMP4 *in vitro*, even in the absence of Smad4. Investigating the effects of manipulating p38/MAPK, ERK1/2, JNK or Pi3k/Akt signalling either *in vivo*, or in AHNSCs *in vitro*, could shed some light on the transcriptional regulation of Id4.

6.5 Crosstalk between BMP and Notch signalling

Both BMP and Notch signalling maintain RGL quiescence in the adult DG (Ables et al., 2010; Ehm et al., 2010; Mira et al., 2010) therefore there could be a degree of crosstalk between the two pathways, something that has been reported to occur in other contexts (Kluppel and Wrana, 2005). I was very interested to explore further the coordination between Notch and BMP4 signalling in the regulation of hippocampal NSCs *in vitro*, as well as to determine more precisely whether Notch signalling regulates Id4 in BMP4-induced quiescence. I therefore inhibited Notch signalling at the level of the receptors using a gamma-secretase inhibitor, in active, ‘shallow’ quiescent (1ng/mL BMP4) and ‘deep’ quiescent (20ng/mL BMP4) AHNSCs. I chose to investigate the role of Notch in both ‘depths’ of quiescence, because Notch is highly context dependent, therefore the interaction with BMP signalling may vary depending on BMP concentration. This was certainly the case, as shown by the expression of *Hes5*; while being strongly suppressed in active and shallow quiescent AHNSCs following Notch inhibition, *Hes5* expression was maintained in deep quiescent AHNSCs the absence of Notch (Figure 5.2B). This result indicates BMP4 is able to induce some canonical target genes of Notch. One could speculate that in the hippocampal niche, stem cells could become refractory to the regulation of Notch signalling, if they receive high levels of BMP signalling. In the aged hippocampus, RGLs are less active, and BMP signalling is higher (Yousef et al., 2015b); perhaps BMP signalling in the aged DG is dominant

over Notch signalling. Notch signalling is dynamically regulated in RGLs of the DG, via cell-cell signalling with IPCs and astrocytes. Perhaps RGLs receiving higher levels of BMP signalling are less able to activate because dynamically regulated Notch target genes that induce quiescence are instead stably induced by BMP. The oscillatory versus stable expression dynamics of Ascl1, Hes1 and Olig2 are known to regulate self-renewal versus differentiation of NPCs in the embryonic mouse (Imayoshi et al., 2013). The difference between Notch-induced and BMP4-induced *Hes5* expression could be the difference between oscillatory and stable expression, therefore determining whether a stem cell self-renews or becomes more deeply quiescent, or differentiates. BMP4-induced quiescent AHNSCs did in fact become more deeply quiescent following Notch inhibition (Figure 5.2Giii), suggesting Notch signalling is required to maintain the low-level of self-renewal observed in quiescent AHNSCs *in vitro*. This result was surprising, as the opposite was expected; loss of Notch signalling via RBPJk deletion in RGLs *in vivo* leads to a massive activation of the stem cell pool (Ehm et al., 2010), therefore Notch inhibition *in vitro* might have been expected to activate BMP4-induced quiescent AHNSCs. This discrepancy could be explained by the difference between inhibiting Notch at the level of the effector RBPJk and the receptors. Studies in which Notch signalling was inhibited by the ablation of Notch1 receptor show a more modest phenotype, with a loss of maintenance of the active RGL fraction, but with no effect on quiescent RGLs (Ables et al., 2010; Lugert et al., 2010). Notch1 ablated RGLs cultured *in vitro* lose the capacity to form self-renewing neurospheres (Ables et al., 2010), a phenotype very similar to what I observe in Notch inhibited quiescent AHNSCs. Notch signalling therefore is required to maintain self-renewal of BMP4-induced AHNSCs, possibly by maintaining oscillatory expression of *Hes1/5* and *Ascl1*. These results also suggest that the *in vitro* model of quiescence developed in this thesis is able to recapitulate the behaviour of RGLs *in vivo*, even with respect to complex signal cross-regulation, further demonstrating it is a highly useful and relevant model for studying adult neural stem cell quiescence.

The method I used to inhibit Notch signalling did not discriminate between the different Notch receptors, rather inhibiting all at the same time (as well as other gamma-secretase regulated receptors). This indiscriminate inhibition could also explain why I see loss of proliferation, rather than activation, of quiescent AHNSCs *in vitro*, because while Notch1 has been shown to be crucial for RGL self-renewal, Notch3 has been identified to maintain quiescence of neural stem cells in the adult zebrafish pallium and

mouse SVZ (Alunni et al., 2013; Kawai et al., 2017). It would be interesting to see whether specifically knocking-out Notch3 is sufficient to activate AHNSCs in BMP4 conditions, and how it regulates stem cell activity differently to Notch1 signalling.

RNA sequencing of Notch-inhibited quiescent AHNSCs revealed that Notch regulated far fewer genes in the context of high BMP4 concentration, compared to low levels of BMP4 (Figure 5.3). This observation further suggests that BMP signalling is able to induce Notch target genes when expressed at high levels. It was striking for example that when BMP4 concentration was high, Notch regulated none of 313 cell cycle genes tested, whereas Notch inhibition in active and shallow quiescent AHNSCs led to the upregulation of cell cycle genes. These results suggest that at low concentrations, BMP4 synergises with Notch to maintain quiescence, whereas at high concentrations, BMP4 dominates over Notch to maintain quiescence. As discussed above, this could have implications for homeostasis of RGLs *in vivo*; if the balance of BMP and Notch signalling becomes deregulated, RGLs could become less easily activated.

Finally, I measured Id4 mRNA and protein expression in Notch-inhibited AHNSCs, to determine whether Notch can regulate Id4 *in vitro*. The results reflected those observed for RBPJk deletion *in vivo*, showing Notch does not strongly regulate Id4 in active or quiescent AHNSCs. Notch3 specifically regulates quiescent SVZ NSCs (Kawai et al., 2017), therefore I would be interested to test whether specific knockdown of Notch3 *in vitro* and *in vivo* can specifically regulate Id4 expression.

6.6 Conclusions and perspectives

The work presented in this thesis has identified Id4 as a novel quiescence factor, required to maintain the quiescent state of adult hippocampal neural stem cells. We have also proposed the molecular mechanisms by which Id4 maintains quiescence. We show that the activation factor Ascl1 is expressed but actively suppressed at the protein level in quiescent RGLs by Id4, which we propose sequesters the E-protein binding partners of Ascl1, rendering Ascl1 unable to bind DNA and activate its target genes, and rapidly targeted for proteasomal degradation. In Figure 6.1 I present the proposed mechanism by which Id4 regulates quiescence, highlighting the complex network of interactions between the different Id proteins, the E-proteins and Ascl1 in different conditions.

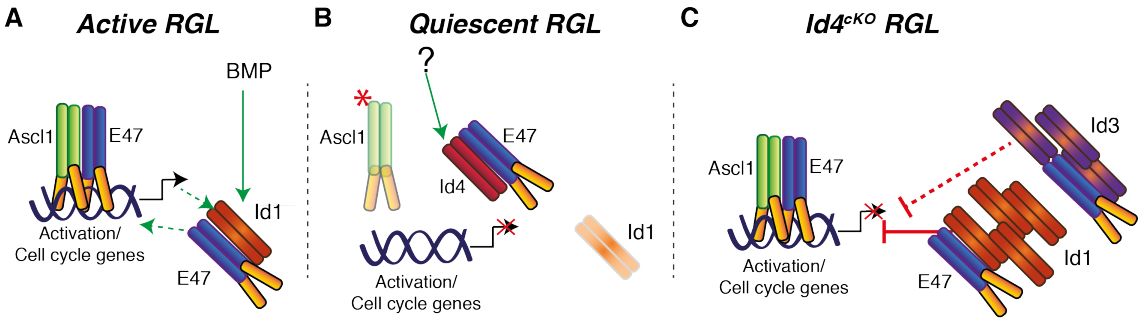

Figure 6.1. Proposed mechanisms regulating the active and quiescent RGL state and *Id4*^{cKO} RGLs

(A) In the active state, Ascl1 (green) and E47 (blue) heterodimerise to bind DNA at E-box sites in Ascl1 target genes, inducing expression of activation and cell cycle genes. Id1 (orange) is expressed in active RGLs downstream of BMP/Smad signalling, and potentially induces stem cell self-renewal gene expression. Id1 may be stabilised by E-proteins.
(B) In the quiescent state, Id4 (red) expression is induced by unknown niche signals, and sequesters the E-proteins, rendering Ascl1 monomeric and targeted for degradation. Id4 also inhibits Id1 protein, possibly by the same mechanism; without E-protein heterodimerisation, Id1 may be more unstable and degraded. Activation/cell cycle genes are not induced.
(C) In *Id4*^{cKO} RGLs, Ascl1 and E47 can heterodimerise, and Id1 and Id3 (purple) proteins are highly upregulated. At high levels, Id1 can suppress the cell cycle, possibly compensating for the loss of Id4. Id3 might also function in this way. Ascl1 protein is not degraded by Id1/3 but competes with the repressive functions of Id1/3 to induce activation of its target genes.
Solid arrows indicate strong evidence for the interaction, dashed lines indicate weak or no evidence/speculation. Red asterisk: ubiquitination.

Adult stem cells, including neural stem cells of the neurogenic niches, must be regulated carefully to ensure life-long maintenance whilst still enabling the production of progenitors for the regeneration of the tissue. The significance of the work presented here firstly lies in the identification of Id4 as a novel regulator of RGL quiescence, and as a potential target of niche signals regulating the activity of RGLs. Secondly, we have made the significant discovery that Ascl1 is even more dynamically regulated in RGLs than previously thought. The observation that Ascl1 is actively transcribed and translated, but inhibited at the protein level in quiescent hippocampal NSCs, could enable rapid response of RGLs to activating stimuli. The multi-level regulation of Ascl1, by transcriptional repressors Hes1/5, the E3-ubiquitn ligase Huwe1, and now by Id4,

indicates that the tight regulation of Ascl1 has evolved as a crucial mechanism for maintaining hippocampal NSCs.

Despite playing central roles in the regulation of neural stem cells during embryonic development, the Id proteins have not been thoroughly studied in the context of adult neurogenesis. We have shown that Id1-4 have different expression patterns in the DG of adult mice, and have demonstrated distinct functions between Id1 and Id4 in the regulation of NSC activity, sharing a function in inhibiting the cell cycle, but showing differential regulation of Ascl1, highlighting Id4 as a unique regulator of Ascl1 protein. Future studies should investigate the function of Id1-3 in the hippocampal niche, to identify novel mechanisms of NSC regulation as well as identifying whether these Ids can compensate for Id4 in maintaining NSC quiescence.

We have also presented a highly tractable *in vitro* model of adult hippocampal neural stem cell quiescence (Figure 3.1), which enabled identification of Id4 as a quiescence factor, as well as elucidating its molecular mechanism. This *in vitro* model of AHNSC quiescence holds tremendous potential for elucidating many more mechanisms of AHNSC regulation.

The full picture of the mechanisms regulating adult NSC quiescence is yet to be fully painted, therefore the discovery of novel mechanisms can help address the gap in our knowledge, particularly regarding the heterogeneity in the response of RGLs to neurogenic stimuli. This knowledge has important clinical implications, including the understanding of why NSCs become more quiescent with age, stress or depression. This knowledge can then be applied to target Id4 for NSC activation as a therapeutic intervention in these disorders, as well as in neurodegenerative diseases.

Reference List

Ables, J.L., Decarolis, N.A., Johnson, M.A., Rivera, P.D., Gao, Z., Cooper, D.C., Radtke, F., Hsieh, J., and Eisch, A.J. (2010). Notch1 is required for maintenance of the reservoir of adult hippocampal stem cells. The Journal of neuroscience : the official journal of the Society for Neuroscience *30*, 10484-10492.

Aguirre, A., Rubio, M.E., and Gallo, V. (2010). Notch and EGFR pathway interaction regulates neural stem cell number and self-renewal. Nature *467*, 323-327.

Ahn, S., and Joyner, A.L. (2005). In vivo analysis of quiescent adult neural stem cells responding to Sonic hedgehog. Nature *437*, 894-897.

Alexson, T.O., Hitoshi, S., Coles, B.L., Bernstein, A., and van der Kooy, D. (2006). Notch signaling is required to maintain all neural stem cell populations--irrespective of spatial or temporal niche. Dev Neurosci *28*, 34-48.

Alfonso, J., Le Magueresse, C., Zuccotti, A., Khodosevich, K., and Monyer, H. (2012). Diazepam binding inhibitor promotes progenitor proliferation in the postnatal SVZ by reducing GABA signaling. Cell Stem Cell *10*, 76-87.

Ali, F.R., Cheng, K., Kirwan, P., Metcalfe, S., Livesey, F.J., Barker, R.A., and Philpott, A. (2014). The phosphorylation status of Ascl1 is a key determinant of neuronal differentiation and maturation in vivo and in vitro. Development *141*, 2216-2224.

Altman, J. (1963). Autoradiographic investigation of cell proliferation in the brains of rats and cats. Anat Rec *145*, 573-591.

Altman, J. (1966). Proliferation and migration of undifferentiated precursor cells in the rat during postnatal gliogenesis. Exp Neurol *16*, 263-278.

Altman, J. (1969). Autoradiographic and histological studies of postnatal neurogenesis. IV. Cell proliferation and migration in the anterior forebrain, with special reference to persisting neurogenesis in the olfactory bulb. The Journal of comparative neurology *137*, 433-457.

Altman, J., and Das, G.D. (1965). Autoradiographic and histological evidence of postnatal hippocampal neurogenesis in rats. The Journal of comparative neurology *124*, 319-335.

Alunni, A., Krecsmarik, M., Bosco, A., Galant, S., Pan, L., Moens, C.B., and Bally-Cuif, L. (2013). Notch3 signaling gates cell cycle entry and limits neural stem cell amplification in the adult pallium. Development *140*, 3335-3347.

Amador-Arjona, A., Elliott, J., Miller, A., Ginbey, A., Pazour, G.J., Enikolopov, G., Roberts, A.J., and Terskikh, A.V. (2011). Primary cilia regulate proliferation of amplifying progenitors in adult hippocampus: implications for learning and memory. The Journal of neuroscience : the official journal of the Society for Neuroscience *31*, 9933-9944.

Anders, S., Pyl, P.T., and Huber, W. (2015). HTSeq--a Python framework to work with high-throughput sequencing data. Bioinformatics *31*, 166-169.

Andersen, J., Urban, N., Achimastou, A., Ito, A., Simic, M., Ullom, K., Martynoga, B., Lebel, M., Goritz, C., Frisen, J.*, et al.* (2014). A transcriptional mechanism integrating inputs from extracellular signals to activate hippocampal stem cells. Neuron *83*, 1085-1097.

Andreu, Z., Khan, M.A., Gonzalez-Gomez, P., Negueruela, S., Hortiguela, R., San Emeterio, J., Ferron, S.R., Martinez, G., Vidal, A., Farinas, I.*, et al.* (2015). The cyclin-dependent kinase inhibitor p27 kip1 regulates radial stem cell quiescence and neurogenesis in the adult hippocampus. Stem Cells *33*, 219-229.

Andreu-Agullo, C., Morante-Redolat, J.M., Delgado, A.C., and Farinas, I. (2009). Vascular niche factor PEDF modulates Notch-dependent stemness in the adult subependymal zone. Nat Neurosci *12*, 1514-1523.

Andrews, S. (2010). FastQC: a quality control tool for high throughput sequence data. Babraham Bioinformatics *[*https://www.bioinformatics.babraham.ac.uk/projects/fastqc/*]*.

Androutsellis-Theotokis, A., Leker, R.R., Soldner, F., Hoeppner, D.J., Ravin, R., Poser, S.W., Rueger, M.A., Bae, S.K., Kittappa, R., and McKay, R.D. (2006). Notch signalling regulates stem cell numbers in vitro and in vivo. Nature *442*, 823-826.

Bai, G., Sheng, N., Xie, Z., Bian, W., Yokota, Y., Benezra, R., Kageyama, R., Guillemot, F., and Jing, N. (2007). Id sustains Hes1 expression to inhibit precocious neurogenesis by releasing negative autoregulation of Hes1. Dev Cell *13*, 283-297.

Ballas, N., Grunseich, C., Lu, D.D., Speh, J.C., and Mandel, G. (2005). REST and its corepressors mediate plasticity of neuronal gene chromatin throughout neurogenesis. Cell *121*, 645-657.

Banasr, M., Hery, M., Printemps, R., and Daszuta, A. (2004). Serotonin-induced increases in adult cell proliferation and neurogenesis are mediated through different and common 5-HT receptor subtypes in the dentate gyrus and the subventricular zone. Neuropsychopharmacology : official publication of the American College of Neuropsychopharmacology *29*, 450-460.

Baptista, P., and Andrade, J.P. (2018). Adult Hippocampal Neurogenesis: Regulation and Possible Functional and Clinical Correlates. Front Neuroanat *12*, 44.

Basak, O., Giachino, C., Fiorini, E., Macdonald, H.R., and Taylor, V. (2012). Neurogenic subventricular zone stem/progenitor cells are Notch1-dependent in their active but not quiescent state. The Journal of neuroscience : the official journal of the Society for Neuroscience *32*, 5654-5666.

Beck, S.E., and Carethers, J.M. (2007). BMP suppresses PTEN expression via RAS/ERK signaling. Cancer Biol Ther *6*, 1313-1317.

Beckervordersandforth, R. (2017). Mitochondrial Metabolism-Mediated Regulation of Adult Neurogenesis. Brain Plast *3*, 73-87.

Beckervordersandforth, R., Ebert, B., Schaffner, I., Moss, J., Fiebig, C., Shin, J., Moore, D.L., Ghosh, L., Trinchero, M.F., Stockburger, C.*, et al.* (2017). Role of Mitochondrial Metabolism in the Control of Early Lineage Progression and Aging Phenotypes in Adult Hippocampal Neurogenesis. Neuron.

Beckervordersandforth, R., Tripathi, P., Ninkovic, J., Bayam, E., Lepier, A., Stempfhuber, B., Kirchhoff, F., Hirrlinger, J., Haslinger, A., Lie, D.C.*, et al.* (2010). In vivo fate mapping and expression analysis reveals molecular hallmarks of prospectively isolated adult neural stem cells. Cell Stem Cell *7*, 744-758.

Berg, D.A., Belnoue, L., Song, H., and Simon, A. (2013). Neurotransmitter-mediated control of neurogenesis in the adult vertebrate brain. Development *140*, 2548-2561.

Berg, D.A., Bond, A.M., Ming, G.L., and Song, H. (2018). Radial glial cells in the adult dentate gyrus: what are they and where do they come from? F1000Res *7*, 277.

Bergmann, O., Liebl, J., Bernard, S., Alkass, K., Yeung, M.S., Steier, P., Kutschera, W., Johnson, L., Landen, M., Druid, H.*, et al.* (2012). The age of olfactory bulb neurons in humans. Neuron *74*, 634-639.

Berninger, B., Costa, M.R., Koch, U., Schroeder, T., Sutor, B., Grothe, B., and Gotz, M. (2007). Functional properties of neurons derived from in vitro reprogrammed postnatal astroglia. The Journal of neuroscience : the official journal of the Society for Neuroscience *27*, 8654-8664.

Bertrand, N., Castro, D.S., and Guillemot, F. (2002). Proneural genes and the specification of neural cell types. Nat Rev Neurosci *3*, 517-530.

Best, S.A., Hutt, K.J., Fu, N.Y., Vaillant, F., Liew, S.H., Hartley, L., Scott, C.L., Lindeman, G.J., and Visvader, J.E. (2014). Dual roles for Id4 in the regulation of estrogen signaling in the mammary gland and ovary. Development *141*, 3159-3164.

Bjornson, C.R., Cheung, T.H., Liu, L., Tripathi, P.V., Steeper, K.M., and Rando, T.A. (2012). Notch signaling is necessary to maintain quiescence in adult muscle stem cells. Stem Cells *30*, 232-242.

Blanpain, C., Lowry, W.E., Geoghegan, A., Polak, L., and Fuchs, E. (2004). Self-renewal, multipotency, and the existence of two cell populations within an epithelial stem cell niche. Cell *118*, 635-648.

Boareto, M., Iber, D., and Taylor, V. (2017). Differential interactions between Notch and ID factors control neurogenesis by modulating Hes factor autoregulation. Development *144*, 3465-3474.

Bohrer, C., Pfurr, S., Mammadzada, K., Schildge, S., Plappert, L., Hils, M., Pous, L., Rauch, K.S., Dumit, V.I., Pfeifer, D.*, et al.* (2015). The balance of Id3 and E47 determines neural stem/precursor cell differentiation into astrocytes. EMBO J *34*, 2804-2819.

Boldrini, M., Fulmore, C.A., Tartt, A.N., Simeon, L.R., Pavlova, I., Poposka, V., Rosoklija, G.B., Stankov, A., Arango, V., Dwork, A.J.*, et al.* (2018). Human Hippocampal Neurogenesis Persists throughout Aging. Cell Stem Cell *22*, 589-599 e585.

Bolger, A.M., Lohse, M., and Usadel, B. (2014). Trimmomatic: a flexible trimmer for Illumina sequence data. Bioinformatics *30*, 2114-2120.

Bonaguidi, M.A., McGuire, T., Hu, M., Kan, L., Samanta, J., and Kessler, J.A. (2005). LIF and BMP signaling generate separate and discrete types of GFAP-expressing cells. Development *132*, 5503-5514.

Bonaguidi, M.A., Peng, C.Y., McGuire, T., Falciglia, G., Gobeske, K.T., Czeisler, C., and Kessler, J.A. (2008). Noggin expands neural stem cells in the adult hippocampus. The Journal of neuroscience : the official journal of the Society for Neuroscience *28*, 9194-9204.

Bonaguidi, M.A., Song, J., Ming, G.L., and Song, H. (2012). A unifying hypothesis on mammalian neural stem cell properties in the adult hippocampus. Curr Opin Neurobiol *22*, 754-761.

Bonaguidi, M.A., Wheeler, M.A., Shapiro, J.S., Stadel, R.P., Sun, G.J., Ming, G.L., and Song, H. (2011). In vivo clonal analysis reveals self-renewing and multipotent adult neural stem cell characteristics. Cell *145*, 1142-1155.

Bond, A.M., Ming, G.L., and Song, H. (2015). Adult Mammalian Neural Stem Cells and Neurogenesis: Five Decades Later. Cell Stem Cell *17*, 385-395.

Bond, A.M., Peng, C.Y., Meyers, E.A., McGuire, T., Ewaleifoh, O., and Kessler, J.A. (2014). BMP signaling regulates the tempo of adult hippocampal progenitor maturation at multiple stages of the lineage. Stem Cells *32*, 2201-2214.

Boulais, P.E., and Frenette, P.S. (2015). Making sense of hematopoietic stem cell niches. Blood *125*, 2621-2629.

Bounpheng, M.A., Dimas, J.J., Dodds, S.G., and Christy, B.A. (1999). Degradation of Id proteins by the ubiquitin-proteasome pathway. FASEB J *13*, 2257-2264.

Bowman, A.N., van Amerongen, R., Palmer, T.D., and Nusse, R. (2013). Lineage tracing with Axin2 reveals distinct developmental and adult populations of Wnt/beta-catenin-responsive neural stem cells. Proc Natl Acad Sci U S A *110*, 7324-7329.

Bracko, O., Singer, T., Aigner, S., Knobloch, M., Winner, B., Ray, J., Clemenson, G.D., Jr., Suh, H., Couillard-Despres, S., Aigner, L.*, et al.* (2012). Gene expression profiling of neural stem cells and their neuronal progeny reveals IGF2 as a regulator of adult hippocampal neurogenesis. The Journal of neuroscience : the official journal of the Society for Neuroscience *32*, 3376-3387.

Bragdon, B., Moseychuk, O., Saldanha, S., King, D., Julian, J., and Nohe, A. (2011). Bone morphogenetic proteins: a critical review. Cell Signal *23*, 609-620.

Braun, S.M., Pilz, G.A., Machado, R.A., Moss, J., Becher, B., Toni, N., and Jessberger, S. (2015). Programming Hippocampal Neural Stem/Progenitor Cells into Oligodendrocytes Enhances Remyelination in the Adult Brain after Injury. Cell reports *11*, 1679-1685.

Breunig, J.J., Sarkisian, M.R., Arellano, J.I., Morozov, Y.M., Ayoub, A.E., Sojitra, S., Wang, B., Flavell, R.A., Rakic, P., and Town, T. (2008). Primary cilia regulate

hippocampal neurogenesis by mediating sonic hedgehog signaling. Proc Natl Acad Sci U S A *105*, 13127-13132.

Breunig, J.J., Silbereis, J., Vaccarino, F.M., Sestan, N., and Rakic, P. (2007). Notch regulates cell fate and dendrite morphology of newborn neurons in the postnatal dentate gyrus. Proc Natl Acad Sci U S A *104*, 20558-20563.

Bronner, M., Hatten, M. (2014). Chapter 15 - Neurogenesis and migration (Elsevier).

Brooks, L.J., and Parrinello, S. (2017). Vascular regulation of glioma stem-like cells: a balancing act. Curr Opin Neurobiol *47*, 8-15.

Bugra, K., Pollard, H., Charton, G., Moreau, J., Ben-Ari, Y., and Khrestchatisky, M. (1994). aFGF, bFGF and flg mRNAs show distinct patterns of induction in the hippocampus following kainate-induced seizures. Eur J Neurosci *6*, 58-66.

Campos, L.S., Decker, L., Taylor, V., and Skarnes, W. (2006). Notch, epidermal growth factor receptor, and beta1-integrin pathways are coordinated in neural stem cells. J Biol Chem *281*, 5300-5309.

Cao, L., Jiao, X., Zuzga, D.S., Liu, Y., Fong, D.M., Young, D., and During, M.J. (2004). VEGF links hippocampal activity with neurogenesis, learning and memory. Nat Genet *36*, 827-835.

Castro, D.S., Martynoga, B., Parras, C., Ramesh, V., Pacary, E., Johnston, C., Drechsel, D., Lebel-Potter, M., Garcia, L.G., Hunt, C.*, et al.* (2011). A novel function of the proneural factor Ascl1 in progenitor proliferation identified by genome-wide characterization of its targets. Genes & development *25*, 930-945.

Chapouton, P., Skupien, P., Hesl, B., Coolen, M., Moore, J.C., Madelaine, R., Kremmer, E., Faus-Kessler, T., Blader, P., Lawson, N.D.*, et al.* (2010). Notch activity levels control the balance between quiescence and recruitment of adult neural stem cells. The Journal of neuroscience : the official journal of the Society for Neuroscience *30*, 7961-7974.

Charville, G.W., and Rando, T.A. (2011). Stem cell ageing and non-random chromosome segregation. Philos Trans R Soc Lond B Biol Sci *366*, 85-93.

Chell, J.M., and Brand, A.H. (2010). Nutrition-responsive glia control exit of neural stem cells from quiescence. Cell *143*, 1161-1173.

Chen, J., Li, Y., Yu, T.S., McKay, R.M., Burns, D.K., Kernie, S.G., and Parada, L.F. (2012). A restricted cell population propagates glioblastoma growth after chemotherapy. Nature *488*, 522-526.

Chen, W., Dong, J., Haiech, J., Kilhoffer, M.C., and Zeniou, M. (2016). Cancer Stem Cell Quiescence and Plasticity as Major Challenges in Cancer Therapy. Stem Cells Int *2016*, 1740936.

Cheung, T.H., and Rando, T.A. (2013). Molecular regulation of stem cell quiescence. Nat Rev Mol Cell Biol *14*, 329-340.

Choe, Y., Pleasure, S.J., and Mira, H. (2015). Control of Adult Neurogenesis by Short-Range Morphogenic-Signaling Molecules. Cold Spring Harb Perspect Biol *8*, a018887.

Choubey, L., Collette, J.C., and Smith, K.M. (2017). Quantitative assessment of fibroblast growth factor receptor 1 expression in neurons and glia. PeerJ *5*, e3173.

Chu, G.C., Dunn, N.R., Anderson, D.C., Oxburgh, L., and Robertson, E.J. (2004). Differential requirements for Smad4 in TGFbeta-dependent patterning of the early mouse embryo. Development *131*, 3501-3512.

Codega, P., Silva-Vargas, V., Paul, A., Maldonado-Soto, A.R., Deleo, A.M., Pastrana, E., and Doetsch, F. (2014). Prospective identification and purification of quiescent adult neural stem cells from their in vivo niche. Neuron *82*, 545-559.

Colak, D., Mori, T., Brill, M.S., Pfeifer, A., Falk, S., Deng, C., Monteiro, R., Mummery, C., Sommer, L., and Gotz, M. (2008). Adult neurogenesis requires Smad4-mediated bone morphogenic protein signaling in stem cells. The Journal of neuroscience : the official journal of the Society for Neuroscience *28*, 434-446.

Coller, H.A., Sang, L., and Roberts, J.M. (2006). A new description of cellular quiescence. PLoS Biol *4*, e83.

Conboy, I.M., Conboy, M.J., Wagers, A.J., Girma, E.R., Weissman, I.L., and Rando, T.A. (2005). Rejuvenation of aged progenitor cells by exposure to a young systemic environment. Nature *433*, 760-764.

Conti, L., Pollard, S.M., Gorba, T., Reitano, E., Toselli, M., Biella, G., Sun, Y., Sanzone, S., Ying, Q.L., Cattaneo, E.*, et al.* (2005). Niche-independent symmetrical self-renewal of a mammalian tissue stem cell. PLoS Biol *3*, e283.

Cook, B.D., and Evans, T. (2014). BMP signaling balances murine myeloid potential through SMAD-independent p38MAPK and NOTCH pathways. Blood *124*, 393-402.

Coolen, M., Katz, S., and Bally-Cuif, L. (2013). miR-9: a versatile regulator of neurogenesis. Frontiers in cellular neuroscience *7*, 220.

Czeh, B., Muller-Keuker, J.I., Rygula, R., Abumaria, N., Hiemke, C., Domenici, E., and Fuchs, E. (2007). Chronic social stress inhibits cell proliferation in the adult medial prefrontal cortex: hemispheric asymmetry and reversal by fluoxetine treatment. Neuropsychopharmacology : official publication of the American College of Neuropsychopharmacology *32*, 1490-1503.

DeCarolis, N.A., Mechanic, M., Petrik, D., Carlton, A., Ables, J.L., Malhotra, S., Bachoo, R., Gotz, M., Lagace, D.C., and Eisch, A.J. (2013). In vivo contribution of nestin- and GLAST-lineage cells to adult hippocampal neurogenesis. Hippocampus *23*, 708-719.

Delgado, A.C., Ferron, S.R., Vicente, D., Porlan, E., Perez-Villalba, A., Trujillo, C.M., P, D.O., and Farinas, I. (2014). Endothelial NT-3 Delivered by Vasculature and CSF Promotes Quiescence of Subependymal Neural Stem Cells through Nitric Oxide Induction. Neuron *83*, 572-585.

Derynck, R., and Zhang, Y.E. (2003). Smad-dependent and Smad-independent pathways in TGF-beta family signalling. Nature *425*, 577-584.

Doetsch, F., Caille, I., Lim, D.A., Garcia-Verdugo, J.M., and Alvarez-Buylla, A. (1999a). Subventricular zone astrocytes are neural stem cells in the adult mammalian brain. Cell *97*, 703-716.

Doetsch, F., Garcia-Verdugo, J.M., and Alvarez-Buylla, A. (1999b). Regeneration of a germinal layer in the adult mammalian brain. Proc Natl Acad Sci U S A *96*, 11619-11624.

Doetsch, F., Verdugo, J.M., Caille, I., Alvarez-Buylla, A., Chao, M.V., and Casaccia-Bonnefil, P. (2002). Lack of the cell-cycle inhibitor p27Kip1 results in selective increase of transit-amplifying cells for adult neurogenesis. The Journal of neuroscience : the official journal of the Society for Neuroscience *22*, 2255-2264.

Dong, J., Huang, S., Caikovski, M., Ji, S., McGrath, A., Custorio, M.G., Creighton, C.J., Maliakkal, P., Bogoslovskaia, E., Du, Z.*, et al.* (2011). ID4 regulates mammary gland development by suppressing p38MAPK activity. Development *138*, 5247-5256.

Douet, V., Arikawa-Hirasawa, E., and Mercier, F. (2012). Fractone-heparan sulfates mediate BMP-7 inhibition of cell proliferation in the adult subventricular zone. Neurosci Lett *528*, 120-125.

Duan, X., Chang, J.H., Ge, S., Faulkner, R.L., Kim, J.Y., Kitabatake, Y., Liu, X.B., Yang, C.H., Jordan, J.D., Ma, D.K.*, et al.* (2007). Disrupted-In-Schizophrenia 1 regulates integration of newly generated neurons in the adult brain. Cell *130*, 1146-1158.

Dumitru, I., Neitz, A., Alfonso, J., and Monyer, H. (2017). Diazepam Binding Inhibitor Promotes Stem Cell Expansion Controlling Environment-Dependent Neurogenesis. Neuron *94*, 125-137 e125.

Duncan, M., DiCicco-Bloom, E.M., Xiang, X., Benezra, R., and Chada, K. (1992). The gene for the helix-loop-helix protein, Id, is specifically expressed in neural precursors. Dev Biol *154*, 1-10.

Ehm, O., Goritz, C., Covic, M., Schaffner, I., Schwarz, T.J., Karaca, E., Kempkes, B., Kremmer, E., Pfrieger, F.W., Espinosa, L.*, et al.* (2010). RBPJkappa-dependent signaling is essential for long-term maintenance of neural stem cells in the adult hippocampus. The Journal of neuroscience : the official journal of the Society for Neuroscience *30*, 13794-13807.

Encinas, J.M., Michurina, T.V., Peunova, N., Park, J.H., Tordo, J., Peterson, D.A., Fishell, G., Koulakov, A., and Enikolopov, G. (2011). Division-coupled astrocytic differentiation and age-related depletion of neural stem cells in the adult hippocampus. Cell Stem Cell *8*, 566-579.

Encinas, J.M., Sierra, A., Valcarcel-Martin, R., and Martin-Suarez, S. (2013). A developmental perspective on adult hippocampal neurogenesis. Int J Dev Neurosci *31*, 640-645.

Encinas, J.M., Vaahtokari, A., and Enikolopov, G. (2006). Fluoxetine targets early progenitor cells in the adult brain. Proc Natl Acad Sci U S A *103*, 8233-8238.

Engel, M.E., McDonnell, M.A., Law, B.K., and Moses, H.L. (1999). Interdependent SMAD and JNK signaling in transforming growth factor-beta-mediated transcription. J Biol Chem *274*, 37413-37420.

Engler, A., Rolando, C., Giachino, C., Saotome, I., Erni, A., Brien, C., Zhang, R., Zimber-Strobl, U., Radtke, F., Artavanis-Tsakonas, S.*, et al.* (2018). Notch2 Signaling Maintains NSC Quiescence in the Murine Ventricular-Subventricular Zone. Cell reports *22*, 992-1002.

Episkopou, V. (2005). SOX2 functions in adult neural stem cells. Trends Neurosci *28*, 219-221.

Eriksson, P.S., Perfilieva, E., Bjork-Eriksson, T., Alborn, A.M., Nordborg, C., Peterson, D.A., and Gage, F.H. (1998). Neurogenesis in the adult human hippocampus. Nat Med *4*, 1313-1317.

Ernst, A., Alkass, K., Bernard, S., Salehpour, M., Perl, S., Tisdale, J., Possnert, G., Druid, H., and Frisen, J. (2014). Neurogenesis in the striatum of the adult human brain. Cell *156*, 1072-1083.

Estrada, C., and Murillo-Carretero, M. (2005). Nitric oxide and adult neurogenesis in health and disease. The Neuroscientist : a review journal bringing neurobiology, neurology and psychiatry *11*, 294-307.

Fabel, K., Fabel, K., Tam, B., Kaufer, D., Baiker, A., Simmons, N., Kuo, C.J., and Palmer, T.D. (2003). VEGF is necessary for exercise-induced adult hippocampal neurogenesis. Eur J Neurosci *18*, 2803-2812.

Fabian, M.R., Sonenberg, N., and Filipowicz, W. (2010). Regulation of mRNA translation and stability by microRNAs. Annu Rev Biochem *79*, 351-379.

Falk, S., Joosten, E., Kaartinen, V., and Sommer, L. (2014). Smad4 and Trim33/Tif1gamma redundantly regulate neural stem cells in the developing cortex. Cerebral cortex *24*, 2951-2963.

Fan, X., Xu, H., Cai, W., Yang, Z., and Zhang, J. (2003). Spatial and temporal patterns of expression of Noggin and BMP4 in embryonic and postnatal rat hippocampus. Brain research Developmental brain research *146*, 51-58.

Ferent, J., Cochard, L., Faure, H., Taddei, M., Hahn, H., Ruat, M., and Traiffort, E. (2014). Genetic activation of Hedgehog signaling unbalances the rate of neural stem cell renewal by increasing symmetric divisions. Stem Cell Reports *3*, 312-323.

Fernando, R.N., Eleuteri, B., Abdelhady, S., Nussenzweig, A., Andang, M., and Ernfors, P. (2011). Cell cycle restriction by histone H2AX limits proliferation of adult neural stem cells. Proc Natl Acad Sci U S A *108*, 5837-5842.

Forsberg, E.C., Passegue, E., Prohaska, S.S., Wagers, A.J., Koeva, M., Stuart, J.M., and Weissman, I.L. (2010). Molecular signatures of quiescent, mobilized and leukemia-initiating hematopoietic stem cells. PLoS ONE *5*, e8785.

Fuentealba, L.C., Obernier, K., and Alvarez-Buylla, A. (2012). Adult neural stem cells bridge their niche. Cell Stem Cell *10*, 698-708.

Fuentealba, L.C., Rompani, S.B., Parraguez, J.I., Obernier, K., Romero, R., Cepko, C.L., and Alvarez-Buylla, A. (2015). Embryonic Origin of Postnatal Neural Stem Cells. Cell *161*, 1644-1655.

Fukada, S., Uezumi, A., Ikemoto, M., Masuda, S., Segawa, M., Tanimura, N., Yamamoto, H., Miyagoe-Suzuki, Y., and Takeda, S. (2007). Molecular signature of quiescent satellite cells in adult skeletal muscle. Stem Cells *25*, 2448-2459.

Fukuda, S., Kato, F., Tozuka, Y., Yamaguchi, M., Miyamoto, Y., and Hisatsune, T. (2003). Two distinct subpopulations of nestin-positive cells in adult mouse dentate gyrus. The Journal of neuroscience : the official journal of the Society for Neuroscience *23*, 9357-9366.

Furuta, M., and Bridges, R.S. (2005). Gestation-induced cell proliferation in the rat brain. Brain research Developmental brain research *156*, 61-66.

Furutachi, S., Matsumoto, A., Nakayama, K.I., and Gotoh, Y. (2013). p57 controls adult neural stem cell quiescence and modulates the pace of lifelong neurogenesis. EMBO J *32*, 970-981.

Gage, F.H., Coates, P.W., Palmer, T.D., Kuhn, H.G., Fisher, L.J., Suhonen, J.O., Peterson, D.A., Suhr, S.T., and Ray, J. (1995). Survival and differentiation of adult neuronal progenitor cells transplanted to the adult brain. Proc Natl Acad Sci U S A *92*, 11879-11883.

Gajera, C.R., Emich, H., Lioubinski, O., Christ, A., Beckervordersandforth-Bonk, R., Yoshikawa, K., Bachmann, S., Christensen, E.I., Gotz, M., Kempermann, G.*, et al.* (2010). LRP2 in ependymal cells regulates BMP signaling in the adult neurogenic niche. J Cell Sci *123*, 1922-1930.

Galea, L.A., Wainwright, S.R., Roes, M.M., Duarte-Guterman, P., Chow, C., and Hamson, D.K. (2013). Sex, hormones and neurogenesis in the hippocampus: hormonal modulation of neurogenesis and potential functional implications. J Neuroendocrinol *25*, 1039-1061.

Galichet, C., Guillemot, F., and Parras, C.M. (2008). Neurogenin 2 has an essential role in development of the dentate gyrus. Development *135*, 2031-2041.

Gao, Z., Ure, K., Ding, P., Nashaat, M., Yuan, L., Ma, J., Hammer, R.E., and Hsieh, J. (2011). The master negative regulator REST/NRSF controls adult neurogenesis by restraining the neurogenic program in quiescent stem cells. The Journal of neuroscience : the official journal of the Society for Neuroscience *31*, 9772-9786.

Garcia, A.D., Doan, N.B., Imura, T., Bush, T.G., and Sofroniew, M.V. (2004). GFAP-expressing progenitors are the principal source of constitutive neurogenesis in adult mouse forebrain. Nat Neurosci *7*, 1233-1241.

Gillotin, S., Davies, J.D., and Philpott, A. (2018). Subcellular localisation modulates ubiquitylation and degradation of Ascl1. Sci Rep *8*, 4625.

Gobeske, K.T., Das, S., Bonaguidi, M.A., Weiss, C., Radulovic, J., Disterhoft, J.F., and Kessler, J.A. (2009). BMP signaling mediates effects of exercise on hippocampal neurogenesis and cognition in mice. PLoS ONE *4*, e7506.

Godoy, M.D., Voegels, R.L., Pinna Fde, R., Imamura, R., and Farfel, J.M. (2015). Olfaction in neurologic and neurodegenerative diseases: a literature review. Int Arch Otorhinolaryngol *19*, 176-179.

Goldman, S.A., and Nottebohm, F. (1983). Neuronal production, migration, and differentiation in a vocal control nucleus of the adult female canary brain. Proc Natl Acad Sci U S A *80*, 2390-2394.

Goncalves, J.T., Schafer, S.T., and Gage, F.H. (2016). Adult Neurogenesis in the Hippocampus: From Stem Cells to Behavior. Cell *167*, 897-914.

Gonzalez-Perez, O., Romero-Rodriguez, R., Soriano-Navarro, M., Garcia-Verdugo, J.M., and Alvarez-Buylla, A. (2009). Epidermal growth factor induces the progeny of subventricular zone type B cells to migrate and differentiate into oligodendrocytes. Stem Cells *27*, 2032-2043.

Gould, E. (2007). How widespread is adult neurogenesis in mammals? Nat Rev Neurosci *8*, 481-488.

Gould, E., Cameron, H.A., Daniels, D.C., Woolley, C.S., and McEwen, B.S. (1992). Adrenal hormones suppress cell division in the adult rat dentate gyrus. The Journal of neuroscience : the official journal of the Society for Neuroscience *12*, 3642-3650.

Gould, E., McEwen, B.S., Tanapat, P., Galea, L.A., and Fuchs, E. (1997). Neurogenesis in the dentate gyrus of the adult tree shrew is regulated by psychosocial stress and NMDA receptor activation. The Journal of neuroscience : the official journal of the Society for Neuroscience *17*, 2492-2498.

Gould, E., Reeves, A.J., Graziano, M.S., and Gross, C.G. (1999). Neurogenesis in the neocortex of adult primates. Science *286*, 548-552.

Gray, J.V., Petsko, G.A., Johnston, G.C., Ringe, D., Singer, R.A., and Werner-Washburne, M. (2004). "Sleeping beauty": quiescence in Saccharomyces cerevisiae. Microbiol Mol Biol Rev *68*, 187-206.

Gregorian, C., Nakashima, J., Le Belle, J., Ohab, J., Kim, R., Liu, A., Smith, K.B., Groszer, M., Garcia, A.D., Sofroniew, M.V.*, et al.* (2009). Pten deletion in adult neural stem/progenitor cells enhances constitutive neurogenesis. The Journal of neuroscience : the official journal of the Society for Neuroscience *29*, 1874-1886.

Griessinger, E., Anjos-Afonso, F., Pizzitola, I., Rouault-Pierre, K., Vargaftig, J., Taussig, D., Gribben, J., Lassailly, F., and Bonnet, D. (2014). A niche-like culture system allowing the maintenance of primary human acute myeloid leukemia-initiating cells: a new tool to decipher their chemoresistance and self-renewal mechanisms. Stem Cells Transl Med *3*, 520-529.

Gritti, A., Parati, E.A., Cova, L., Frolichsthal, P., Galli, R., Wanke, E., Faravelli, L., Morassutti, D.J., Roisen, F., Nickel, D.D.*, et al.* (1996). Multipotential stem cells from the adult mouse brain proliferate and self-renew in response to basic fibroblast growth

factor. The Journal of neuroscience : the official journal of the Society for Neuroscience *16*, 1091-1100.

Groszer, M., Erickson, R., Scripture-Adams, D.D., Dougherty, J.D., Le Belle, J., Zack, J.A., Geschwind, D.H., Liu, X., Kornblum, H.I., and Wu, H. (2006). PTEN negatively regulates neural stem cell self-renewal by modulating G0-G1 cell cycle entry. Proc Natl Acad Sci U S A *103*, 111-116.

Gu, Z., Lamb, P.W., and Yakel, J.L. (2012). Cholinergic coordination of presynaptic and postsynaptic activity induces timing-dependent hippocampal synaptic plasticity. The Journal of neuroscience : the official journal of the Society for Neuroscience *32*, 12337-12348.

Guillemot, F. (2007). Spatial and temporal specification of neural fates by transcription factor codes. Development *134*, 3771-3780.

Guillemot, F., and Hassan, B.A. (2017). Beyond proneural: emerging functions and regulations of proneural proteins. Curr Opin Neurobiol *42*, 93-101.

Hall, A.K., and Miller, R.H. (2004). Emerging roles for bone morphogenetic proteins in central nervous system glial biology. J Neurosci Res *76*, 1-8.

Han, H., Tanigaki, K., Yamamoto, N., Kuroda, K., Yoshimoto, M., Nakahata, T., Ikuta, K., and Honjo, T. (2002). Inducible gene knockout of transcription factor recombination signal binding protein-J reveals its essential role in T versus B lineage decision. Int Immunol *14*, 637-645.

Han, J., Calvo, C.F., Kang, T.H., Baker, K.L., Park, J.H., Parras, C., Levittas, M., Birba, U., Pibouin-Fragner, L., Fragner, P*., et al.* (2015). Vascular endothelial growth factor receptor 3 controls neural stem cell activation in mice and humans. Cell reports *10*, 1158-1172.

Hansen, D.V., Lui, J.H., Parker, P.R., and Kriegstein, A.R. (2010). Neurogenic radial glia in the outer subventricular zone of human neocortex. Nature *464*, 554-561.

Hitoshi, S., Alexson, T., Tropepe, V., Donoviel, D., Elia, A.J., Nye, J.S., Conlon, R.A., Mak, T.W., Bernstein, A., and van der Kooy, D. (2002). Notch pathway molecules are essential for the maintenance, but not the generation, of mammalian neural stem cells. Genes & development *16*, 846-858.

Hochgerner, H., Zeisel, A., Lonnerberg, P., and Linnarsson, S. (2018). Conserved properties of dentate gyrus neurogenesis across postnatal development revealed by single-cell RNA sequencing. Nat Neurosci *21*, 290-299.

Hsieh, J. (2012). Orchestrating transcriptional control of adult neurogenesis. Genes & development *26*, 1010-1021.

Huang, G.J., and Herbert, J. (2006). Stimulation of neurogenesis in the hippocampus of the adult rat by fluoxetine requires rhythmic change in corticosterone. Biological psychiatry *59*, 619-624.

Huttmann, A., Liu, S.L., Boyd, A.W., and Li, C.L. (2001). Functional heterogeneity within rhodamine123(lo) Hoechst33342(lo/sp) primitive hemopoietic stem cells revealed by pyronin Y. Exp Hematol *29*, 1109-1116.

Imayoshi, I., Isomura, A., Harima, Y., Kawaguchi, K., Kori, H., Miyachi, H., Fujiwara, T., Ishidate, F., and Kageyama, R. (2013). Oscillatory control of factors determining multipotency and fate in mouse neural progenitors. Science *342*, 1203-1208.

Imayoshi, I., and Kageyama, R. (2011). The role of Notch signaling in adult neurogenesis. Molecular neurobiology *44*, 7-12.

Imayoshi, I., and Kageyama, R. (2014a). bHLH factors in self-renewal, multipotency, and fate choice of neural progenitor cells. Neuron *82*, 9-23.

Imayoshi, I., and Kageyama, R. (2014b). Oscillatory control of bHLH factors in neural progenitors. Trends Neurosci *37*, 531-538.

Imayoshi, I., Sakamoto, M., Yamaguchi, M., Mori, K., and Kageyama, R. (2010). Essential roles of Notch signaling in maintenance of neural stem cells in developing and adult brains. The Journal of neuroscience : the official journal of the Society for Neuroscience *30*, 3489-3498.

Jang, M.H., Bonaguidi, M.A., Kitabatake, Y., Sun, J., Song, J., Kang, E., Jun, H., Zhong, C., Su, Y., Guo, J.U*., et al.* (2013a). Secreted frizzled-related protein 3 regulates activity-dependent adult hippocampal neurogenesis. Cell Stem Cell *12*, 215-223.

Jang, M.H., Kitabatake, Y., Kang, E., Jun, H., Pletnikov, M.V., Christian, K.M., Hen, R., Lucae, S., Binder, E.B., Song, H*., et al.* (2013b). Secreted frizzled-related protein 3 (sFRP3) regulates antidepressant responses in mice and humans. Molecular psychiatry *18*, 957-958.

Jaskelioff, M., Muller, F.L., Paik, J.H., Thomas, E., Jiang, S., Adams, A.C., Sahin, E., Kost-Alimova, M., Protopopov, A., Cadinanos, J*., et al.* (2011). Telomerase reactivation reverses tissue degeneration in aged telomerase-deficient mice. Nature *469*, 102-106.

Jen, Y., Manova, K., and Benezra, R. (1997). Each member of the Id gene family exhibits a unique expression pattern in mouse gastrulation and neurogenesis. Dev Dyn *208*, 92-106.

Jessberger, S., and Gage, F.H. (2008). Stem-cell-associated structural and functional plasticity in the aging hippocampus. Psychology and aging *23*, 684-691.

Jessberger, S., and Parent, J.M. (2015). Epilepsy and Adult Neurogenesis. Cold Spring Harb Perspect Biol *7*.

Jin, K., Sun, Y., Xie, L., Batteur, S., Mao, X.O., Smelick, C., Logvinova, A., and Greenberg, D.A. (2003). Neurogenesis and aging: FGF-2 and HB-EGF restore neurogenesis in hippocampus and subventricular zone of aged mice. Aging Cell *2*, 175-183.

Jin, K., Zhu, Y., Sun, Y., Mao, X.O., Xie, L., and Greenberg, D.A. (2002). Vascular endothelial growth factor (VEGF) stimulates neurogenesis in vitro and in vivo. Proc Natl Acad Sci U S A *99*, 11946-11950.

Joo, S., Kim, J.Y., Lee, E., Hong, N., Sun, W., and Nam, Y. (2015). Effects of ECM protein micropatterns on the migration and differentiation of adult neural stem cells. Sci Rep *5*, 13043.

Jung, S., Park, R.H., Kim, S., Jeon, Y.J., Ham, D.S., Jung, M.Y., Kim, S.S., Lee, Y.D., Park, C.H., and Suh-Kim, H. (2010). Id proteins facilitate self-renewal and proliferation of neural stem cells. Stem cells and development *19*, 831-841.

Kageyama, R., Ohtsuka, T., Shimojo, H., and Imayoshi, I. (2008). Dynamic Notch signaling in neural progenitor cells and a revised view of lateral inhibition. Nat Neurosci *11*, 1247-1251.

Kang, W., and Hebert, J.M. (2015). FGF Signaling Is Necessary for Neurogenesis in Young Mice and Sufficient to Reverse Its Decline in Old Mice. The Journal of neuroscience : the official journal of the Society for Neuroscience *35*, 10217-10223.

Kapsimali, M., Kloosterman, W.P., de Bruijn, E., Rosa, F., Plasterk, R.H., and Wilson, S.W. (2007). MicroRNAs show a wide diversity of expression profiles in the developing and mature central nervous system. Genome Biol *8*, R173.

Karpowicz, P., Morshead, C., Kam, A., Jervis, E., Ramunas, J., Cheng, V., and van der Kooy, D. (2005). Support for the immortal strand hypothesis: neural stem cells partition DNA asymmetrically in vitro. J Cell Biol *170*, 721-732.

Katz, S., Cussigh, D., Urban, N., Blomfield, I., Guillemot, F., Bally-Cuif, L., and Coolen, M. (2016). A Nuclear Role for miR-9 and Argonaute Proteins in Balancing Quiescent and Activated Neural Stem Cell States. Cell reports *17*, 1383-1398.

Kawaguchi, D., Furutachi, S., Kawai, H., Hozumi, K., and Gotoh, Y. (2013). Dll1 maintains quiescence of adult neural stem cells and segregates asymmetrically during mitosis. Nature communications *4*, 1880.

Kawahara, H., Imai, T., and Okano, H. (2012). MicroRNAs in Neural Stem Cells and Neurogenesis. Frontiers in neuroscience *6*, 30.

Kawai, H., Kawaguchi, D., Kuebrich, B.D., Kitamoto, T., Yamaguchi, M., Gotoh, Y., and Furutachi, S. (2017). Area-Specific Regulation of Quiescent Neural Stem Cells by Notch3 in the Adult Mouse Subependymal Zone. The Journal of neuroscience : the official journal of the Society for Neuroscience *37*, 11867-11880.

Kazanis, I., Lathia, J.D., Vadakkan, T.J., Raborn, E., Wan, R., Mughal, M.R., Eckley, D.M., Sasaki, T., Patton, B., Mattson, M.P.*, et al.* (2010). Quiescence and activation of stem and precursor cell populations in the subependymal zone of the mammalian brain are associated with distinct cellular and extracellular matrix signals. The Journal of neuroscience : the official journal of the Society for Neuroscience *30*, 9771-9781.

Kempermann, G. (2011a). The pessimist's and optimist's views of adult neurogenesis. Cell *145*, 1009-1011.

Kempermann, G. (2011b). Seven principles in the regulation of adult neurogenesis. Eur J Neurosci *33*, 1018-1024.

Kempermann, G. (2012). New neurons for 'survival of the fittest'. Nat Rev Neurosci *13*, 727-736.

Kempermann, G., Gage, F.H., Aigner, L., Song, H., Curtis, M.A., Thuret, S., Kuhn, H.G., Jessberger, S., Frankland, P.W., Cameron, H.A.*, et al.* (2018). Human Adult Neurogenesis: Evidence and Remaining Questions. Cell Stem Cell *23*, 25-30.

Kim, D., Pertea, G., Trapnell, C., Pimentel, H., Kelley, R., and Salzberg, S.L. (2013). TopHat2: accurate alignment of transcriptomes in the presence of insertions, deletions and gene fusions. Genome Biol *14*, R36.

Kim, E.J., Ables, J.L., Dickel, L.K., Eisch, A.J., and Johnson, J.E. (2011). Ascl1 (Mash1) defines cells with long-term neurogenic potential in subgranular and subventricular zones in adult mouse brain. PLoS ONE *6*, e18472.

Kim, K.H., and Sederstrom, J.M. (2015). Assaying Cell Cycle Status Using Flow Cytometry. Curr Protoc Mol Biol *111*, 28 26 21-11.

Kippin, T.E., Martens, D.J., and van der Kooy, D. (2005). p21 loss compromises the relative quiescence of forebrain stem cell proliferation leading to exhaustion of their proliferation capacity. Genes & development *19*, 756-767.

Kluppel, M., and Wrana, J.L. (2005). Turning it up a Notch: cross-talk between TGF beta and Notch signaling. Bioessays *27*, 115-118.

Knobloch, M., Braun, S.M., Zurkirchen, L., von Schoultz, C., Zamboni, N., Arauzo-Bravo, M.J., Kovacs, W.J., Karalay, O., Suter, U., Machado, R.A.*, et al.* (2013). Metabolic control of adult neural stem cell activity by Fasn-dependent lipogenesis. Nature *493*, 226-230.

Knobloch, M., Pilz, G.A., Ghesquiere, B., Kovacs, W.J., Wegleiter, T., Moore, D.L., Hruzova, M., Zamboni, N., Carmeliet, P., and Jessberger, S. (2017). A Fatty Acid Oxidation-Dependent Metabolic Shift Regulates Adult Neural Stem Cell Activity. Cell reports *20*, 2144-2155.

Knoth, R., Singec, I., Ditter, M., Pantazis, G., Capetian, P., Meyer, R.P., Horvat, V., Volk, B., and Kempermann, G. (2010). Murine features of neurogenesis in the human hippocampus across the lifespan from 0 to 100 years. PLoS ONE *5*, e8809.

Kokovay, E., Wang, Y., Kusek, G., Wurster, R., Lederman, P., Lowry, N., Shen, Q., and Temple, S. (2012). VCAM1 is essential to maintain the structure of the SVZ niche and acts as an environmental sensor to regulate SVZ lineage progression. Cell Stem Cell *11*, 220-230.

Kriegstein, A., and Alvarez-Buylla, A. (2009). The glial nature of embryonic and adult neural stem cells. Annu Rev Neurosci *32*, 149-184.

Kronenberg, G., Reuter, K., Steiner, B., Brandt, M.D., Jessberger, S., Yamaguchi, M., and Kempermann, G. (2003). Subpopulations of proliferating cells of the adult

hippocampus respond differently to physiologic neurogenic stimuli. The Journal of comparative neurology *467*, 455-463.

Kuhn, H.G., Dickinson-Anson, H., and Gage, F.H. (1996). Neurogenesis in the dentate gyrus of the adult rat: age-related decrease of neuronal progenitor proliferation. The Journal of neuroscience : the official journal of the Society for Neuroscience *16*, 2027-2033.

Kuhn, H.G., Winkler, J., Kempermann, G., Thal, L.J., and Gage, F.H. (1997). Epidermal growth factor and fibroblast growth factor-2 have different effects on neural progenitors in the adult rat brain. The Journal of neuroscience : the official journal of the Society for Neuroscience *17*, 5820-5829.

Kukekov, V.G., Laywell, E.D., Suslov, O., Davies, K., Scheffler, B., Thomas, L.B., O'Brien, T.F., Kusakabe, M., and Steindler, D.A. (1999). Multipotent stem/progenitor cells with similar properties arise from two neurogenic regions of adult human brain. Exp Neurol *156*, 333-344.

Kuwabara, T., Hsieh, J., Muotri, A., Yeo, G., Warashina, M., Lie, D.C., Moore, L., Nakashima, K., Asashima, M., and Gage, F.H. (2009). Wnt-mediated activation of NeuroD1 and retro-elements during adult neurogenesis. Nat Neurosci *12*, 1097-1105.

Kvajo, M., McKellar, H., Arguello, P.A., Drew, L.J., Moore, H., MacDermott, A.B., Karayiorgou, M., and Gogos, J.A. (2008). A mutation in mouse Disc1 that models a schizophrenia risk allele leads to specific alterations in neuronal architecture and cognition. Proc Natl Acad Sci U S A *105*, 7076-7081.

Kwon, J.S., Everetts, N.J., Wang, X., Wang, W., Della Croce, K., Xing, J., and Yao, G. (2017). Controlling Depth of Cellular Quiescence by an Rb-E2F Network Switch. Cell reports *20*, 3223-3235.

Lai, K., Kaspar, B.K., Gage, F.H., and Schaffer, D.V. (2003). Sonic hedgehog regulates adult neural progenitor proliferation in vitro and in vivo. Nat Neurosci *6*, 21-27.

Langmead, B., and Salzberg, S.L. (2012). Fast gapped-read alignment with Bowtie 2. Nat Methods *9*, 357-359.

Larsson, O., Zetterberg, A., and Engstrom, W. (1985). Cell-cycle-specific induction of quiescence achieved by limited inhibition of protein synthesis: counteractive effect of addition of purified growth factors. J Cell Sci *73*, 375-387.

Lasorella, A., Benezra, R., and Iavarone, A. (2014). The ID proteins: master regulators of cancer stem cells and tumour aggressiveness. Nat Rev Cancer *14*, 77-91.

Lasorella, A., Noseda, M., Beyna, M., Yokota, Y., and Iavarone, A. (2000). Id2 is a retinoblastoma protein target and mediates signalling by Myc oncoproteins. Nature *407*, 592-598.

Lathia, J.D., Mack, S.C., Mulkearns-Hubert, E.E., Valentim, C.L., and Rich, J.N. (2015). Cancer stem cells in glioblastoma. Genes & development *29*, 1203-1217.

Lavado, A., and Oliver, G. (2014). Jagged1 is necessary for postnatal and adult neurogenesis in the dentate gyrus. Dev Biol *388*, 11-21.

Laywell, E.D., Rakic, P., Kukekov, V.G., Holland, E.C., and Steindler, D.A. (2000). Identification of a multipotent astrocytic stem cell in the immature and adult mouse brain. Proc Natl Acad Sci U S A *97*, 13883-13888.

Lazarini, F., and Lledo, P.M. (2011). Is adult neurogenesis essential for olfaction? Trends Neurosci *34*, 20-30.

Lazarov, O., and Marr, R.A. (2013). Of mice and men: neurogenesis, cognition and Alzheimer's disease. Frontiers in aging neuroscience *5*, 43.

Lee, A., Kessler, J.D., Read, T.A., Kaiser, C., Corbeil, D., Huttner, W.B., Johnson, J.E., and Wechsler-Reya, R.J. (2005). Isolation of neural stem cells from the postnatal cerebellum. Nat Neurosci *8*, 723-729.

Leeman, D.S., Hebestreit, K., Ruetz, T., Webb, A.E., McKay, A., Pollina, E.A., Dulken, B.W., Zhao, X., Yeo, R.W., Ho, T.T.*, et al.* (2018). Lysosome activation clears aggregates and enhances quiescent neural stem cell activation during aging. Science *359*, 1277-1283.

Leung, C.T., Coulombe, P.A., and Reed, R.R. (2007). Contribution of olfactory neural stem cells to tissue maintenance and regeneration. Nat Neurosci *10*, 720-726.

Li, G., Fang, L., Fernandez, G., and Pleasure, S.J. (2013). The ventral hippocampus is the embryonic origin for adult neural stem cells in the dentate gyrus. Neuron *78*, 658-672.

Liboska, R., Ligasova, A., Strunin, D., Rosenberg, I., and Koberna, K. (2012). Most anti-BrdU antibodies react with 2'-deoxy-5-ethynyluridine -- the method for the effective suppression of this cross-reactivity. PLoS ONE *7*, e51679.

Liddelow, S.A., and Barres, B.A. (2017). Reactive Astrocytes: Production, Function, and Therapeutic Potential. Immunity *46*, 957-967.

Lie, D.C., Colamarino, S.A., Song, H.J., Desire, L., Mira, H., Consiglio, A., Lein, E.S., Jessberger, S., Lansford, H., Dearie, A.R.*, et al.* (2005). Wnt signalling regulates adult hippocampal neurogenesis. Nature *437*, 1370-1375.

Lieberwirth, C., Liu, Y., Jia, X., and Wang, Z. (2012). Social isolation impairs adult neurogenesis in the limbic system and alters behaviors in female prairie voles. Horm Behav *62*, 357-366.

Lim, D.A., Tramontin, A.D., Trevejo, J.M., Herrera, D.G., Garcia-Verdugo, J.M., and Alvarez-Buylla, A. (2000). Noggin antagonizes BMP signaling to create a niche for adult neurogenesis. Neuron *28*, 713-726.

Lin, H. (2002). The stem-cell niche theory: lessons from flies. Nat Rev Genet *3*, 931-940.

Lin, T.N., Te, J., Lee, M., Sun, G.Y., and Hsu, C.Y. (1997). Induction of basic fibroblast growth factor (bFGF) expression following focal cerebral ischemia. Brain Res Mol Brain Res *49*, 255-265.

Ling, F., Kang, B., and Sun, X.H. (2014). Id proteins: small molecules, mighty regulators. Curr Top Dev Biol *110*, 189-216.

Lingbeck, J.M., Trausch-Azar, J.S., Ciechanover, A., and Schwartz, A.L. (2005). E12 and E47 modulate cellular localization and proteasome-mediated degradation of MyoD and Id1. Oncogene *24*, 6376-6384.

Liu, A., and Niswander, L.A. (2005). Bone morphogenetic protein signalling and vertebrate nervous system development. Nat Rev Neurosci *6*, 945-954.

Liu, H., Adler, A.S., Segal, E., and Chang, H.Y. (2007). A transcriptional program mediating entry into cellular quiescence. PLoS Genet *3*, e91.

Liu, X., Wang, Q., Haydar, T.F., and Bordey, A. (2005). Nonsynaptic GABA signaling in postnatal subventricular zone controls proliferation of GFAP-expressing progenitors. Nat Neurosci *8*, 1179-1187.

Llorens-Bobadilla, E., Zhao, S., Baser, A., Saiz-Castro, G., Zwadlo, K., and Martin-Villalba, A. (2015). Single-Cell Transcriptomics Reveals a Population of Dormant Neural Stem Cells that Become Activated upon Brain Injury. Cell Stem Cell *17*, 329-340.

Lugert, S., Basak, O., Knuckles, P., Haussler, U., Fabel, K., Gotz, M., Haas, C.A., Kempermann, G., Taylor, V., and Giachino, C. (2010). Quiescent and active hippocampal neural stem cells with distinct morphologies respond selectively to physiological and pathological stimuli and aging. Cell Stem Cell *6*, 445-456.

Lyden, D., Young, A.Z., Zagzag, D., Yan, W., Gerald, W., O'Reilly, R., Bader, B.L., Hynes, R.O., Zhuang, Y., Manova, K.*, et al.* (1999). Id1 and Id3 are required for neurogenesis, angiogenesis and vascularization of tumour xenografts. Nature *401*, 670-677.

Madisen, L., Zwingman, T.A., Sunkin, S.M., Oh, S.W., Zariwala, H.A., Gu, H., Ng, L.L., Palmiter, R.D., Hawrylycz, M.J., Jones, A.R.*, et al.* (2010). A robust and high-throughput Cre reporting and characterization system for the whole mouse brain. Nat Neurosci *13*, 133-140.

Mak, G.K., Enwere, E.K., Gregg, C., Pakarainen, T., Poutanen, M., Huhtaniemi, I., and Weiss, S. (2007). Male pheromone-stimulated neurogenesis in the adult female brain: possible role in mating behavior. Nat Neurosci *10*, 1003-1011.

Marques-Torrejon, M.A., Porlan, E., Banito, A., Gomez-Ibarlucea, E., Lopez-Contreras, A.J., Fernandez-Capetillo, O., Vidal, A., Gil, J., Torres, J., and Farinas, I. (2013). Cyclin-dependent kinase inhibitor p21 controls adult neural stem cell expansion by regulating Sox2 gene expression. Cell Stem Cell *12*, 88-100.

Martini, M., Cenci, T., D'Alessandris, G.Q., Cesarini, V., Cocomazzi, A., Ricci-Vitiani, L., De Maria, R., Pallini, R., and Larocca, L.M. (2013). Epigenetic silencing of Id4 identifies a glioblastoma subgroup with a better prognosis as a consequence of an inhibition of angiogenesis. Cancer *119*, 1004-1012.

Martynoga, B., Mateo, J.L., Zhou, B., Andersen, J., Achimastou, A., Urban, N., van den Berg, D., Georgopoulou, D., Hadjur, S., Wittbrodt, J.*, et al.* (2013). Epigenomic

enhancer annotation reveals a key role for NFIX in neural stem cell quiescence. Genes & development *27*, 1769-1786.

McKee, C., and Chaudhry, G.R. (2017). Advances and challenges in stem cell culture. Colloids Surf B Biointerfaces *159*, 62-77.

Meier-Stiegen, F., Schwanbeck, R., Bernoth, K., Martini, S., Hieronymus, T., Ruau, D., Zenke, M., and Just, U. (2010). Activated Notch1 target genes during embryonic cell differentiation depend on the cellular context and include lineage determinants and inhibitors. PLoS ONE *5*, e11481.

Mercier, F., and Douet, V. (2014). Bone morphogenetic protein-4 inhibits adult neurogenesis and is regulated by fractone-associated heparan sulfates in the subventricular zone. J Chem Neuroanat *57-58*, 54-61.

Merkle, F.T., Fuentealba, L.C., Sanders, T.A., Magno, L., Kessaris, N., and Alvarez-Buylla, A. (2014). Adult neural stem cells in distinct microdomains generate previously unknown interneuron types. Nat Neurosci *17*, 207-214.

Merkle, F.T., Mirzadeh, Z., and Alvarez-Buylla, A. (2007). Mosaic organization of neural stem cells in the adult brain. Science *317*, 381-384.

Mikawa, S., Wang, C., and Sato, K. (2006). Bone morphogenetic protein-4 expression in the adult rat brain. The Journal of comparative neurology *499*, 613-625.

Miller, B.R., and Hen, R. (2015). The current state of the neurogenic theory of depression and anxiety. Curr Opin Neurobiol *30*, 51-58.

Mira, H., Andreu, Z., Suh, H., Lie, D.C., Jessberger, S., Consiglio, A., San Emeterio, J., Hortiguela, R., Marques-Torrejon, M.A., Nakashima, K.*, et al.* (2010). Signaling through BMPR-IA regulates quiescence and long-term activity of neural stem cells in the adult hippocampus. Cell Stem Cell *7*, 78-89.

Mirescu, C., and Gould, E. (2006). Stress and adult neurogenesis. Hippocampus *16*, 233-238.

Monaghan, A.P., Grau, E., Bock, D., and Schutz, G. (1995). The mouse homolog of the orphan nuclear receptor tailless is expressed in the developing forebrain. Development *121*, 839-853.

Moore, K.A., and Lemischka, I.R. (2006). Stem cells and their niches. Science *311*, 1880-1885.

Morizur, L., Chicheportiche, A., Gauthier, L.R., Daynac, M., Boussin, F.D., and Mouthon, M.A. (2018). Distinct Molecular Signatures of Quiescent and Activated Adult Neural Stem Cells Reveal Specific Interactions with Their Microenvironment. Stem Cell Reports *11*, 565-577.

Mosher, K.I., and Schaffer, D.V. (2018). Influence of hippocampal niche signals on neural stem cell functions during aging. Cell Tissue Res *371*, 115-124.

Mourikis, P., Sambasivan, R., Castel, D., Rocheteau, P., Bizzarro, V., and Tajbakhsh, S. (2012). A critical requirement for notch signaling in maintenance of the quiescent skeletal muscle stem cell state. Stem Cells *30*, 243-252.

Mourikis, P., and Tajbakhsh, S. (2014). Distinct contextual roles for Notch signalling in skeletal muscle stem cells. BMC Dev Biol *14*, 2.

Moustakas, A., and Heldin, C.H. (2005). Non-Smad TGF-beta signals. J Cell Sci *118*, 3573-3584.

Mu, Y., Gudey, S.K., and Landstrom, M. (2012). Non-Smad signaling pathways. Cell Tissue Res *347*, 11-20.

Mudo, G., Belluardo, N., Mauro, A., and Fuxe, K. (2007). Acute intermittent nicotine treatment induces fibroblast growth factor-2 in the subventricular zone of the adult rat brain and enhances neuronal precursor cell proliferation. Neuroscience *145*, 470-483.

Mudo, G., Bonomo, A., Di Liberto, V., Frinchi, M., Fuxe, K., and Belluardo, N. (2009). The FGF-2/FGFRs neurotrophic system promotes neurogenesis in the adult brain. J Neural Transm (Vienna) *116*, 995-1005.

Mukherjee, S., Brulet, R., Zhang, L., and Hsieh, J. (2016). REST regulation of gene networks in adult neural stem cells. Nature communications *7*, 13360.

Murai, K., Qu, Q., Sun, G., Ye, P., Li, W., Asuelime, G., Sun, E., Tsai, G.E., and Shi, Y. (2014). Nuclear receptor TLX stimulates hippocampal neurogenesis and enhances learning and memory in a transgenic mouse model. Proc Natl Acad Sci U S A *111*, 9115-9120.

Nam, H.S., and Benezra, R. (2009). High levels of Id1 expression define B1 type adult neural stem cells. Cell Stem Cell *5*, 515-526.

Namba, T., Mochizuki, H., Onodera, M., Mizuno, Y., Namiki, H., and Seki, T. (2005). The fate of neural progenitor cells expressing astrocytic and radial glial markers in the postnatal rat dentate gyrus. Eur J Neurosci *22*, 1928-1941.

Nguyen, L., Malgrange, B., Breuskin, I., Bettendorff, L., Moonen, G., Belachew, S., and Rigo, J.M. (2003). Autocrine/paracrine activation of the GABA(A) receptor inhibits the proliferation of neurogenic polysialylated neural cell adhesion molecule-positive (PSA-NCAM+) precursor cells from postnatal striatum. The Journal of neuroscience : the official journal of the Society for Neuroscience *23*, 3278-3294.

Niola, F., Zhao, X., Singh, D., Castano, A., Sullivan, R., Lauria, M., Nam, H.S., Zhuang, Y., Benezra, R., Di Bernardo, D*., et al.* (2012). Id proteins synchronize stemness and anchorage to the niche of neural stem cells. Nat Cell Biol *14*, 477-487.

Niola, F., Zhao, X., Singh, D., Sullivan, R., Castano, A., Verrico, A., Zoppoli, P., Friedmann-Morvinski, D., Sulman, E., Barrett, L*., et al.* (2013). Mesenchymal high-grade glioma is maintained by the ID-RAP1 axis. J Clin Invest *123*, 405-417.

Niu, W., Zou, Y., Shen, C., and Zhang, C.L. (2011). Activation of postnatal neural stem cells requires nuclear receptor TLX. The Journal of neuroscience : the official journal of the Society for Neuroscience *31*, 13816-13828.

Nochi, R., Kato, T., Kaneko, J., Itou, Y., Kuribayashi, H., Fukuda, S., Terazono, Y., Matani, A., Kanatani, S., Nakajima, K.*, et al.* (2012). Involvement of metabotropic glutamate receptor 5 signaling in activity-related proliferation of adult hippocampal neural stem cells. Eur J Neurosci *36*, 2273-2283.

O'Shea, A., Cohen, R.A., Porges, E.C., Nissim, N.R., and Woods, A.J. (2016). Cognitive Aging and the Hippocampus in Older Adults. Frontiers in aging neuroscience *8*, 298.

Oh, J., Daniels, G.J., Chiou, L.S., Ye, E.A., Jeong, Y.S., and Sakaguchi, D.S. (2014). Multipotent adult hippocampal progenitor cells maintained as neurospheres favor differentiation toward glial lineages. Biotechnol J *9*, 921-933.

Ohkubo, Y., Uchida, A.O., Shin, D., Partanen, J., and Vaccarino, F.M. (2004). Fibroblast growth factor receptor 1 is required for the proliferation of hippocampal progenitor cells and for hippocampal growth in mouse. The Journal of neuroscience : the official journal of the Society for Neuroscience *24*, 6057-6069.

Ohtsuka, T., Imayoshi, I., Shimojo, H., Nishi, E., Kageyama, R., and McConnell, S.K. (2006). Visualization of embryonic neural stem cells using Hes promoters in transgenic mice. Mol Cell Neurosci *31*, 109-122.

Oishi, K., Watatani, K., Itoh, Y., Okano, H., Guillemot, F., Nakajima, K., and Gotoh, Y. (2009). Selective induction of neocortical GABAergic neurons by the PDK1-Akt pathway through activation of Mash1. Proc Natl Acad Sci U S A *106*, 13064-13069.

Otsuki, L., and Brand, A.H. (2018). Cell cycle heterogeneity directs the timing of neural stem cell activation from quiescence. Science *360*, 99-102.

Ottone, C., Krusche, B., Whitby, A., Clements, M., Quadrato, G., Pitulescu, M.E., Adams, R.H., and Parrinello, S. (2014). Direct cell-cell contact with the vascular niche maintains quiescent neural stem cells. Nat Cell Biol *16*, 1045-1056.

Packer, A.N., Xing, Y., Harper, S.Q., Jones, L., and Davidson, B.L. (2008). The bifunctional microRNA miR-9/miR-9* regulates REST and CoREST and is downregulated in Huntington's disease. The Journal of neuroscience : the official journal of the Society for Neuroscience *28*, 14341-14346.

Palma, V., Lim, D.A., Dahmane, N., Sanchez, P., Brionne, T.C., Herzberg, C.D., Gitton, Y., Carleton, A., Alvarez-Buylla, A., and Ruiz i Altaba, A. (2005). Sonic hedgehog controls stem cell behavior in the postnatal and adult brain. Development *132*, 335-344.

Palmer, T.D., Markakis, E.A., Willhoite, A.R., Safar, F., and Gage, F.H. (1999). Fibroblast growth factor-2 activates a latent neurogenic program in neural stem cells from diverse regions of the adult CNS. The Journal of neuroscience : the official journal of the Society for Neuroscience *19*, 8487-8497.

Palmer, T.D., Ray, J., and Gage, F.H. (1995). FGF-2-responsive neuronal progenitors reside in proliferative and quiescent regions of the adult rodent brain. Mol Cell Neurosci *6*, 474-486.

Palmer, T.D., Willhoite, A.R., and Gage, F.H. (2000). Vascular niche for adult hippocampal neurogenesis. The Journal of comparative neurology *425*, 479-494.

Patel, D., Morton, D.J., Carey, J., Havrda, M.C., and Chaudhary, J. (2015). Inhibitor of differentiation 4 (ID4): From development to cancer. Biochim Biophys Acta *1855*, 92-103.

Paul, A., Chaker, Z., and Doetsch, F. (2017). Hypothalamic regulation of regionally distinct adult neural stem cells and neurogenesis. Science *356*, 1383-1386.

Pereira, S.F., Gonzalez, R.L., Jr., and Dworkin, J. (2015). Protein synthesis during cellular quiescence is inhibited by phosphorylation of a translational elongation factor. Proc Natl Acad Sci U S A *112*, E3274-3281.

Petrova, R., Garcia, A.D., and Joyner, A.L. (2013). Titration of GLI3 repressor activity by sonic hedgehog signaling is critical for maintaining multiple adult neural stem cell and astrocyte functions. The Journal of neuroscience : the official journal of the Society for Neuroscience *33*, 17490-17505.

Peverali, F.A., Ramqvist, T., Saffrich, R., Pepperkok, R., Barone, M.V., and Philipson, L. (1994). Regulation of G1 progression by E2A and Id helix-loop-helix proteins. EMBO J *13*, 4291-4301.

Pevny, L.H., and Nicolis, S.K. (2010). Sox2 roles in neural stem cells. Int J Biochem Cell Biol *42*, 421-424.

Pilz, G.A., Bottes, S., Betizeau, M., Jorg, D.J., Carta, S., Simons, B.D., Helmchen, F., and Jessberger, S. (2018). Live imaging of neurogenesis in the adult mouse hippocampus. Science *359*, 658-662.

Pineda, J.R., Daynac, M., Chicheportiche, A., Cebrian-Silla, A., Sii Felice, K., Garcia-Verdugo, J.M., Boussin, F.D., and Mouthon, M.A. (2013). Vascular-derived TGF-beta increases in the stem cell niche and perturbs neurogenesis during aging and following irradiation in the adult mouse brain. EMBO Mol Med *5*, 548-562.

Porlan, E., Morante-Redolat, J.M., Marques-Torrejon, M.A., Andreu-Agullo, C., Carneiro, C., Gomez-Ibarlucea, E., Soto, A., Vidal, A., Ferron, S.R., and Farinas, I. (2013). Transcriptional repression of Bmp2 by p21(Waf1/Cip1) links quiescence to neural stem cell maintenance. Nat Neurosci *16*, 1567-1575.

Qu, Q., Sun, G., Li, W., Yang, S., Ye, P., Zhao, C., Yu, R.T., Gage, F.H., Evans, R.M., and Shi, Y. (2010). Orphan nuclear receptor TLX activates Wnt/beta-catenin signalling to stimulate neural stem cell proliferation and self-renewal. Nat Cell Biol *12*, 31-40; sup pp 31-39.

Rahme, G.J., and Israel, M.A. (2015). Id4 suppresses MMP2-mediated invasion of glioblastoma-derived cells by direct inactivation of Twist1 function. Oncogene *34*, 53-62.

Rai, K.S., Hattiangady, B., and Shetty, A.K. (2007). Enhanced production and dendritic growth of new dentate granule cells in the middle-aged hippocampus following intracerebroventricular FGF-2 infusions. Eur J Neurosci *26*, 1765-1779.

Ramón y Cajal, S. (1928). Degeneration and regeneration of the nervous system. Oxford, England: Clarendon Press.

Ray, J., Peterson, D.A., Schinstine, M., and Gage, F.H. (1993). Proliferation, differentiation, and long-term culture of primary hippocampal neurons. Proc Natl Acad Sci U S A *90*, 3602-3606.

Rebo, J., Mehdipour, M., Gathwala, R., Causey, K., Liu, Y., Conboy, M.J., and Conboy, I.M. (2016). A single heterochronic blood exchange reveals rapid inhibition of multiple tissues by old blood. Nature communications *7*, 13363.

Renault, V.M., Rafalski, V.A., Morgan, A.A., Salih, D.A., Brett, J.O., Webb, A.E., Villeda, S.A., Thekkat, P.U., Guillerey, C., Denko, N.C.*, et al.* (2009). FoxO3 regulates neural stem cell homeostasis. Cell Stem Cell *5*, 527-539.

Revest, J.M., Dupret, D., Koehl, M., Funk-Reiter, C., Grosjean, N., Piazza, P.V., and Abrous, D.N. (2009). Adult hippocampal neurogenesis is involved in anxiety-related behaviors. Molecular psychiatry *14*, 959-967.

Reynolds, B.A., and Weiss, S. (1992). Generation of neurons and astrocytes from isolated cells of the adult mammalian central nervous system. Science *255*, 1707-1710.

Riccio, A. (2018). RNA targeting and translation in axons. Science *359*, 1331-1332.

Richards, L.J., Kilpatrick, T.J., and Bartlett, P.F. (1992). De novo generation of neuronal cells from the adult mouse brain. Proc Natl Acad Sci U S A *89*, 8591-8595.

Rigolet, M., Rich, T., Gross-Morand, M.S., Molina-Gomes, D., Viegas-Pequignot, E., and Junien, C. (1998). cDNA cloning, tissue distribution and chromosomal localization of the human ID4 gene. DNA Res *5*, 309-313.

Risso, D., Ngai, J., Speed, T.P., and Dudoit, S. (2014). Normalization of RNA-seq data using factor analysis of control genes or samples. Nat Biotechnol *32*, 896-902.

Risso, D., Schwartz, K., Sherlock, G., and Dudoit, S. (2011). GC-content normalization for RNA-Seq data. BMC Bioinformatics *12*, 480.

Robinson, M.D., McCarthy, D.J., and Smyth, G.K. (2010). edgeR: a Bioconductor package for differential expression analysis of digital gene expression data. Bioinformatics *26*, 139-140.

Rodriguez Viales, R., Diotel, N., Ferg, M., Armant, O., Eich, J., Alunni, A., Marz, M., Bally-Cuif, L., Rastegar, S., and Strahle, U. (2015). The helix-loop-helix protein id1 controls stem cell proliferation during regenerative neurogenesis in the adult zebrafish telencephalon. Stem Cells *33*, 892-903.

Rolando, C., and Taylor, V. (2014). Neural stem cell of the hippocampus: development, physiology regulation, and dysfunction in disease. Curr Top Dev Biol *107*, 183-206.

Romero-Lanman, E.E., Pavlovic, S., Amlani, B., Chin, Y., and Benezra, R. (2012). Id1 maintains embryonic stem cell self-renewal by up-regulation of Nanog and repression of Brachyury expression. Stem cells and development *21*, 384-393.

Roy, N.S., Benraiss, A., Wang, S., Fraser, R.A., Goodman, R., Couldwell, W.T., Nedergaard, M., Kawaguchi, A., Okano, H., and Goldman, S.A. (2000). Promoter-targeted selection and isolation of neural progenitor cells from the adult human ventricular zone. J Neurosci Res *59*, 321-331.

Ruckh, J.M., Zhao, J.W., Shadrach, J.L., van Wijngaarden, P., Rao, T.N., Wagers, A.J., and Franklin, R.J. (2012). Rejuvenation of regeneration in the aging central nervous system. Cell Stem Cell *10*, 96-103.

Ruzinova, M.B., and Benezra, R. (2003). Id proteins in development, cell cycle and cancer. Trends Cell Biol *13*, 410-418.

Ryan, S.M., O'Keeffe, G.W., O'Connor, C., Keeshan, K., and Nolan, Y.M. (2013). Negative regulation of TLX by IL-1beta correlates with an inhibition of adult hippocampal neural precursor cell proliferation. Brain Behav Immun *33*, 7-13.

Samanta, J., and Kessler, J.A. (2004). Interactions between ID and OLIG proteins mediate the inhibitory effects of BMP4 on oligodendroglial differentiation. Development *131*, 4131-4142.

Sanai, N., Tramontin, A.D., Quinones-Hinojosa, A., Barbaro, N.M., Gupta, N., Kunwar, S., Lawton, M.T., McDermott, M.W., Parsa, A.T., Manuel-Garcia Verdugo, J.*, et al.* (2004). Unique astrocyte ribbon in adult human brain contains neural stem cells but lacks chain migration. Nature *427*, 740-744.

Santarelli, L., Saxe, M., Gross, C., Surget, A., Battaglia, F., Dulawa, S., Weisstaub, N., Lee, J., Duman, R., Arancio, O.*, et al.* (2003). Requirement of hippocampal neurogenesis for the behavioral effects of antidepressants. Science *301*, 805-809.

Schofield, R. (1978). The relationship between the spleen colony-forming cell and the haemopoietic stem cell. Blood Cells *4*, 7-25.

Scott, I.C., Steiglitz, B.M., Clark, T.G., Pappano, W.N., and Greenspan, D.S. (2000). Spatiotemporal expression patterns of mammalian chordin during postgastrulation embryogenesis and in postnatal brain. Dev Dyn *217*, 449-456.

Sedlmeier, G., and Sleeman, J.P. (2017). Extracellular regulation of BMP signaling: welcome to the matrix. Biochem Soc Trans *45*, 173-181.

Seib, D.R., Corsini, N.S., Ellwanger, K., Plaas, C., Mateos, A., Pitzer, C., Niehrs, C., Celikel, T., and Martin-Villalba, A. (2013). Loss of Dickkopf-1 restores neurogenesis in old age and counteracts cognitive decline. Cell Stem Cell *12*, 204-214.

Seri, B., Garcia-Verdugo, J.M., Collado-Morente, L., McEwen, B.S., and Alvarez-Buylla, A. (2004). Cell types, lineage, and architecture of the germinal zone in the adult dentate gyrus. The Journal of comparative neurology *478*, 359-378.

Seri, B., Garcia-Verdugo, J.M., McEwen, B.S., and Alvarez-Buylla, A. (2001). Astrocytes give rise to new neurons in the adult mammalian hippocampus. The Journal of neuroscience : the official journal of the Society for Neuroscience *21*, 7153-7160.

Sharma, P., Chinaranagari, S., and Chaudhary, J. (2015). Inhibitor of differentiation 4 (ID4) acts as an inhibitor of ID-1, -2 and -3 and promotes basic helix loop helix (bHLH) E47 DNA binding and transcriptional activity. Biochimie *112*, 139-150.

Shen, Q., Goderie, S.K., Jin, L., Karanth, N., Sun, Y., Abramova, N., Vincent, P., Pumiglia, K., and Temple, S. (2004). Endothelial cells stimulate self-renewal and expand neurogenesis of neural stem cells. Science *304*, 1338-1340.

Shen, Q., Wang, Y., Kokovay, E., Lin, G., Chuang, S.M., Goderie, S.K., Roysam, B., and Temple, S. (2008). Adult SVZ stem cells lie in a vascular niche: a quantitative analysis of niche cell-cell interactions. Cell Stem Cell *3*, 289-300.

Shetty, A.K., Hattiangady, B., and Shetty, G.A. (2005). Stem/progenitor cell proliferation factors FGF-2, IGF-1, and VEGF exhibit early decline during the course of aging in the hippocampus: role of astrocytes. Glia *51*, 173-186.

Shi, Y., Chichung Lie, D., Taupin, P., Nakashima, K., Ray, J., Yu, R.T., Gage, F.H., and Evans, R.M. (2004). Expression and function of orphan nuclear receptor TLX in adult neural stem cells. Nature *427*, 78-83.

Shin, J., Berg, D.A., Zhu, Y., Shin, J.Y., Song, J., Bonaguidi, M.A., Enikolopov, G., Nauen, D.W., Christian, K.M., Ming, G.L.*, et al.* (2015). Single-Cell RNA-Seq with Waterfall Reveals Molecular Cascades underlying Adult Neurogenesis. Cell Stem Cell *17*, 360-372.

Shou, J., Rim, P.C., and Calof, A.L. (1999). BMPs inhibit neurogenesis by a mechanism involving degradation of a transcription factor. Nat Neurosci *2*, 339-345.

Sierra, A., Beccari, S., Diaz-Aparicio, I., Encinas, J.M., Comeau, S., and Tremblay, M.E. (2014). Surveillance, phagocytosis, and inflammation: how never-resting microglia influence adult hippocampal neurogenesis. Neural plasticity *2014*, 610343.

Sierra, A., Encinas, J.M., Deudero, J.J., Chancey, J.H., Enikolopov, G., Overstreet-Wadiche, L.S., Tsirka, S.E., and Maletic-Savatic, M. (2010). Microglia shape adult hippocampal neurogenesis through apoptosis-coupled phagocytosis. Cell Stem Cell *7*, 483-495.

Signer, R.A., Magee, J.A., Salic, A., and Morrison, S.J. (2014). Haematopoietic stem cells require a highly regulated protein synthesis rate. Nature *509*, 49-54.

Silva-Vargas, V., and Doetsch, F. (2014). A new twist for neurotrophins: endothelial-derived NT-3 mediates adult neural stem cell quiescence. Neuron *83*, 507-509.

Singh, S.K., Singh, S., Gadomski, S., Sun, L., Pfannenstein, A., Magidson, V., Chen, X.F., Kozlov, S., Tessarollo, L., Klarmann, K.D.*, et al.* (2018). Id1 ablation protects hematopoietic stem cells from stress-Induced exhaustion and aging. . Cell Stem Cell *In press.*

Sonenberg, N., and Hinnebusch, A.G. (2009). Regulation of translation initiation in eukaryotes: mechanisms and biological targets. Cell *136*, 731-745.

Song, J., Zhong, C., Bonaguidi, M.A., Sun, G.J., Hsu, D., Gu, Y., Meletis, K., Huang, Z.J., Ge, S., Enikolopov, G.*, et al.* (2012a). Neuronal circuitry mechanism regulating adult quiescent neural stem-cell fate decision. Nature *489*, 150-154.

Song, M.S., Salmena, L., and Pandolfi, P.P. (2012b). The functions and regulation of the PTEN tumour suppressor. Nat Rev Mol Cell Biol *13*, 283-296.

Sorrells, S.F., Paredes, M.F., Cebrian-Silla, A., Sandoval, K., Qi, D., Kelley, K.W., James, D., Mayer, S., Chang, J., Auguste, K.I.*, et al.* (2018). Human hippocampal neurogenesis drops sharply in children to undetectable levels in adults. Nature *555*, 377-381.

Sottocornola, R., and Lo Celso, C. (2012). Dormancy in the stem cell niche. Stem Cell Res Ther *3*, 10.

Spalding, K.L., Bergmann, O., Alkass, K., Bernard, S., Salehpour, M., Huttner, H.B., Bostrom, E., Westerlund, I., Vial, C., Buchholz, B.A.*, et al.* (2013). Dynamics of hippocampal neurogenesis in adult humans. Cell *153*, 1219-1227.

Sriuranpong, V., Borges, M.W., Strock, C.L., Nakakura, E.K., Watkins, D.N., Blaumueller, C.M., Nelkin, B.D., and Ball, D.W. (2002). Notch signaling induces rapid degradation of achaete-scute homolog 1. Mol Cell Biol *22*, 3129-3139.

Stark, S.M., Yassa, M.A., and Stark, C.E. (2010). Individual differences in spatial pattern separation performance associated with healthy aging in humans. Learning & memory *17*, 284-288.

Steiner, B., Klempin, F., Wang, L., Kott, M., Kettenmann, H., and Kempermann, G. (2006). Type-2 cells as link between glial and neuronal lineage in adult hippocampal neurogenesis. Glia *54*, 805-814.

Steiner, B., Zurborg, S., Horster, H., Fabel, K., and Kempermann, G. (2008). Differential 24 h responsiveness of Prox1-expressing precursor cells in adult hippocampal neurogenesis to physical activity, environmental enrichment, and kainic acid-induced seizures. Neuroscience *154*, 521-529.

Suh, H., Consiglio, A., Ray, J., Sawai, T., D'Amour, K.A., and Gage, F.H. (2007). In vivo fate analysis reveals the multipotent and self-renewal capacities of Sox2+ neural stem cells in the adult hippocampus. Cell Stem Cell *1*, 515-528.

Suhonen, J.O., Peterson, D.A., Ray, J., and Gage, F.H. (1996). Differentiation of adult hippocampus-derived progenitors into olfactory neurons in vivo. Nature *383*, 624-627.

Sun, Y., Hu, J., Zhou, L., Pollard, S.M., and Smith, A. (2011). Interplay between FGF2 and BMP controls the self-renewal, dormancy and differentiation of rat neural stem cells. J Cell Sci *124*, 1867-1877.

Sun, Y., Jin, K., Xie, L., Childs, J., Mao, X.O., Logvinova, A., and Greenberg, D.A. (2003). VEGF-induced neuroprotection, neurogenesis, and angiogenesis after focal cerebral ischemia. J Clin Invest *111*, 1843-1851.

Tavazoie, M., Van der Veken, L., Silva-Vargas, V., Louissaint, M., Colonna, L., Zaidi, B., Garcia-Verdugo, J.M., and Doetsch, F. (2008). A specialized vascular niche for adult neural stem cells. Cell Stem Cell *3*, 279-288.

Tong, C.K., Chen, J., Cebrian-Silla, A., Mirzadeh, Z., Obernier, K., Guinto, C.D., Tecott, L.H., Garcia-Verdugo, J.M., Kriegstein, A., and Alvarez-Buylla, A. (2014). Axonal control of the adult neural stem cell niche. Cell Stem Cell *14*, 500-511.

Trapnell, C., Hendrickson, D.G., Sauvageau, M., Goff, L., Rinn, J.L., and Pachter, L. (2013). Differential analysis of gene regulation at transcript resolution with RNA-seq. Nat Biotechnol *31*, 46-53.

Trapnell, C., Williams, B.A., Pertea, G., Mortazavi, A., Kwan, G., van Baren, M.J., Salzberg, S.L., Wold, B.J., and Pachter, L. (2010). Transcript assembly and quantification by RNA-Seq reveals unannotated transcripts and isoform switching during cell differentiation. Nat Biotechnol *28*, 511-515.

Trejo, J.L., Llorens-Martin, M.V., and Torres-Aleman, I. (2008). The effects of exercise on spatial learning and anxiety-like behavior are mediated by an IGF-I-dependent mechanism related to hippocampal neurogenesis. Mol Cell Neurosci *37*, 402-411.

Tsai, R.Y. (2016). Balancing self-renewal against genome preservation in stem cells: How do they manage to have the cake and eat it too? Cell Mol Life Sci *73*, 1803-1823.

Tzivion, G., Dobson, M., and Ramakrishnan, G. (2011). FoxO transcription factors; Regulation by AKT and 14-3-3 proteins. Biochim Biophys Acta *1813*, 1938-1945.

Urban, N., and Guillemot, F. (2014). Neurogenesis in the embryonic and adult brain: same regulators, different roles. Frontiers in cellular neuroscience *8*, 396.

Urban, N., van den Berg, D.L., Forget, A., Andersen, J., Demmers, J.A., Hunt, C., Ayrault, O., and Guillemot, F. (2016). Return to quiescence of mouse neural stem cells by degradation of a proactivation protein. Science *353*, 292-295.

van Praag, H., Kempermann, G., and Gage, F.H. (1999). Running increases cell proliferation and neurogenesis in the adult mouse dentate gyrus. Nat Neurosci *2*, 266-270.

van Praag, H., Schinder, A.F., Christie, B.R., Toni, N., Palmer, T.D., and Gage, F.H. (2002). Functional neurogenesis in the adult hippocampus. Nature *415*, 1030-1034.

Villeda, S.A., Luo, J., Mosher, K.I., Zou, B., Britschgi, M., Bieri, G., Stan, T.M., Fainberg, N., Ding, Z., Eggel, A*., et al.* (2011). The ageing systemic milieu negatively regulates neurogenesis and cognitive function. Nature *477*, 90-94.

Vinals, F., Reiriz, J., Ambrosio, S., Bartrons, R., Rosa, J.L., and Ventura, F. (2004). BMP-2 decreases Mash1 stability by increasing Id1 expression. EMBO J *23*, 3527-3537.

Walker, T.L., and Kempermann, G. (2014). One mouse, two cultures: isolation and culture of adult neural stem cells from the two neurogenic zones of individual mice. J Vis Exp, e51225.

Wang, C., Liu, F., Liu, Y.Y., Zhao, C.H., You, Y., Wang, L., Zhang, J., Wei, B., Ma, T., Zhang, Q.*, et al.* (2011). Identification and characterization of neuroblasts in the subventricular zone and rostral migratory stream of the adult human brain. Cell Res *21*, 1534-1550.

Wang, L.H., and Baker, N.E. (2015). E Proteins and ID Proteins: Helix-Loop-Helix Partners in Development and Disease. Dev Cell *35*, 269-280.

Wapinski, O.L., Vierbuchen, T., Qu, K., Lee, Q.Y., Chanda, S., Fuentes, D.R., Giresi, P.G., Ng, Y.H., Marro, S., Neff, N.F.*, et al.* (2013). Hierarchical mechanisms for direct reprogramming of fibroblasts to neurons. Cell *155*, 621-635.

Webb, A.E., Pollina, E.A., Vierbuchen, T., Urban, N., Ucar, D., Leeman, D.S., Martynoga, B., Sewak, M., Rando, T.A., Guillemot, F.*, et al.* (2013). FOXO3 shares common targets with ASCL1 genome-wide and inhibits ASCL1-dependent neurogenesis. Cell reports *4*, 477-491.

Werner, S., Unsicker, K., and von Bohlen und Halbach, O. (2011). Fibroblast growth factor-2 deficiency causes defects in adult hippocampal neurogenesis, which are not rescued by exogenous fibroblast growth factor-2. J Neurosci Res *89*, 1605-1617.

Winner, B., and Winkler, J. (2015). Adult neurogenesis in neurodegenerative diseases. Cold Spring Harb Perspect Biol *7*, a021287.

Woodbury, M.E., and Ikezu, T. (2014). Fibroblast growth factor-2 signaling in neurogenesis and neurodegeneration. J Neuroimmune Pharmacol *9*, 92-101.

Xu, X., Han, J., Ito, Y., Bringas, P., Jr., Deng, C., and Chai, Y. (2008). Ectodermal Smad4 and p38 MAPK are functionally redundant in mediating TGF-beta/BMP signaling during tooth and palate development. Dev Cell *15*, 322-329.

Yeh, C.Y., Asrican, B., Moss, J., Quintanilla, L.J., He, T., Mao, X., Casse, F., Gebara, E., Bao, H., Lu, W.*, et al.* (2018). Mossy Cells Control Adult Neural Stem Cell Quiescence and Maintenance through a Dynamic Balance between Direct and Indirect Pathways. Neuron *99*, 493-510 e494.

Yeo, H., Lyssiotis, C.A., Zhang, Y., Ying, H., Asara, J.M., Cantley, L.C., and Paik, J.H. (2013). FoxO3 coordinates metabolic pathways to maintain redox balance in neural stem cells. EMBO J *32*, 2589-2602.

Yin, H., Price, F., and Rudnicki, M.A. (2013). Satellite cells and the muscle stem cell niche. Physiol Rev *93*, 23-67.

Yokota, Y., Mansouri, A., Mori, S., Sugawara, S., Adachi, S., Nishikawa, S., and Gruss, P. (1999). Development of peripheral lymphoid organs and natural killer cells depends on the helix-loop-helix inhibitor Id2. Nature *397*, 702-706.

Yoshimura, S., Takagi, Y., Harada, J., Teramoto, T., Thomas, S.S., Waeber, C., Bakowska, J.C., Breakefield, X.O., and Moskowitz, M.A. (2001). FGF-2 regulation of neurogenesis in adult hippocampus after brain injury. Proc Natl Acad Sci U S A *98*, 5874-5879.

Yoshimura, S., Teramoto, T., Whalen, M.J., Irizarry, M.C., Takagi, Y., Qiu, J., Harada, J., Waeber, C., Breakefield, X.O., and Moskowitz, M.A. (2003). FGF-2 regulates neurogenesis and degeneration in the dentate gyrus after traumatic brain injury in mice. J Clin Invest *112*, 1202-1210.

Young, S.Z., Taylor, M.M., and Bordey, A. (2011). Neurotransmitters couple brain activity to subventricular zone neurogenesis. Eur J Neurosci *33*, 1123-1132.

Yousef, H., Conboy, M.J., Morgenthaler, A., Schlesinger, C., Bugaj, L., Paliwal, P., Greer, C., Conboy, I.M., and Schaffer, D. (2015a). Systemic attenuation of the TGF-beta pathway by a single drug simultaneously rejuvenates hippocampal neurogenesis and myogenesis in the same old mammal. Oncotarget *6*, 11959-11978.

Yousef, H., Morgenthaler, A., Schlesinger, C., Bugaj, L., Conboy, I.M., and Schaffer, D.V. (2015b). Age-Associated Increase in BMP Signaling Inhibits Hippocampal Neurogenesis. Stem Cells *33*, 1577-1588.

Yuan, H., Chen, R., Wu, L., Chen, Q., Hu, A., Zhang, T., Wang, Z., and Zhu, X. (2015). The regulatory mechanism of neurogenesis by IGF-1 in adult mice. Molecular neurobiology *51*, 512-522.

Yuan, T.F., Li, J., Ding, F., and Arias-Carrion, O. (2014). Evidence of adult neurogenesis in non-human primates and human. Cell Tissue Res *358*, 17-23.

Yue, F., Bi, P., Wang, C., Shan, T., Nie, Y., Ratliff, T.L., Gavin, T.P., and Kuang, S. (2017). Pten is necessary for the quiescence and maintenance of adult muscle stem cells. Nature communications *8*, 14328.

Yun, K., Mantani, A., Garel, S., Rubenstein, J., and Israel, M.A. (2004). Id4 regulates neural progenitor proliferation and differentiation in vivo. Development *131*, 5441-5448.

Zetterberg, A., and Larsson, O. (1985). Kinetic analysis of regulatory events in G1 leading to proliferation or quiescence of Swiss 3T3 cells. Proc Natl Acad Sci U S A *82*, 5365-5369.

Zhang, C.L., Zou, Y., He, W., Gage, F.H., and Evans, R.M. (2008). A role for adult TLX-positive neural stem cells in learning and behaviour. Nature *451*, 1004-1007.

Zhao, C., Sun, G., Li, S., and Shi, Y. (2009). A feedback regulatory loop involving microRNA-9 and nuclear receptor TLX in neural stem cell fate determination. Nat Struct Mol Biol *16*, 365-371.

Zupanc, G.K., Hinsch, K., and Gage, F.H. (2005). Proliferation, migration, neuronal differentiation, and long-term survival of new cells in the adult zebrafish brain. The Journal of comparative neurology *488*, 290-319.

Zupanc, G.K., and Horschke, I. (1995). Proliferation zones in the brain of adult gymnotiform fish: a quantitative mapping study. The Journal of comparative neurology *353*, 213-233.